Developing Anti-p53/HLA-A*0201 T-Cell Receptor Mimic Antibodies for Cancer Immunotherapy

Iva Trenevska

St Catherine's College
University of Oxford

Thesis submitted for the degree of Doctor of Philosophy

Hilary Term 2019

Developing Anti-p53/HLA-A*0201 T-Cell Receptor Mimic Antibodies for Cancer Immunotherapy

Iva Trenevska, St Catherine's College, University of Oxford

Thesis submitted for the degree of Doctor of Philosophy, Hilary Term 2019

Abstract

T-cell receptor mimic (TCRm) antibodies target a dual antigen epitope consisting of a peptide derived from an intracellular protein, and the major histocompatibility complex class I (MHC-I) molecule that presents the peptide at the cell surface. As traditional antibodies typically target cell surface or secreted antigens, TCRm antibodies advantageously expand the range of targetable antigens to include peptides derived from intracellular proteins.

This thesis describes the development of TCRm antibodies targeting peptides that are derived from the wild type p53 protein and are presented by human leukocyte antigen (HLA)-A2. We further characterised the specificity and safety of the T1-116C TCRm antibody, which was the most extensively studied TCRm antibody in the laboratory prior to the start of this DPhil project. We showed that T1-116C labels primary AML and myeloma cells. We investigated the specificity of the T1-116C TCRm antibody for the $p53_{65-73}$ peptide, RMPEAAPPV, by substituting each amino acid within the peptide individually, and showed that T1-116C recognises multiple tumour antigens. Using *in silico* analysis we identified 271 potentially cross-reactive peptides. We tested a panel of 25 peptides that are conserved in mice *in vitro*, showing that T1-116C binds peptides derived from a broad range of normal tissues.

Despite these findings, *in vivo* testing of T1-116C cross-reactivity in human HLA-A2 transgenic mice demonstrated that T1-116C does not cause toxicity to normal mouse tissues.

We also generated chimeric antigen receptors (CARs) for T-cell therapy using the single chain variable fragment of p53-targeting TCRm antibodies to provide the CAR specificity. We found that the CAR derived from T2-2A, a TCRm antibody that targets the $p53_{187\text{-}197}$ peptide, GLAPPQHLIRV, demonstrated superior specificity for target peptide-HLA-A2 tetramers and cell lines to the T1-116C CAR. Through these studies, the T2-2A TCRm antibody has emerged as a potential therapeutic agent when used in the CAR format.

Declaration of Authentication

I declare that all of the work presented in this thesis was performed by me, and in no way forms part of another thesis at this or any other University. Contributions made by others have been acknowledged in this thesis. The work described in this thesis was performed under the co-supervision of Prof Alison Banham and Dr Demin Li, at the Nuffield Division of Clinical Laboratory Sciences, Radcliffe Department of Medicine, University of Oxford.

Iva Trenevska

Oxford

January 2019

Acknowledgements

I would like to thank my co-supervisors, Prof Alison Banham and Dr Demin Li, for their supervision, guidance, patience and support throughout this DPhil project.

I would also like to thank all of the members of Prof Banham's laboratory for their invaluable help throughout this project: Dr Massimo Masiero, Dr Amanda Anderson, Dr Duncan Gascoyne, Miss Carol Bentley (especially for teaching me laboratory techniques when I first came to the lab), Miss Tasneem Hassanali, Mr Koon Ang Hwee, Miss Dian Wang, Miss Linden Lyne, Dr Ling Felce, Miss Hayley Spearman, Dr Simon Brooks and Miss Hayley Hayjung Han. A particular thank you to Dr Massimo Masiero and Dr Amanda Anderson for their help and guidance, on both an academic and personal level.

I would like to thank those who provided materials and technical expertise, without which this thesis would not have been possible: Prof Paresh Vyas and his laboratory (University of Oxford) for providing primary AML samples and clinicopathological patient data, Dr Karthik Ramasamy (University of Oxford) for providing primary myeloma samples, Dr Uzi Gileadi (MRC Human Immunology Unit, University of Oxford) for providing HHD mice, Dr Esther Bridges (University of Oxford) for her help in organising the *in vivo* experiment and for providing technical expertise, and Dr Mariolina Salio (MRC WIMM, University of Oxford) for kindly gifting antibodies, and HHD and C57BL/6 mice.

A special thank you to my mother and sister for their unconditional love, support and help throughout every stage of my life – especially through the most stressful times! Without you, I would not be here today. Finally, a big thank you to my family and friends for helping me weather the storms. This journey has been a transformative experience, and it would not have been the same without you.

Table of Contents

List of Figures

List of Tables

List of Abbreviations

5' and 3'	5 prime and 3 prime end of DNA molecule
^{51}Cr	chromium-51 radionuclide
β2M	beta-2 microglobulin
ADC	antibody-drug conjugate
ADCC	antibody-dependent cellular cytotoxicity
ADCP	antibody-dependent cellular phagocytosis
ALL	acute lymphocytic leukaemia
AML	acute myeloid leukaemia
ANOVA	analysis of variance
APC	allophycocyanin
APC	anitgen-presenting cell
AWERB	Animal Welfare and Ethical Review Body
BCA	bicinchoninic assay
BIMAS	Bioinformatics and Molecular Analysis Section
BiTE	bispecific T-cell engager
bp	base pair
BRCA	breast cancer antigen
BSA	bovine serum albumin
BV421	Brilliant Violet™ 421
C_H	constant heavy chain
C_L	constant light chain
CAIX	carbonic anhydrase IX
CAR	chimeric antigen receptor
CD3	cluster of differentiation 3
CD3ζ	CD3 zeta chain
CD8	cluster of differentiation 8
CD20	cluster of differentiation 20
CD107a	cluster of differentiation 107a
CDC	complement-dependent cytotoxicity
cDNA	complementary deoxyribonucleic acid
CDR	complementarity determining region
CEA	carcinoembryonic antigen
CLL	chronic lymphocytic leukaemia
CMV	cytomegalovirus
CRS	cytokine release syndrome
CTL	cytotoxic T-lymphocyte
CTLA-4	cytotoxic T-lymphocyte-associated antigen 4
DiBsAb	dimeric bispecific antibody
DMEM	Dulbecco's modified Eagle's medium
DMSO	dimethyl sulphoxide
DNA	deoxyribonucleic acid

dNTP	deoxyribonucleotide triphosphate
E. coli	*Eschericia coli*
EF-1α	elongation factor-1α
EGFR	epidermal growth factor receptor
EGFRvIII	epidermal growth factor receptor variant III
ELISA	enzyme-linked immunosorbent assay
ELISpot	enzyme-linked immunospot assay
ER	endoplasmic reticulum
ERK	extracellular signal-regulated kinase
Fab	fragment antigen-binding
FACS	fluorescence activated cell sorting
FBS	foetal bovine serum
Fc	fragment crystallisable
FcγRIIIa	Fcγ receptor IIIa
FcγRIIb	Fcγ receptor IIIb
FDA	Food and Drug Administration
FITC	fluorescein isothiocyanate
FPLC	fast protein liquid chromatography
GFP	green fluorescent protein
GMP	good manufacturing practice
gp100	glycoprotein 100 (also PMEL)
H&E	haematoxylin and eosin
HER2	human epidermal growth factor receptor 2 (also neu or ErbB2)
HHD	human HLA-A2 transgenic mouse
hIgG1	human IgG1
HLA	human leukocyte antigen
HNSCC	head and neck squamous cell carcinoma
HPV	human papilloma virus
HRP	horseradish peroxidase
IEDB	Immune Epitope Database
IFN-γ	interferon-γ
Ig	immunoglobulin
IgG	immunoglobulin G
IHC	immunohistochemistry
IL-2	interleukin-2
ImmTAC	immune-mobilising monoclonal TCRs against cancer
INN	international non-proprietary name
IPTG	isopropyl β-D-1-thiogalactopyranoside
ITAM	immunoreceptor tyrosine-based activation motif
JNK	c-Jun N-terminal kinase
kb	kilobase
K_D	dissociation constant
LAMP	lysosomal associated membrane glycoprotein
LB	Luria-Bertani
LMP2A	latent membrane protein 2A
LSLB	low salt Luria-Bertani

mAb	monoclonal antibody
MAGE-A1	melanoma associated antigen 1
MAGE-A3	melanoma associated antigen 3
MART-1	melanoma antigen recognised by T cells-1
MFI	mean fluorescence intensity
MHC-I	major histocompatibility complex class I
mRNA	messenger RNA
NF-κB	nuclear factor-κB
NFAT	nuclear factor of activated T cells
NHL	non-Hodgkin's lymphoma
NK cell	natural killer cell
NSCLC	non-small cell lung cancer
NY-ESO-1	New York esophageal squamous cell carcinoma-1
OD	optical density
ORF	open reading frame
p53GLA	$p53_{187-197}$ peptide GLAPPQHLIRV
p53RMP	$p53_{65-73}$ peptide RMPEAAPPV
PAGE	polyacrylamide gel electrophoresis
PASD1	PAS domain-containing protein 1
PBMCs	peripheral blood mononuclear cells
PBS	phosphate buffered saline
PCR	polymerase chain reaction
PD-1	programmed cell death 1
PD-L1	programmed cell death 1 ligand 1
PE	phycoerythrin
PE38	38 kDa Pseudomonas exotoxin
pHLA	peptide-HLA
PMA	phorbol 12-myristate 13-acetate
pMHC	peptide-MHC-I
PR1	pathogenesis-related protein 1
PS-SCL	positional scanning synthetic combinatorial peptide library
PTK	protein tyrosine kinase
RCC	renal cell carcinoma
RNA	ribonucleic acid
rpm	revolutions per minute
RPMI	Roswell Park Memorial Institute
scFv	single chain variable fragment
SD	standard deviation
sdAb	single domain antibody
SDS	sodium dodecyl sulphate
SDS-PAGE	sodium dodecyl sulphate polyacrylamide gel electrophoresis
SOC	super optimal broth with catabolite repression
SV40	simian virus 40
T1-116CV1	T1-116C humanised antibody variant 1
T1-116CV2	T1-116C humanised antibody variant 2
TAA	tumour-associated antigen

TAE	Tris base, acetic acid and EDTA
TAP	transporter of antigen processing
TB	Terrific Broth
TCR	T-cell receptor
TCRm	T-cell receptor mimic antibody
TERT	telomerase reverse transcriptase
TK-	thymidine kinase negative
TP53	tumour protein 53
TSA	tumour-specific antigen
Tyr	tyrosinase
V_H	variable heavy chain
V_L	variable light chain
VEGF	vascular endothelial growth factor
VEGFR	vascular endothelial growth factor receptor
VSV-G	vesicular stomatitis virus G glycoprotein
WBCs	white blood cells
wt	wild type
WT1	Wilms tumour 1
Zap70	zeta chain of T-cell receptor associated protein kinase 70kDa

1 Introduction

1.1 Antibody immunotherapy in cancer

Cancer is one of the leading causes of death in the UK and worldwide. In 2016, 28% of all deaths in the UK were attributed to cancer (CRUK). Cancer can be caused by environmental and genetic factors, and it encompasses a range of diseases that affect many different tissue types in the body. As a result of this, there is no universal cancer therapy that is suitable for all patients. Surgery, radiotherapy, and chemotherapy were the first cancer therapies, which were initially used in the 20th Century (DeVita & Chu, 2008). They continue to form a significant part of the standard treatment regimen for cancer today. However these treatments have low efficacy and are associated with tumour recurrence; for example surgery is ineffective at eradicating cancer in patients with metastases that will go on to propagate the cancer. There are also side effects associated with radiotherapy and chemotherapy, which target rapidly dividing cells in the body with inadequate differentiation between normal and cancer cells, causing undesirable damage to healthy tissues. The limitations of these treatments and the rise in cancer incidence and mortality call for alternative therapies with superior efficacy.

Monoclonal antibodies (mAbs), a form of passive immunotherapy, are therapeutic agents used for the treatment of cancer. In the late 19th century, antibodies were first discovered in immune sera and infused intravenously into patients for the

treatment of infectious disease, when their potential to treat disease was first recognised (Scott *et al.*, 2012a). Progress was made in the production of mAbs with the advent of inbred mice and hybridoma technology (Köhler & Milstein, 1975; Scott *et al.*, 2012b). However the early therapeutic use of mouse mAbs in patients resulted in undesirable immune responses to murine immunoglobulins (Blottière *et al.*, 1991). This led to the development of humanisation techniques, where most murine sequences (those not required for binding specificity) were replaced with their human counterparts, which enabled the generation of mAbs that elicit a minimal immune response, thereby revolutionising the field of therapeutic mAbs (Jones *et al.*, 1986). The structure of an antibody is depicted in Figure 1.1.

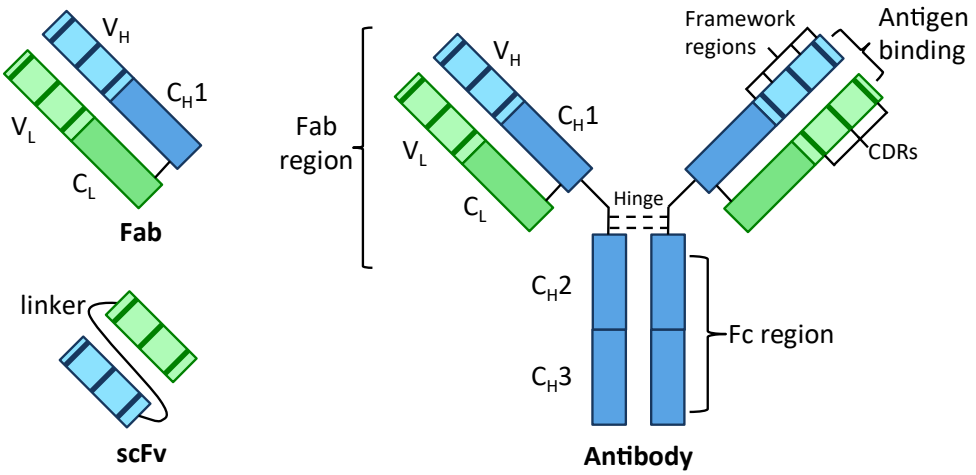

mAb type	Protein sequence	Nomenclature (example)
Murine	Fully murine	-o- (e.g. ibritumomab tiuxetan)
Chimeric	Human constant region with murine variable region	-xi- (e.g. rituximab)
Humanised	Human except for murine CDRs	-zu- (e.g. trastuzumab)
Human	Fully human	-u- (e.g. panitumumab)

Figure 1.1 – Antibody structure
The structure of an antibody is depicted with its component regions. mAbs consist of a heavy chain (C_H1-3 and V_H) and a light chain (C_L and V_L) sequence, where both chains have a constant (C) region and a variable (V) region. The antigen binding region constitutes the variable light (V_L) chain region and the variable heavy (V_H) chain region. Both the V_L and the V_H chains have three complementarity determining regions (CDRs), which bind to specific epitopes on the target. Framework regions surround the CDRs. The fragment crystallisable region (Fc region) is used to engage immune effector functions. The fragment antigen-binding (Fab) region can be used as an antigen-targeting moiety without the full mAb structure. A single chain variable fragment (scFv), which consists of the V_L and the V_H chains of a mAb linked by a flexible linker, can also be used alone to target antigens. The table summarises the characteristics of murine, chimeric, humanised and human mAb types. Diagram modified from Hansel *et al.*, 2010.

Following decades of research, mAbs have now become established cancer therapeutics, as well as being used for the treatment of other conditions, such as autoimmune and infectious disease (Casadevall, 1996). One of the first mAbs approved for cancer treatment was rituximab, which is a chimeric anti-CD20 mAb approved in 1997 for the treatment of follicular B-cell non-Hodgkin's lymphoma (NHL) (Oldham & Dillman, 2008). There are currently 29 Food and Drug

Administration (FDA)-approved mAbs targeting a variety of tumour antigens for the treatment of cancers and these are summarised in Table 1.1. Therapeutic mAbs continue to be developed for different conditions, and importantly, there are established methods for mAb manufacture, delivery, regulatory approval, and validated therapeutic mechanisms of action.

Table 1.1 – FDA–approved mAbs for cancer immunotherapy

INN (Commercial name; Company)	Target	Type	Isotype	Indication	Mode of action	First FDA approval date
Rituximab (Rituxan®; Genentech)	CD20	Chimeric	IgG1	NHL, CLL	ADCC; CDC; induction of apoptosis	26 Nov 1997
Trastuzumab (Herceptin®; Genentech)	HER2	Humanised	IgG1	Breast cancer, gastric cancer	Inhibition of HER2 signalling; ADCC	25 Sep 1998
Ibritumomab tiuxetan (Zevalin®; Spectrum Pharmaceuticals)	CD20	Murine	IgG1	NHL	Delivery of the radioisotope yttrium-90 (^{90}Y)	19 Feb 2002
Cetuximab (Erbitux®; Eli Lilly)	EGFR	Chimeric	IgG1	Metastatic colorectal cancer, head and neck cancer	Receptor antagonist inhibits EGFR signalling; ADCC	12 Feb 2004
Bevacizumab (Avastin®; Genentech)	VEGF	Humanised	IgG1	Metastatic colorectal cancer, NSCLC, glioblastoma, renal cell carcinoma, cervical cancer, ovarian cancer	Inhibition of VEGF signalling	26 Feb 2004
Panitumumab (Vectibix®; Amgen)	EGFR	Human	IgG2	Metastatic colorectal cancer	Inhibition of EGFR signalling	27 Sep 2006
Ofatumumab (Arzerra®; GlaxoSmithKline)	CD20	Human	IgG1	CLL	ADCC; CDC	26 Oct 2009
Ipilimumab (Yervoy®; Bristol-Myers Squibb)	CTLA-4	Human	IgG1	Metastatic melanoma, renal cell carcinoma, metastatic colorectal cancer	Inhibition of CTLA-4 signalling (Immune check point inhibitor)	25 Mar 2011
Brentuximab vedotin (Adcetris®; Seattle Genetics Inc.)	CD30	Chimeric ADC	IgG1	Hodgkin lymphoma, anaplastic large cell lymphoma, mycosis fungoides	Delivery of monomethyl auristatin E toxin (antimitotic agent)	19 Aug 2011

INN (Commercial name; Company)	Target	Type	Isotype	Indication	Mode of action	First FDA approval date
Denosumab (Xgeva®; Amgen)	RANKL	Human	IgG2	Treatment of bone loss in patients with bone metastases from solid tumours and MM	Binds RANKL and prevents its activating RANK (its receptor)	19 Sep 2011
Pertuzumab (Perieta®; Genentech)	HER2	Humanised	IgG1	Metastatic breast cancer	Inhibition of HER2 dimerisation and signalling	8 Jun 2012
Ado-trastuzumab emtansine (Kadcyla®; Genentech)	HER2	Humanised ADC	IgG1	Breast cancer	Inhibition of HER2 signalling; ADCC; delivery of cytotoxic drug, DM1	22 Feb 2013
Obinutuzumab (Gazyva®; Genentech)	CD20	Humanised	IgG1	CLL, follicular lymphoma	ADCC; induction of apoptosis	1 Nov 2013
Ramucirumab (Cyramza®; Eli Lilly)	VEGFR2	Human	IgG1	Gastric cancer, NSCLC, metastatic colorectal cancer	Receptor antagonist inhibiting angiogenesis	21 Apr 2014
Pembrolizumab (Keytruda®; Merck)	PD-1	Humanised	IgG4	Metastatic melanoma, non-squamous NSCLC, HNSCC, Hodgkin lymphoma, bladder cancer, gastric cancer	Immune check point inhibitor	4 Sep 2014
Blinatumomab (Blincyto®; Amgen)	CD19/ CD3 BiTE	Murine BiTE	scFV	ALL	Links T cells (via CD3) to malignant B cells (via CD19)	3 Dec 2014
Nivolumab (Opdivo®; Bristol-Myers Squibb)	PD-1	Human	IgG4	Metastatic melanoma, lung cancer, renal cell carcinoma, Hodgkin lymphoma, head and neck cancer, bladder cancer, colorectal cancer, hepatocellular carcinoma	Immune check point inhibitor	22 Dec 2014

INN (Commercial name; Company)	Target	Type	Isotype	Indication	Mode of action	First FDA approval date
Dinutuximab (Unituxin®; United Therapeutics)	GD2	Chimeric	IgG1	Paediatric high-risk neuroblastoma	ADCC; CDC	10 Mar 2015
Daratumumab (Darzalex®; Janssen Biotech)	CD38	Human	IgG1	Multiple myeloma	ADCC; CDC; ADCP; induction of apoptosis	16 Nov 2015
Necitumumab (Portrazza®; Eli Lilly)	EGFR	Human	IgG1	Metastatic squamous NSCLC	Receptor antagonist blocking EGFR signalling	24 Nov 2015
Elotuzumab (Empliciti®; Bristol-Myers Squibb)	SLAMF7	Humanised	IgG1	Multiple myeloma	Natural killer cell activation; ADCC	30 Nov 2015
Atezolizumab (Tecentriq®; Genentech)	PD-L1	Humanised	IgG1	Metastatic NSCLC	Immune check point inhibitor	18 May 2016
Olaratumab (Lartruvo®; Eli Lilly)	PDGFRα	Human	IgG1	Soft tissue sarcoma	Inhibits signalling	19 Oct 2016
Avelumab (Bavencio®; EMD Serono)	PD-L1	Human	IgG1	Metastatic Merkel cell carcinoma	Immune check point inhibitor	23 Mar 2017
Durvalumab (Imfinzi®; AstraZeneca)	PD-L1	Human	IgG1	Urothelial carcinoma	Immune check point inhibitor	1 May 2017
Inotuzumab ozogamicin (Besponsa®; Pfizer)	CD22	Humanised ADC	IgG4	ALL	Delivery of calicheamicin toxin	17 Aug 2017
Gemtuzumab ozogamicin (Mylotarg®; Pfizer)	CD33	Humanised ADC	IgG4	AML	Delivery of calicheamicin toxin	1 Sep 2017

INN (Commercial name; Company)	Target	Type	Isotype	Indication	Mode of action	First FDA approval date
Moxetumomab pasudotox-tdfk (Lumoxiti®; AstraZeneca)	CD22	Murine; scFv with PE38 immunotoxin	scFv	Relapsed or refractory hairy cell leukaemia in adults	Delivery of truncated form of *Pseudomonas* exotoxin PE38	13 Sep 2018
Cemiplimab-rwlc (Libtayo®; Regeneron Pharma Inc.)	PD-1	Human	IgG4	Cutaneous squamous cell carcinoma	Immune check point inhibitor	28 Sep 2018

The antibodies that are currently approved by the FDA for cancer immunotherapy are listed in chronological order of approval. The international non-proprietary name (INN), the trade name and the manufacturing company of each mAb is listed. ADC – antibody-drug conjugate; ADCC – antibody-dependent cellular cytotoxicity; ADCP– antibody-dependent cellular phagocytosis; ALL – acute lymphocytic leukaemia; AML – acute myeloid leukaemia; BiTE – bispecific T-cell engager; CDC – complement-dependent cytotoxicity; CLL – chronic lymphocytic leukaemia; HNSCC – head and neck squamous cell carcinoma; MM – multiple myeloma; NHL – non-Hodgkin's lymphoma; NSCLC – non-small cell lung cancer; scFv – single chain variable fragment. Gemtuzumab ozogamicin was initially approved in 2000 for the treatment of AML, but withdrawn in 2010 because of safety concerns. It was approved again in 2017 for the treatment of patients with CD33+ AML. Table modified from https://www.antibodysociety.org.

The ideal target for cancer immunotherapies, such as mAbs, is a tumour-specific antigen (TSA), which is only expressed on cancer cells. However the availability of TSAs is limited, therefore therapies also target tumour-associated antigens (TAAs) (Neller *et al.*, 2008). TAAs are essentially self-antigens that are expressed on both normal cells and tumour cells, but certain differences in their molecular characteristics allow discrimination between healthy and malignant cells, for example their physiological expression may be restricted to early embryonic development, or they can be overexpressed or expressed at an aberrant location in tumour cells (Vigneron, 2015). Tumour antigens with wider therapeutic application are preferred target antigens for the development of novel cancer immunotherapies as described in a National Cancer Institute pilot project prioritising cancer antigens for translational research (Cheever *et al.*, 2009). Examples of tumour antigens are summarised in Table 1.2.

Table 1.2 – Tumour antigens for cancer immunotherapy

Antigen type	Characteristics	Example	Tumour type
Oncofoetal	Expressed in foetal tissues and somatic cancer cells	CEA	Colorectal
Oncoviral	Produced by tumorigenic viruses	HPV	Cervical
Cancer testis	Expressed in adult reproductive tissues and cancer cells	MAGE NY-ESO-1	Multiple: Breast, bladder, lung
Differentiation products	Expression confined mostly to a single cell type	Tyrosinase, Melan-A/MART-1, gp100/ pmel17	Melanoma

Antigen type	Characteristics	Example	Tumour type
Mutated gene products	Expression restricted to cancer cells due to genetic mutation	BRCA1/2 Ras p53	Breast, ovarian Multiple: Colon, breast, lung
Aberrant post-translational modification	Altered phosphorylation, glycosylation etc.	Mucin-1	Breast
Overexpressed	Expressed in normal and cancer cells, but expression very high in cancer cells	HER2/neu p53	Breast, ovarian Multiple
Angiogenesis targets	Growth factors or their receptors involved in tumour angiogenesis	VEGF VEGFR	Tumour vasculature
Idiotypic	Cancerous B or T cells expressing the same Ig or TCR clonotype	Ig TCR	Lymphoma, leukaemia, myeloma

Tumour antigens are listed according to their molecular features. Some antigens can belong to multiple categories. For example, the p53 protein can be both mutated and overexpressed in cancers, and so it can be classified as both. BRCA – breast cancer antigen; CEA – carcinoembryonic antigen; Her2/neu – human epidermal growth factor receptor 2; HPV – human papilloma virus; MAGE – melanoma associated antigen; MART-1 – melanoma antigen recognised by T cells-1; NY-ESO-1 – New York esophageal squamous cell carcinoma-1; VEGF – vascular endothelial growth factor; VEGFR – vascular endothelial growth factor receptor. The table is composed of information from the following references: Neller *et al.*, 2008, Vigneron, 2015, and Cheever *et al.*, 2009.

1.1.1 Mechanisms of action

mAbs have been shown to function through a variety of mechanisms (Figure 1.2). Some mAbs function by direct tumour cell killing via modulating the function of cell surface receptors. For example, trastuzumab functions by blocking the dimerisation of HER2 receptors, which in turn inhibits signalling that drives cell proliferation (Scott *et al.*, 2012a).

mAbs can engage the immune system to mediate cell killing through complement-dependent cytotoxicity (CDC), antibody-dependent cellular cytotoxicity (ADCC), antibody-dependent cellular phagocytosis (ADCP) and the regulation of T-cell

function (Scott *et al.*, 2012b). The Fc portion of mAbs is crucial for the initiation of CDC, ADCC and ADCP. CDC occurs through the classical complement pathway where the mAb-antigen complex is recognised by complement proteins, initiating the complement cascade, which results in tumour cell killing and the recruitment of immune effector cells, such as macrophages (Scott *et al.*, 2012b). Cognate Fc receptors on macrophages and natural killer (NK) cells can also bind to the Fc portion of mAbs, leading to phagocytosis of the target cells by macrophages (ADCP), or ADCC by NK cells. ADCC occurs when the Fc receptors on NK cells bind the Fc region of the mAbs bound to their target on a tumour cell. This interaction causes NK cells to release their cytotoxic granules, which contain perforin and granzyme B. The perforin will form pores in the membrane of the tumour cell for the entry of granzyme B, which initiates a caspase cascade that will ultimately result in apoptosis of the tumour cell (Scott *et al.*, 2012b). Rituximab is an example of an approved mAb that mediates some of its therapeutic effect through ADCC.

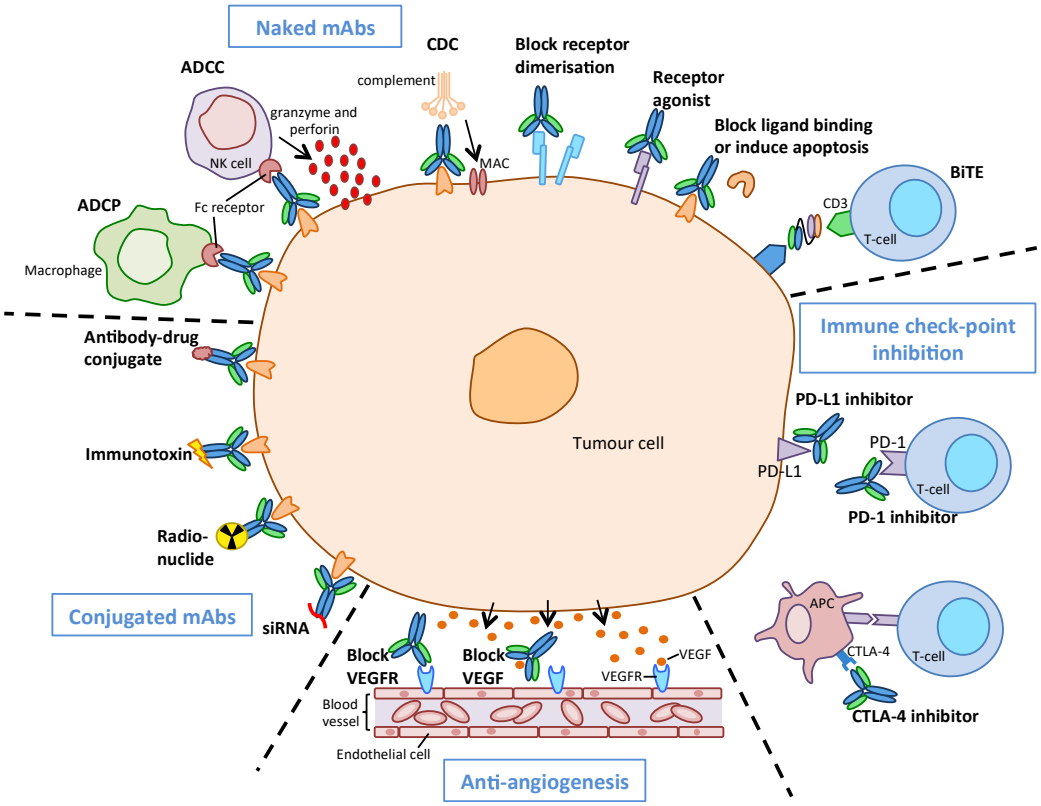

Figure 1.2 – mAb mechanisms of action.
The different mechanisms of action of mAbs are illustrated in four categories: naked mAbs, immune check-point inhibition, anti-angiogenesis and conjugated mAbs. mAbs can engage the immune system and mediate a therapeutic effect through ADCP, ADCC and CDC. mAbs can block receptor dimerisation or ligand binding to receptors. They can induce apoptosis or act as receptor agonists that activate cellular pathways. The scFv of two different mAbs can be joined by a linker to form a bispecific T-cell engager (BiTE), which links T cells to a tumour cell, thereby facilitating T-cell activation against the tumour cell. mAbs can enable direct cell killing by delivering a conjugated drug, toxin, radioisotope or small interfering RNA (siRNA) to a tumour cell. mAbs can inhibit immune checkpoints thereby enhancing anti-tumour immunity, and they can also inhibit angiogenesis in the tumour microenvironment, which has the effect of slowing tumour growth. ADCC – antibody-dependent cellular cytotoxicity; ADCP – antibody-dependent cellular phagocytosis; CDC – complement-dependent cytotoxicity; CTLA-4 – cytotoxic T-lymphocyte-associated antigen 4; MAC – membrane attack complex; PD-1 – programmed cell death 1; PD-L1 – programmed cell death 1 ligand 1; scFv – single chain variable fragment; VEGF(R) – vascular endothelial growth factor (receptor). Diagram modified from Weiner, 2015.

In addition to the tumour cells themselves, different cells within the tumour microenvironment can also be targeted using mAbs. mAbs can be used as immune modulators to directly activate T cells by blocking T-cell inhibitory receptors or their ligands such as programmed cell death 1 (PD-1), programmed cell death 1 ligand 1

(PD-L1) or cytotoxic T-lymphocyte-associated antigen 4 (CTLA-4). The latter is targeted by the approved mAb ipilimumab (Weiner, 2015). The tumour vasculature and stroma are also being studied extensively for their contribution to tumour growth and as potential targets for mAbs (Weiner, 2015). The approved mAb bevacizumab targets a soluble ligand, vascular endothelial growth factor (VEGF), which plays a role in tumour angiogenesis. By binding to VEGF, bevacizumab delays angiogenesis, thereby limiting the tumour blood supply and consequently limiting delivery of oxygen and nutrients that would enhance tumour growth (Ferrara *et al.*, 2004).

1.1.2 Limitations of mAb therapy

Despite the clinical successes of mAbs, there are some limitations to their efficacy and use. The generation of clinical-grade mAbs is associated with high production costs and is time-consuming and laborious; large-scale antibody synthesis requires the culturing of mammalian cells to substantial volumes, with multiple subsequent purification steps, while adhering to good manufacturing practice (GMP) conditions (Chames *et al.*, 2009). mAbs are also large proteins, which have a size of approximately 150kDa. Their large size is not a burden when mAbs circulate freely in the blood for the treatment of haematological malignancies. However, when mAbs have to penetrate tissues in order to access solid tumours, their large size can be a hindrance (Chames *et al.*, 2009). Heterogeneous tumour vasculature, leaky vessels and high interstitial fluid pressure impede the diffusion of mAbs, and thereby limit their therapeutic efficacy in solid tumours. Furthermore, mAbs are seldom used as

first-line treatments for cancer, and are predominantly administered in conjunction with chemotherapy and radiotherapy (Chames *et al.*, 2009). However the use of such therapies weakens the immune system that some mAbs depend on for their mechanism of action. Therefore the use of chemo- or radiotherapy with mAbs can be counterproductive by limiting the efficacy of mAbs. Side effects due to off-target binding with systemic circulation of mAbs have also been reported and include immune-related toxicities (Hansel *et al.*, 2010). The potential severity of adverse reactions when using mAbs was demonstrated in a first-in-human study of TGN1412, a CD28 superagonist mAb (Stebbings *et al.*, 2007). Administration of the mAb resulted in a severe cytokine-release syndrome (CRS) that led to the hospitalisation of the six human subjects that received the mAb in the study due to multiple organ failure (Hünig, 2012). No such toxicity had been identified in the preclinical models used for testing and the lessons learned from this trial have been used to improve their future safety.

An additional limitation of traditional mAbs, which is particularly relevant to this DPhil project, is their restricted repertoire of targetable antigens. Due to their large size, mAbs cannot cross the cell membrane and are therefore limited to targeting cell surface or soluble antigens (Scott *et al.*, 2012b). This is a disadvantage because there are many intracellular disease-associated antigens, which represent potential therapeutic targets. According to Polanski & Anderson, analysis of the subcellular distribution of 1261 cancer biomarkers showed that 41% are intracellular proteins. However as they are inaccessible to mAbs, they cannot be exploited (Polanski & Anderson, 2007). In order to overcome this inaccessibility, intracellular antibodies

(also referred to as intrabodies) have been developed. Intracellular antibodies can consist of an scFv, or their size can be minimised even further by using a single heavy chain or light chain variable region domain (intracellular domain antibodies). Extracellular immune effector mechanisms cannot be recruited by intracellular antibodies or by intracellular antibody fragments that lack an Fc region. They therefore mediate effector functions by directly neutralising their target, by targeting proteins within subcellular compartments (e.g. endoplasmic reticulum (ER) targeting to degrade the target protein) or inducing caspase activation and programmed cell death. Different methods have been investigated for the delivery of intracellular antibodies, some of which include: (i) a gene therapy-like approach that uses vectors to enable expression of the intracellular antibodies within the cell, or (ii) intracellular antibodies or DNA encoding the antibody can also be encapsulated in liposomes, nanoparticles or exosomes, which are targeted to a specific cell, where they are then internalised by endocytosis. More information on using antibodies to target intracellular proteins can be found in our published review (Trenevska *et al.*, 2017). An alternative strategy to overcome the inaccessibility of mAbs to intracellular antigens, which is the subject of this DPhil project, is to harness the major histocompatibility complex class I (MHC-I) peptide presentation pathway by using T-cell receptor mimic antibodies.

1.2 T-cell receptor mimic (TCRm) antibodies

There are several approaches for harnessing the MHC-I peptide presentation pathway for therapeutic purposes. These include the use of recombinant TCRs as

targeting agents, as well as the development of T-cell receptor mimic (TCRm) antibodies, which recognise MHC-I-presented peptides in a similar way to the TCR of CD8+ T cells.

The MHC-I peptide presentation pathway is an immune surveillance mechanism that enables the immune system to monitor whether cells are synthesising foreign or mutant proteins as a result of infection or cancer. Thus it enables the detection and subsequent elimination of infected or cancerous cells. Newly synthesised intracellular proteins are processed, through proteasome-dependent or proteasome-independent pathways, into peptides that are 8 to 11 amino acid residues long (Rock & Goldberg, 1999). These peptides are then loaded onto MHC-I molecules in the ER, and the peptide-MHC-I (pMHC) complex is transported to the cell surface, where it is displayed for recognition by the T-cell receptor (TCR) of CD8+ T cells (Rock & Goldberg, 1999) (Figure 1.3). The MHC-I molecule comprises a heterodimer of a heavy chain of three α domains and a light chain, β2-microglobulin (β2M). Under normal physiological conditions, the peptides presented on the cell surface by MHC-I are derived from normal autologous proteins that are not recognised by CD8+ T cells due to prior development of immune tolerance to self-antigens (Rock *et al.*, 2004). In contrast, if a cell is infected by a virus or if a cell expresses the protein product of mutant genes, MHC-I will display foreign peptides at the cell's surface for which there is no immune tolerance, triggering CD8+ T cells to kill the cell.

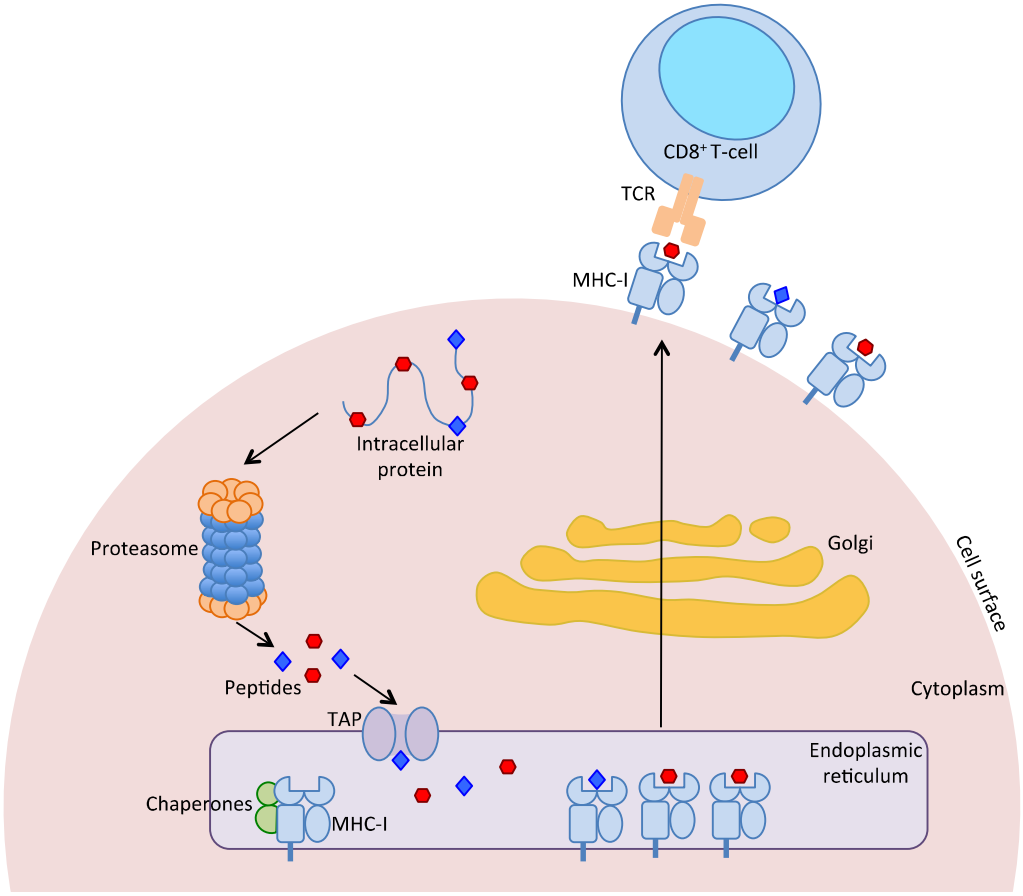

Figure 1.3 – MHC-I antigen presentation.
Intracellular proteins are processed into short peptides through the proteasome. The peptides enter the endoplasmic reticulum through the transporter of antigen processing (TAP), where they bind to the peptide-binding groove of MHC-I and stabilise the MHC-I molecule. The pMHC complex is then transported through the Golgi apparatus and presented on the cell surface. Once at the cell surface, the TCR of CD8+ T cells recognises the pMHC complex as part of the body's immune surveillance mechanism. Diagram modified from Yewdell *et al.*, 2003.

The following content in Section 1.2 is an excerpt, which has been modified and updated where necessary, from the published review that was predominantly written by the candidate: Trenevska I., Li D. and Banham A.H. (2017). Therapeutic antibodies against intracellular tumor antigens. *Frontiers in Immunology*, *8*, 1001.

TCRm antibodies (also referred to as TCR-like antibodies) target disease-associated pMHC complexes, and are similar to the TCR because their target epitope consists of both the peptide and the MHC-I molecule (Figure 1.4). Thus TCRm antibodies are distinctive from classical mAbs because they have a dual antigen epitope and their

binding is both peptide-specific and MHC-restricted (Weidanz *et al.*, 2011; Cohen & Reiter, 2013). They recognise peptides derived from intracellular proteins and so advantageously expand the mAb repertoire of targetable antigens to include intracellular proteins. Another advantage of TCRm antibodies is that they combine the intricate tumour specificity of TCRs with the biological properties of antibodies, which do not succumb to immune regulatory mechanisms that obstruct T-cell function in the tumour microenvironment (Dahan & Reiter, 2012). Like conventional mAbs, TCRm antibodies cause tumour killing through ADCC and CDC, as well as inducing apoptosis in breast cancer cells through a caspase-dependent pathway (Verma *et al.*, 2011; Li *et al.*, 2017a). In addition to successes using naked TCRm antibodies, there have also been reports of their anti-tumour activity when they are conjugated to toxins (Denkberg *et al.*, 2003; Klechevsky *et al.*, 2008). The ability of TCRm mAbs to target intracellular antigens has also been applied to cellular therapies in the development of chimeric antigen receptor (CAR) T cells (Oren *et al.*, 2014; Zhang *et al.*, 2014).

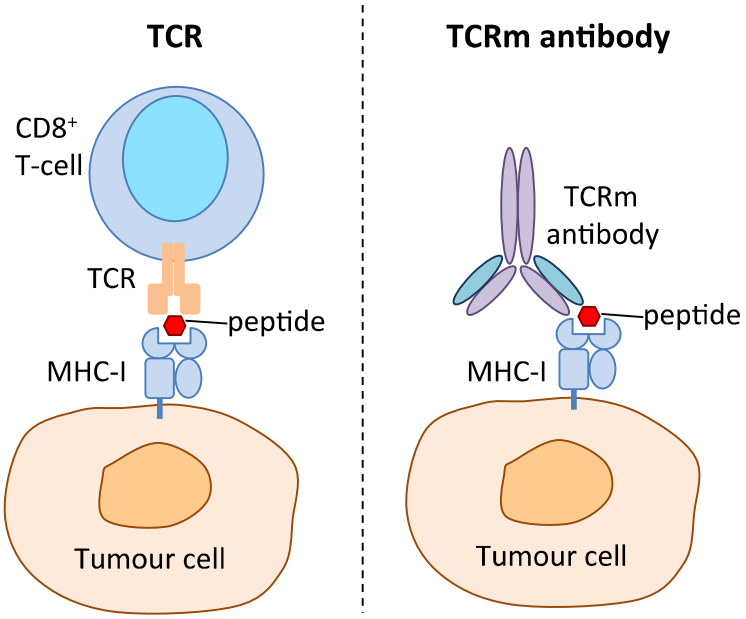

Figure 1.4 – TCR and TCRm antibody target recognition.
The diagram highlights that the TCR of CD8+ T cells and TCRm antibodies both recognise pMHC complexes on the cell surface in a similar way.

1.2.1 TCRm antibodies published to date

While TCRm antibodies can be used for therapeutic purposes, they are also widely used as research tools for the study of antigen presentation and recognition, as well as for structural studies. Further to this, there is potential to use them as theranostics, which combine diagnostic utility to determine target epitope presentation and therapeutic activity within a single agent. Some of the TCRm antibody therapeutics have shown promise in both *in vitro* and *in vivo* studies, however none of them have advanced to clinical studies as yet. The target peptides of such reagents are typically derived from either viral antigens (including HIV and Hepatitis B antigens) or cancer antigens, and they are commonly presented by either the HLA-A*0201 or the HLA-A*2402 MHC-I haplotype (Sastry *et al.*, 2011). The cancer-targeting TCRm antibodies published to date are summarised in Table 1.3.

Table 1.3 - TCRm antibodies for cancer immunotherapy

Target	Epitope sequence	MHC haplotype	TCRm antibody name	Isotype/ format	Cancer indications investigated	Isolation method	Reference
MAGE-A1	EADPTGHSY	HLA-A*0101	Fab-G8	Fab	Melanoma	Phage	(Chames *et al.*, 2000)
hTERT	ILAKFLHWL	HLA-A*0201	4A9, 4G9	Fab	Melanoma, prostate	Phage	(Lev *et al.*, 2002)
hTERT	RLVDDFLLV	HLA-A*0201	3H2, 3G3	Fab	Melanoma, prostate	Phage	(Lev *et al.*, 2002)
GP100	KTWGQYWQV	HLA-A*0201	G2D12, G3G4	Fab	Melanoma	Phage	(Denkberg *et al.*, 2002)
GP100	IMDQVPFSV	HLA-A*0201	1A9, 1C8, 1A11, 1A7	Fab	Melanoma	Phage	(Denkberg *et al.*, 2002)
GP100	YLEPGPVTV/A	HLA-A*0201	2F1, 2B2, 2C5, 2D1	Fab	Melanoma	Phage	(Denkberg *et al.*, 2002)
MAGE-A1	EADPTGHSY	HLA-A*0101	Fab-Hyb3	Fab	Melanoma	Phage	(Chames *et al.*, 2002)
MUC1	LLLTVLTVV	HLA-A*0201	M2F5, M3A1, M3B8, M3C8	Fab	Breast	Phage	(Cohen *et al.*, 2002)
GP100	IMDQVPFSV	HLA-A*0201	G1	scFv-PE38	Melanoma	Phage	(Denkberg *et al.*, 2003)
NY-ESO-1	SLIMWITQC	HLA-A*0201	3M4E5	Fab	Melanoma	Phage	(Held *et al.*, 2004)
MAGE3	FLWGPRALV	HLA-A*0201	7D4, 8A11, 2G12, 9E6	-	-	Hybridoma	(Bernardeau *et al.*, 2005)
hCGβ	GVLPALPQV	HLA-A*0201	3.2G1/RL4B	mIgG2a	Ovarian, colon, breast	Hybridoma	(Wittman *et al.*,2006; Verma *et al.*, 2010a;)

Target	Epitope sequence	MHC haplotype	TCRm antibody name	Isotype/ format	Cancer indications investigated	Isolation method	Reference
Her2/Neu	KIFGSLAFL	HLA-A*0201	1B8	IgG1	Breast, colon	Hybridoma	(Weidanz *et al.*, 2006)
MART-1/Melan-A	EAAGIGILTV/ ELAGIGILTV	HLA-A*0201	-	Fab	Melanoma	Phage	(Held *et al.*, 2007)
TARP	FLRNFSLML	HLA-A*0201	Fab D2	Fab-PE38	Breast, prostate	Phage	(Epel *et al.*, 2008)
hCGβ	GVLPALPQV	HLA-A*0201	1B10	IgG1	-	Hybridoma	(Neethling *et al.*, 2008)
hCGβ	TMTRVLQGV	HLA-A*0201	3F9	IgG1	-	Hybridoma	(Neethling *et al.*, 2008)
MART-1/Melan-A	EAAGIGILTV	HLA-A*0201	CAG10, CLA12	Fab-PE38	Melanoma	Phage	(Klechevsky *et al.*, 2008)
Tyrosinase	YMDGTMSQV	HLA-A*0201	TA2	Fab	Melanoma	Phage	(Michaeli *et al.*, 2009)
p68	YLLPAIVHI	HLA-A*0201	RL6A	mIgG2a	Breast	Hybridoma	(Verma *et al.*, 2010b)
Proteinase 3	VLQELNVTV	HLA-A*0201	8F4/ h8F4-CAR	IgG2a/ scFv for CAR	AML	Hybridoma	(Sergeeva *et al.*,2011; Ma *et al.*, 2016;)
MIF	FLSELTQQL	HLA-A*0201	RL21A	IgG2a	Breast	Hybridoma	(Hawkins *et al.*, 2011)
WT1	RMFPNAPYL	HLA-A*0201	ESK1/ ESK1-BiTE	hIgG1/ scFv for BiTE	Mesothelioma, leukaemia, ovarian, colon	Phage	(Dao *et al.*, 2013; Dao *et al.*, 2015)
GP100	ITDQVPFSV	HLA-A*0201	GPA7	sdAb/CAR	Melanoma	Phage	(Zhang *et al.*, 2014)

Target	Epitope sequence	MHC haplotype	TCRm antibody name	Isotype/ format	Cancer indications investigated	Isolation method	Reference
HA-1H	VLHDDLLEA	HLA-A*0201	#131	scFv	Leukaemia	Phage	(Inaguma *et al.*, 2014)
WT1	RMFPNAPYL	HLA-A*0201	F2, F3	Fab	-	Phage	(Oren *et al.*, 2014)
WT1	RMFPNAPYL	HLA-A*0201	Clone45	scFv	Leukaemia	Phage	(Zhao *et al.*, 2015)
MAGE-A1	EADPTGHSY	HLA-A1	Fab-Hyb3, Fab-G8	scFv coupled to liposomes	Melanoma	Phage	(Saeed *et al.*, 2016)
p53	RMPEAAPPV	HLA-A*0201	T1-116C	IgG1	Breast	Hybridoma	(Li *et al.*, 2017a)
p53	GLAPPQHLIRV	HLA-A*0201	T2-108A, T2-2A, T2-116A	IgG1, IgG2a, IgG1	-	Hybridoma	(Li *et al.*, 2017b)
p53	RMPEAAPPV	HLA-A*0201	T1-29D, T1-84C	IgG1, IgG2b	-	Hybridoma	(Li *et al.*, 2017b)
RNA helicase p68	YLLPAIVHI	HLA-A*0201	YLL-Ab labelled with saporin or duocarmycin (ADC)	mIgG (isotype not specified)	Breast, colon	Hybridoma	(Lowe *et al.*, 2017)
HER2/neu	KIFGSLAFL	HLA-A*0201	KIF-Ab labelled with saporin or duocarmycin (ADC)	mIgG (isotype not specified)	Breast	Hybridoma	(Lowe *et al.*, 2017)
MIF	FLSELTQQL	HLA-A*0201	FLS-Ab labelled with saporin or duocarmycin (ADC)	mIgG (isotype not specified)	Breast, colon	Hybridoma	(Lowe *et al.*, 2017)
CEA	YLSGADLNL	HLA-A*0201	YLSG-Ab1 to -Ab6 labelled with duocarmycin (ADCs)	YLSG-Ab1,2,4,6 are IgG1; YLSG-Ab3,5 are IgG2b	Colon	Hybridoma	(Lowe *et al.*, 2017)
PRAME	ALYVDSLFFL	HLA-A*0201	Pr20, Pr20M	hIgG1	Leukaemia, lymphoma, melanoma, breast, colon	Phage	(Chang *et al.*, 2017)

Target	Epitope sequence	MHC haplotype	TCRm antibody name	Isotype/ format	Cancer indications investigated	Isolation method	Reference
LMP2A	CLGGLLTMV	HLA-A*0201	Clones 26, 38, 40, 61 and clone 38-2	hIgG1, DiBsAb	EBV-related malignancies	Phage	(Ahmed *et al.*, 2018)

Published TCRm antibodies targeting cancer antigens are listed. ADC – antibody-drug conjugate; AML – acute myeloid leukaemia; CAR – chimeric antigen receptor; DiBsAb – dimeric bispecific antibody; EBV – Epstein-Barr virus; Fab – fragment antigen-binding; hIgG1 – human IgG1; PE38 – 38 kDa immunotoxin, which is a truncated form of *Pseudomonas* exotoxin; scFv – single chain variable fragment; sdAb – single domain antibody that has a single antigen-binding domain. Table updated from Trenevska *et al.*, 2017.

1.2.2 Selecting TCRm antibody targets

The ideal target for a TCRm antibody would be a disease-specific pMHC complex that is presented at high density on the target cell surface, while being absent from normal cells. As for traditional mAbs, the tumour antigens in Table 1.2 are also potential therapeutic targets for TCRm antibodies; for example peptides from mutated, overexpressed and oncofoetal proteins are potential TCRm antibody targets (Warren & Holt, 2010). The target peptides must have a high affinity for the patient's MHC and form a stable complex that persists on the cell surface, allowing recognition by TCRm antibodies. It is important to consider that it is the presentation of the epitope, and not expression of the antigen, that will determine the availability of antibody binding sites. Peptides undergo various steps of processing from their original protein before being presented on MHC-I. Therefore the level of protein expression and its half-life, the rate of peptide processing, MHC-I levels and the presentation of the peptide by MHC-I can all affect the epitope density at the cell surface. Proteins must be stable and translated in sufficient quantities to allow peptide processing, and it has been shown that overexpressed proteins with shorter half-lives are more likely to be presented than ones with longer half-lives (Bassani-Sternberg *et al.*, 2015).

Furthermore, it has been reported that tumours can downregulate their surface MHC expression as an immune evasion mechanism, suggesting that such tumours will be less susceptible to TCRm therapy (Khanna, 1998; Angell *et al.*, 2014). The possibility of this evasion mechanism must be considered when selecting both target

antigens and disease indications. Targeting an antigen with a functional role in tumour biology will also help avoid loss of the antigen from the tumour cells under subsequent therapeutic selection pressure. In order to ensure the safety of TCRm antibodies, the expression of the targets on normal healthy tissues must be considered when developing these as therapeutics.

1.2.3 Challenges in TCRm antibody therapy

It is crucial that a TCRm antibody does not recognise MHC-I alone, as this molecule is found on most nucleated cells. Therefore a TCRm antibody must be specific for the pMHC complex containing the target peptide, which also highlights that it should not cross-react with other processed peptides that might be presented on normal tissues. As a TCRm antibody recognises only few amino acid residues in the peptide, it is crucial to assess which other processed peptides possess the same amino acids at those positions and whether these would pose any risk of TCRm cross-reactivity. The importance of this is exemplified in a clinical trial of an affinity-enhanced TCR, which targeted an epitope from the cancer testis antigen MAGE-A3 (Linette *et al.*, 2013). Following investigation of the cause of unexpected side effects of the therapy, it was discovered that the TCR also recognised an epitope on the unrelated protein Titin, which is expressed in cardiac tissue. The cardiac toxicity resulting from the recognition of Titin led to two patient deaths. This cross-reactivity was not observed in normal tissue screening and the Titin peptide was not conserved in mice. However, a limitation of the *in silico* screening by amino acid substitution that was used to identify the Titin cross-reactivity (Cameron *et al.*, 2013) is that it may identify

a wider variety of potentially cross-reactive peptides than can be functionally evaluated. Furthermore, even potentially cross-reactive peptides shown to bind MHC-I in T2 stabilisation assays may not be processed endogenously or presented on the cell surface in normal tissues.

1.3 Chimeric antigen receptor (CAR) T-cell therapy

Cellular therapies represent another immunotherapeutic strategy that has evolved into an exciting field of research since autologous tumour-infiltrating cells were successfully adoptively transferred into metastatic melanoma patients in the 1980s (Rosenberg *et al.*, 1988; Kolb *et al.*, 1990). Subsequent gene transfer techniques developed in the 1990s enabled the modification of T-cell specificity using TCRs or chimeric antigen receptors (CARs) (Sadelain *et al.*, 2017).

CARs are transmembrane recombinant TCR fusion proteins that endow T cells with new antigen specificity (Figure 1.5). The intracellular portion of the CAR is composed of the ζ chain of the CD3 complex (CD3ζ) that normally associates with the TCR to activate downstream intracellular signalling pathways. The transmembrane region of the CAR crosses the cell membrane and it is followed by a spacer that links the extracellular portion. The extracellular portion is commonly composed of an scFv derived from a mAb, which confers the targeting specificity of the CAR (Kuwana *et al.*, 1987; Brocker *et al.*, 1993; Eshhar *et al.*, 1993;). This description of a first generation CAR represents the earliest model of the synthetic receptor (Sadelain *et al.*, 2009). While first generation CARs successfully recognised their target antigen,

they exhibited weak T-cell responses and low persistence as a result of their poor signalling capacity (Brocker & Karjalainen, 1995; Gong *et al.*, 1999). Second generation CARs included a single costimulatory domain in the intracellular portion of the CAR, in addition to the CD3ζ chain. The costimulatory domain is typically derived from either CD28 or 4-1BB, and reinforces the signalling capacity of CAR-transduced T cells by enhancing their cytotoxicity, persistence and proliferation (Krause *et al.*, 1998; Maher *et al.*, 2002). Third generation CARs include two costimulatory domains in the intracellular portion of the CAR in addition to the CD3ζ chain. To date, second generation CARs have been studied most extensively and shown the greatest promise (Gross & Eshhar, 2016), culminating in the recent FDA approval of two CD19-targeting second generation CARs (Sadelain, 2017) (Table 1.4).

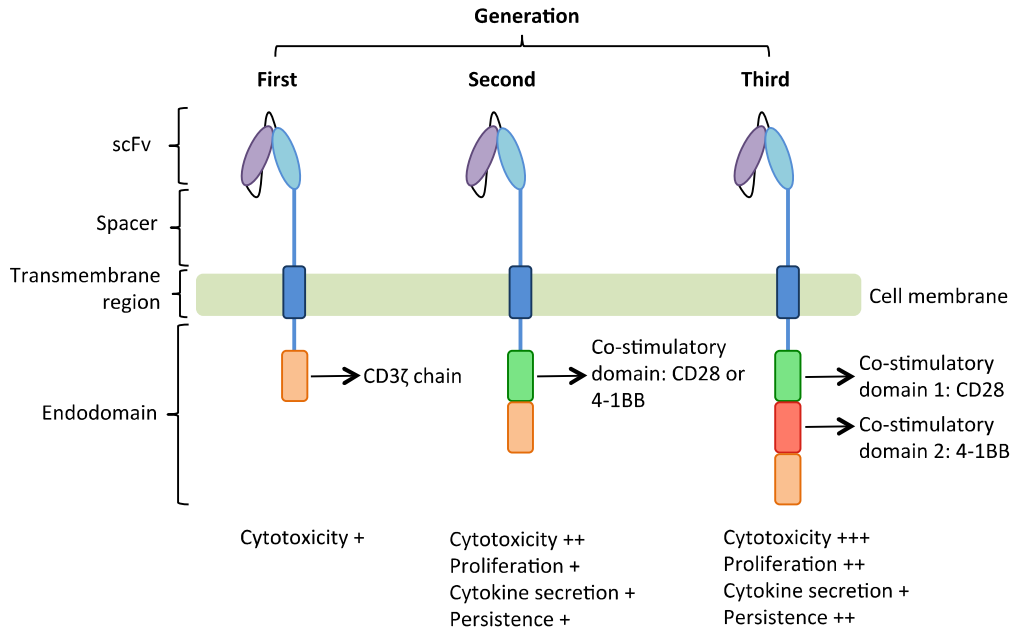

Figure 1.5 – CAR structure and generations.
CARs are composed of an scFv derived from a mAb, which provides the targeting moiety. There is a spacer region between the scFv and the transmembrane region. The endodomain of the three different generations of CARs has a CD3ζ activating domain, but they differ in the number of co-stimulatory domains present in the endodomain, which enhance the listed T-cell functions.

An advantage of CARs is that they use an scFv to direct their specificity, therefore CARs can also be MHC-independent when the targeting moiety is not provided by TCRs or TCRm antibodies (Gross & Eshhar, 2016). By incorporating an scFv, CARs also combine the fine specificity of mAbs with the potent functionality of T cells. Advantageously, CAR T cells can target low-density antigens where naked mAbs would not be effective. They also directly mediate their own cytotoxic effector functions upon target recognition, while many mAbs rely on recruiting host immune cells to mediate their therapeutic effect, which is not always effective in cancer patients who are immunocompromised.

Table 1.4 – FDA-approved CARs targeting CD19

INN; commercial name	Indication	Co-stimulatory domain	Company name; approval date
Tisagenlecleucel; Kymriah®	(i) B-cell ALL in children and young adults (ii) Relapsed/refractory large B-cell lymphoma in adults	4-1BB	Novartis; (i) August 2017 (ii) May 2018
Axicabtagene Ciloleucel; Yescarta®	Relapsed/refractory large B-cell lymphoma in adults	CD28	Kite Pharma/ Gilead; October 2018

CAR T-cell therapies were recently approved for the first time and are the first FDA-approved gene therapy. The two approved CAR T-cell therapies both target CD19, but have a different co-stimulatory region. INN – international non-proprietary name. Information in table summarised from Sadelain, 2017.

1.3.1 Anti-CD19 CAR T-cell therapy

CARs targeting the CD19 antigen have been the most extensively studied and were the first to be clinically approved. CD19 was selected as a target antigen because its expression in normal tissues is limited to the B-cell lineage, therefore any on-target

off-tumour toxicity would be restricted to B-cell aplasia (Gross & Eshhar, 2016). Although this is an undesirable side effect, it can be managed clinically with immunoglobulin (Ig) replacement therapy. CD19 is frequently expressed in B-cell leukaemias and lymphomas, and will therefore have wide clinical applicability (Gross & Eshhar, 2016). In comparison to other potential B-cell targets (such as CD20 and CD22), CD19 has broader and higher expression, which makes it a more attractive target for haematological malignancies (Brentjens *et al.*, 2003; Lebien & Tedder, 2008). Finally, CARs are more efficient at achieving clinical responses in haematological cancers than in solid tumours, therefore CD19 represented an ideal platform to further the development of CAR T-cell therapy and advance its application to other target antigens.

CAR T-cell therapy is a personalised therapy that is administered through adoptive cell transfer (Figure 1.6). Clinical trial data showed remarkable responses in paediatric and adult patients with relapsed or refractory NHL, CLL and ALL (Kochenderfer *et al.*, 2010; Porter *et al.*, 2011; Brentjens *et al.*, 2013). Larger studies were performed to validate the initial findings, and they showed similar results, with the most striking finding being the durable nature of the clinical responses in patients with no alternative treatment options (Maude *et al.*, 2018; Park *et al.*, 2018). Clinical findings have helped improve the design of CARs by demonstrating that mouse sequences in the CAR can activate the host immune system, leading to CAR T-cell rejection and limited clinical responses. The use of fully human CAR sequences correlated with better relapse-free survival in leukaemia patients because

the absence of immunogenicity presented by murine sequences allowed improved CAR T-cell persistence (Sadelain *et al.*, 2017).

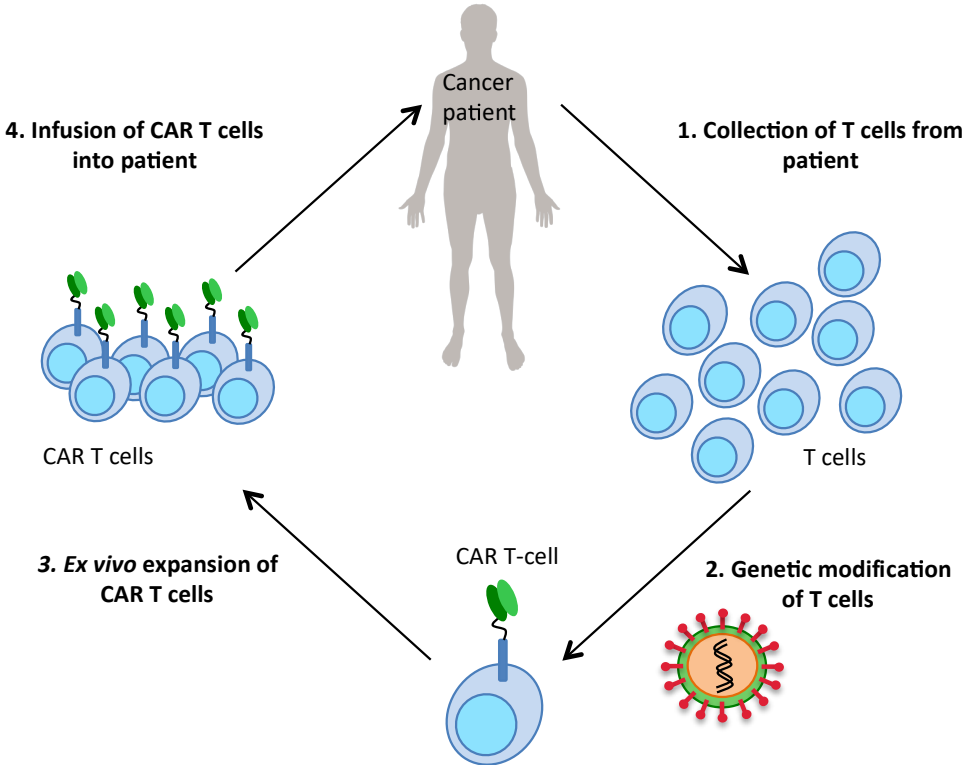

Figure 1.6 – Adoptive cell transfer for CAR T-cell therapy.
T cells are collected from the cancer patient and they are transduced with a viral vector that encodes the CAR. The genetically modified CAR T cells are expanded *ex vivo* and they are then infused into the patient for therapy.

1.3.2 Challenges in CAR T-cell therapy

The use of CAR T cells to treat solid tumours remains a major challenge (Rosenberg, 2014). There is evidence that T cells have the capacity to eradicate solid tumours as shown by infusions of tumour-infiltrating lymphocytes in advanced cancers, such as melanoma, as well as responses being observed to immune checkpoint therapy (Rosenberg *et al.*, 1988; Postow *et al.*, 2015). CAR T cells targeting solid tumours are faced with obstacles presented by the tumour microenvironment, such as interstitial

pressure and irregular blood vessels that limit their homogeneous access to the entire tumour (Rosenberg, 2014). Heterogeneous antigen expression between cancer cells within the tumour also limits the efficacy of therapy (Rosenberg, 2014). Thus the availability and selection of suitable target antigens for CAR T-cell therapy is perhaps one of the most critical factors that delays the expansion of CAR T-cell therapy beyond haematological malignancies.

Target selection is crucial in limiting on-target off-tumour toxicity, and it determines the therapeutic safety and success of a CAR (Sadelain *et al.*, 2017). It is essential to consider the tissue distribution of a candidate antigen and to evaluate the potential for toxicity due to on-target recognition of the same antigen on normal cells (Rosenberg, 2014). The safety risk posed by CAR T-cell therapy was exemplified in a clinical study targeting the transmembrane carbonic anhydrase IX (CAIX) antigen in renal cell carcinoma (RCC). CAIX is also expressed on epithelial cells in bile ducts, where cross-reactivity with these healthy cells resulted in toxicity (Lamers *et al.*, 2006; Lamers *et al.*, 2013). Similarly, a CAR targeting Her 2 (neu/ErbB2) reacted with the low level expression of Her2 in cardiopulmonary epithelia, causing severe on-target off-tumour toxicity that resulted in a fatality and early termination of the clinical trial (Morgan *et al.*, 2010).

The toxicity caused by on-target off-tumour CAR T-cell activity for B-cell antigens, such as CD19, can lead to B-cell aplasia (Lebien & Tedder, 2008). CARs can also cause CRS (Davila *et al.*, 2014; Maude *et al.*, 2014), which can be fatal and is characterised by increased serum cytokine levels, fever, neurological toxicities, hypotension and

hypoxia (Davila *et al.*, 2014; Lee *et al.*, 2014; Teachey *et al.*, 2016). CRS correlates with CAR T-cell activation causing elevated levels of cytokines, such as IL-6. This is typically controlled using an anti-IL-6 receptor antagonist mAb (tocilizumab) that has been approved for use in CAR T-cell-induced CRS (Grupp *et al.*, 2013; Davila *et al.*, 2014).

Various strategies are being investigated to increase the safety of CARs. For example, combinatorial antigen recognition by two CARs (one with the intracellular activation domain, and the second with the co-stimulation domain) requires the presence of two target antigens on a tumour cell in order to activate complete CAR T-cell activation (Gross & Eshhar, 2016). Alternatively, in the inhibitory CAR approach, T cells co-express an activating CAR (targeting a tumour antigen) and an inhibitory CAR (targeting a normal antigen), which has a T-cell inhibitory signalling domain. The inhibitory CAR impedes CAR T-cell activation when both the activating and inhibitory CARs engage their targets (Gross & Eshhar, 2016). Additionally, suicide genes can accompany CAR genes and they can be used to eliminate CAR T cells when necessary (Gross & Eshhar, 2016). Examples include the suicide gene that encodes the herpes simplex virus (HSV) thymidine kinase, which phosphorylates the prodrug ganciclovir (a guanosine analogue); this strategy blocks DNA replication and ultimately results in cell death (Bonini *et al.*, 1997). Another example is the inducible caspase 9 gene, which encodes a fusion polypeptide of: (i) a truncated human caspase 9, and (ii) a mutated protein that binds the nontoxic FK506 drug (Straathof *et al.*, 2005; Di Stasi *et al.*, 2011). Once the FK506 drug is administered, it binds to the mutated FK506-binding protein and leads to dimerisation of the fusion polypeptides, which is

required in order to initiate apoptosis. Thus both methods require the administration of a drug, in addition to the presence of the suicide gene, and thereby allow selective elimination of CAR T cells.

The cost associated with the development and administration of CAR T-cell therapy is a disadvantage (Sadelain, 2017). For the currently FDA-approved CAR T-cell therapies, Kymriah is estimated to cost $475,000 per treatment, while Yescarta is slightly cheaper, at $373,000 per treatment (Vormittag *et al.*, 2018). Compared to mAbs, the cost of CAR T-cell therapy is significantly higher and remains an obstacle to its wider clinical application. To address this, researchers are endeavouring to develop "universal" CAR T cells, which are intended to serve as an off-the-shelf therapy that can be applied to any patient. Gene-editing techniques (Qasim *et al.*, 2017) or T cells generated from human embryonic stem cells and induced pluripotent stem cells, could be useful in the development of such off-the-shelf CAR T cells with appropriate histocompatibility that do not trigger immune rejection (Themeli *et al.*, 2015).

1.4 p53 as a target antigen for cancer immunotherapy

The p53 protein, encoded by the *TP53* gene, is a transcription factor that controls a variety of biological processes, including the cell cycle, DNA repair, metabolism, apoptosis and senescence (Vogelstein *et al.*, 2000). Germline mutations in *TP53* lead to the development of Li-Fraumeni syndrome, which is a rare autosomal dominant condition that causes a predisposition to cancer (Li & Fraumeni, 1969a; Li &

Fraumeni, 1969b). As one of the key characteristics of many cancer cells is uncontrolled cell growth, the ability of p53 to stop progress through the cell cycle is critical for tumour suppression (Vogelstein *et al.*, 2000). The *TP53* gene is expressed at low levels in normal cells, however it is mutated in approximately 50% of human malignancies, where there is increased expression of the mutated p53 protein and aberrant p53 function (Freed-Pastor & Prives, 2012). 80% of the *TP53* mutations in cancer are missense mutations, which produce a full-length mutated p53 protein that has a prolonged half-life and increased stability (Strano *et al.*, 2007). Hotspot missense mutations have been found in the *TP53* gene, which define residues that are mutated at a higher frequency than would be expected to occur by chance. The hotspot residues are R175, G245, R248, R249, R273 and R282, and these six amino acids are mutated in multiple cancers at varying frequencies (Freed-Pastor & Prives, 2012). The three most frequent missense mutations at hotspot residues are: R175H (4.6% frequency), R248Q (3.5% frequency) and R273H (3.1% frequency), however these hotspot residues can also be mutated to other amino acids, increasing their mutational frequency further still (Freed-Pastor & Prives, 2012). Collectively, mutations at the six hotspot residues constitute almost one third of all *TP53* gene mutations (Freed-Pastor & Prives, 2012). The stable mutant p53 protein is usually more abundant than its wild type (wt) counterpart; it has the ability to impede the wt p53 protein in preventing cellular transformation and can lead to gain-of-function transformation. This is achieved by the formation of tetramers composed of both mutant and wt p53, wherein the mutant p53 protein exercises dominant negative inhibition of the wt p53 protein (Freed-Pastor & Prives, 2012). Due to its extensive

involvement in human oncogenesis, wt p53 has been prioritised as a target for cancer therapy by a National Cancer Institute pilot study (Cheever *et al.*, 2009).

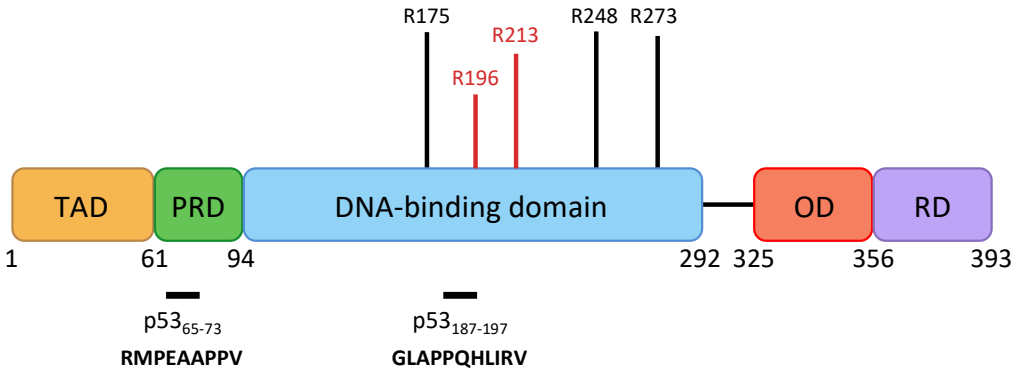

Figure 1.7 – p53 protein domains and common mutation locations.
The domains of the p53 protein, from the N-terminus to the C-terminus, are: the transactivation domain (TAD), the proline-rich domain (PRD), the DNA-binding domain, the oligomerisation domain (OD, also known as the tetramerisation domain), and the C-terminal regulatory domain (RD). Some of the most common mutations in the p53 protein are indicated above the schematic diagram of the protein: the three most common missense mutations are indicated in black, and the two most frequent nonsense mutations are indicated in red. The numbers below the schematic diagram indicate the amino acid positions. The positions of the peptides that are the subject of this thesis, $p53_{65\text{-}73}$ and $p53_{187\text{-}197}$, are also indicated, along with the amino acid sequence that they represent. $p53_{65\text{-}73}$ is located in the proline-rich domain, while $p53_{187\text{-}197}$ is located in the DNA-binding domain. Diagram modified from Joerger and Fersht, 2010.

1.4.1 Rationale for targeting wild type p53 rather than mutated p53 epitopes

Mutant p53-derived peptides would be ideal tumour antigens because they are TSAs that are not found in normal cells. However p53 mutations in cancer patients are extremely diverse, and as a consequence, mutant p53-targeted immunotherapies would be laborious, expensive and commercially not viable as they would require the sequencing of each patient's tumour to identify their specific mutation and the subsequent production of a personalised therapy (Offringa *et al.*, 2000; Theobald & Offringa, 2003). A further limitation is that not all mutated regions of p53 will form part of a peptide that can be processed and presented by MHC-I. This is

corroborated by the limited reports of mutant p53 T-cell epitopes (Yanuck *et al.*, 1993). Furthermore, this type of immunotherapy would be ineffective against tumours that overexpress wt p53 due to mutation or deregulation of proteins that regulate p53 expression levels and peptide presentation (Offringa *et al.*, 2000). For example, a mutated *TP53* allele was used in a DNA vaccine, which prevented growth of tumours presenting the mutated peptide, however the vaccine had no effect against tumours that presented other p53 mutants or overexpressed wt p53 (Humar *et al.*, 2009). Advantageously, directing immunotherapy at wt p53 epitopes enables the targeting of tumours that have aberrant p53 expression or function as a result of mutations in p53 at a position that does not affect the integrity of the wt epitope and mutations in proteins that regulate p53 levels, such as MDM2 and p14ARF, or due to viral oncogene expression, such as HPV (Theobald & Offringa, 2003).

In order to increase the applicability of p53-targeting cancer immunotherapies, focus has primarily been directed at wt p53 epitopes (Theobald, 1995; Vierboom *et al.*, 1997; Vierboom *et al.*, 2000; Kuball *et al.*, 2002; Kuckelkorn *et al.*, 2002). Humoural immune response studies in cancer patients have shown that both wt and mutant p53 epitopes can be recognised, and that mutant p53 does not contain immunodominant epitopes that would make it a more attractive target than wt p53 (Labrecque *et al.*, 1993). High copy numbers of wt p53-MHC-I complexes on cancer cells, in contrast to low copy numbers on normal cells, have been reported as a key difference between malignant and normal cells (Theobald *et al.*, 1998; Vierboom *et al.*, 2000; Kuckelkorn *et al.*, 2002). It is suggested that this is due to the increased turnover, and thereby the increased processing of p53 in tumours with modest

steady-state levels of expression. Thus it is p53 turnover, rather than high steady-state levels of p53, that dictates T-cell killing of tumour cells (Vierboom *et al.*, 2000). This is exemplified by a report where p53-specific T cells were able to recognise tumours without detectable p53 protein expression in patients with HPV infection, which is associated with increased p53 proteasomal degradation (Theoret *et al.*, 2008). There is evidence that wt p53-specific T cells can differentiate between tumour cells and normal cells that present p53 epitopes (Nijman *et al.*, 2005). Moreover, cytotoxic T lymphocytes (CTLs) and T-helper cells targeting wt p53 can not only recognise tumour cells presenting these peptides *in vitro*, but they can also kill target tumour cells *in vivo* (Vierboom *et al.*, 1997; Zwaveling *et al.*, 2002).

1.5 TCRm antibodies targeting wild type p53 peptides

Two patents, WO 2005/116072 and WO 2007/030451, describe a TCRm targeting the $p53_{264\text{-}272}$ peptide. However there are some disadvantages associated with targeting this peptide. Researchers have reported difficulties in detecting and producing cytotoxic T cells against the $p53_{264\text{-}272}$ epitope in cancer patients who display p53 accumulation, which has given rise to the speculation that there is aberrant processing and presentation of the $p53_{264\text{-}272}$ epitope in cancer patients (Hoffmann *et al.*, 2002; DeLeo *et al.*, 2008). This suggests that the $p53_{264\text{-}272}$ peptide may not be widely applicable and therefore is not an ideal target for cancer immunotherapy. Furthermore, the $p53_{264\text{-}272}$ peptide is C-terminal to the two most frequent non-sense *TP53* mutations, R196X and R213X. These mutations occur in approximately 8% of patients and cause premature termination of translation,

producing a p53 protein that is truncated at the C-terminus (Khoo *et al.*, 2014; Zhang *et al.*, 2018). Therefore patients with these mutations would not present the target $p53_{264-272}$ epitope and would be excluded from this therapy.

Thus there is demand for widely applicable p53-targeting TCRm antibodies that overcome the disadvantages of targeting the $p53_{264-272}$ peptide. Multiple wt p53 peptides have been studied for the purpose of developing vaccines. Some of these HLA-A2-restricted wt p53 peptides include $p53_{65-73}$, $p53_{149-157}$, $p53_{187-197}$, and $p53_{217-255}$ (DeLeo *et al.*, 2008; Nijman *et al.*, 2011).

Before the start of this DPhil project, TCRm antibodies were generated in our laboratory targeting wt p53-derived peptides ($p53_{65-73}$ and $p53_{187-197}$) presented by HLA-A2. Residues 65 to 73 of the human p53 protein represent the amino acid sequence RMPEAAPPV, while residues 187 to 197 represent the amino acid sequence GLAPPQHLIRV. These peptides have been previously described in the literature (Houbiers *et al.*, 1993; Nijman *et al.*, 1994; Barfoed *et al.*, 2000; Würtzen *et al.*, 2001). An advantage of targeting these wt p53 peptides is that they are N-terminal to the truncating p53 mutations R196X and R213X. Patients that have these mutations should still be able to present the $p53_{65-73}$ peptide (p53RMP peptide) and therefore be able to benefit from therapy with a TCRm mAb targeting the p53RMP peptide. The $p53_{187-197}$ peptide (p53GLA peptide) is also N-terminal to the R213X mutation, however it includes the arginine residue (R) at position 196 (R196) in its sequence, which means that R196X mutations fall within the p53GLA peptide sequence, potentially affecting its availability to therapeutic agents. Overall, TCRm

mAbs targeting p53RMP or p53GLA peptides have the potential for wider clinical applicability than ones targeting more C-terminal peptides, and their applicability is also maximised by targeting peptides that are presented by HLA-A2, which is one of the more common HLA haplotypes.

The TCRm production protocol used to generate the TCRm mAbs in our laboratory involved the immunisation of MF1 or BALB/c mice with human or chimeric MHC-I tetramers presenting p53 peptides (Li *et al.*, 2017a; Li *et al.*, 2017b). Antibodies that cross-reacted with non-specific tetramers (i.e. tetramers that contained a non-target peptide) were discarded. Of the remaining TCRm antibodies, four hybridoma clones (T1-116C, T2-2A, T1-29D and T2-108A) displayed specific recognition of their target p53 peptide when presented by HLA-A*0201 on the surface of T2 cells. The T1-116C TCRm mAb against p53RMP had been studied extensively in our laboratory prior to the start of this DPhil project. T1-116C was selected for further development as it was the only TCRm mAb that immunolabelled a variety of cancer cell lines in addition to peptide-presenting T2 cells. A patent for T1-116C has been published (WO2017037440A1), and it includes data that was generated prior to this DPhil project, as well as some of the data that has been produced within the scope of this project.

Data obtained before this DPhil project showed that T1-116C recognised HLA-$A2^{+}$/$p53^{+}$ cancer cell lines by flow cytometry, and it also had the capacity to engage immune effector functions (ADCC, CDC and ADCP) against target cell lines, which are important for therapeutic efficacy. Internalisation of T1-116C was shown to occur

three hours after incubation with target cells, indicating that T1-116C can be suitable for use as an ADC. Furthermore, using triple receptor negative breast cancer xenografts *in vivo* showed that T1-116C can prevent xenograft engraftment and it can also impede growth of an established xenograft (Li *et al.*, 2017a).

In order to further develop T1-116C and assess its potential for clinical application, we tested the specificity and safety of T1-116C. In addition to this, we also investigated whether T1-116C and T2-2A, a TCRm antibody that was generated alongside T1-116C, could be used to provide the targeting moiety for the generation of a CAR. This thesis focuses largely on two TCRm mAbs, T1-116C and T2-2A (the latter targets p53GLA), and describes the studies performed to further assess their clinical potential.

1.6 DPhil project aims

The aims of this DPhil project are as follows:

1) To further evaluate the specificity of T1-116C for its target p53RMP peptide.
2) To assess the safety of T1-116C using *in vitro*, *in silico* and *in vivo* methods, in order to validate its specificity profile and assess its clinical potential.
3) To generate p53-targeting CARs using anti-p53 TCRm antibodies and to test their specificity *in vitro*, expanding the use of anti-p53 TCRm antibodies beyond the naked TCRm antibody platform.

2 Materials and Methods

2.1 Tissue culture

2.1.1 Cell culture

Cells were cultured in the appropriate growth media (Table 2.1) and supplemented with 10% or 20% foetal bovine serum (FBS), 2mM L-glutamine and 1% penicillin (50 units/ml)-streptomycin (50µg/ml) solution (all from Gibco). Cells were cultured in a 5% CO_2 incubator at 37°C and were regularly tested for mycoplasma infection. Experiments were conducted prior to reaching 15 passages.

Hybridoma cells were cultured in a designated hybridoma cell culture room. They were cultured as described above, in Roswell Park Memorial Institute-1640 medium (RPMI-1640), supplemented as above and with the addition of 1% Ultroser G (PALL Life Sciences, 15950-017) and 2% HAT supplement (Gibco, 21060017), which is used to select for fused hybridoma cells. HAT supplement contains sodium hypoxanthine (5mM) and thymidine (0.8mM), which provide pre-formed purines and pyrimidines for DNA synthesis by the fused hybridoma cells, and aminopterin (20µM), which is a folic acid antagonist that inhibits *de novo* nucleoside biosynthesis. During the fusion process three types of cells are present: (i) fused hybridoma cells (spleen + myeloma), (ii) spleen cells, and (iii) myeloma cells that are HGPRT enzyme deficient. Spleen cells do not replicate in culture and will therefore be eliminated. Myeloma cells are eliminated because the aminopterin in the HAT-supplemented media blocks *de novo* DNA synthesis, forcing the cells to use the salvage pathway to replicate.

However because the HGPRT enzyme is required for the salvage pathway, only myeloma fusions, which have the HGPRT enzyme from the spleen cells, will be able to replicate using the hypoxanthine and thymidine in the media (Mak & Saunders, 2006).

2.1.2 Cell lines and primary cells

The cell lines used in experiments are summarised in Table 2.1. Additionally, primary AML samples were kindly gifted from Prof Paresh Vyas and primary myeloma samples from Dr Karthik Ramasamy, both at the John Radcliffe Hospital, Oxford. Studies with these primary samples were performed under approved ethics held by these clinicians and all patients gave informed consent for the use of their tissues for research.

Table 2.1 – Cell lines used in experimental procedures.

Cell line	Origin	Growth media	Supplier	Experiment
A549	Lung adenocarcinoma	RPMI-1640 + 10% FBS	N/A	IL-2 ELISA
CEM	T-cell (T-ALL)	RPMI-1640 + 10% FBS	Georges Delsol (Toulouse, France), between 2000 and 2004	IL-2 ELISA
Granta-519	B-cell (mantle cell NHL)	RPMI-1640 + 10% FBS	Leibniz Institute DSMZ prior to 2000	Flow cytometry; IL-2 ELISA
HCT-116	Colorectal carcinoma	DMEM + 10% FBS	Dr Francesco Pezzella (University of Oxford)	IL-2 ELISA
HEK293	Human embryonic kidney epithelial cells	RPMI-1640 + 10% FBS	N/A	IL-2 ELISA

Cell line	Origin	Growth media	Supplier	Experiment
HEK293-p53	Human embryonic kidney epithelial cells over-expressing wild type (wt) p53	RPMI-1640 + 10% FBS	Generated "in-house" by Demin Li	IL-2 ELISA
HEK293T	Human embryonic kidney epithelial cells	RPMI-1640 + 10% FBS	N/A	Transfection
HL-60	Promyeloblast (acute promyelocytic leukaemia)	DMEM + 20% FBS	Prof Alain Townsend (University of Oxford), prior to 2000	IL-2 ELISA
Jurkat	T-cell	RPMI-1640 + 10% FBS	Sir William Dunn School of Pathology (University of Oxford), prior to 2000	Transduced with CARs
Jurkat HLA-A2	T-cell expressing HLA-A2	RPMI-1640 + 10% FBS	Generated "in-house" by Demin Li	IL-2 ELISA
MCF-7	Human epithelial mammary gland adenocarcinoma (breast cancer)	DMEM + 10% FBS	CRUK Clare Hall Laboratories, 2004	IL-2 ELISA
MDA-MB-231	Human epithelial mammary gland adenocarcinoma (breast cancer)	DMEM + 10% FBS	ATCC 2004	IL-2 ELISA
MO1043	B-cell (CLL)	RPMI-1640 + 10% FBS	Prof Dalla-Favera (Columbia University), 2014	IL-2 ELISA; CD107a degranulation assay
MOLT4	T-cell (T-ALL)	RPMI-1640 + 10% FBS	Necker Hospital, Paris, prior to 2000	IL-2 ELISA
NCIH-1395	Lung adenocarcinoma	RPMI-1640 + 10% FBS	ATCC 2014	IL-2 ELISA
OCI-Ly8	B-cell (DLBCL)	RPMI-1640 + 10% FBS	Leibniz Institute DSMZ 2004	IL-2 ELISA; CD107a degranulation assay
SW480	Colorectal adenocarcinoma	DMEM + 10% FBS	Leibniz Institute DSMZ 2004	IL-2 ELISA
T2	B-cell deficient in the TAP	RPMI-1640 + 10% FBS	Prof Alain Townsend, University of Oxford, prior to 2000	T2 assays (routinely used for the study of peptide presentation by MHC-I); flow cytometry
T2-116A	Hybridoma	RPMI-1640 + 10% FBS + HAT	Generated "in-house"	RNA extraction

Cell line	Origin	Growth media	Supplier	Experiment
T2-2A	Hybridoma	RPMI-1640 + 10% FBS + HAT	Generated "in-house"	RNA extraction

The origin and growth media of cell lines is listed alongside the experimental purpose of their use. DMEM – Dulbecco's Modified Eagle Medium. N/A – information not available; DSMZ – German Collection of Microorganisms and Cell Cultures. ATCC- American Tissue Culture Collection; TAP – transporter of antigen processing.

2.1.3 Cell passage

The growth rate of individual cell lines determined how frequently the cell lines were split and the sub-culturing ratio; the latter varied from 1:2, 1:5 to 1:10. For the sub-culturing of adherent cell lines, the culture medium was removed and the cells were washed with phosphate buffered saline (PBS, Gibco). PBS was removed and 3ml of trypsin/EDTA (Gibco) solution was added to the flask, which was incubated at 37°C for 5 minutes or until the cells detached from the surface of the flask. Supplemented medium was added to the flask, at four times the volume of trypsin, in order to dilute the proteolytic action of trypsin, and the cells were transferred to a Falcon tube. Cells were centrifuged at 1500x*g* for 5 minutes to form a pellet. Medium was decanted from the Falcon tube and cells were resuspended in the required volume of fresh medium. The required proportion of cell suspension was transferred to a new sterile tissue culture flask, which was labelled appropriately and placed in a 5% CO_2 incubator at 37°C.

2.1.4 Cell freezing and thawing

Cells were counted prior to freezing, and the volume that corresponded to the required number of cells was transferred to a Falcon tube for centrifugation at 1500x*g*, for 5 minutes. The medium was decanted from the Falcon tube and the cell pellet was resuspended in 1ml of FBS with 10% dimethyl sulphoxide (DMSO, Sigma-Aldrich). Cells were immediately transferred to cryovials (Greiner Bio-One), which were placed in a Mr Frosty (Thermo Scientific) filled with isopropanol (VWR), and transferred to a -80°C freezer. After 24 hours, cells were transferred to liquid nitrogen storage.

For thawing, cryovials containing frozen cells were removed from liquid nitrogen storage and immediately thawed in a 37°C water bath. As soon as the cells were thawed, they were transferred from the cryovials to a Falcon tube that contained 20ml of supplemented medium. Cells were centrifuged at 1500x*g*, for 5 minutes, and the medium was decanted. Cells were counted, resuspended in fresh media and transferred to a sterile tissue culture flask: 5ml media for resuspension in a T-25 tissue culture flask or 15-20ml media for resuspension in a T-75 tissue culture flask (Greiner Bio-One). Cells were then placed in a 5% CO_2 incubator at 37°C for further expansion.

2.2 Flow cytometry and fluorescence-activated cell sorting

The expression of cell surface markers was detected using flow cytometry (FACS). Flow cytometry is often referred to as FACS, which was originally used to describe

fluorescence-activated cell sorting. Flow cytometry and FACS are widely used as interchangeable terms in the literature. Where there is specific reference to fluorescence-activated cell sorting in this thesis, it is described as FACS sorting.

2.2.1 Table of antibodies used in experiments

The antibodies that were used in flow cytometry and enzyme-linked immunosorbent assays (ELISAs) are summarised in Table 2.2.

Table 2.2 – Antibodies used in flow cytometry and ELISA experiments.

Antibody	Manufacturer	Catalogue number (Clone)	Dilution
Isotype control antibodies			
mIgG1	R&D Systems	MAB002 (11711R)	1:100
mIgG2a (anti-keyhole limpet haemocyanin)	R&D Systems	MAB003 (133304)	1:100
mIg2a (anti-fluorescein) (HHD experiment)	Absolute Antibody	-	20mg/kg
mIgG2b	BioRad Laboratories	MCA691	1:10
mIgG1-FITC/PE	Dako	X0956	1:100
mIgG1-PE	eBiosciences	12-4714-42 (P3.6.2.8.1)	5µl/test
mIgG1-APC	BD Biosciences	554681 (MOPC-21)	5µl/test
mIgG2b-APC	R&D Systems	IC0041A (133303)	1:100
hIgG1 (anti-fluorescein)	Absolute Antibody	Ab00102-10.0 (4-4-20e)	10µg/ml

Antibody	Manufacturer	Catalogue number (Clone)	Dilution
Antibodies originally generated "in-house"			
mT1-116C hIgG1 (anti-p53RMP-HLA-A2)	"In-house"	T1-116C	10µg/ml
hT1-116C hIgG1 V1 (anti-p53RMP-HLA-A2)	"In-house"	T1-116CV1	10µg/ml
T1-116C-PE (anti-p53RMP-HLA-A2)	BioLegend	T1-116C-PE	10µg/ml
T1-116CV1-mIgG2a (HHD experiment)	Absolute Antibody	T1-116CV1	20mg/kg
T2-2A (anti-p53GLA-HLA-A2)	"In-house"	T2-2A	10µg/ml
T2-108A (anti-p53GLA-HLA-A2)	"In-house"	T2-108A	10µg/ml
Secondary antibodies			
Anti-mouse IgG-APC	ThermoFisher	A10539	1:200
Anti-mouse IgG-PE	Dako	R0480	1:100
Anti-human IgG-APC	Jackson ImmunoResearch Inc.	109-136-098	1:200
Anti-human IgG-PE	Jackson ImmunoResearch Inc.	109-116-170	1:100
Anti-mouse IgG HRP-conjugated	Sigma Aldrich	A9044	1:1000
Anti-human IgG HRP-conjugated	Sigma Aldrich	62-8420	1:2000
Other antibodies			
Anti-human HLA-A2 (BB7.2)	BioRad Laboratories	MCA2090 (BB7.2)	10µg/ml
Anti-human HLA-A2 (BB7.2)-FITC	BioLegend	343304 (BB7.2)	10µg/ml
Anti-human HLA-A2 (BB7.2)-APC	eBioscience	17-9876-42 (BB7.2)	10µg/ml
Anti-β2M (BBM.1)	Sigma-Aldrich	MA1-26040 (BBM.1)	10µg/ml

Antibody	Manufacturer	Catalogue number (Clone)	Dilution
Anti-human p53-APC	R&D Systems	IC13551A (184727)	1:100
Anti-CD11b-PE	BioLegend	101207 (M1/70)	1:200
Anti-Gr1-biotin	Invitrogen	13-5931-81 (RB6-8C5)	1:100
Streptavidin-PerCP eFluor™710	Invitrogen	46-4317-82	1:500
Anti-CD19-APC	Invitrogen	17-0193-80 (eBio1D3)	1:100
Anti-CD3-BV421	BioLegend	100227 (17A2)	1:100
Anti-human CD3-PE	BioLegend	317410 (OKT3)	5µl/test
Anti-human CD107a-APC	BD Biosciences	560664 (H4A3)	5µl/test

Antibodies are listed with the manufacturer name, catalogue number, clone and dilutions are provided. The secondary antibodies are polyclonal antibodies; all other antibodies are monoclonal. Streptavidin-PerCP eFluor™710 is not an antibody but is displayed here as it was used in combination with the Anti-Gr1-biotin antibody instead of a secondary antibody.

2.2.2 Cell surface antibody staining for flow cytometry analysis

Cells that had just been thawed, as per the above protocol in 2.1.4, were first washed with supplemented RPMI-1640, and then a general staining protocol was followed. Cells were washed with FACS wash (PBS with 2% FBS and 0.1% sodium azide), and incubated with 100µl primary antibody at the dilution specified in Table 2.2 above, for 30 minutes at 4°C. Cells were washed again before staining with the relevant secondary antibody for 20 minutes at 4°C. After a final wash the cells were fixed (PBS with 1% paraformaldehyde) and analysed using a flow cytometer (FACSCalibur™, BD Biosciences). This method was also used to stain T2 cells with

primary antibody (T1-116C or BB7.2) and secondary antibody in T2 stabilisation assays.

In the case of staining with fluorophore-conjugated antibodies, cells were washed and incubated with the conjugated antibody, at the dilution specified in Table 2.2 above, for 30 minutes at 4°C. Cells were then washed and fixed (PBS with 1% paraformaldehyde) prior to being analysed using a FACSCalibur™. This method was used to stain primary AML and myeloma cells with fluorophore-conjugated T1-116C and BB7.2 antibodies.

For the staining of white blood cells (WBCs) from human HLA-A2 transgenic (HHD) mice, blood was collected and red blood cells were lysed with a red blood cell lysis buffer (Sigma Aldrich, R7757). The WBCs were washed with FACS wash (PBS with 2% FBS and 0.1% sodium azide) and stained with antibodies according to the general staining protocol in order to assess immune cell populations. Flow cytometry was performed using an LSRFortessa™ (BD Biosciences).

2.2.3 Tetramer staining of transiently transfected or transduced cells

Laboratory stocks of monomers of different peptides complexed with HLA-A2 were tetramerised with streptavidin-APC (eBioscience, 17-4317-82). The laboratory stocks are aliquots of monomers of HLA-A2 complexed with peptide, which had previously been refolded and biotinylated by other members of the laboratory as described below in 2.7.3, and which were stored in a -80°C freezer. When required, a monomer

aliquot (100µg) was thawed and then mixed on a rotating wheel with 25µl streptavidin-APC at 4°C, for 30 minutes. Three further doses of 8µl streptavidin-APC were added to the monomers at 30 minute intervals, while rotating at 4°C. Streptavidin and biotin were used because each streptavidin can bind up to four biotin molecules, forming a very strong non-covalent interaction and thereby enabling the tetramerisation of biotinylated monomers (Dundas *et al.*, 2013). The use of tetramers has previously been described in the literature (Altman *et al.* 1996). The monomers were left to tetramerise overnight at 4°C. Tetramers were used fresh the following day, or were stored at 4°C and used for up to 1 month after tetramerisation. Transfected or transduced cells were harvested and washed with FACS wash (PBS with 2% FBS and 0.1% sodium azide) before being stained with 100µl of tetramer (at 10µg/ml), for 30 minutes at room temperature. The cells were then washed with FACS wash and fixed (PBS with 1% paraformaldehyde) for flow cytometry analysis.

2.2.4 Intracellular antibody staining

Cells were washed with FACS wash. 10X BD FACS™ Permeabilizing Solution 2 (BD Biosciences, 340973) was diluted 1 in 10 in deionised water. After centrifugation of the cells at 1500x*g*, the supernatant was discarded and the cells were resuspended in 500µl of 1X BD FACS Permeabilizing Solution 2. Samples were vortexed and incubated at room temperature for 10 minutes. Cells were then washed with FACS wash and stained with anti-human p53-APC antibody (R&D Systems, IC13551A) or mIgG2b-APC isotype control antibody (R&D Systems, IC0041A). Cells were vortexed and incubated for 30 minutes in the dark, at room temperature. Finally, the cells

were washed (PBS with 2% FBS and 0.1% sodium azide) and then fixed (PBS with 1% paraformaldehyde) prior to flow cytometry analysis using a FACSCalibur™ (BD Biosciences).

2.2.5 Flow cytometry results analysis

Fixed cells were analysed using a FACSCalibur™ (BD Biosciences) in all cases, except in the analysis of WBCs from HHD mice, where an LSRFortessa™ (BD Biosciences) was used. Data was analysed using FlowJo software (Tree Star Inc.).

2.3 Enzyme-linked immunosorbent assay (ELISA)

2.3.1 T1-116C and BB7.2 antibody

An ELISA plate was coated with 100µl of 10µg/ml extravidin in PBS, at 4°C overnight. The plate was washed with PBS/0.1% Tween-20, blocked with PBS/1% BSA for 1 hour at room temperature, and then washed again. The plate was coated with p53RMP-HLA-A2 monomer or flu-HLA-A2 monomer for 1 hour at room temperature (100µL of 1µg/ml monomer). The plate was washed three times and 100µL of antibody, at 10µg/ml, was added in the combinations summarised in Figure 2.1. Antibody was incubated for 30 minutes at room temperature.

	Reagents added at each step	
Well contents	**STEP 1**	**STEP 2**
Isotype control	PBS	Isotype control
T1-116C only	PBS	T1-116C
BB7.2 only	PBS	BB7.2
T1-116C and BB7.2 simultaneously	PBS	T1-116C and BB7.2
BB7.2 first; T1-116C second	BB7.2	T1-116C
T1-116C first; BB7.2 second	T1-116C	BB7.2

Figure 2.1 – Antibody combinations added to the T1-116C and BB7.2 ELISA plate.

The plate was washed three times between each step. After 'STEP 2' the wells were washed three times again. Then to one half of the plate 100µl of HRP-conjugated anti-mouse secondary antibody (Sigma Aldrich, A9044) was added at 1:1000 dilution in order to detect the BB7.2 antibody, while 100µl of HRP-conjugated anti-human secondary antibody (Sigma Aldrich, 62-8420) was added to the other half of the plate at 1:2000 dilution, in order to detect the T1-116C antibody. The secondary antibody was incubated for 30 minutes at room temperature, in the dark. The plate was washed three times, 50µl of ABTS substrate (Roche, 10102946001) were added per well, and the plate was developed for 20 minutes on a shaker. The absorbance was measured at 405nm using a plate reader (Sunrise, Tecan) powered by Magellan software (Tecan).

2.3.2 T1-116C recognition of p53RMP-HLA-A2 fusion protein

An ELISA plate was coated with 100µl extravidin at 10µg/ml in PBS, at 4°C overnight. The plate was washed with PBS/0.1% Tween-20 and blocked with PBS/1% BSA for 1 hour at room temperature. The plate was washed and then 100µl refolded biotinylated monomers were added at 1µg/ml, and the plate was incubated for 1 hour at room temperature. After washing, 100µl of BB7.2 (Bio-Rad, MCA2090), BBM.1 (Sigma-Aldrich, MA1-26040) or T1-116C antibodies were added at 10µg/ml, and incubated for 1 hour at room temperature. The plate was washed and 100µl of HRP-conjugated anti-mouse secondary antibody (Sigma Aldrich, A9044) was added at a 1:1000 dilution and incubated for 30 minutes in the dark. The plate was washed and developed for 20 minutes with 100µl ABTS substrate solution (Roche). The absorbance was recorded at 405nm using a plate reader and Magellan software (Tecan).

2.3.3 Interleukin-2 (IL-2)

Target and effector cell lines were resuspended at 10^5 cells per 100µl of complete RPMI-1640. Cells were plated at a 1:1 ratio (i.e. 10^5 target cells versus 10^5 effector cells, amounting to a total volume of 200µl). CAR-transduced Jurkat and non-transduced Jurkat cells were also chemically stimulated with phorbol 12-myristate 13-acetate (PMA, at 50ng/ml, Sigma-Aldrich, P1585) and ionomycin (at 1µg/ml, Sigma-Aldrich, I9657) as a positive control. The plates were incubated overnight, for approximately 18 hours at 37°C, then centrifuged at 1500x*g* for 5 minutes the next day, and supernatants were harvested for cytokine secretion testing. ELISA was

performed according to the protocol provided by the supplier (Human IL-2 DuoSet ELISA kit, R&D Systems, DY202). ABTS solution was used as the peroxidase substrate and the plate was developed for 20 minutes on a shaker. Absorbance was recorded at 405nm using Magellan software (Tecan) and a plate reader (Sunrise, Tecan). An example of the co-culture plate setup for Jurkat cells transduced with the T2-2A CAR is illustrated in Figure 2.2.

In experiments where TCRm antibody (T2-2A or T2-108A) was added for competitive blocking in the IL-2 ELISA, an additional step was added to the protocol. Target cells were first plated, and TCRm antibody was added to the plated target cells at 10µg/ml, for 30 minutes at 37°C. Jurkat or T2-2A-CAR-Jurkat cells were then added, and the ensuing steps described earlier in this IL-2 ELISA protocol were followed.

	1	2	3	4	5	6	7	8	9	10	11	12
Jurkat	T2 unpulsed			T2 flu peptide			T2 p53RMP peptide			T2 p53GLA peptide		
T2-2A CAR	T2 unpulsed			T2 flu peptide			T2 p53RMP peptide			T2 p53GLA peptide		
Jurkat	NCI-H1395			MDA-MB-231			SW480			HEK293		
T2-2A CAR	NCI-H1395			MDA-MB-231			SW480			HEK293		
Jurkat	HEK293-p53			OCI-Ly8			MO1043			Jurkat-HLA-A2		
T2-2A CAR	HEK293-p53			OCI-Ly8			MO1043			Jurkat-HLA-A2		
Jurkat	Granta-519			PMA/Ionomycin			RPMI-1640			-	-	-
T2-2A CAR	Granta-519			PMA/Ionomycin			RPMI-1640			Jurkat		

Figure 2.2 – Co-culture plate setup for the T2-2A CAR-transduced Jurkat cells.
The target cell lines, PMA/ionomycin and RPMI-1640 were plated in triplicates and the T2-2A CAR-transduced Jurkat cells (T2-2A CAR) or non-transduced Jurkat cells (Jurkat) were added to each well. T2 cells were either mock pulsed (unpulsed) or pulsed with flu peptide, p53RMP peptide or p53GLA peptide. PMA/ionomycin was used as a positive control that chemically simulates IL-2 production. RPMI-1640 was used as a negative control (media alone with no target cells). The white wells (-) were empty.

2.4 T2 stabilisation assays

Synthesised peptides (Sigma-Aldrich) were dissolved in DMSO to make stocks at a concentration of 50mM. T2 cells were washed in serum-free RPMI-1640 and plated at 10^5 cells/100µl/well, in a flat-bottom 96-well plate (Greiner Bio-One). Peptides were diluted into 100µl serum-free media and added to the cells to a final concentration of 50µM. Cells were incubated overnight for 16 hours, in a 5% CO_2 incubator at 37°C, and then harvested for flow cytometry analysis.

2.5 T1-116C administration in HLA-A2 transgenic (HHD) mice

Animal experiments were approved by the Oxford University Animal Welfare and Ethical Review Body (AWERB) and governed by the appropriate UK Home Office project and personal licences (project licence number PPL 30-3197, personal licence number PIL ICC9D0F04).

HHD mice (6-8 week old females, n=5 per group) were a kind gift from Uzi Gileadi at the MRC Human Immunology Unit, University of Oxford. HHD mice are transgenic for human HLA-A2; they express human β2M, which is covalently linked to the α1 and α2 domains of human HLA-A2, while the α3, transmembrane and cytoplasmic domains of the molecule originate from murine H-2D^{b} (Pascolo *et al.*, 1997). During the study, animals were monitored regularly for welfare signs, in addition to routine husbandry care, and their body weights were measured twice weekly. They were injected intraperitoneally twice weekly, for a total of 17 interventions, with 20mg/kg T1-116CV1-mIgG2a (Absolute Antibody) or an isotype control antibody (Absolute Antibody). Mice were housed at the Biomedical Services facility at the John Radcliffe Hospital, Oxford. The facility houses mice in temperature-controlled rooms, within individually ventilated cages. Mice had continuous access to sterile water and formulated food. There were five female mice per cage, in mixed groups of isotype control or T1-116C treated mice.

2.5.1 Haematoxylin and eosin staining of tissues

Six organs (heart, liver, kidney, lungs, spleen and colon) from each mouse were harvested and fixed in formalin (Sigma-Aldrich, HT501128) for two days, at 4°C. Fixed

organs were processed using a Tissue-Tek VIP 5Jr. processor (Sakura) and embedded in paraffin (VWR). Tissue sections (4µm thick) were cut using a microtome (Leica RM 2135) and stained with haematoxylin (Thermo Scientific, 6765009), followed by counterstaining with eosin (Sigma-Aldrich, HT110216) as per the manufacturer's protocol. VectaMount™ mounting medium (Vector Labs, H-5000) and cover slips (VWR) were placed on the tissues before leaving overnight to dry. Tissues were visualised using an Olympus BX51 microscope and photos acquired with an Olympus DP70 digital camera and DP controller software (Olympus). Slides were analysed by a qualified pathologist (Dr Francesco Pezzella, University of Oxford) who was blinded to treatment.

2.6 Molecular biology protocols

2.6.1 Polymerase chain reaction (PCR)

PCR is used to amplify specific regions of DNA flanked by complementary primer pairs (a forward and a reverse primer that are each ≈20 nucleotides long). PCR is performed through repetition of three steps at different temperatures: (i) denaturation – double stranded DNA is heated to separate the complementary strands; (ii) annealing – primers bind to single stranded DNA at a region flanking the target DNA; and (iii) extension – DNA polymerase synthesises a DNA strand complementary to the target sequence by moving along the template strand and extending the DNA from the –OH group provided at the 3' end of the primer. These three steps are repeated 25-35 times (in cycles) in order to exponentially amplify the target DNA region. Pfu DNA polymerase was used, which is a thermostable

polymerase that has 5’ to 3’ polymerase activity, and it also has 3’ to 5’ exonuclease (proofreading) activity for high fidelity DNA synthesis. The reagents for the PCR reaction setup are listed in Table 2.3.

Table 2.3 – PCR setup.

Reagent	**Volume (µl)**
H_2O (Severn Biotech Ltd.)	37
10x Pfu buffer (Invitrogen)	5
dNTP (Invitrogen)	2.5
Primer 1 (forward)	2.5
Primer 2 (reverse)	2.5
Pfu DNA polymerase (Invitrogen)	0.5
Template DNA	0.1-1
Total volume	**≈50**

The reagents for the PCR setup are summarised, with their volume and the order in which they were added.

Once the reactions were set up, the PCRs were performed using an MJ Research Chromo4 thermal cycler. The PCR steps are summarised in Table 2.4, with the temperatures and durations of each step. A total of 30 cycles were performed and PCR products were then analysed using agarose gel electrophoresis.

Table 2.4 – Standard PCR cycles.

Step	Temperature	Duration
Denature template	95°C	5 minutes
Denaturation	95°C	1 minute
Annealing	60°C	1 minute
Extension	72°C	2 minutes

In each cycle of the PCR, denaturation, annealing and extension were repeated consecutively, for a total of 30 cycles.

2.6.2 Agarose gel electrophoresis

The sizes of PCR products and DNA fragments from restriction enzyme digests were estimated using agarose gel electrophoresis. Agarose gels were prepared by adding agarose powder (Sigma-Aldrich) to 1X TAE buffer and slowly heating the mixture in a microwave until boiling, in order to dissolve the agarose. The agarose content of the gel varied depending on the size of the DNA bands that were to be visualised; for DNA bands smaller than 500bp, a 2% gel was used; for DNA bands between 500bp to 1kb, a 1.5% gel was used; while for DNA bands larger than 1kb, a 1% gel was used. Once the agarose/TAE buffer mixture was partially cooled, GelRed® (Biotium) was added at a 10,000-fold dilution and swirled to mix. The gel was cast in a mould and left to cool and set. 10µl of DNA were supplemented with 2µl of 6X loading dye (Thermo Fisher, R0611) and mixed by pipetting before loading into the wells of the agarose gel. Samples were loaded in separate wells and run alongside a DNA ladder: either HyperLadder™ 1kb (Bioline, BIO-33026) or GelPilot 100bp Plus Ladder (Qiagen, 239045), in order to enable the estimation of DNA size. Samples were run at

100 volts for approximately 60 minutes in electrophoresis tanks (BioRad Laboratories), and DNA bands were visualised by UV transillumination using a gel doc system (Syngene). When required, DNA bands were extracted from the gel by cutting the bands out under UV light using a clean scalpel (Swann Morton), followed by DNA extraction using the Wizard® SV Gel and PCR Clean-UP gel extraction kit (Promega).

2.6.3 Gateway recombination cloning system: TOPO cloning and LR recombination

The Invitrogen Gateway® recombination cloning technology (Thermo Fisher) was used for the cloning and subcloning of CAR genes. Purified PCR products were cloned into the pENTR®/D-TOPO® entry vector (Thermo Fisher) according to the manufacturer's protocol. The entry vector contains *att*L recombination sites that flank the newly ligated DNA fragment of interest. An LR recombination reaction was then performed according to the manufacturer's protocol, in order to subclone the desired DNA fragment from the pENTR®/D-TOPO® entry vector into the expression vector pLenti7.3/V5-DEST™ (Thermo Fisher), which has *att*R recombination sites. The expression vector pLenti7.3/V5-DEST™ is a lentiviral expression vector that is designed for high target gene expression in mammalian cells (dividing and non-dividing). In pLenti7.3/V5-DEST™, target gene expression is under a cytomegalovirus (CMV) promoter. There is also a GFP selection marker, which is under a simian virus 40 (SV40) promoter.

2.6.4 Transformation of competent bacterial cells by heat shock

One Shot® TOP10 (ThermoFisher) competent *Escherichia coli* (*E. coli*) cells were thawed on ice for 30 minutes. DNA was added and mixed very gently by stirring. The reaction was incubated on ice for a further 30 minutes. The *E. coli* were then heat shocked in a water bath at 42°C for 30 seconds and immediately transferred onto ice for an incubation of 2 minutes. 250µl of SOC medium (Thermo Fisher, 15544034) were added to the reaction and the tubes were incubated in a rotary shaker for 1 hour, at 37°C. The samples were then plated on preheated agar plates containing the appropriate antibiotic. The plates were cultured overnight at 37°C, and checked the following morning for bacterial colonies.

2.6.5 Plasmid amplification

Individual colonies were picked from each plate and transferred to 5ml of Terrific Broth (TB, Sigma-Aldrich) for a miniprep, or 250ml of TB for a maxiprep DNA isolation procedure, supplemented with the appropriate antibiotic (ampicillin at 100 µg/ml; kanamycin at 50 µg/ml). The bacterial cultures were incubated overnight in a rotary shaker, at 37°C.

2.6.6 Isolation of plasmid DNA

Isolation of plasmid DNA was performed using either the Qiagen miniprep or maxiprep kit, depending on the size of the amplification and the amount of DNA required. Restriction enzyme digest and DNA sequencing were used to verify the

identity and integrity of the amplified plasmid DNA. Purified DNA samples were quantified using a NanoDrop spectrophotometer (Thermo Fisher).

2.6.7 Restriction enzyme digest

Restriction endonucleases were used to digest plasmid DNA in order to validate and screen for the presence of specific DNA fragments. Reactions were set up as summarised in Table 2.5.

Table 2.5 – Restriction enzyme digest setup.

Reagent	**Volume (µl)**
Plasmid DNA	0.5µg (e.g 5µl for 0.1 µg/µl concentration)
Restriction enzyme 1	0.25
Restriction enzyme 2	0.25
Reaction buffer	1
Nuclease-free water	Up to 10µl
Total volume	**10**

The reaction components and volumes are listed. Nuclease-free water was from Severn Biotech Ltd.

In the case of multiple samples, a mastermix (excluding the DNA) was made and aliquoted into tubes where DNA was then added individually. Restriction enzymes and reaction buffers were from New England Biolabs (NEB). Samples were incubated at 37°C for 1 hour prior to performing agarose gel electrophoresis. Samples that matched the expected size were validated by DNA sequencing.

2.6.8 DNA sequence analysis

DNA sequencing was performed by a commercial service provided by Source Bioscience, Oxford.

2.6.9 Cloning of CAR genes

The CAR genes were commercially synthesised (GeneArt Gene Synthesis, Thermo Fisher) and then were PCR-amplified using commercially synthesised primers (Eurofins). The primer sequences were: 5'-CACCATGCCTATGGGCAGCCTGCAGC-3' (forward primer), and 5'-TTATCTAGGGGGCAGGGCCTG-3' (reverse primer). PCR products were then purified and ligated into the entry vector pENTR®/D-TOPO® (Invitrogen). One Shot® TOP10 *E. coli* cells (Invitrogen) were transformed with the ligation reaction according to standard transformation protocol. The plasmid DNA was purified using the Qiagen miniprep kit and protocol (Qiagen). The CAR genes were subcloned from the pENTR®/D-TOPO® entry vector into the expression vector pLenti7.3/V5-DEST (Invitrogen) by LR recombination, using the Gateway® LR Clonase® II Enzyme Mix kit and protocol (Invitrogen). The CAR genes were sequenced to confirm their sequence integrity.

2.6.10 RNA extraction and reverse transcription to generate cDNA

Total RNA was extracted from the T2-2A and T2-116A hybridoma cell lines using the RNeasy mini kit (Qiagen, 74104) according to the manufacturer's protocol. The RNA was then reverse transcribed in order to obtain cDNA (Table 2.6). A mastermix of dNTPs and random primers was made and 2µl added per reaction tube, while RNA

and water were added individually. The contents of each tube were mixed by pipetting up and down, and were then spun down before placing in a thermal cycler (MJ Research PTC-200) for 5 minutes at 70°C, for step 1 of the reverse transcription. For step 2, a mastermix of the reagents listed in Table 2.6 was made and the appropriate volume was added to the reaction from step 1. The reaction components were mixed by pipetting and spun down to ensure all reagents were at the bottom of the tube, and then placed in the thermal cycler (MJ Research PTC-200). The temperatures and times used for the cDNA synthesis protocol were: (i) 25°C for 5 minutes, (ii) 55°C for 1 hour and (iii) 70°C for 15 minutes. Reagents for the reverse transcription were from Invitrogen (Invitrogen, 18080093).

Table 2.6 – Reverse transcription of RNA.

Step 1	
Reagent	**Volume**
Nuclease-free water	Up to 13µl
dNTPs	1µl
Random primers	1µl
RNA	1.5µg (→ calculate required volume)
Total volume	**13**
Step 2	
Reagent	**Volume**
Nuclease-free water	1µl
DTT	1µl
Buffer 5X	4µl
Superscript III enzyme	1µl
Total volume	**7µl**

The reaction components and their volumes are summarised. DTT – dithiothreitol.

2.6.11 Cloning of antibody variable region cDNA

After obtaining cDNA from the T2-2A and T2-116A hybridoma cell lines, PCRs were performed in order to clone the antibody variable regions. Three PCRs were performed to amplify the heavy chain genes and three PCRs were performed to amplify the light chain genes, each with a combination of multiple primers. Forward primers annealed to a highly conserved stretch of nucleotide sequence in the framework 1 region that is shared by *Ig* variable (V_H and V_L) genes, and reverse primers annealed to the DNA region encoding the beginning (5' end) of the constant regions of the γ heavy and κ light chains, as described in the literature (Dübel *et al.*, 1994; Dattamajumdar *et al.*, 1996; Brocks *et al.*, 2001). Multiple primers and PCRs were performed in order to cover sequence variability in an unknown *Ig* variable region. Table 2.7 summarises the PCR setup for the amplification of the heavy chain and light chain genes.

Table 2.7 – PCR setup for amplification of murine *Ig* variable heavy and light chain genes.

PCR	Reverse Primers	Forward Primer
Heavy chain PCR 1	MHV.B1 – B4	MHC.F
Heavy chain PCR 2	MHV.B5 – B8	
Heavy chain PCR 3	MHV.B9 – B12	
Light chain PCR 1	MKV.B1 – B4	MKC.F
Light chain PCR 2	MKV.B5 – B7	
Light chain PCR 3	MKV.B8 – B10	

Three PCRs with different primer combinations were performed for the heavy chain genes and for the light chain genes.

The PCR products of all three heavy chain PCRs were pooled together, as were those of all three light chain PCRs. The sequences of the primers used (Brocks *et al.*, 2001) are listed in Table 2.8. The pooled PCR products were then run on an agarose gel. For each sample, a band the size of ≈350 base pairs was cut out of the gel and extracted (Wizard® SV Gel and PCR Clean-UP gel extraction kit, Promega). The extracted PCR products were cloned into the Zero Blunt® TOPO® vector (Invitrogen, 450245) according to the manufacturer's protocol. The Zero Blunt® TOPO® vector was then used to transform One Shot® TOP10 *E. coli* (protocol 2.6.4). Colonies were picked for both the heavy chain and light chain genes, and they were amplified in TB (protocol 2.6.5). Minipreps were performed to isolate the plasmid DNA, which was then analysed using EcoRI restriction digestion. DNA was quantified (Nanodrop) and verified by sequencing with the M13 forward (5´-GTAAAACGACGGCCAG-3´) and M13 reverse (5´-CAGGAAACAGCTATGAC-3´) primers. We were unable to isolate the variable heavy chain gene sequence of the T2-116A antibody, therefore T2-116A was no longer pursued. The variable heavy and light chain genes of the T2-2A antibody were successfully amplified, and along with existing *Ig* variable region sequences available for the T1-29D antibody, were used to construct CARs (illustrated in Figure 5.12).

Table 2.8 – DNA sequences of primers used to amplify murine *Ig* variable heavy and light chain regions.

Primer name	Nucleotide sequence 5' to 3'
Variable heavy chain region primers	
MHV.B1	GATGTGAAGCTTCAGGAGTC
MHV.B2	CAGGTGCAGCTGAAGGAGTC
MHV.B3	CAGGTGCAGCTGAAGCAGTC
MHV.B4	CAGGTTACTCTGAAAGAGTC
MHV.B5	GAGGTCCAGCTGCAACAATCT
MHV.B6	GAGGTCCAGCTGCAGCAGC
MHV.B7	CAGGTCCAACTGCAGCAGCCT
MHV.B8	GAGGTGAAGCTGGTGGAGTC
MHV.B9	GAGGTGAAGCTGGTGGAATC
MHV.B10	GATGTGAACTTGGAAGTGTC
MHV.B11	GAGGTCCAGCTGCAACAGTC
MHV.B12	GAGGTGCAGCTGGAGGAGTC
MHC.F	GCCAGTGGATAGTCAGATGGGGGTGTCGTTTTGGC
Variable light chain region primers	
MKV.B1	GATGTTTTGATGACCCAAACT
MKV.B2	GATATTGTGATGACGCAGGCT
MKV.B3	GATATTGTGATAACCCAG
MKV.B4	GACATTGTGCTGACCCAATCT
MKV.B5	GACATTGTGATGACCCAGTCT
MKV.B6	GATATTGTGCTAACTCAGTCT

Primer name	Nucleotide sequence 5' to 3'
MKV.B7	GATATCCAGATGACACAGACT
MKV.B8	GACATCCAGCTGACTCAGTCT
MKV.B9	CAAATTGTTCTCACCCAGTCT
MKV.B10	GACATTCTGATGACCCAGTCT
MKC.F	GGATACAGTTGGTGCAGCATC

Primer sequences are described in Brocks *et al.*, 2001.

2.6.12 Constructs

The constructs made and used in the studies conducted during this DPhil project are summarised in Table 2.9.

Table 2.9 – Constructs made and used in experimental procedures.

Construct	Description	Purpose
pET-9c-p53RMP-HLA-A2	pET-9c vector expressing the p53RMP peptide fused to the heavy chain of HLA-A2	To assess the affinity of T1-116C for its target
pLenti7.3-T1-116C-CAR-V_LV_H	pLenti7.3 vector expressing the T1-116C CAR in the V_LV_H orientation	To test the suitability of T1-116C for use in a CAR
pLenti7.3-T1-116C-CAR-V_HV_L	pLenti7.3 vector expressing the T1-116C CAR in the V_HV_L orientation	To test the suitability of T1-116C for use in a CAR
pLenti7.3-T2-2A-CAR	pLenti7.3 vector expressing the T2-2A CAR	To test the suitability of T2-2A for use in a CAR
pLenti7.3-T1-29D-CAR	pLenti7.3 vector expressing the T1-29D CAR	To test the suitability of T1-29D for use in a CAR

2.7 Production of recombinant p53RMP-HLA-A2 fusion protein

2.7.1 Cloning of covalently linked p53RMP-HLA-A2 monomer

The affinity of T1-116C had been previously measured by binding T1-116C to a non-covalently linked trimer of: (i) the p53RMP peptide, (ii) the heavy chain of HLA-A2, and (iii) β2M. The measured affinity was lower than expected for an antibody with *in vivo* activity, therefore we tested whether the relatively low affinity could have partially resulted from the disassembly of the trimer complex used. We used a p53RMP peptide that was covalently linked to the heavy chain of HLA-A2 through a flexible glycine-serine linker, in order to prevent disassembly of the p53RMP peptide from HLA-A2. The covalently linked p53RMP-HLA-A2 gene was synthesised using a commercial supplier (Eurofins) and provided in the commercial vector pEX-A2. Plasmid DNA was propagated by transforming One Shot® TOP10 *E. coli* cells (Invitrogen), and then purified using the Qiagen miniprep kit (Qiagen), following the manufacturer's instructions. The covalently linked p53RMP-HLA-A2 gene was cloned from the pEX-A2 commercial vector into the pET-9c expression vector, by restriction enzyme digestion using NdeI and BamHI restriction endonucleases (NEB), gel extraction (Wizard® SV Gel and PCR Clean-UP gel extraction kit, Promega) and ligation (T4 DNA ligase, NEB). The final construct was sequenced commercially to validate the sequence integrity of the insert.

2.7.2 Expression of recombinant fusion protein

Plasmid DNA of pET-9c-p53RMP-HLA-A2 (pET-9c vector containing the fused p53RMP-HLA-A2 gene) was purified and used to transform BL21 (DE3) *E. coli*. The

advantages of using BL21 (DE3) *E. coli* for recombinant protein expression are that they are deficient in the Lon and OmpT proteases, which degrade foreign proteins and they have an *hsd*SB mutation that prevents DNA methylation and degradation. Furthermore, the gene of interest in the pET-9c vector is under a T7 promoter that is recognised by T7 RNA polymerase. The phage T7 RNA polymerase gene (λDE3) is integrated into the BL21 (DE3) *E. coli* chromosome and is expressed under the control of the *lacUV5* promoter; therefore isopropyl β-D-1-thiogalactopyranoside (IPTG), a molecular mimic of allolactose (which is a lactose metabolite that instigates *lac* operon transcription), can be used to induce recombinant protein expression under control of the *lac* operon (Rosano & Ceccarelli, 2014). Colonies were grown and picked for amplification into low salt Luria-Bertani (LSLB) medium, and IPTG was used to induce recombinant protein expression. The protocol was initially performed to identify the optimal IPTG concentration (0.5mM) and induction time (4 hours at 37°C) using small scale (5ml LSLB) cultures and induction of the recombinant p53RMP-HLA-A2 protein was then analysed using sodium dodecyl sulphate polyacrylamide gel electrophoresis (SDS-PAGE). Recombinant protein expression was then induced on a larger scale (1 litre LSLB) in BL21 (DE3) *E. coli*. Insoluble inclusion bodies containing the recombinant p53RMP-HLA-A2 fusion protein were purified using BugBuster (Merck, 70584), according to the manufacturer's protocol. The purity and molecular weight of the recombinant p53RMP-HLA-A2 fusion protein was validated using SDS-PAGE.

2.7.3 Refolding of recombinant p53RMP-HLA-A2 fusion protein with β2-microglobulin

As described in the literature (Garboczi *et al.* 1992), the recombinant p53RMP-HLA-A2 protein was refolded with β2M to make p53RMP-HLA-A2-β2M monomers. The recombinant p53RMP-HLA-A2 protein (7.5mg) and β2M (12.5mg) were added to 500ml of refolding buffer (100mM Tris-Cl pH 8.0, 400mM L-Arginine, 2mM EDTA, 5mM reduced glutathione, 0.5mM oxidised glutathione and 0.1 mM phenylmethylsulphonyl fluoride [PMSF]) and left to stir overnight at 4°C. A further 7.5mg of recombinant p53RMP-HLA-A2 protein were added to the refolding buffer and left to refold while stirring for 48 hours, at 4°C. The refolded protein was concentrated and the buffer was exchanged for 10mM Tris-Cl pH8.0. The refolded protein was biotinylated using the BirA biotin-protein ligase reaction kit (Avidity LLC, BirA-500), according to the manufacturer's protocol (in order to enable tetramerisation of monomers for future applications). The biotinylated p53RMP-HLA-A2-β2M protein was then purified by fast protein liquid chromatography (FPLC), using an AKTA Purifier with a Sephadex 75 column (both from GE Healthcare), which separates different proteins in the solution based on their size. The p53RMP-HLA-A2-β2M monomers in FPLC buffer (20mM Tris-Cl pH8.0) were isolated, concentrated to 1mg/ml, aliquoted into 50µg or 100µg and stored at -80°C. When required, aliquots were thawed and tetramerised using streptavidin-APC (eBioscience, 17-4317-82), as described above in protocol 2.2.3. FPLC fractions were validated for protein size using SDS-PAGE. Protein refolding was validated using the ELISA assay described in 2.3.2.

2.7.4 Sodium dodecyl sulphate polyacrylamide gel electrophoresis (SDS-PAGE)

The protein concentration of whole cell lysates or FPLC fractions was quantified using the Pierce™ BCA Protein Assay Kit (Thermo Fisher, 23227), according to the manufacturer's protocol. For SDS-PAGE analysis, protein samples were disrupted and the protein was denatured by heating at 95°C for 5 minutes in sample loading buffer (NuPage™ LDS Sample buffer, Invitrogen, NP0007). Samples (10µg/lane) were loaded into NuPage™ 4-12% Bis-Tris pre-cast gels (Invitrogen, NP0322BOX) and run using NuPage™ MES SDS Running Buffer (Invitrogen, NP0002). Proteins were separated at 200 volts for 45 minutes. Spectra™ Multicolor Broad Range Protein Ladder (Thermo Fisher, 26634) was loaded in the first lane as the protein standard. After gel electrophoresis, proteins were visualised by staining with Coomassie dye (Imperial™ Protein Stain, Thermo Fisher, 24615) for 1 hour, according to the manufacturer's protocol.

2.8 Transfection and transduction protocols

2.8.1 Transient transfection of HEK293T cells

HEK293T cells were plated at $6x10^5$ cells in 2ml of media in a 6-well plate and incubated overnight in a 5% CO_2 incubator at 37°C. At 70% confluence the next day, HEK293T cells were transfected with 2µg of plasmid DNA (pLenti7.3 vector backbone containing one CAR gene) using FuGene® transfection reagent (Promega, E2311), according to the manufacturer's protocol. The cells were returned to the 5% CO_2 incubator at 37°C for 48 hours before being harvested, washed with FACS wash and analysed for GFP expression using a FACSCalibur™ (BD Biosciences).

2.8.2 Lentiviral transduction to generate Jurkat cell line with stable CAR expression

The calcium phosphate transfection method was used to transfect HEK293T cells with the CAR constructs. VSV-G, pLP1 and pLP2 plasmids were used for lentiviral packaging (ViraPower^{TM} kit, Invitrogen). Cells were incubated for 72 hours in a 5% CO_2 incubator at 37°C before culture supernatants were transferred to Ultraclear ultracentrifuge tubes (Beckman) and supplemented with complete RPMI-1640 media into a volume of 38ml. Culture supernatants were centrifuged at 28,000rpm in a Beckman Optima L-90K ultracentrifuge, using an SW28 rotor (Beckman Coulter), for 3 hours at 4°C. Supernatants were discarded and pellets resuspended with the backflow. $0.5x10^6$ Jurkat cells were harvested, resuspended with the virus particles and incubated in a 5% CO_2 incubator for 1 hour at 37°C. Cells were then supplemented with 10ml of complete RPMI medium and cultured for 3 days in a 5% CO_2 incubator at 37°C. Cells were subsequently harvested and washed 10 times with complete RPMI-1640, over a period of 1 week, in order to become virus-free. CAR-transduced GFP-positive cells were FACS sorted by the Flow Cytometry Facility in the Experimental Medicine Division, Nuffield Department of Medicine, University of Oxford, using a FACSAria III (BD Biosciences). FACS sorted cells were transferred to sterile tissue culture flasks in complete RPMI-1640, and cultured at 37°C in a 5% CO_2 incubator for further expansion.

2.9 CD107a degranulation assay

Target cells and effector cells (Jurkat-T2-2A-CAR cells) were plated at a 1:1 ratio of 10^5 cells, each resuspended in 50µl of complete RPMI-1640 media per well. Target cells were plated first in a 96-well U-bottom plate (Greiner Bio-One), and effector cells were added to the corresponding wells containing target cells to achieve a total volume of 100µl/well. Anti-CD107a-APC antibody was added to each well, at 5µl/well. Cells were incubated for 1 hour, at 37°C in a 5% CO_2 incubator. Monensin (BD GolgiStop, BD Biosciences, 554724) was diluted 1 in 10 in PBS, and 5µl was added per well. When the anti-CD107a-APC antibody is internalised in endosomes or lysosomes, monensin is required to prevent the acidification of these compartments and the degradation of the endocytosed antibody by proteases, in order to preserve the fluorescent signal of the antibody and enable its detection using flow cytometry (Betts *et al.*, 2003). Cells were incubated for 5 hours in a 5% CO_2 incubator, at 37°C, then washed with FACS wash, and stained with anti-CD3-PE antibody for 30 minutes at 4°C. Cells were washed with FACS wash and fixed (PBS with 1% paraformaldehyde) before being analysed using a FACSCalibur™ (BD Biosciences).

2.10 Collagenase treatment of mouse organs for FACS analysis of cell surface markers

Five organs (spleen, lungs, liver, heart, kidneys) and blood were resected from an untreated HHD and a C57BL/6 mouse. The lungs, liver, heart and kidneys were placed on glass petri dishes in a small volume of collagenase solution (collagenase type 2 at 3mg/ml in HBSS per organ, Worthington Biochem Corp., LS004174). These

organs were cut as finely as possible with two scalpels and then placed in individual Falcon tubes with 3ml of collagenase solution. The Falcon tubes were taped to a rotary shaker and incubated at 37°C for 30 minutes. The spleens were kept in PBS and cut into fine pieces without collagenase treatment. The samples were centrifuged at 450x*g* for 5 minutes. The supernatant was discarded and the samples were resuspended in 1ml of FACS wash. The samples were filtered using Sysmex CellTrics 50µm disposable filters (Sysmex, 04-004-2327) into clean Falcon tubes and spun at 450x*g* for 5 minutes. Supernatants were discarded and the samples were aliquoted into wells of a 96-well U-bottom plate. Blood was also collected into heparinised tubes and red blood cells were lysed with red blood cell lysis buffer (Sigma-Aldrich, R7757) before washing the WBCs and plating in the 96-well U-bottom plate. Human PBMCs were thawed as described previously, and washed in FACS wash prior to aliquoting into the 96-well U-bottom plate. All samples were blocked with normal mouse serum for 15 minutes at room temperature. The samples were stained with fluorophore-conjugated BB7.2-APC (anti-HLA-A2 mAb) and T1-116C-PE antibodies, as described previously. They were then washed with FACS wash and fixed (PBS with 1% paraformaldehyde), before being analysed using a FACSCalibur™.

2.11 Statistical analyses

Data is presented as the mean of replicates ± standard deviation. The one-way analysis of variance (ANOVA) was used to assess whether there was a significant difference when the means of more than 2 groups were compared, using GraphPad

software (Prism). The student's t-test was used to analyse the difference between the means of 2 groups. Statistical significance is expressed as the p-value (p), which is denoted by an asterisk (*) on the graph, where: * = $p \leq 0.05$; ** = $p \leq 0.01$; *** = $p \leq 0.001$; **** = $p \leq 0.0001$.

3 Defining the Specificity of T1-116C for the p53RMP Peptide

3.1 Introduction

TCRm antibodies have a dual antigen epitope, recognising both the peptide and the MHC-I molecule. An MHC-I molecule can present different peptides, hence it is the peptide that predominantly determines the specificity of binding for a TCRm antibody. The length of the peptide presented by MHC-I molecules can vary by a few amino acid residues, however TCRm antibodies will generally only make contact with a few key residues within the peptide (Rock *et al.*, 2002). This allows scope for amino acid variation at the other positions within the peptide while still retaining TCRm antibody binding. The safety implications of this are that peptides derived from normal tissue antigens may also be recognised by tumour-targeting TCRm antibodies if they conserve both the key MHC-I anchor residues and the residues crucial for antibody binding. Therefore it is critical to define the target peptide epitope requirements of TCRm antibodies in order to assess their specificity and identify any potentially cross-reactive peptides. There are only a limited number of reports with direct evidence of TCRm antibody binding and specificity derived from the crystal structures of TCRm antibodies with their dual antigen target (Hülsmeyer *et al.*, 2005; Mareeva *et al.*, 2008; Stewart-Jones *et al.*, 2009; Ataie *et al.*, 2016). Amino acid substitutions within peptides, in conjunction with the use of databases and *in silico* binding prediction tools can also be used to assess TCRm specificity. Researchers in the field predominantly report alanine substitutions within their target peptide to further define the specificity of their TCRm antibodies (Sergeeva *et al.*, 2011; Dao *et*

al., 2013; Zhao *et al.*, 2015; Chang *et al.*, 2017; Lowe *et al.*, 2017; Ahmed *et al.*, 2018).

We had received feedback from Cancer Research UK Commercial Partners (Dr Chris Baker) that companies evaluating TCRm antibodies from other laboratories had sometimes found that their TCRm antibodies recognised cancer cell lines, however they did not bind primary tumours. Thus we first aimed to test whether T1-116C was capable of recognising primary tumours by *ex vivo* staining AML and myeloma samples derived from patients. T1-116C binding to primary tumours is important because its ability to mediate a therapeutic effect against cancer is dependent on it being able to recognise primary cancer cells. We then performed comprehensive amino acid substitutions within the p53RMP peptide in order to map the T1-116C epitope.

3.2 T1-116C staining of primary tumour cells

To assess whether T1-116C could recognise primary tumours, which would be essential for its clinical efficacy, we were kindly gifted primary AML (from Dr Paresh Vyas, Oxford) and primary myeloma samples (from Dr Karthik Ramasamy, Oxford). We stained these with an anti-HLA-A2 antibody (BB7.2) to determine their HLA-A2 profile and with T1-116C.

3.2.1 BB7.2 antibody modulated T1-116C staining

The initial staining of the AML samples was performed with a simultaneous double antibody staining protocol using both BB7.2-FITC antibody and T1-116C-PE antibody.

Directly conjugated antibodies having different fluorophores were used to perform double staining where each sample was stained with both antibodies in the same step of the protocol. In addition to this, a proportion of each of the samples was used to perform single antibody staining with each antibody separately, as a control for the double antibody staining and for the optimisation of the compensation setting on the flow cytometer. We stained with BB7.2 to determine the HLA-A2 profile of each sample in order to evaluate whether T1-116C binding demonstrated the expected HLA-A2-restricted binding pattern.

Three AML samples were used in the first staining experiment, where we found that samples AML1250 and AML471 were HLA-A2-positive and T1-116C-negative in their respective single antibody staining samples (Figure 3.1). AML471 showed only a slight T1-116C-positive shift, making it difficult to conclude that this was true T1-116C staining (Figure 3.1, panel D). In the double antibody staining, both of these samples unexpectedly became T1-116C-positive (Figure 3.1, panel B). One possible explanation was that staining simultaneously with the BB7.2 antibody somehow potentiated the staining of the T1-116C antibody to the point where T1-116C-negative samples became positive. The third sample, AML279, was negative for HLA-A2 expression and T1-116C binding. It is also possible that BB7.2 stabilised HLA-A2 expression at the cell surface, thereby leading to an increase in T1-116C staining.

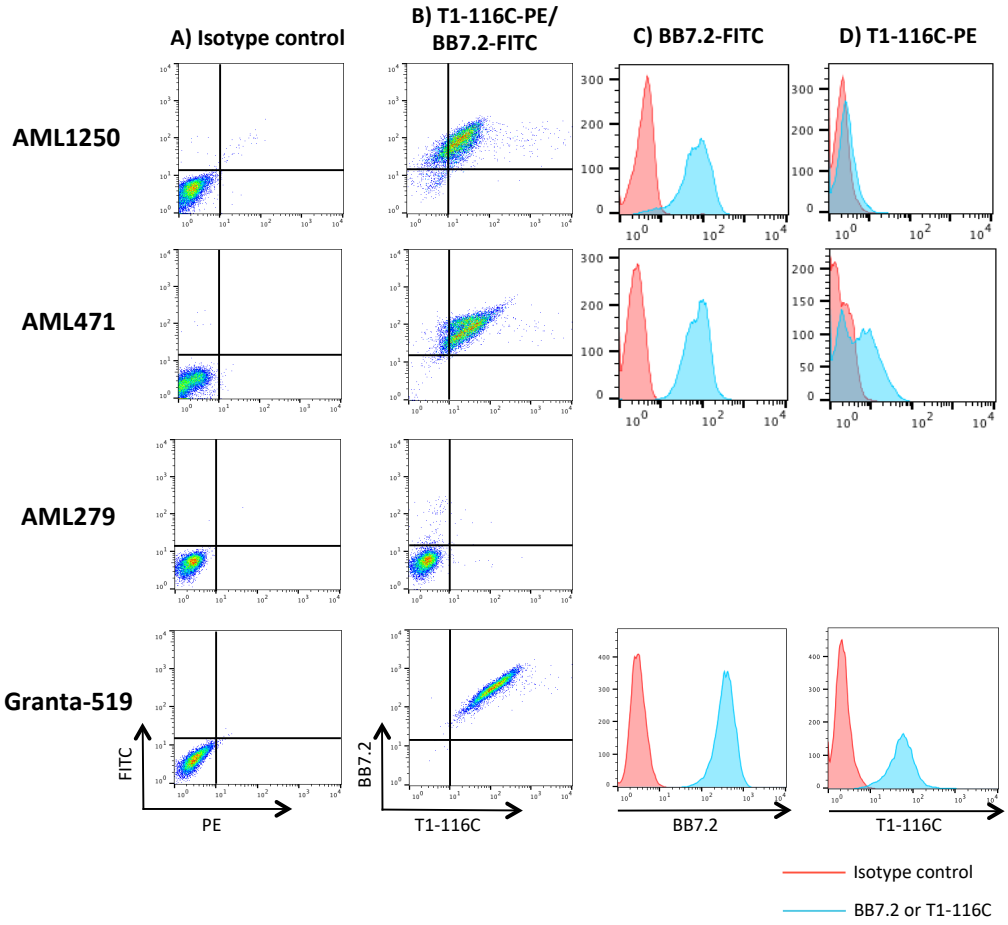

Figure 3.1 – Staining of AML samples with BB7.2-FITC and T1-116C-PE.
Three AML samples were stained with an isotype control (A), or with BB7.2-FITC and T1-116C-PE simultaneously (B). Of the three samples, only two (AML1250 and AML471) had a sufficient number of cells to perform single antibody staining as controls (C and D). Granta-519 cells were used as a positive control, as they are both HLA-A2- and T1-116C-positive.

In order to explain why this occurred, Granta-519 and T2 cell lines were used to validate the results observed with the conjugated antibodies. The Granta-519 cell line is both HLA-A2- and T1-116C-positive, whereas the T2 cell line is HLA-A2-positive but T1-116C-negative (unless pulsed with the p53RMP target peptide). We performed BB7.2 and T1-116C double antibody staining, as well as separate single antibody staining (Figure 3.2). We found that in the Granta-519 cells, the T1-116C positivity was slightly stronger in the double antibody stained sample, compared to the T1-116C antibody staining alone. However, the most striking finding was that the T2 cells, which were T1-116C-negative in the single antibody staining, were T1-116C-positive in the BB7.2 and T1-116C double antibody staining (Figure 3.2, panel A). Importantly, both HLA-A2 (which is also the target of the BB7.2 antibody) and the p53RMP peptide comprise the T1-116C epitope. Thus, among a number of options, there may be either an interaction between the two antibodies, or HLA-A2 binding by BB7.2 may lead to conformational changes at the epitope that alter T1-116C binding.

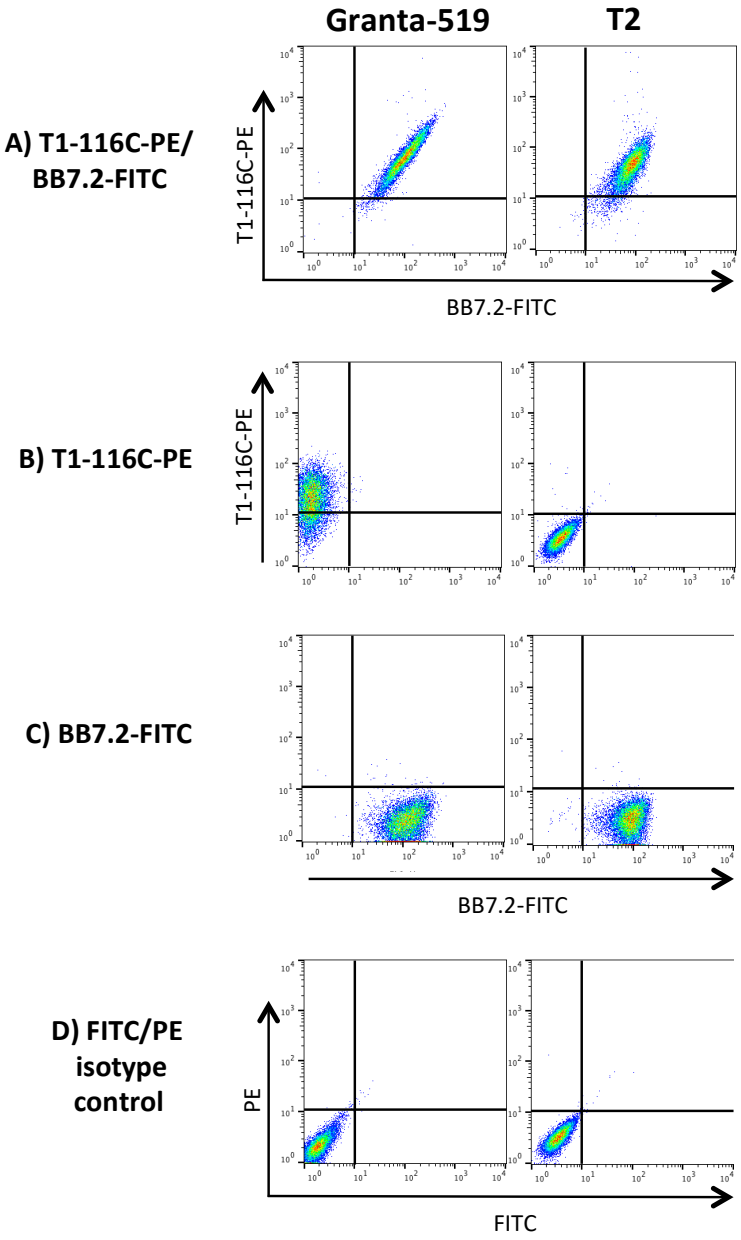

Figure 3.2 – BB7.2 and T1-116C antibody staining of Granta-519 and T2 cells.
Granta-519 and T2 cells were stained with both T1-116C-PE and BB7.2-FITC simultaneously (A), T1-116C-PE only (B), BB7.2-FITC only (C) or an isotype control (D). Granta-519 cells are both HLA-A2- and T1-116C-positive, as expected. T2 cells are HLA-A2-positive but T1-116C-negative in the single antibody staining, however in the double antibody staining, T2 cells become T1-116C-positive.

To investigate whether the observed results were due to antibody-antigen interactions at the cell surface, we performed an ELISA to determine whether these results would also be reproduced in a cell-free system (Figure 3.3). We coated an ELISA plate with the p53RMP-HLA-A2 monomer, or an irrelevant flu-HLA-A2 monomer as a negative control. To assess antibody binding, we added the antibodies either alone, or together, in the different possible combinations (both antibodies simultaneously; BB7.2 first and T1-116C second; or T1-116C first and BB7.2 second). The results showed that the T1-116C single antibody staining was comparable to that of the BB7.2 and T1-116C double antibody combinations. Overall there was no significant difference between the T1-116C staining alone and the double antibody staining combinations, suggesting that the flow cytometry results obtained previously may be due to antibody-antigen interactions at the cell surface, or perhaps due to the conjugation of the PE fluorophore to T1-116C, as an unconjugated T1-116C antibody was used in the ELISA.

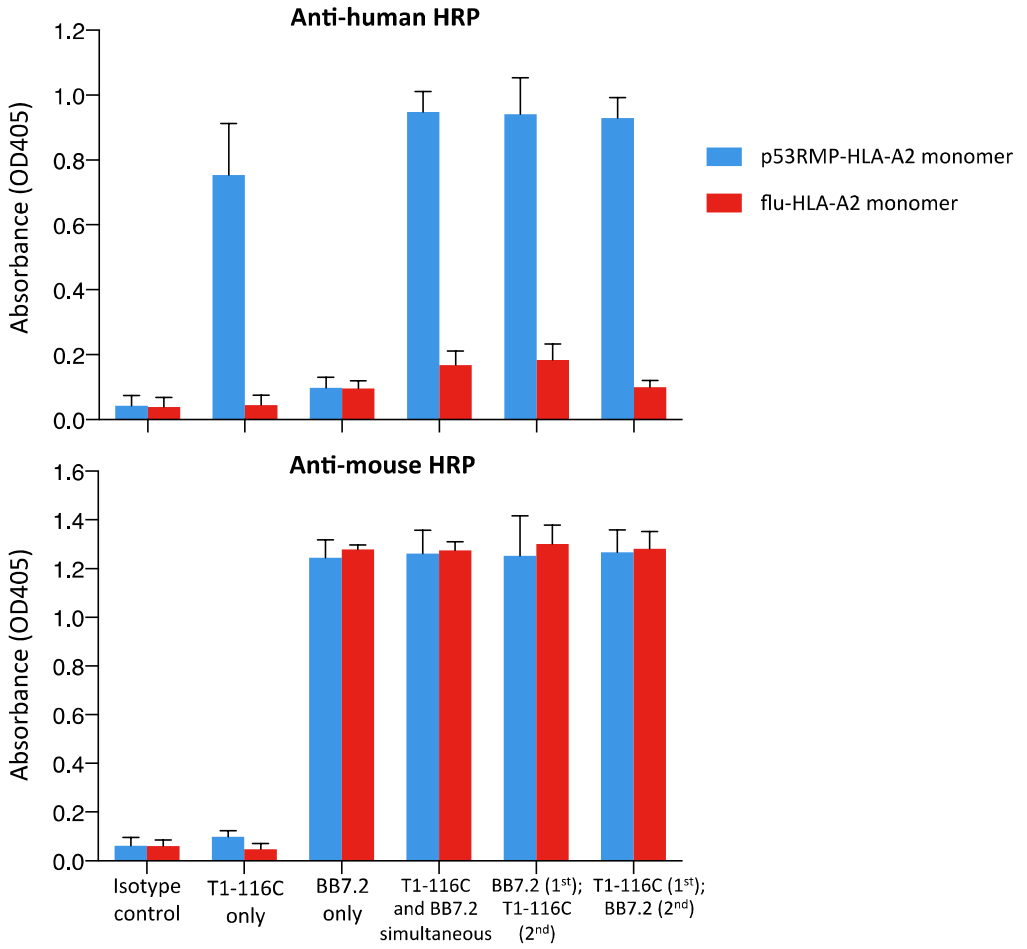

Figure 3.3 – ELISA to determine whether BB7.2 modulates T1-116C binding in a cell-free system.

An ELISA plate was coated with either the target p53RMP-HLA-A2 monomer (blue) or a negative control flu-HLA-A2 monomer (red). The T1-116C antibody used was in the human IgG1 isotype, while the BB7.2 antibody was in the mouse IgG2b isotype, hence they can be differentiated by using either anti-human or anti-mouse HRP-conjugated secondary antibodies. The antibodies were added to the ELISA plate in the different possible combinations: T1-116C alone, BB7.2 alone, the two antibodies simultaneously, BB7.2 first and T1-116C second, or T1-116C first and BB7.2 second. In the anti-human HRP graph, which shows the detection of only the T1-116C antibody, there is no significant difference between the different antibody combinations for the p53RMP-HLA-A2 monomer. One-way ANOVA was used for the statistical analysis. In the anti-mouse HRP plate, as expected, BB7.2 is detected in all samples that contain the BB7.2 antibody. Absorbance was measured at 405nm. n=3.

As the directly conjugated T1-116C-PE antibody was shown to work well in single antibody labelling, we decided to perform single antibody labelling of further AML samples, with either T1-116C-PE or BB7.2-FITC, in order to avoid any potential problems caused by double labelling.

3.2.2 T1-116C staining of primary AML samples

When performing single antibody staining, of the remaining previously unstained seven AML samples, five samples (AML524, AML1234, AML806, AML856 and AML1181) were HLA-A2-positive (Figure 3.4). Of the five HLA-A2-positive samples, one sample was convincingly T1-116C-positive (AML1234).

Information on the clinical characteristics of the AML patients that the samples were derived from was kindly provided by Prof. Vyas's laboratory (Table 3.1). Data for the gender and sample source is not available for all patients. The majority of patients are above the age of 50, with the exception of one paediatric patient (AML279). As only one sample (AML1234) was positive for T1-116C, we cannot draw any conclusions about the clinical characteristics of patients that could benefit from T1-116C use, whether as a diagnostic or a therapeutic antibody. A larger number of primary samples would have to be tested for this purpose.

Table 3.1 – Clinical characteristics of AML patients.

Sample	Gender	Age	Stage	Sample source
AML524	Female	64	Diagnosis	PB
AML821	Male	52	Diagnosis	-
AML1234	-	61	Diagnosis	PB
AML795	Male	66	Diagnosis	BM
AML806	Female	51	Diagnosis	PB
AML856	Male	69	Diagnosis	BM
AML1181	-	63	Diagnosis	PB
AML279	-	12	Diagnosis	-
AML1250	-	60	Diagnosis	-
AML471	-	60	Diagnosis	PB

The gender, age, stage at sample acquisition, and sample source are provided where available. All samples were taken at diagnosis. PB – peripheral blood; BM – bone marrow. Bone marrow samples were taken from the posterior iliac crest.

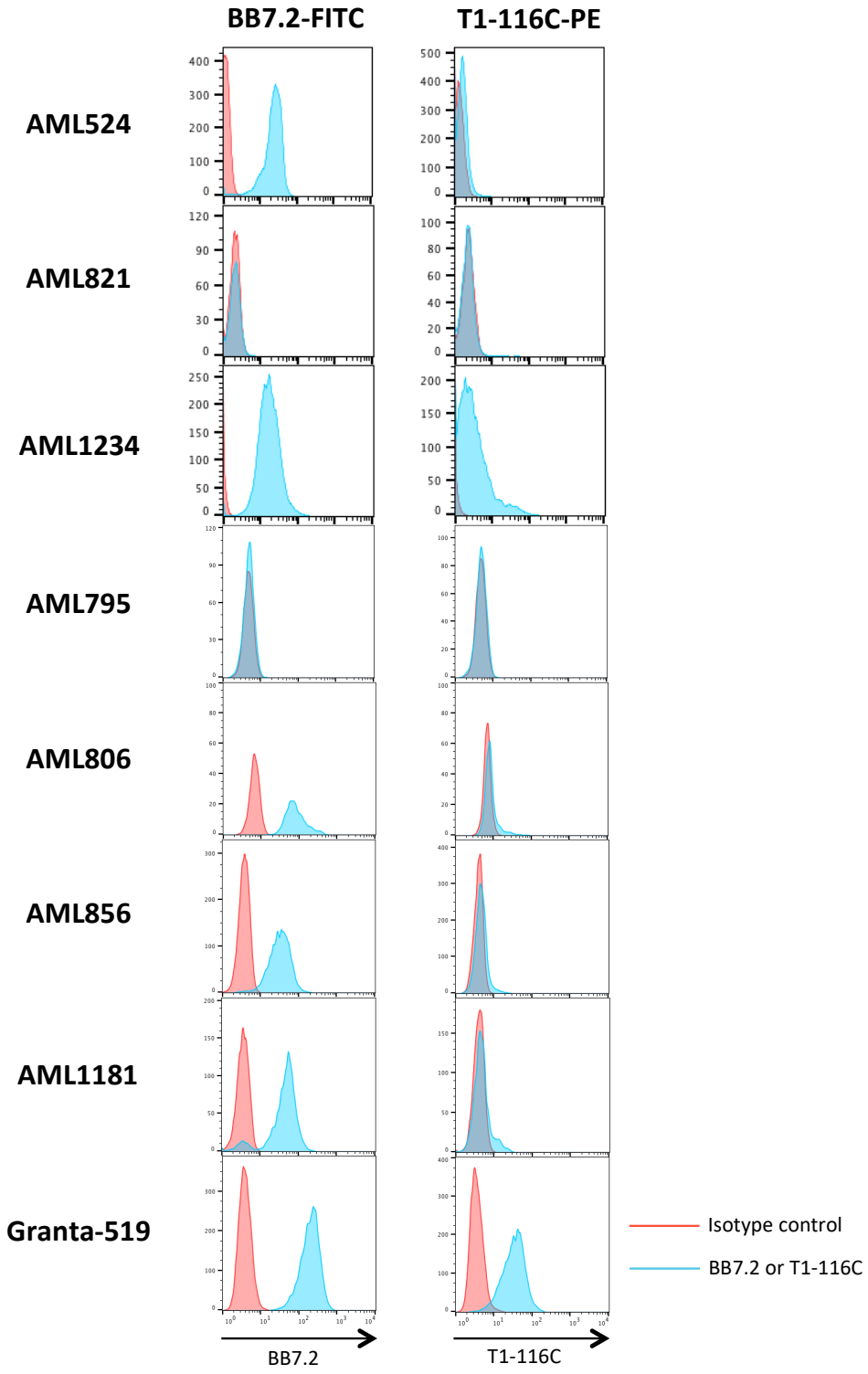

Figure 3.4 – BB7.2 and T1-116C binding profiles of primary AML samples.
Primary AML samples were stained with BB7.2 to determine their HLA-A2 profile (left panels), and with T1-116C (right panels). Samples AML524, AML1234, AML806, AML856, and AML1181, are HLA-A2 positive. Of the HLA-A2-positive samples, only sample AML1234 is T1-116C-positive; the other samples are T1-116C-negative. Red histograms represent the isotype control antibody, and blue histograms represent BB7.2 staining (left panels) or T1-116C staining (right panels). The Granta-519 cell line was used as a positive control because it is both HLA-A2- and T1-116C-positive.

3.2.3 T1-116C staining of primary myeloma samples

Thirteen primary myeloma samples were stained with BB7.2-FITC and T1-116C-PE to determine whether T1-116C could recognise myeloma cells (Figure 3.5). Myeloma samples were obtained from the bone marrow in the posterior iliac crest, but there was no further clinicopathological data available for these patients. Six of the thirteen myeloma samples were HLA-A2-positive (BBH13232, BBH12937, H0283, H0439, H0637 and BBH11468). Of these six samples, one was clearly T1-116C-positive (H0439).

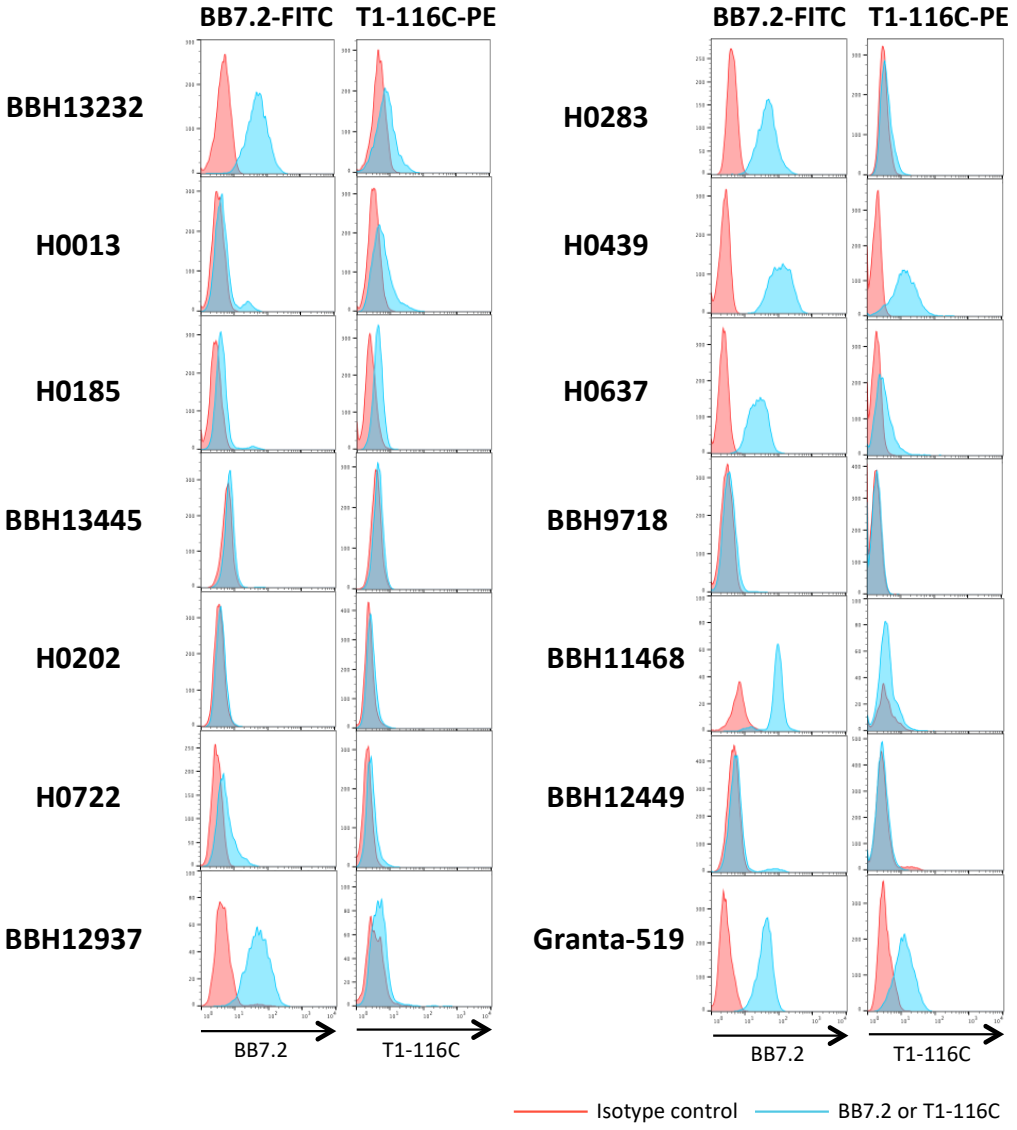

Figure 3.5 – BB7.2 and T1-116C binding profiles of primary myeloma samples.
Primary myeloma samples were stained with BB7.2 to assess their HLA-A2 profile (left panels), and with T1-116C (right panels). Of the thirteen primary myeloma samples, six were HLA-A2-positive (BBH13232, BBH12937, H0283, H0439, H0637 and BBH11468). Of the HLA-A2-positive samples, sample H0439 is also T1-116C-positive. Samples BBH13232 and H0637 are weakly T1-116C positive. Red histograms represent the isotype control antibody, while blue histograms represent BB7.2 staining or T1-116C staining. Granta-519 cells were used as a positive control.

The staining results of the primary AML and myeloma samples are an important step in characterising the T1-116C antibody. They show that T1-116C can recognise primary tumour samples and importantly, these also represent cancers where T1-116C could potentially be clinically applicable. An advantage of using haematological malignancies is that T1-116C binding can be assessed easily using flow cytometry. In these indications T1-116C could be used as a theranostic: both as a diagnostic reagent to stratify patients, and as a therapeutic agent. There is great diversity between patients at the molecular level, even if they present with the same type of cancer, therefore T1-116C will not be suitable for all patients. Patients must be HLA-A2-positive, and within this patient group, all will not present the targeted p53RMP peptide. Therefore the use of T1-116C to stratify patients could be helpful in determining who is likely to benefit from T1-116C therapy. Overall, these results showed that T1-116C can recognise primary AML and myeloma cells, and indicated that further antibody characterisation was worthwhile.

3.3 Validation of alanine and glycine scanning data

Alanine scanning is routinely used in the field to determine the necessity for each amino acid in the target peptide for TCRm antibody binding, as well as for TCR binding. As TCRm antibodies do not make contact with all of the amino acids in the target peptide, it is important to identify which amino acids are part of the TCRm epitope, in order to be able to predict potentially cross-reactive peptides. This step is crucial to characterising the safety of the antibody and to advancing its clinical development.

3.3.1 An initial consensus binding sequence was identified through alanine and glycine scanning

Prior to the start of this DPhil project, our laboratory substituted each amino acid in the p53RMP peptide, one at a time, for either alanine or glycine (Figure 3.6, patent WO2017037440A1). The peptides with the substituted amino acids were synthesised and used to pulse T2 cells. T2 cells were then stained individually with the (i) BB7.2 and (ii) T1-116C antibodies in order to determine the effect that the substitution had on (i) HLA-A2 presentation and (ii) T1-116C binding, using the mean fluorescence intensity (MFI) of antibody staining. The original amino acids at positions where alanine and/or glycine substitution reduced T1-116C binding by more than 50% of the binding observed with the wt p53RMP peptide were considered to be crucial for T1-116C binding and/or MHC-I binding. The initial consensus binding sequence that was derived from the alanine and glycine scanning was: RXPXXAPXV, where X is any natural amino acid. This indicated that the amino acids at positions 1, 3, 6, 7 and 9 were crucial for T1-116C binding, while amino acid variation at the other positions still produced more than 50% of the T1-116C binding observed with the wt p53RMP peptide. One notable finding in both the alanine and glycine scanning data was that both required arginine in position 1; substitution of the amino acid at position 1 for either alanine or glycine completely abrogated T1-116C binding without any reduction in HLA-A2 presentation, indicating that this position is crucial for antibody binding to the p53RMP peptide but not for binding to MHC-I.

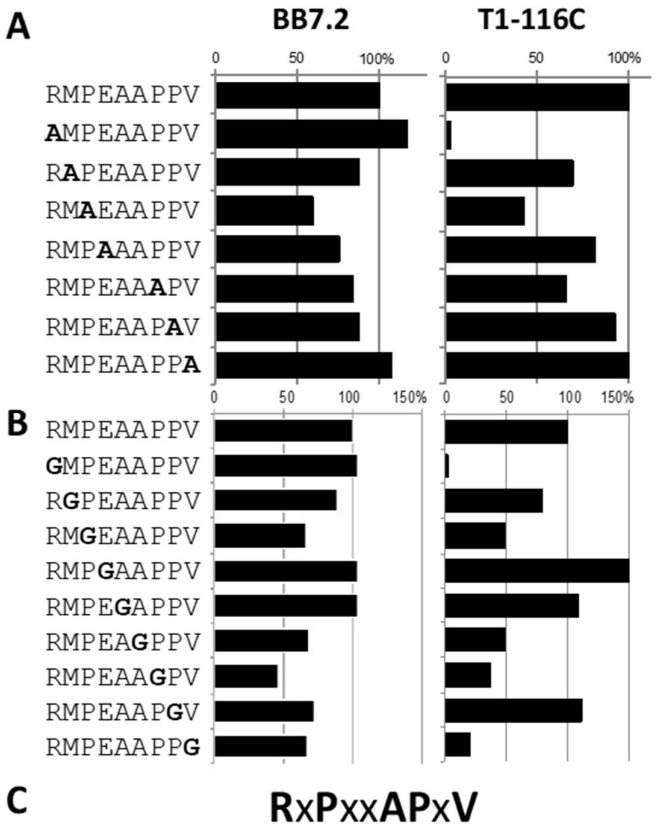

Figure 3.6 – Alanine and glycine scanning identified an initial T1-116C binding consensus sequence.

Individual amino acids in the p53RMP peptide were substituted with either (A) alanine or (B) glycine. The mutant peptides were tested in T2 stabilisation assays. We assessed the effect that the amino acid substitution had on HLA-A2 presentation, using anti-HLA-A2 mAb (BB7.2), and on T1-116C binding. The bar graphs depict the mean fluorescence intensity (MFI) of antibody binding for each substituted peptide relative to the wt p53RMP peptide. The results showed that arginine (R) in position 1 was essential for T1-116C binding, with substitutions at this position having no effect on HLA-A2 presentation. (C) An initial T1-116C consensus recognition motif, RXPXXAPXV, was derived from the amino acid positions in (A) and/or (B) where substitution reduced T1-116C binding to less than 50% of the binding observed with the wt p53RMP peptide. X represents any natural amino acid. This figure originates from the published patent for T1-116C and was performed by other laboratory members prior to the start of this DPhil project.

3.4 T1-116C recognised peptides derived from cancer related proteins that do not match the initial binding consensus sequence

To further test the validity of the RXPXXAPXV consensus sequence, we selected extensively studied cancer T-cell epitopes, which retained the critical arginine (R) in position 1, but which were mismatched at other positions in the consensus sequence. We tested peptides derived from the cancer-related proteins Wilms Tumour 1 (WT1), melanoma-associated antigen MG50 (MG50), tyrosinase (Tyr), melanocyte lineage-specific antigen glycoprotein 100 (GP100) and New York esophageal squamous cell carcinoma-1 (NY-ESO-1) in T2 stabilisation assays (Figure 3.7). We found that T1-116C stained T2 cells presenting each of these peptides to differing degrees despite the fact that they did not fully adhere to the initial binding consensus sequence. These findings suggested that T1-116C could recognise multiple cancer antigens, and that the initial consensus sequence derived from the *in vitro* alanine and glycine scanning alone was insufficient for the prediction of potentially cross-reactive peptides.

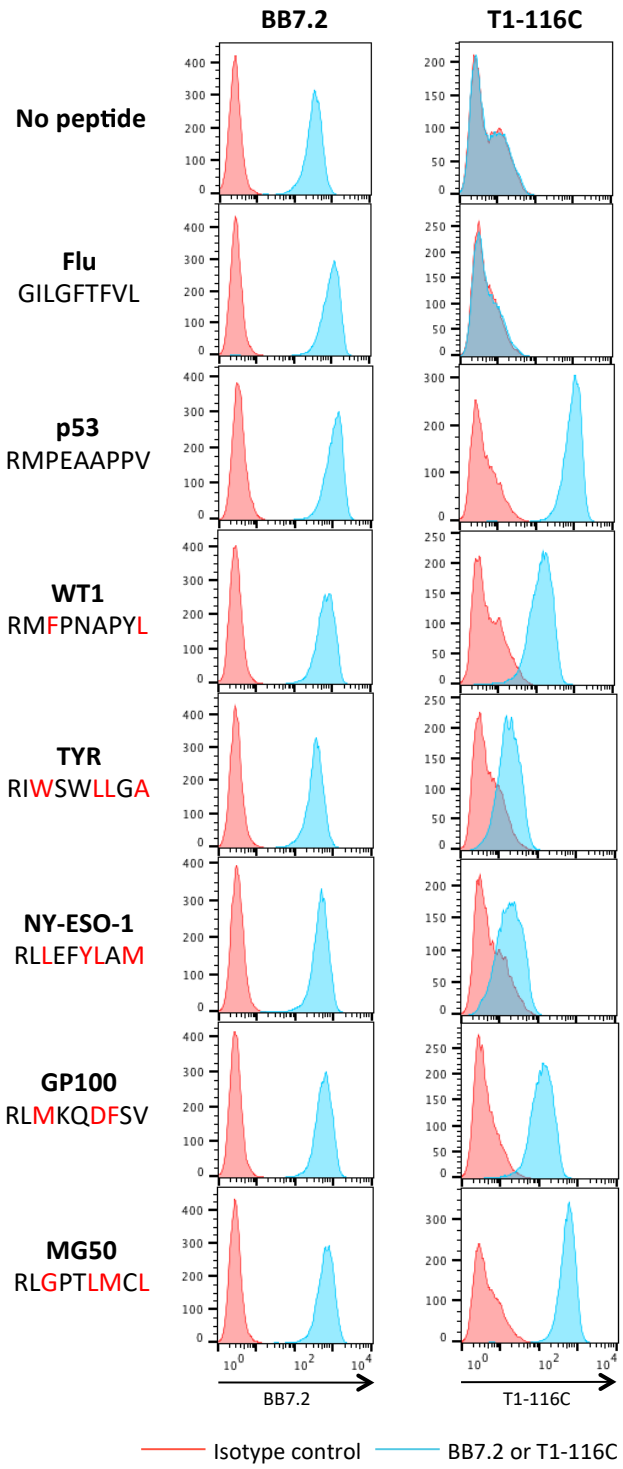

Figure 3.7 – Cancer-related peptides that do not comply with the initial binding consensus sequence were recognised by T1-116C.

Peptides derived from cancer-related proteins WT1, Tyr, NY-ESO-1, gp100, and MG50, which have an arginine at position 1 (R1), but which do not match the initial T1-116C binding consensus sequence fully, were synthesised and tested in T2 stabilisation assays. Peptide-pulsed T2 cells were stained with BB7.2 to assess HLA-A2 presentation, and with T1-116C. Amino acid residues highlighted in red represent those that mismatch the initial consensus sequence. An irrelevant peptide derived from influenza A virus (GILGFTFVL) was used as a negative control. Red histograms represent the isotype control antibody, while blue histograms represent BB7.2 or T1-116C staining. One representative experiment of three independent biological replicates is shown.

3.5 Comprehensive amino acid substitution of the p53RMP peptide identified a more complex binding consensus

To further assess the specificity of T1-116C and to overcome the limitations presented by the alanine and glycine scanning, we performed a comprehensive amino acid substitution where each amino acid within the p53RMP peptide was substituted for each of the remaining 19 natural amino acids. This generated a panel of 172 peptides that were tested in T2 stabilisation assays. The aim of doing a comprehensive scanning mutagenesis was to obtain a more complete specificity profile for T1-116C that would allow us to better predict potentially cross-reactive peptides.

3.5.1 Position 1 in p53RMP is crucial for T1-116C recognition while positions 2 and 9 are important for HLA-A2 peptide presentation

The comprehensive scanning mutagenesis revealed that the arginine in position 1 is absolutely indispensable for T1-116C binding (Figure 3.8). This data indicated that arginine at position 1 comprises part of the T1-116C epitope, because substitutions at position 1 rarely decreased MHC-I presentation. Thus the lack of T1-116C staining was not due to an absence of peptide presentation by MHC-I because the BB7.2 staining showed that the substituted peptides were presented by MHC-I. The lack of T1-116C staining was observed because arginine at position 1 forms a critical part of the T1-116C epitope on the p53RMP peptide (Figure 3.8 and 3.9). Furthermore the results showed that substitutions at positions 2 and 9 had the greatest effect on peptide presentation by HLA-A2 (BB7.2 staining in Figure 3.9A). This is in accordance

with positions 2 and 9 being the anchor residues, which bind to the MHC-I molecule. Certain substitutions at these positions reduced HLA-A2 presentation and consequently also impaired T1-116C binding (Figure 3.9B).

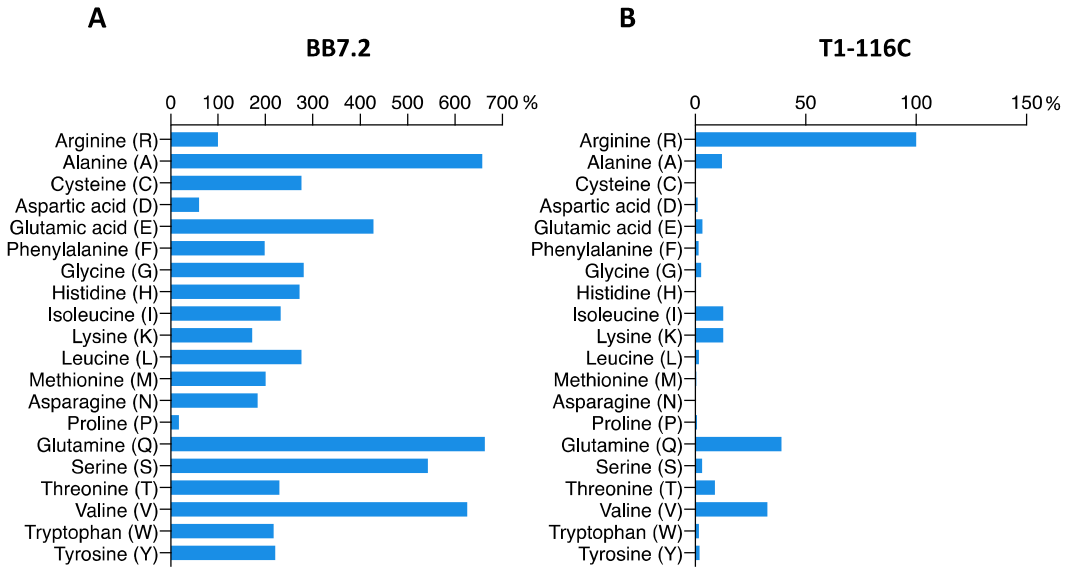

Figure 3.8 – Arginine at position 1 (R1) is crucial for T1-116C binding.
(A) BB7.2 staining of T2 cells pulsed with all of the peptides substituted at position 1 with the amino acid indicated on the y-axis. (B) T1-116C binding profile of peptides substituted at position 1 indicated that arginine in position 1 is crucial for T1-116C binding. The bar graphs represent the MFI of antibody staining compared to the wt p53RMP peptide (the first peptide on the y-axis). The data represent averages of two independent biological replicates.

Figure 3.9 – Comprehensive amino acid substitution identified a complex binding consensus.

Each amino acid within the p53RMP peptide was replaced, one at a time, with each of the remaining 19 natural amino acids, generating 172 peptides for testing in T2 stabilisation assays. Peptide-pulsed T2 cells were stained with (A) anti-HLA-A2 antibody BB7.2 or (B) T1-116C. Antibody binding was categorised, relative to the binding observed with the wt p53RMP peptide, and using the MFI values, as: enhanced (>100%), maintained (50-100%), reduced (25-50%), or severely diminished (<25%). The data represent averages of two independent biological replicates.

3.5.2 Substitutions in the p53RMP peptide that retain T1-116C binding

Table 3.2 summarises the substitutions within the p53RMP peptide that maintain or enhance T1-116C binding. The results of the comprehensive mutagenesis suggested that T1-116C does not bind to the central amino acids that a TCR would commonly recognise (Wucherpfennig, 2010). Indeed, no change at the central position 5 impaired T1-116C binding. The results suggest that T1-116C binds to the N-terminus of the p53RMP peptide. Position 9 at the C-terminus also tolerated little variation from the original sequence, but this is likely due to position 9 being the anchor residue involved in HLA-A2 binding. It is important to note that not all peptides that

will match this new complex consensus sequence will be properly processed in the cell or capable of binding HLA-A2 for presentation at the cell surface. Therefore not all predicted peptides would be functionally cross-reactive and bind T1-116C.

Table 3.2 – Summary of the complex T1-116C binding consensus derived from the comprehensive amino acid substitution.

Position in peptide	Original amino acid	Substitutions that retain T1-116C binding
1	R	None
2	M	A, C, G, I, L, Q, S, T, V, W
3	P	A, C, D, H, L, M, Q, S, V, W, Y
4	E	A, C, D, G, K, M, N, P, Q, S, V
5	A	All
6	A	C, D, E, F, G, H, I, L, M, N, P, Q, S, T, V, W, Y
7	P	A, C, D, E, F, H, I, K, L, M, Q, S, T, V, W, Y
8	P	A, C, E, F, G, H, I, L, M, N, Q, R, S, V, W, Y
9	V	A, C, I, L

The table shows the amino acid substitutions at each position within p53RMP that retain at least 50% of the T1-116C binding observed with the wt p53RMP peptide.

3.6 Discussion

As the majority of the previous T1-116C experiments had been performed *in vitro* using cancer cell lines, it was important to establish that T1-116C could recognise primary tumour cells before pursuing its further development. The laboratory previously found that advantageously T1-116C does not recognise HLA-A2-positive healthy peripheral blood mononuclear cells (PBMCs) (patent WO2017037440A1). Staining of primary AML and myeloma tumour samples confirmed that T1-116C can

recognise primary cells derived from both haematological malignancies, thereby showing promise for its clinical application in these diseases. Optimising the staining protocol for these experiments also revealed that double staining with the directly conjugated BB7.2 and T1-116C antibodies simultaneously potentiated T1-116C staining on cells that were negative when stained only with T1-116C, perhaps as a result of BB7.2 stabilising HLA-A2 cell surface expression. Double antibody labelling with TCRm antibodies that recognise an antigen comprising a dual epitope, such as T1-116C, was not pursued further in order to avoid inconsistencies in staining.

The primary AML and myeloma sample sizes were small; we therefore focused primarily on flow cytometry analysis in this initial experiment, in order to determine whether any HLA-A2-positive samples were also T1-116C-positive. In future experiments, it would be important to obtain more samples, particularly those with higher cell counts, in order to cross-validate HLA-A2 and p53 expression in the primary cells using alternative methods in addition to flow cytometry. For example genotyping could be performed to determine the HLA haplotype of the patient, and cellular p53 expression could be assessed using immunocytochemistry. This would be particularly important for samples that are found to be positive for both BB7.2 and T1-116C by flow cytometry, as it would provide an alternative method to confirm the HLA-A2 and p53 expression profiles of the primary samples.

As TCRm antibodies recognise a dual antigen epitope composed of the MHC-I molecule and the bound peptide, we attempted to define the peptide specificity of T1-116C in order to assess its safety. Alanine and glycine scanning of the p53RMP

peptide had previously defined an initial consensus binding sequence. However, we experimentally verified additional target peptides that did not conform to this initial consensus but were still recognised by T1-116C. We therefore proceeded to perform a more comprehensive scanning mutagenesis, which has given us novel insight into the T1-116C epitope, revealing that the consensus sequence is not as conservative as originally concluded based on only the alanine and glycine scanning data.

Scanning mutagenesis is an established technique that is used to define the role that individual amino acids play within a protein-protein or protein-substrate interaction (Cunningham & Wells, 1989; Weiss *et al.*, 2000). By mutating individual residues at the interface of protein-protein interactions, it is possible to deduce the contribution of a particular residue to protein function. In particular, alanine scanning is widely used due to its favourable biological and chemical properties. Alanine is a non-bulky amino acid that only has a methyl group; therefore alanine substitution removes any side chain that may have been presented by the original amino acid beyond the β-carbon that forms part of the peptide backbone, and so alanine does not change the conformation of the backbone (Lefèvre *et al.*, 1997). This allows the role of individual side chains to be determined, and alanine substitution also does not introduce electrostatic or steric effects (Lefèvre *et al.*, 1997). It was first used to determine the residues contributing to the interaction of human growth hormone with the extracellular domain of its receptor (Cunningham *et al.*, 1989).

In the epitope mapping of TCRm antibodies, it is primarily alanine scanning that is used to determine the key residues in the target peptide that contribute to TCRm

binding (Sergeeva *et al.*, 2011; Dao *et al.*, 2013; Zhao *et al.*, 2015; Chang *et al.*, 2017; Lowe *et al.*, 2017; Ahmed *et al.*, 2018). One of the more extensive substitution analyses, which was not only limited to alanine substitutions, was reported by Ataie *et al.* in describing the crystal structure of ESK1 (a TCRm targeting the WT1 peptide RMFPNAPYL presented by HLA-A2) (Ataie *et al.*, 2016). They used their structural analysis to identify two potentially cross-reactive peptides, which they then validated experimentally (Ataie *et al.*, 2016). In addition to this, they also tested approximately two dozen substituted peptides in T2 assays, where they focused on analysing the effect of various substitutions at certain positions within the peptide that were determined to interact with ESK1 from their crystal structure data (Ataie *et al.*, 2016).

Alanine scanning, followed by a comprehensive "X-scanning", the term used to describe the amino acid substitution approach using each of the remaining 19 naturally occurring amino acids (similar to what we have described in this thesis), has been used in the specificity and safety assessment of immune-mobilising monoclonal TCRs against cancer (ImmTACs) (Harper *et al.*, 2018). Harper *et al.* used peptide-pulsed T2 cells to assess whether any of the substituted peptides trigger T-cell activation and interferon-γ (IFN-γ) release. The X-scan revealed that ImmTAC-nyeso (ImmTAC targeting the NY-ESO-1 peptide, SLLMWITQC, presented by HLA-A2) recognised peptides with substituted amino acids that had been missed by the initial alanine scanning. Thus a more exhaustive TCR motif assessment is achieved through the X-scan, and this motif was then analysed *in silico* using their in-house database of mass spectrometry-identified peptides that are presented by human cell lines. Any

peptides that match the TCR binding motif, and that have been shown to be presented by HLA-A2, are then tested further due to the risk of cross-reactivity. The alanine scanning and X-scan approach used by Harper *et al.* is similar to the safety and specificity testing that we have performed for T1-116C. As we were assessing the specificity of a naked antibody, we analysed T1-116C binding to peptide-pulsed T2 cells by flow cytometry, whereas Harper *et al.* analysed ImmTAC-nyeso-driven T-cell activation because the ImmTAC molecules function by redirecting T cells. Similar to Harper *et al.*, we also used *in silico* analysis to identify potentially cross-reactive peptides, which we then validated *in vitro* (Chapter 4).

Although more laborious, we have shown that performing a comprehensive scanning mutagenesis has provided a more complete definition of the specificity of T1-116C than alanine and glycine scanning alone. Substitutions can impair T1-116C peptide recognition through impairing antibody binding and/or MHC-I presentation. This has important safety implications because it enables the identification of potentially cross-reactive peptides, which would have been overlooked based on the alanine and glycine scanning alone.

Re-examining the sequences of the five cancer-related peptides from Figure 3.7 after obtaining the results from both the alanine and glycine scanning and the comprehensive scanning, shows that the comprehensive scanning mutagenesis defined the consensus binding sequence more fully than the alanine and glycine scanning. However it still does not predict all of the peptides that can bind T1-116C (Table 3.3). All five cancer-related peptides mismatch the initial consensus sequence

at multiple residues, whereas only three mismatch the new complex consensus sequence at a single residue. Although the complex consensus is more accurate, this indicates that even with the more comprehensive scanning mutagenesis, it is still difficult to precisely predict potentially cross-reactive peptides.

Table 3.3 – Cancer-related peptides and their sequence conformity to the initial and to the complex binding consensus sequences.

Protein	Peptide	Initial consensus RXPXXAPXV	Complex consensus
WT1	RMFPNAPYL	RMFPNAPYL	RMFPNAPYL
GP100	RLMKQDFSV	RLMKQDFSV	RLMKQDFSV
Tyrosinase	RIWSWLLGA	RIWSWLLGA	RIWSWLLGA
NY-ESO-1	RLLEFYLAM	RLLEFYLAM	RLLEFYLAM
MG50	RLGPTLMCL	RLGPTLMCL	RLGPTLMCL

The sequence of each of the peptides derived from the five different cancer-related proteins is shown. Their conformity to the initial binding consensus derived from the alanine and glycine scanning is summarised, with any non-conforming amino acids highlighted in red. Amino acids that do not conform to the more complex consensus derived from the comprehensive scanning are highlighted in blue.

It is also important to note that the approach we used will fail to identify the consequences of multiple amino acid substitutions within p53RMP. To study the effect of amino acid substitutions at multiple residues within the p53RMP peptide on T1-116C binding, combinatorial peptide libraries could potentially be used in the positional scanning format (positional scanning synthetic combinatorial peptide libraries, PS-SCLs). PS-SCLs can be synthesised for peptides of different lengths, including nonamers such as p53RMP (Pinilla *et al.*, 1995). The library consists of peptide mixtures: in each mixture, one amino acid at a specific position remains

constant while the amino acids at the remaining positions vary with each of the 20 natural amino acids (Pinilla *et al.*, 1995). PS-SCLs have been used to identify peptides and to study the specificity of CD8+ T cells, for example to identify peptides recognised by tumour-reactive CTLs or to study TCR degeneracy (Pinilla *et al.*, 2001; Wooldridge *et al.*, 2012). PS-SCLs could potentially be used to assess the specificity of TCRm antibodies by pulsing cells, such as T2 cells, with peptide library mixtures and evaluating TCRm specificity. However, this approach requires multiple rounds of peptide synthesis and testing once antibody-binding amino acids at each position are identified in order to test all possible combinations of the identified amino acids and narrow down the search to a single or a few cross-reactive peptides (Gray & Brown, 2014). A disadvantage of this approach is that the peptide libraries are synthesised without consideration of peptide loading on MHC-I, therefore it is important to assess whether any identified peptides can be presented on HLA-A2 and to determine whether they occur naturally and pose a genuine safety risk.

Given that the specificity of T1-116C is not as stringent as suggested by the initial consensus sequence, we cannot be certain that the T1-116C staining observed in the primary tumour samples is p53-specific. For example, WT1 expression, and also the presentation of the T1-116C cross-reactive RMFPNAPYL peptide derived from WT1, have been reported in both AML and myeloma (Scheibenbogen *et al.*, 2002; Rezvani *et al.*, 2005; Tyler *et al.*, 2013; Koehne, 2017; Koehne *et al.*, 2017). WT1 has been described as an immunotherapeutic target for these indications and the RMFPNAPYL peptide is an important epitope for the development of such therapies (Koehne, 2017). Therefore we cannot rule out the possibility that the T1-116C binding

observed in the primary AML and myeloma samples resulted from T1-116C binding to the HLA-A2-presented WT1-derived peptide rather than the p53RMP peptide. It is also possible that both peptides were recognised, or that other cross-reactive peptides were recognised. WT1 was prioritised as the top target for cancer immunotherapy in the National Cancer Institute Pilot study (Cheever *et al.*, 2009), and T1-116C could potentially be used to detect the RMFPNAPYL peptide for research applications.

As T1-116C recognises a dual antigen target, it is important to consider the contribution of both the HLA-A2 molecule and the peptide to T1-116C binding, in order to better understand T1-116C specificity. The MHC-I molecule is a heterodimer composed of a heavy chain (which consists of three α domains) and a light chain (β2M) (Neefjes *et al.*, 2011). MHC-I molecules are unstable under physiological conditions. Interaction with a peptide stabilises MHC-I and is therefore critical for the folding and assembly of the MHC-I molecule, enabling its transport to the cell surface (Rock & Goldberg, 1999). As the MHC-I heavy chain folds, it forms a groove that will bind peptides that are 8 to 11 amino acid residues long (Neefjes *et al.*, 2011). Peptides bind to the MHC-I groove principally with their N- and C- terminal residues, as well as with the side chains of some central residues (Rock *et al.*, 2004). Thus, while the peptides are similar in length, they can differ significantly in sequence, particularly in the residues that do not bind to the MHC-I molecule. Through this system, a small number of different MHC-I molecules can present a much larger number of peptides to CD8+ T cells, which express TCRs that are specific for both the MHC-I alleles and the bound peptides (Rock *et al.*, 2004).

It is clear that arginine at position 1 of the peptide forms part of the T1-116C epitope. This is similar to ESK1, where solving its crystal structure with its target showed that ESK1 binds HLA-A2 close to the arginine at position 1 (R1) in the RMFPNAPYL peptide, and it contacts two residues at the N-terminus of the peptide: R1 and proline at position 4 (P4) (Ataie *et al.*, 2016). Substitutions at position 1 highlighted that the positively-charged R1 is crucial for ESK1 binding: substitutions with an uncharged but sterically similar amino acid to arginine (citrulline), or with amino acids that are also positively charged but chemically different (lysine and histidine) decreased or eliminated ESK1 binding. The part of ESK1 that binds R1 is highly negatively charged, thus the positively charged arginine balances the electrostatic forces by providing the ideal countercharge (Ataie *et al.*, 2016). It is possible that similar electrostatic forces govern the T1-116C binding to R1 of the p53RMP peptide and this could be tested in the future using a peptide with citrulline at position 1.

Our results suggested that the contact residues of T1-116C in the HLA-A2 molecule are based around the N-terminus of the peptide. BB7.2 binds HLA-A2 at the C-terminus of the α2 domain, which is in the vicinity of the N-terminus of the peptide in the HLA-A2 peptide-binding groove (Hogan & Brown, 1992). Thus it is possible that the HLA-A2 epitopes of both T1-116C and BB7.2 are in close proximity. The simultaneous staining of primary AML samples with T1-116C and BB7.2 suggested that BB7.2 binding can modulate T1-116C binding. It is possible that BB7.2 binding to its epitope causes a conformational change in the HLA-A2 molecule that somehow

modulates T1-116C binding, perhaps by making the T1-116C epitope on HLA-A2 more easily accessible to T1-116C, but at the expense of losing peptide specificity and displaying non-specific binding as a result.

Sergeeva *et al.* mapped the HLA-A2 epitope of their PR-1-targeting TCRm, 8F4, by pulsing T2 cells with the target peptide and then staining them simultaneously with 8F4 and with BB7.2 mAb or MA2.1 (a different anti-HLA-A2 mAb) at increasing concentrations (Sergeeva *et al.*, 2011). They found that 8F4 binding to PR1-pulsed T2 cells was partially blocked by BB7.2 or MA2.1. They explained that because the HLA-A2 epitope of BB7.2 includes a residue at position 169, and that of MA2.1 includes a residue at position 170, both of which are at the C-terminus of the α2 domain (Hogan & Brown, 1992), it is possible that these residues also form part of the 8F4 TCRm epitope on HLA-A2. The amino acid at position 1 in the 8F4 target peptide was also crucial for 8F4 binding, thus emphasising that 8F4 binding was focused on the N-terminus of the peptide and the α2 domain of the HLA-A2 molecule (Sergeeva *et al.*, 2011). In contrast to their findings, simultaneous staining with T1-116C and BB7.2 did not decrease T1-116C binding. Nevertheless, without the crystal structure of T1-116C with its target peptide and HLA-A2, it is difficult to draw conclusions about its target epitopes.

HLA-A2 is the most extensively studied MHC-I allele and the most common allele in Caucasians. The anchor residues in HLA-A2 are at position 2 and position 9 of the peptide, where it has been found that the dominant anchoring amino acids are: leucine at position 2, and leucine or valine at position 9 (Barouch *et al.*, 1995). This is

consistent with the data obtained from the comprehensive peptide scanning, where these amino acids at positions 2 and 9 enable peptide presentation by HLA-A2. The different subtypes of HLA-A2 can differ by as little as one amino acid in the peptide-binding groove, and this can determine the peptide motif that can be presented by a specific subtype (Barouch *et al.*, 1995; Sudo *et al.*, 1995). The crystal structure of the ESK1 TCRm antibody with its WT1-derived target peptide RMFPNAPYL, revealed that ESK1 binds an epitope on HLA-A*02:01 that is conserved among multiple HLA-A2 subtypes, thereby expanding its application to a wider population of patients (Ataie *et al.*, 2016). Similar findings were reported with the LMP2A-targeting TCRm, which in addition to recognising HLA-A*02:01, also recognised HLA-A*02:02, HLA-A*02:04 and HLA-A*02:06 (Ahmed *et al.*, 2018). The HLA-A2 suballeles expressed by the primary AML and myeloma samples in our experiments were unknown. The BB7.2 antibody recognises at least five different HLA-A2 subtypes, including HLA-A*02:01, HLA-A*02:02, HLA-A*02:03, HLA-A*02:05 and HLA-A*02:06 (Hilton & Parham, 2013). Thus the primary cancer samples that we tested would be BB7.2-positive if they expressed any of these subtypes, and not only if they expressed HLA-A*02:01. Therefore it is possible that T1-116C may also display specificity for multiple HLA-A2 subtypes like the two aforementioned TCRm antibodies. This would be an advantage, as it would expand the number of patients that could benefit from therapy with T1-116C, provided that the different subtypes can also present the p53RMP peptide.

Methods to test the suballele specificity include the one employed by Ahmed *et al.*, who used artificial antigen-presenting cells (APCs) pulsed with the target peptide of

their TCRm (Ahmed *et al.*, 2018). Six different artificial APC lines were tested, each stably expressing a different HLA-A2 subtype, and the results were analysed using flow cytometry. Whereas Ataie *et al.* used modelling to predict six HLA-A2 subtypes that would retain both ESK1 binding and RMFPNAPYL peptide binding. They then validated these experimentally, using biotinylated, immobilised HLA subtype and RMFPNAPYL peptide complexes and measuring binding affinity of ESK1 by surface plasmon resonance (Ataie *et al.*, 2016). It will be important to study the suballele specificity of T1-116C, perhaps using similar approaches to these, in order to further define its specificity, not only for the p53RMP peptide but also for the HLA-A*02:01 subtype.

The *in vitro* techniques available for the epitope mapping of TCRm antibodies are limited because of their dual antigen epitope and the requirement for human MHC-I. Although the comprehensive scanning has provided valuable information about T1-116C specificity, further work is required to better define its epitope. As mentioned above, another important piece of information that can be extracted from crystal structures relates to the binding orientation of the antibody-peptide-MHC-I complex. The crystal structure of ESK1 revealed that it binds its target at the N-terminus (Ataie *et al.*, 2016). In contrast, the crystal structure of Fab-Hyb3 with its MAGE-A1 peptide presented by HLA-A1 revealed that Fab-Hyb3 recognises the C-terminus of the peptide and it also has a different binding orientation to ESK1 (Hülsmeyer *et al.*, 2005). There is also a report of a different binding orientation exemplified by the crystal structure of a Fab antibody that targets the NY-ESO-$1_{157–165}$ peptide presented by HLA-A*02:01 (Stewart-Jones *et al.*, 2009). This Fab antibody binds in a diagonal

orientation across the peptide presented by the MHC-I molecule, thus making contact with residues in the central portion of the peptide (Stewart-Jones *et al.*, 2009). This last example simulates the canonical binding orientation of TCRs, which generally bind in a diagonal conformation that allows numerous contacts with the peptide, and in particular, with the central residues of the peptide (Wucherpfennig, 2010). TCRm antibodies can bind less than half of the peptide with high affinity, whereas TCRs have low affinity and their most diverse CDRs are focused over the length of the peptide, rather than at the termini (Wucherpfennig, 2010). Thus, while TCRs tend to bind only in a canonical diagonal orientation, TCRm antibodies display greater variation by employing both canonical and non-canonical binding orientations wherein the peptide and the MHC-I molecule contribute differing amounts to TCRm binding. From our current results it is likely that T1-116C binding is focused at the N-terminus of the peptide. If there were a possibility to solve the crystal structure of T1-116C with its target in the future, it would allow us to visualise the orientation of T1-116C binding to its target and the key contact residues in both the peptide and the MHC-I molecule.

The ability of T1-116C to target multiple tumour antigens could be an advantage as it could counter the immune evasion mechanisms of cancers, which under the selective pressure of therapy, can lose their antigenicity through a process known as cancer immunoediting (Beatty & Gladney, 2015). For this reason, combination therapies are effective in the treatment of cancer, and the targeting of multiple cancer antigens combined in one TCRm antibody such as T1-116C could be advantageous. Additionally, this could expand T1-116C applicability to a wider range

of cancers and patients. However, even if a TCRm antibody were to target multiple tumour antigens, this would not prevent immune evasion from occurring through the downregulation of MHC-I. Therefore combination therapy with two therapeutics that have distinct mechanisms of action is likely to be more effective (Campoli & Ferrone, 2008). Moreover, an important disadvantage of targeting multiple tumour antigens and potentially a wide variety of other normal antigens, as predicted by the comprehensive scanning, is that predicting specificity becomes more difficult and assembling a safety profile becomes precarious. These are likely to be obstacles in obtaining regulatory approval for testing T1-116C in humans.

In conclusion, while the comprehensive amino acid scanning has defined the specificity of T1-116C for the p53RMP peptide more accurately than alanine and glycine scanning alone, it has also revealed the possibility for multiple cross-reactive peptides. These will have to be identified and tested in order to further assess the specificity of T1-116C and the implications for its clinical development.

4 Validating the Specificity and Safety of T1-116C

4.1 Introduction

The findings from investigating the specificity of T1-116C in the previous chapter revealed that its specificity and safety must be assessed further, and potentially through alternative methods than the scanning mutagenesis used thus far. The comprehensive scanning mutagenesis demonstrated that alanine and glycine scanning alone is insufficient for predicting cross-reactive peptides. Importantly, it revealed that the T1-116C consensus sequence is less conservative than initially thought and therefore the possibility for variation in the target peptide sequence is far greater than originally anticipated. Potentially cross-reactive T1-116C epitopes presented on healthy cells could pose a serious safety risk.

As it is not possible to test all potentially cross-reactive peptides and human cell types *in vitro*, *in silico* analysis of the data can be used to identify the most relevant peptides that should be prioritised for further experimental validation. For example, it is important to assess whether the peptides can be properly processed and presented by HLA-A2. Furthermore, the tissue expression patterns of the proteins that the identified peptides originate from also give an idea of the safety risk posed by cross-reactivity with specific peptides. For example, the safety risk posed by cross-reactivity with a protein that is ubiquitously expressed could be anticipated to be more serious than that posed by cross-reactivity with a protein whose expression is

restricted to one tissue (unless that tissue itself performs a vital function and the toxicity caused cannot be managed clinically).

4.2 Characterisation of T1-116C epitopes using the Immune Epitope Database

In silico screening of an epitope database is a practical method available for the identification of a large quantity of cross-reactive peptides that match the consensus sequence and that are known to be processed and presented by MHC-I. One such database is the Immune Epitope Database (IEDB), which logs experimentally validated MHC-I-presented peptides (as well as MHC-II peptides). It is possible to search the database for peptides presented by specific HLA haplotypes. By using high-throughput approaches such as mass spectrometry analysis of peptides eluted from MHC-I purified from healthy and disease samples, the sequence of individual bound peptides can be identified (Hunt *et al.*, 2007; Stern, 2007). This has increased the volume of data available in databases such as the IEDB, and can be used to inform the way that *in vitro* experiments are conducted. An IEDB search could be used to identify all reported peptides that are presented by HLA-A*02:01 and that match the complex consensus binding sequence derived form the T1-116C comprehensive scanning mutagenesis (www.iedb.org).

We searched the IEDB for HLA-A*02:01-restricted peptides that match the complex T1-116C consensus sequence and identified 271 potentially cross-reactive peptides. The 271 peptides are listed in Appendix A. The peptides are derived from a diverse

range of antigens, which are broadly expressed across different tissues. Some of the antigens that the peptides are derived from are tissue-specific, while others are ubiquitously expressed in humans, and some are also derived from antigens that are associated with cancer. The expression and functional profiles of 25 potentially cross-reactive and widely expressed antigens, whose peptide sequences are conserved in mice, are summarised in Table 4.1. With the aim of subsequently testing T1-116C safety *in vivo* in an HLA-A2 transgenic mouse model, it was also important to establish whether the peptides identified from the IEDB search were conserved in mice. Fortunately, approximately 60% of the peptides identified through the IEDB search were conserved in mice.

Table 4.1 - Expression and functional profiles of widely expressed normal tissue antigens identified in the IEDB search.

Gene	Protein	Peptide	Expression	Molecular function
MTF2	Metal-response element-binding transcription factor 2	RVPPVPPNV	Ubiquitously expressed	Chromatin regulator involved in DNA binding
USP9Y	Probable ubiquitin carboxyl-terminal hydrolase FAF-Y	RLWGEPVNL	Ubiquitously expressed	Involved in Ubl conjugation pathway
DUSP2	Dual specificity protein phosphatase 2	RLDEAFDFV	Expressed in haematopoietic tissues	Regulates mitogenic signal transduction
LMNA	Prelamin-A/C	RLADALQEL	Ubiquitously expressed	Intermediate filaments that provide structural stability
INPP5B	Type II inositol 1,4,5-trisphosphate 5-phosphatase	RLVGIMLLL	Expressed in most tissues with lower levels in adipose tissue	Hydrolase involved in the regulation of calcium signalling
KANK2	KN motif and ankyrin repeat domain-containing protein 2	RLLDYVVNI	Strongly expressed in cervix, colon, heart, kidney and lung. Also in kidney	Involved in the regulation of transcription and apoptosis
SNX4	Sorting nexin-4	RVADRLYGV	Expressed across most tissues with highest levels in placenta and spleen	Involved in protein transport

Gene	Protein	Peptide	Expression	Molecular function
ARHGAP30	Rho GTPase activating protein 30	RLYDKFAEA	Expressed across various tissues, with highest expression in lymph nodes, tonsil and spleen	Involved in GTPase activation
TRIP12	E3 ubiquitin-protein ligase TRIP12	RLLDTNPEI	Expressed across most tissues. Enriched in testis	Involved in DNA damage repair and in the Ubl conjugation pathway
CBX6	Chromobox protein homolog 6	RISDVHFSV	Expressed across most tissues	Chromatin regulator involved in transcription regulation
MCM7	DNA replication licensing factor MCM7	RLAQHITYV	Expressed in highly proliferative cells in the immune organs, gastrointestinal tract and skin	Involved in the cell cycle and DNA replication
G6PC2	Glucose-6-phosphatase 2	RLLCALTSL	Expressed in pancreas	Involved in gluconeogenesis
NIPBL	Nipped-B-like protein	RLMDNSTSV	Ubiquitously expressed	Activator involved in transcription regulation
VRK2	Serine/threonine-protein kinase VRK2	RMLDVLEYI	Ubiquitously expressed	Regulates several signal transduction pathways and is involved in host-virus interaction

Gene	Protein	Peptide	Expression	Molecular function
KRT18	Keratin, type I cytoskeletal 18	RLAADDFRV	Colon, placenta, liver, exocervix and glandular epithelium	Involved in transport and filament reorganisation
AKAP8L	A-kinase anchor protein 8-like	RMWEDPMGA	Ubiquitously expressed	mRNA processing and transcription
BRD4	Bromodomain-containing protein 4	RLAELQEQL	Ubiquitously expressed	Chromatin regulator
TRRAP	Transformation/transcription domain-associated protein	RVYERLLYV	Ubiquitously expressed	Activator and chromatin regulator involved in transcription
UBE2L3	Ubiquitin-conjugating enzyme E2 L3	RLMKELEEI	Ubiquitous, with highest expression in testis	Transcription regulation
NFIB	Nuclear factor 1 B-type	RQADKVWRL	Ubiquitously expressed	Activator involved in DNA replication and transcription
MSH6	DNA mismatch repair protein Msh6	RLLSKIHNV	Ubiquitously expressed	Involved in DNA damage repair

Gene	Protein	Peptide	Expression	Molecular function
KDM1A	Lysine-specific histone demethylase 1A	RLLEATSYL	Ubiquitously expressed	Transcription regulation
VAMP1	Vesicle-associated membrane protein 1	RLQQTQAQV	Enriched in nervous system, skeletal muscle and adipose tissue. Found in gastrointestinal tract	Involved in the targeting and/or fusion of transport vesicles to their target membrane
PRKD2	Serine/threonine-protein kinase D2	RQASLSISV	Ubiquitously expressed but enriched in lymphoid tissues	Kinase involved in adaptive immunity, angiogenesis and cell adhesion
ACTB	Actin, cytoplasmic 1	RMQKEITAL	Ubiquitously expressed in all eukaryotic cells	Involved in various types of cell motility

The expression and molecular function of antigens from a selection of 25 peptides identified in the IEDB search, whose peptide sequence is conserved in mice, are listed. UniProt and The Human Protein Atlas databases were used to acquire information on expression and molecular function.

4.2.1 Validation of T1-116C recognition of predicted murine cross-reactive epitopes derived from normal tissue antigens

The next step after identifying the potentially cross-reactive peptides was to further test the validity of the consensus sequence by verifying that T1-116C recognises these peptides *in vitro*. It would be time-consuming to test all 271 identified peptides *in vitro*, and we have already demonstrated that additional peptides that do not fully match the consensus can be recognised. Therefore, we selected the 25 peptides listed in Table 4.1 above, which are conserved in mice and which are derived from proteins that are broadly expressed in normal human tissues.

As a future aim was to test the safety of the T1-116C antibody *in vivo*, we also decided to use the humanised T1-116C antibody in this experiment. Thus the T1-116C antibody was used in two formats: (i) the chimeric format (murine T1-116C fused to human IgG1), which was used to generate all of the data thus far, and (ii) the humanised format (T1-116CV1), which will be used in future *in vivo* studies as this format is more clinically relevant. The T1-116C antibody was humanised by CDR grafting (Lonza, UK) prior to the start of this DPhil project. Of the sixteen humanised variants produced, four antibodies retained comparable affinity and peptide specificity to the parental antibody. Two variants, T1-116CV1 and T1-116CV2, also displayed binding to cancer cell lines and T2 cells pulsed with glycine- or alanine-substituted peptides that was comparable to that of the parental antibody. T1-116CV1 was selected as the lead candidate as it had the most similar affinity and specificity profile to the parental antibody.

The 25 selected peptides were each tested in T2 stabilisation assays and the staining intensity of T1-116C, T1-116CV1 and BB7.2 was categorised as strong (+++), medium (++), weak (+) or no (-) binding (Table 4.2). Histograms showing the antibody staining of T2 cells pulsed with the 25 peptides are presented in Appendix B. Notably, a small number of peptides did not bind HLA-A2, as indicated by the absence of increased BB7.2 staining. The two different formats of the T1-116C antibody performed similarly with regard to their peptide recognition profile (Table 4.2). The peptides were spread more or less evenly between the four labelling intensity categories, and approximately a quarter of the peptides were not recognised by T1-116C or T1-116CV1, despite matching the consensus sequence. Thus, even with the *in silico* analysis derived from the comprehensive scanning, it was still not possible to precisely predict individual functionally T1-116C cross-reactive epitopes.

Table 4.2 - T1-116C binding of peptides retrieved from the IEDB.

Gene	Protein	Peptide	T1-116C	T1-116CV1	BB7.2
TP53	**Cellular tumor antigen p53**	**RMPEAAPPV**	+++	+++	+++
MTF2	Metal-response element-binding transcription factor 2	RVPPVPPNV	+++	+++	+++
USP9Y	Probable ubiquitin carboxyl-terminal hydrolase FAF-Y	RLWGEPVNL	+++	+++	+++
DUSP2	Dual specificity protein phosphatase 2	RLDEAFDFV	+++	+++	+++
LMNA	Prelamin-A/C	RLADALQEL	+++	+++	+++
INPP5B	Type II inositol 1,4,5-trisphosphate 5-phosphatase	RLVGIMLLL	+++	++	+++
KANK2	KN motif and ankyrin repeat domain-containing protein 2	RLLDYVVNI	++	++	+++
SNX4	Sorting nexin-4	RVADRLYGV	++	++	++
ARHGAP30	Rho GTPase activating protein 30	RLYDKFAEA	++	++	++

Gene	Protein	Peptide	T1-116C	T1-116CV1	BB7.2
TRIP12	E3 ubiquitin-protein ligase TRIP12	RLLDTNPEI	++	++	++
CBX6	Chromobox protein homolog 6	RISDVHFSV	++	++	++
MCM7	DNA replication licensing factor MCM7	RLAQHITYV	++	+	++
G6PC2	Glucose-6-phosphatase 2	RLLCALTSL	+	+	++
NIPBL	Nipped-B-like protein	RLMDNSTSV	+	+	++
VRK2	Serine/threonine-protein kinase VRK2	RMLDVLEYI	+	+	++
KRT18	Keratin, type I cytoskeletal 18	RLAADDFRV	+	+	+
AKAP8L	A-kinase anchor protein 8-like	RMWEDPMGA	+	+	++
BRD4	Bromodomain-containing protein 4	RLAELQEQL	+	+	+
TRRAP	Transformation/transcription domain-associated protein	RVYERLLYV	+	+	++
UBE2L3	Ubiquitin-conjugating enzyme E2 L3	RLMKELEEI	+	+	+
NFIB	Nuclear factor 1 B-type	RQADKVWRL	-	-	+
MSH6	DNA mismatch repair protein Msh6	RLLSKIHNV	-	-	+
KDM1A	Lysine-specific histone demethylase 1A	RLLEATSYL	-	-	+
VAMP1	Vesicle-associated membrane protein 1	RLQQTQAQV	-	-	-
PRKD2	Serine/threonine-protein kinase D2	RQASLSISV	-	-	-
ACTB	Actin, cytoplasmic 1	RMQKEITAL	-	-	-

Peptides matching the complex binding consensus were identified by searching the IEDB. 25 peptides derived from antigens with broad normal tissue distribution, and sequence conservation in mice, were tested in T2 stabilisation assays for binding by the chimeric T1-116C antibody and the humanised variant T1-116CV1. The MFI of antibody staining was used to indicate strong (+++), medium (++), weak (+) or no (-) binding, respectively. The cut-off MFI values for each category were: MFI >100 for (+++); MFI 50-100 for (++); MFI 15-50 for (+); MFI <15 for (-); n=3.

4.3 Administration of T1-116C in HHD mice exhibited no toxicity

After identifying potentially cross-reactive peptides using the IEDB and validating that some of those derived from normal tissues and conserved in mice can be recognised by T1-116C *in vitro*, the safety of T1-116C was further assessed *in vivo*. This was to enable testing of recognition of an unbiased selection of target peptides, with the acknowledged limitations that approximately one third of the potential human target peptides are not conserved in mice and that mice may not always process and present the same peptides as humans. For this experiment we used the human HLA-A2 transgenic (HHD) mouse model. The efficacy of the T1-116C antibody had previously been tested against triple receptor negative breast cancer xenografts *in vivo* (Li *et al.*, 2017a). T1-116C was shown to both prevent xenograft engraftment (Figure 4.1) and to delay growth of an established xenograft (Figure 4.2). These two experiments were performed by other lab members, prior to the start of this DPhil project and are also published in Li *et al.,* 2017a.

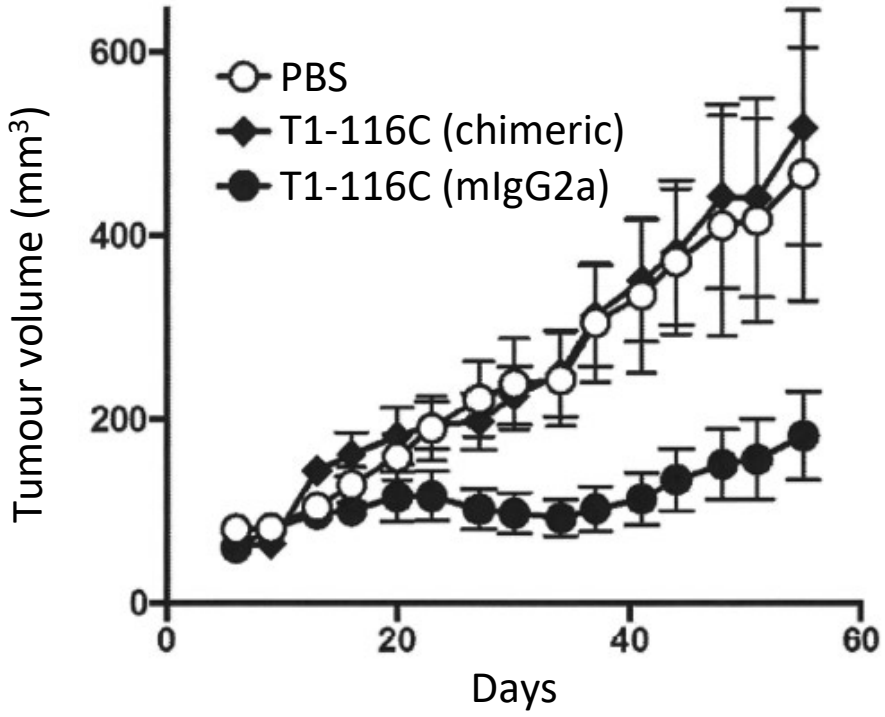

Figure 4.1 - T1-116C prevented engraftment of a triple receptor negative breast cancer xenograft *in vivo*.

$1x10^7$ human breast cancer MDA-MB-231 cells were injected subcutaneously into BALB/c nu/nu mice (n=10). PBS alone was administered as a control. T1-116C antibody was administered in two formats: a chimeric T1-116C format (human IgG1 isotype), and a murine T1-116C with a murine IgG2a isotype (T1-116C mIgG2a).. Antibodies were administered intraperitoneally, twice weekly (10 mg/kg) from the time of tumour inoculation. The mIgG2a T1-116C antibody, but not the chimeric hIgG1 T1-116C antibody significantly inhibited tumour growth ($P<0.0001$). This experiment was performed prior to the start of this DPhil project, by other members of our laboratory.

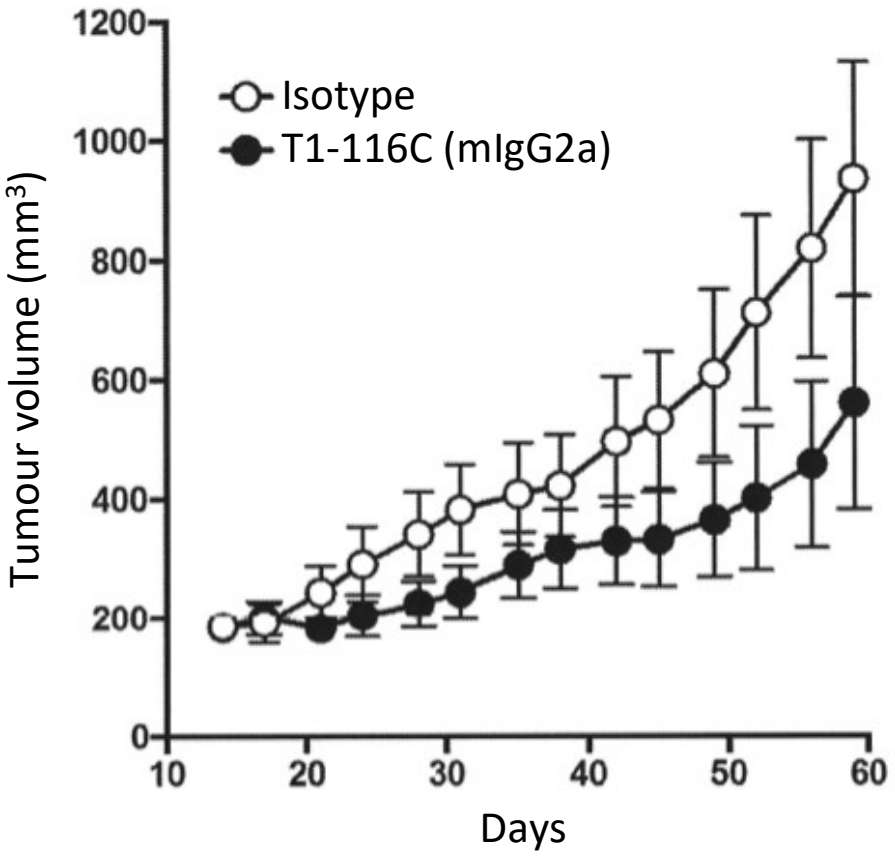

Figure 4.2 - T1-116C inhibited growth of an established triple receptor negative breast cancer xenograft *in vivo.*

$1x10^7$ human breast cancer MDA-MB-231 cells were injected subcutaneously into BALB/c nu/nu mice (n=9). T1-116C antibody (mIgG2a isotype) or an anti-fluorescein isotype control antibody was administered intraperitoneally, twice weekly (10 mg/kg), after the tumours had been growing for 14 days and had reached an average size of $150mm^3$. The T1-116C mIgG2a antibody significantly inhibited tumour growth ($P<0.0001$). This experiment was performed prior to the start of this DPhil project, by other members of our laboratory.

4.3.1 Experimental design

The aim of our study was to investigate whether T1-116C administration over a two-month period causes toxicity in mice. We chose to administer the antibody over a two-month period in order to be able to observe any acute toxicity, as well as any toxicity that may arise after prolonged exposure to the antibody, which would otherwise be missed with a shorter treatment period. The study design involved two groups: (i) an isotype control mIgG2a antibody treated group, and (ii) the T1-116CV1 antibody treated group. Each group was composed of five female HHD mice that were between six to eight weeks old at the start of the experiment. The dose that was administered was 20mg/kg. In the previous *in vivo* experiments where the efficacy of the T1-116C antibody was tested against triple receptor negative breast cancer xenografts, the antibody dose administered was 10mg/kg. We used twice the dose in order to ensure the safety of T1-116C administration even at a higher dose than was shown to be therapeutically effective. Both of the antibodies used were in the mIgG2a isotype in order to maximise engagement of murine immune effector cells and also to prevent the development of antibodies to a human Fc domain that might have functionally impaired the antibody if the animals mounted an immune response after repeat administration. Only the mIgG2a T1-116C antibody impaired tumour xenograft growth *in vivo*, when compared to hIgG1 (Figure 4.1), further indicating that mIgG2a was the most suitable isotype for this experiment. The antibody was delivered through intraperitoneal injection and a total of seventeen injections were administered. The mice were sacrificed at the end of the experiment. Figure 4.3 is a timeline of the experimental procedures.

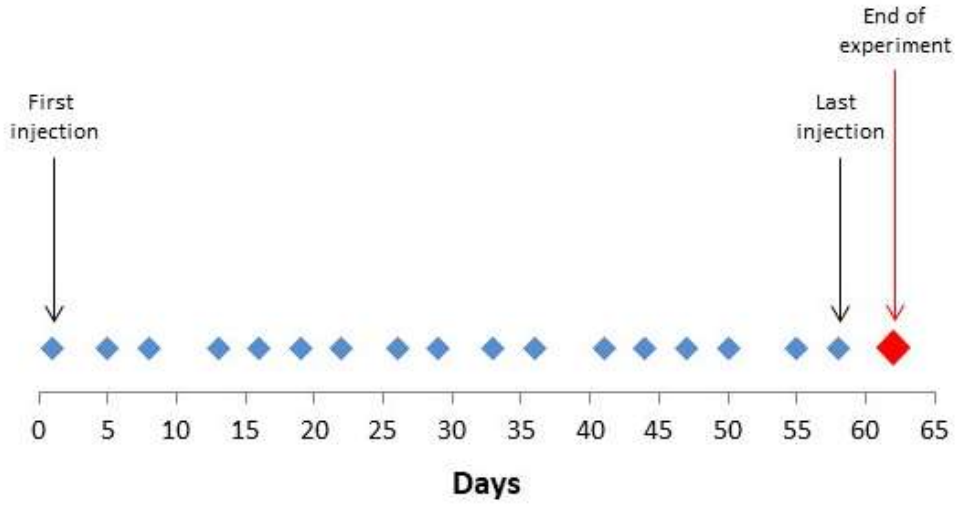

Figure 4.3 - Timeline of the *in vivo* experiment.
Each blue mark represents the administration of one intraperitoneal injection. The first injection was administered on day 1, and the last (seventeenth) injection was administered on day 58. The red mark represents the termination of the experiment on day 62.

4.3.2 T1-116C did not affect body weight

In addition to regular husbandry care, the mice were monitored daily for signs of adverse effects and changes in behaviour. Throughout the experiment, the weight of the mice was recorded at least twice weekly. The mice showed no signs of any adverse effects and there was no significant difference in body weight between the T1-116CV1 and the control group. Figure 4.4A summarises the average of the weights in each group. Figure 4.4B shows the weight of each animal through the course of the experiment and clarifies that the larger error bars observed towards the end of the experiment in Figure 4.4A are due to animals whose weight was already above or below the average for that group at the start of the experiment. Therefore the large error bars are not due to an effect of antibody treatment but rather due to natural differences between animals.

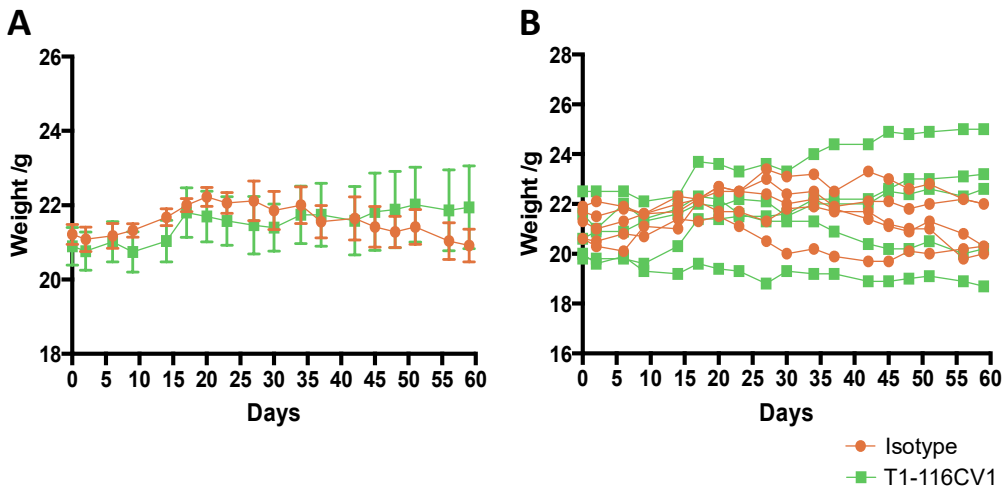

Figure 4.4 - T1-116CV1 did not affect the body weight of HHD mice.
Mice were monitored for signs of adverse effects throughout the course of treatment. This included measuring mouse body weights at least twice weekly to assess whether antibody administration had an effect on body weight. (A) The graph represents the mean ± SD. There was no significant difference between the isotype control (orange) and T1-116CV1 (green) groups. The student's t-test was used for statistical analysis. (B) The graph represents the weight of each individual mouse throughout the experiment.

4.3.3 Analysis of blood cell populations showed no expansion of immune cell subsets

In order to assess whether the administration of T1-116CV1 caused any activation of the immune system in the treated mice, we studied the immune cell populations in their blood. Blood was collected from each animal and the red blood cells were lysed. Granulocytes were identified by staining with anti-Gr1 and anti-CD11b antibodies, whereas lymphocyte populations were identified by staining with anti-CD19 antibody for B cells, and anti-CD3 antibody for T cells. There was no significant difference in the three immune cell subsets between the T1-116CV1 and control groups, suggesting that there was no expansion of these immune cell subsets. Figure 4.5 shows representative results for each group following flow cytometry analysis.

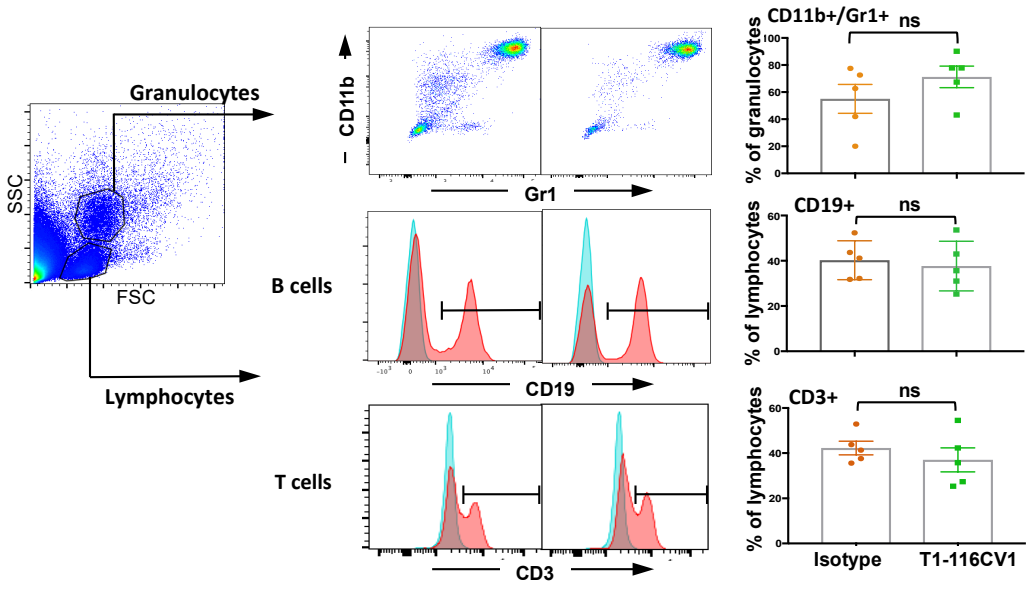

Figure 4.5 - Effect of T1-116C treatment on blood cell subsets in HHD mice.
Blood was collected from the mice and the blood cell subsets were analysed in order to determine whether antibody administration resulted in immune cell activation. Antibodies against CD11b and Gr1 were used to identify the granulocytes, while antibodies against CD19 and CD3 were used to identify the B and T cells respectively. The flow cytometry plots are representative of the results observed in each treatment group. The bar graphs represent the mean ± SD (n=5). No significant difference in the percentages of cells was observed between the T1-116CV1 and the control group. The student's t-test was used for the statistical analysis.

4.3.4 Histology demonstrated no signs of toxicity in tissues

To detect whether T1-116CV1 administration caused any tissue damage at the histological level, we performed haematoxylin and eosin (H&E) staining of six organs (heart, lungs, liver, kidney, spleen, colon), which were resected from all of the animals at the end of the experiment. If there were damage at the histological level, we would expect to see changes to the normal architecture of the affected organs, and infiltration of immune cells could also occur if there were any adverse reactions to antibody administration. Following H&E staining, there was no histological evidence of toxicity as a result of T1-116CV1 treatment. A qualified pathologist, who was blinded to treatment, independently verified the results. Figure 4.6 shows

representative H&E images from the tissues harvested from both the T1-116CV1 and the control group.

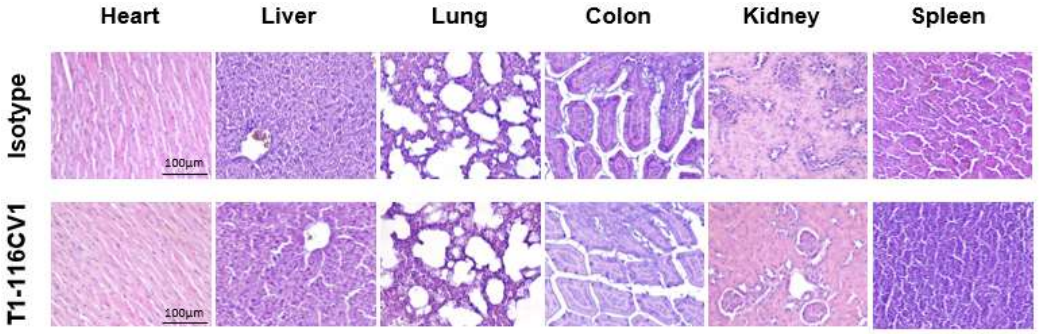

Figure 4.6 - T1-116C administration caused no histological toxicity in HHD mice.
Six organs (heart, lungs, liver, kidneys, spleen and colon) were resected from the mice in order to determine whether antibody administration caused damage to the architecture and structure of the tissues. Tissue sections were stained with H&E. There were no histological signs of toxicity and no significant differences between the two groups. Representative images at 10X magnification are shown.

There were initially some concerns that the sections of the lungs, for both the T1-116CV1 and the control group, looked as if the layers of cells were thicker than usual for lung tissue, and there seemed to be fewer alveolar air spaces than expected, based on the architecture of human lungs. To further investigate this observation, we obtained lungs from an untreated HHD mouse and an untreated C57BL/6 mouse (which is the strain that the HHD mouse is derived from). We stained sections of the lungs with H&E, and we found that the sections looked similar to those of the HHD mice treated with the isotype control and T1-116CV1 antibodies. This confirmed that the lung tissue was comparable to normal lung tissue from untreated mice, thereby further indicating that there is no histological evidence of damage. Figure 4.7 shows representative images of the untreated HHD and C57BL/6 mouse lungs stained with H&E.

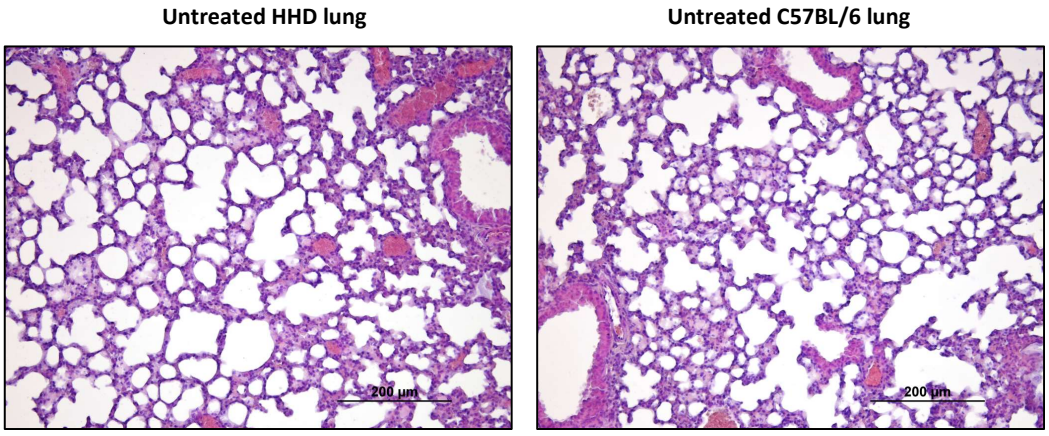

Figure 4.7 - Haematoxylin and eosin stained lung of untreated HHD and C57BL/6 mouse. Images show H&E stained lung sections from an untreated HHD mouse and from an untreated C57BL/6 mouse. Lung structure in the untreated mice is similar to that of the mice treated with T1-116CV1 and the isotype control antibodies. Images were taken at 10X magnification.

4.3.5 Validation of HLA-A2 expression in HHD mouse

While the HHD mouse is widely used for testing vaccines and other therapeutics targeting human HLA-A2 presented peptides, information on the expression of HLA-A2 in different tissues of the HHD mouse (it should be ubiquitously expressed [Pascolo *et al.*, 1997]), and how expression levels compare to those in humans, is important when assessing the significance of the absence of any toxicity.

To verify the level of cell surface human HLA-A2 expression in the HHD mouse model, and whether HLA-A2 is distributed evenly across different tissues, we stained cells from the spleen, lungs, heart, kidney, liver and blood *ex vivo*. We stained tissues from an untreated HHD mouse and from an untreated C57BL/6 mouse (as a negative control) with APC-conjugated anti-human HLA-A2 antibody (BB7.2-APC). We also stained the tissues with T1-116C-PE in order to investigate whether any binding to these tissues would be observed by flow cytometry. Figure 4.8 shows that, of the six

tissues tested, only the spleen, lungs and blood were HLA-A2-positive by flow cytometry. We used frozen human PBMCs that are known to be HLA-A2-positive as a positive control (Buffy 12, 16, 27 and 28). In comparison to the human PBMCs, the level of HLA-A2 staining is lower in the HHD spleen, lungs and blood. This could indicate that the HLA-A2 levels in HHD mice are lower than in humans and therefore not directly comparable. The C57BL/6 mouse tissues were all HLA-A2-negative, as expected. For the T1-116C staining, all tissues of both the HHD and C57BL/6 mouse and all human PBMCs were negative, as anticipated.

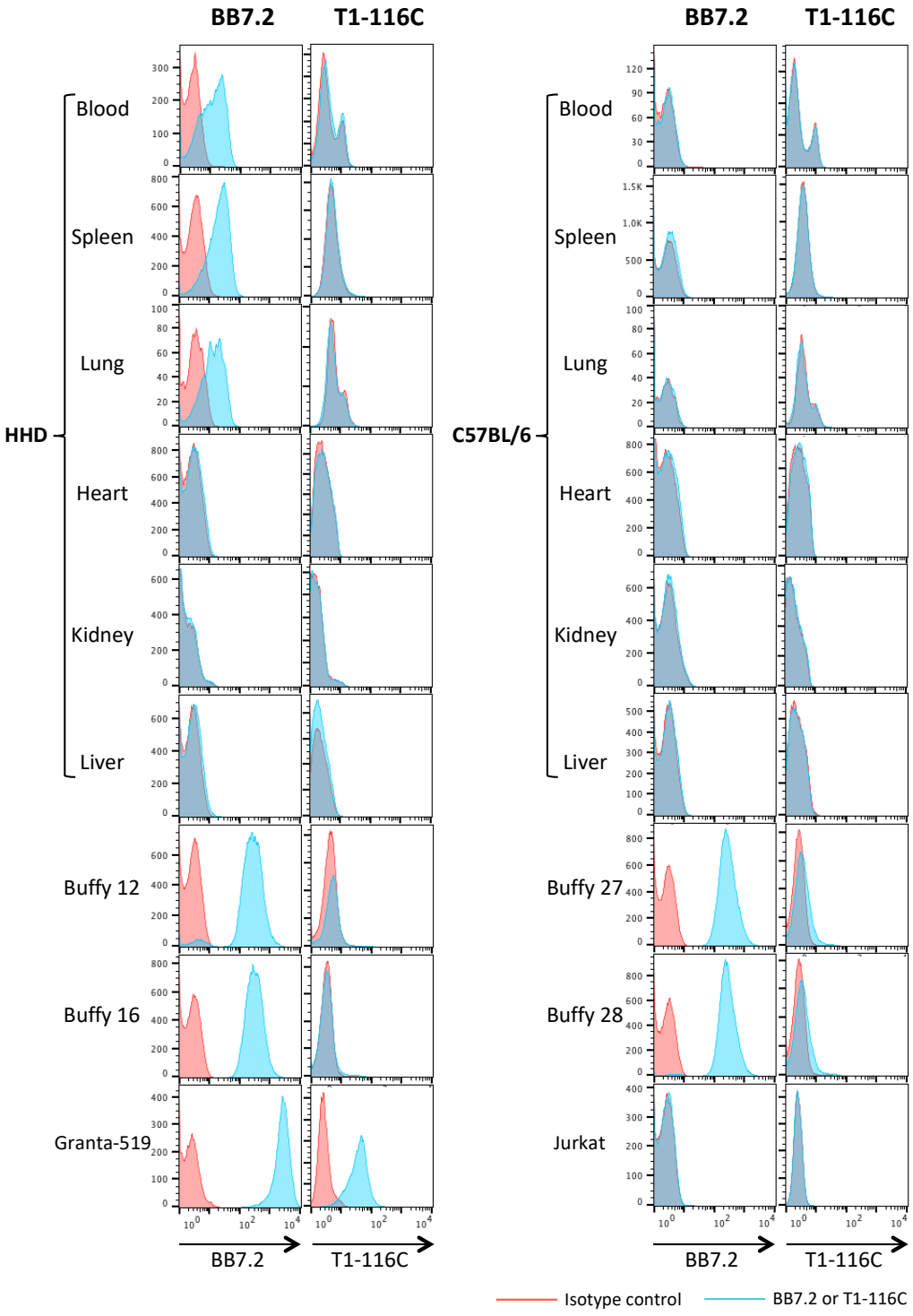

Figure 4.8 – *Ex vivo* HLA-A2 expression in tissues from an HHD mouse.
BB7.2-APC antibody was used to detect HLA-A2 expression in an untreated HHD mouse and an untreated C57BL/6 mouse. The blood, spleen and lungs of the HHD mouse are positive for HLA-A2. All other mouse tissues are HLA-A2-negative. Human PBMCs (Buffy 12, 16, 27 and 28) were used as a positive control for the comparison of human HLA-A2 levels. All samples were negative for T1-116C (T1-116C-PE antibody was used). The Granta-519 cell line was used as a positive control for BB7.2 and T1-116C staining, whereas the Jurkat cell line was used as a negative control.

4.4 Discussion

Our aim was to use the complex consensus derived from the comprehensive scanning mutagenesis to define the range of peptides potentially capable of binding the T1-116C antibody. As the complex consensus suggested the possibility for great variety in the sequences of T1-116C binding peptides, data mining the IEDB enabled us to narrow down the search to HLA-A*02:01-restricted, experimentally validated epitopes, which still matched the complex consensus. As we were aware of peptides that bound T1-116C but still failed to match the complex consensus (Table 3.3), even testing all 271 peptides identified in the IEDB search would still not comprehensively identify all cross-reactive peptides. Therefore we selected 25 peptides derived from normal tissue antigens, whose sequence was conserved in mice, for *in vitro* validation. This enabled us to test how robust the more complex consensus is, and whether using the consensus sequence in combination with data mining the IEDB is a robust method for predicting functionally cross-reactive peptides.

The IEDB is a useful resource for the *in silico* identification of potentially cross-reactive peptides because it can be used to narrow down the search to peptides that match the complex binding consensus, and importantly, the peptides identified have previously been shown to bind to HLA-A*02:01, which addresses the question of whether a peptide can be appropriately processed and presented at the cell surface. The IEDB was established in 2004 and it provides up-to-date data that is curated from all publications available in PubMed (Vita *et al.*, 2015). It is the largest database, containing more than 450 000 peptidic epitopes (Vita *et al.*, 2018). Due to the unique binding preferences of different MHC-I alleles, there are also tools for

MHC-I binding prediction, which can be used to assess peptides that can bind a specific MHC-I haplotype. Examples include SYFPEITHI and Bioinformatics and Molecular Analysis Section (BIMAS), which are allele-specific prediction tools that use algorithms based on experimental data (Parker *et al.*, 1994; Rammensee *et al.*, 1999). SYFPEITHI was one of the first prediction tools, and it has been used to predict cancer-associated peptides, however it has not been updated since 2012 (Backert & Kohlbacher, 2015; Snyder & Chan, 2015). While *in silico* prediction tools are very useful, they also have some limitations because the predicted MHC-I binding profile is not always accurate when validated *in vitro* (Snyder & Chan, 2015).

This observation was also made in our laboratory when the initial T1-116C consensus sequence, RXPXXAPXV, was compared to sequences in the UniProtKB/Swiss-Prot protein database using the ScanProsite tool, and 19 human peptides matching the T1-116C consensus were identified (patent WO2017037440A1). SYFPEITHI and BIMAS were used to predict the HLA-A2 binding profiles of the 19 peptides. They accurately predicted the three strongest HLA-A2 binding peptides, but did not manage to predict all of the peptides that can bind HLA-A2; *in vitro* validation using T2 stabilisation assays showed that some peptides that were predicted not to bind HLA-A2, were in fact BB7.2-positive (patent WO2017037440A1). We used the IEDB to identify cross-reactive peptides because the IEDB houses experimentally validated epitopes. However the results showed that the peptides predicted using the IEDB were not all functionally T1-116C cross-reactive *in vitro* using T2 stabilisation assays, despite matching the consensus sequence. It is important to note that the peptides that did not bind T1-116C were also the ones that had the weakest or no BB7.2

binding; therefore it is likely that the lack of T1-116C binding resulted from a lack of peptide binding to HLA-A2. It is possible that this was due to peptide synthesis error, or due to variation between experiments and different experimental techniques. These findings highlight the need to use both *in silico* and *in vitro* methods to test the specificity of T1-116C because limiting the analysis to one method alone does not accurately define the T1-116C pattern of peptide recognition.

In order to assess whether T1-116C recognition of a broad range of epitopes could cause damage to normal tissues, we tested the safety of T1-116C in the HHD mouse model. Human HLA-A2 transgenic mice have been used previously to assess the potential toxicity of TCRm antibodies due to the recognition of broadly presented cross-reactive peptides. A study investigating the ESKM TCRm mAb, which targets the WT1-derived peptide RMFPNAPYL presented by HLA-A*02:01, used HLA-A2 transgenic mice to assess the toxicity of ESKM (Veomett *et al.*, 2014). They assessed the WBC populations in the mice, and the histology of lymphoid and major organs, where they found no differences between the ESKM and isotype treated groups. They also assessed surface HLA-A2 expression using the BB7.2 mAb and flow cytometry, finding that spleen and bone marrow levels were higher than those in the thymus. ESKM's target peptide is conserved in mice, which enables the study of both on-target and off-target reactivity in this case. The same mouse model was used to assess the toxicity of TCRm mAb Pr20, targeting the PRAME-derived peptide ALYVDSLFFL presented by HLA-A*02:01 (Chang *et al.*, 2017). They performed a biodistribution study and showed that, like the isotype control mAb, Pr20 does not localise to any specific organ. Similar to the p53 peptide targeted by T1-116C, they

acknowledge that the ALYVDSLFFL target peptide is not conserved in murine PRAME. However they explain that transgenic HLA-A2 mice can still be used for toxicity studies as they can present potentially cross-reactive peptides derived from murine proteins that are also present in human proteins.

It has been shown that human peptides can be presented and targeted in human HLA-A2 transgenic mice. An example is the WT1 peptide, RMFPNAPYL, which is conserved in mice and is also recognised by T1-116C. RMFPNAPYL was shown to be processed and presented by the transgenic HLA-A2 of HHD mice in a DNA vaccine study (Chaise *et al.*, 2008). This study also revealed that there was sufficient HLA-A2 expression to present WT1 peptides and provoke an immune response in HHD mice. The HHD mouse model has also been used in another study to test PASD1 peptides for DNA vaccines (Joseph-Pietras *et al.*, 2010). Similarly, sufficient HLA-A2 was available to present PASD1 peptides and generate an immune response. Conforti *et al.* generated an HHD mouse model expressing transgenic CEA in order to study immune responses to DNA vaccines, again highlighting that there is sufficient expression of HLA-A2 and presentation of peptides for immune recognition (Conforti *et al.*, 2009). Although it should be noted that fewer presented epitopes are generally needed for T-cell mediated immunity than to engage antibody-dependent immune effector functionality.

The species barrier is an important limitation of using the HHD mouse model; interspecies differences in peptide sequence conservation, patterns of antigen expression, antigen processing and presentation preclude the study of all human

epitopes in this model. For example, the T1-116C target p53 peptide itself is not conserved in mice, and cross-reactivity of the MAGE-A3 TCR with Titin would have not been discovered in this model because the Titin peptide is also not conserved in mice (Cameron *et al.*, 2013). In addition, while we validated multiple T1-116C bound peptides that are conserved in humans and mice *in vitro*, we cannot confirm that each was presented *in vivo*. Similarly, had we observed toxicity in this model, it would not be clear which epitope was cross-reactive and the cause of the toxicity, nor whether the epitope is conserved in humans and whether it would provoke a similar immune response in humans as well.

Despite these limitations, the HHD mouse model is one of the best available preclinical models for testing T1-116C safety *in vivo* because of its expression of transgenic HLA-A2. As the majority of the peptides predicted using the IEDB share sequence conservation in mice, this is an appropriate model for assessing whether the broad range of epitopes recognised by T1-116C might cause damage to healthy tissues, while bearing in mind that only a proportion of the epitopes will be conserved in humans, with the rest being mouse-specific. Furthermore, this approach is not limited to epitopes that match a pre-defined consensus, which we have shown does not fully define the T1-116C antibody specificity.

The p53RMP peptide is not conserved in mice; therefore we would not be able to observe on-target toxicity arising from recognition of the target epitope in this model. However, p53 knockout mice are known to be viable (Donehower *et al.*, 1992) and there have been many studies of drugs targeting p53 such that tissues

affected by on-target toxicity are already known (Gudkov & Komarova, 2010). In order to study the possibility of normal tissue toxicity caused by on-target p53 binding *in vivo*, HHD mice would have to be crossed with mice expressing human p53 protein. However, this approach would not address the additional cross-reactive, human-specific epitopes recognised by T1-116C. It would also be a time-consuming project as it would require the generation of the HHD/human p53 transgenic mice, and initial *in vitro* testing would be needed to determine whether the p53RMP peptide would be processed correctly in murine cells and presented by transgenic HLA-A2.

Regarding the levels of immune cell subsets, no significant difference was observed between those of isotype control and T1-116CV1-treated mice. It would be important to test the blood of untreated HHD mice to assess whether the levels observed in our experiment are representative of the normal range of these immune cell subsets in untreated HHD mice. If administration of T1-116CV1 were to have a detrimental effect on murine tissues, we speculated that this could possibly lead to an increase in immune cell numbers through the engagement of the Fc region of T1-116CV1 by the Fc receptors of murine immune cells, such as B cells, monocytes and neutrophils (hence the use of T1-116CV1 with a mIgG2a isotype). These cells would then become activated and would proliferate, potentially resulting in a detectable increase in the quantities of immune cells. Due to availability and practicality, we only had five mice per group. Increasing the number of mice per group would increase the power of the data, and a power analysis should be performed for future *in vivo* experiments in order to ensure that a clinically meaningful magnitude of

change can be observed through the experimental design. Despite this limitation of the experiment, taking all of the data (mouse body weights, immune cell subsets and histology) into consideration collectively indicates that there was no toxicity caused by the administration of T1-116CV1.

It is important to evaluate the HLA-A2 expression level in the HHD mouse model because HLA-A2 forms part of the T1-116C dual antigen epitope and so its availability at the cell surface is critical. In order to assess if HLA-A2 was expressed at a comparable level to human cells, and whether it was distributed evenly across all tissues, we stained tissues from an HHD mouse and a C57BL/6 mouse with BB7.2. Of the six tissues tested, only the spleen, lungs and blood were HLA-A2 positive by flow cytometry. In comparison to the human PBMCs, the level of HLA-A2 was lower in the HHD mouse tissues (Figure 4.8). This could indicate that the HLA-A2 levels in HHD mice are lower than in humans and therefore not directly comparable. In the future it would be better to evaluate multiple animals, as it is also possible that the variation in HLA-A2 expression was due to the small sample size or due to experimental error. The heart, kidney and liver were HLA-A2-negative by flow cytometry. The T1-116C antibody showed no binding to any of the tissues, including the HLA-A2-positive tissues, confirming that there was: (i) no non-specific binding to HLA-A2 alone, and (ii) no recognition of potentially cross-reactive peptides presented by HLA-A2, consistent with the lack of toxicity observed in the *in vivo* experiment.

It is difficult to conclude whether the collagenase treatment of the HHD and C57BL/6 mouse tissues could have modified the conformational HLA-A2 epitope of BB7.2, and

thereby impaired the detection of HLA-A2 in these tissues. However, the lungs were found to be HLA-A2-positive despite also being treated with collagenase, indicating that the collagenase treatment *per se* did not completely impair the BB7.2 epitope in this case. BB7.2 binds to human HLA-A2 at the α2 domain, which is part of the HHD transgene (Hogan & Brown, 1992); therefore BB7.2 should be able to bind HLA-A2 in HHD mice as it does wt HLA-A2 (unless there is a conformational difference in the HHD molecule that impairs BB7.2 binding). Bhattacharya *et al.* described HLA-A2 transgene expression in brain endothelial cells while studying the RL6A TCRm mAb against an HLA-A2-presented peptide derived from p68 RNA helicase protein (Bhattacharya *et al.*, 2010). They analysed the HLA-A2 expression levels of brain endothelial cells in five different strains of human HLA-A2 transgenic mice, including HHD mice, using the BB7.2 mAb and flow cytometry. Mice generally showed weak positivity for HLA-A2, which was enhanced after IFN-γ stimulation for 2 days (Bhattacharya *et al.*, 2010). They used dendritic cells from the spleen as a positive control, and these showed higher HLA-A2 expression levels than the brain endothelial cells. In our experiment, we found that the heart, kidney and liver were HLA-A2-negative by flow cytometry. We would expect the HLA-A2 transgene to be expressed in all tissues, as the mice are homozygous for the transgene; therefore it is possible that the levels of HLA-A2 expression in these tissues were too low to detect by flow cytometry. It would be interesting to stimulate the cells with IFN-γ *ex vivo* and assess whether HLA-A2 levels become detectable by flow cytometry due to HLA-A2 upregulation in inflammatory conditions.

An alternative method to test the level of HLA-A2 expression across different HHD tissues could be by immunohistochemistry (IHC) analysis of frozen tissues, using frozen human tissues as a positive control (frozen tissues preserve the conformation of proteins; formalin-fixed paraffin-embedded tissues would not be suitable because HLA-A2 will be denatured as a result of formalin fixation). However IHC will also detect intracellular HLA-A2, therefore it will not indicate the level of HLA-A2 available on the cell surface for antibody binding. We performed flow cytometry analysis, and an advantage of using this method is that the antibody has better access to target cells in suspension. This resembles the *in vivo* environment more closely than using frozen tissue sections where only a cross-section of an organ is available, which provides a snapshot of a restricted area. However, as explained above, a limitation of flow cytometry could be that it is not sufficiently sensitive to detect low levels of the HLA-A2 transgene expressed in murine tissues.

A limitation of using the humanised T1-116CV1 antibody for the HHD experiment is that its efficacy has not previously been tested *in vitro* or *in vivo*. The *in vitro* efficacy of the original T1-116C antibody has been published, as well as its *in vivo* efficacy against breast cancer xenografts as described previously (Li *et al.*, 2017a). Since then, the specificity profile of the humanised T1-116CV1 antibody has been tested by other members in our laboratory, and although the results show that T1-116CV1 has similar specificity to the original antibody, there is a possibility that it does not bind as strongly as the original antibody (unpublished data). Therefore it will be important to test the efficacy of T1-116CV1 *in vitro* to determine its ability to kill cells expressing the target peptide or cross-reactive peptides. Demonstrating the *in vivo*

efficacy of T1-116CV1 against human tumour xenografts would dispel any doubt that off-target toxicity is not observed in the HHD model because the humanised variant does not bind as strongly to its target as the murine T1-116C does. We used the humanised T1-116CV1 antibody because it was the clinically relevant format with which to study toxicity and therefore it would provide the most useful data for the potential future development of T1-116C for clinical applications.

To conclude, we searched the IEDB for potentially cross-reactive peptides to inform further *in vitro* validation of the T1-116C specificity. This revealed that not all predicted peptides were functionally cross-reactive *in vitro*, reiterating the difficulty of accurately defining the specificity of T1-116C. Importantly, it also showed that T1-116C binding is not limited to tumour antigens because T1-116C also binds peptides derived from broadly expressed normal tissue antigens. Despite this, no toxicity was observed in T1-116CV1-treated HHD mice *in vivo*. These results are encouraging, although it is important to acknowledge the limitations of using the HHD mouse model. The use of a combination of *in silico*, *in vitro* and *in vivo* methods has been crucial to further evaluate the T1-116C specificity for the p53RMP peptide and its safety. To better define the safety profile of T1-116C in humans, imaging studies with a T1-116C antibody that was unable to engage immune effector functions could enable its biodistribution in normal tissues to be safely characterised (Wang *et al.*, 2018). T1-116C has already been used for tumour imaging in xenograft studies, indicating its applicability to such an approach (Li *et al.*, 2017a), however an important disadvantage of this approach is the large cost involved.

5 Developing CARs Using p53-Targeting TCRm Antibodies

5.1 Introduction

In addition to assessing the specificity of the T1-116C antibody and its therapeutic potential as a naked antibody, we also evaluated the specificity of a CAR designed using the T1-116C scFv. The benefit of this approach is that the target specificity of the TCRm antibody is retained while also taking advantage of the cytotoxic activity of the CAR-expressing T cells. This mechanism of action is different to that of naked TCRm antibodies, which harness immune effector functions to mediate a therapeutic effect through ADCC, ADCP and CDC. The T1-116C TCRm antibody is the most extensively studied of the laboratory's TCRm antibodies and is the only one that has been previously humanised and patented. Hence it was logical to first investigate its suitability for the CAR platform, in parallel with further validating its specificity. Testing the T1-116C CAR showed that it lacked sufficient target peptide specificity; it subsequently became important to investigate the suitability of the other TCRm antibodies generated in the laboratory for the development of CARs because T1-116C may have characteristics that make it more suitable for use as a naked antibody, while one of the other TCRm antibodies may be more suitable for a CAR. This chapter will first describe studies with the T1-116C TCRm antibody, and then the T2-2A, T2-116A and T1-29D TCRm antibodies, focusing predominantly on the T2-2A TCRm antibody.

5.2 Covalently linking the p53RMP peptide to MHC-I to assess TCRm affinity

Unlike the other TCRm antibodies generated in the laboratory, the affinity of the murine, chimeric and humanised variants of T1-116C had been previously determined (although the affinity of the other TCRm antibodies has not been tested, titrating peptides in T2 assays has shown that the other antibodies bind their target more effectively at lower concentrations of peptide than T1-116C does). The dissociation constant (K_D) of murine and humanised T1-116C was measured prior to the start of this DPhil project by Lonza Biologics PLC. Quartz crystal microbalance assay was used and the affinity of the chimeric T1-116C antibody binding to p53RMP-HLA-A2 monomers was approximately 1μM. The p53RMP-HLA-A2 monomer used in the experiment was a non-covalently linked trimer comprising the p53RMP peptide, the HLA-A2 heavy chain, and β2M. As the affinity of T1-116C measured using this method was found to be lower than expected for an antibody with *in vivo* anti-tumour activity, we speculated that the relatively low affinity could partially be due to the spontaneous disassembly of the trimer complex. If the p53RMP-HLA-A2 can be stabilised then we might be able to evaluate the true binding affinity of T1-116C, without the influence of the instability of the antigen.

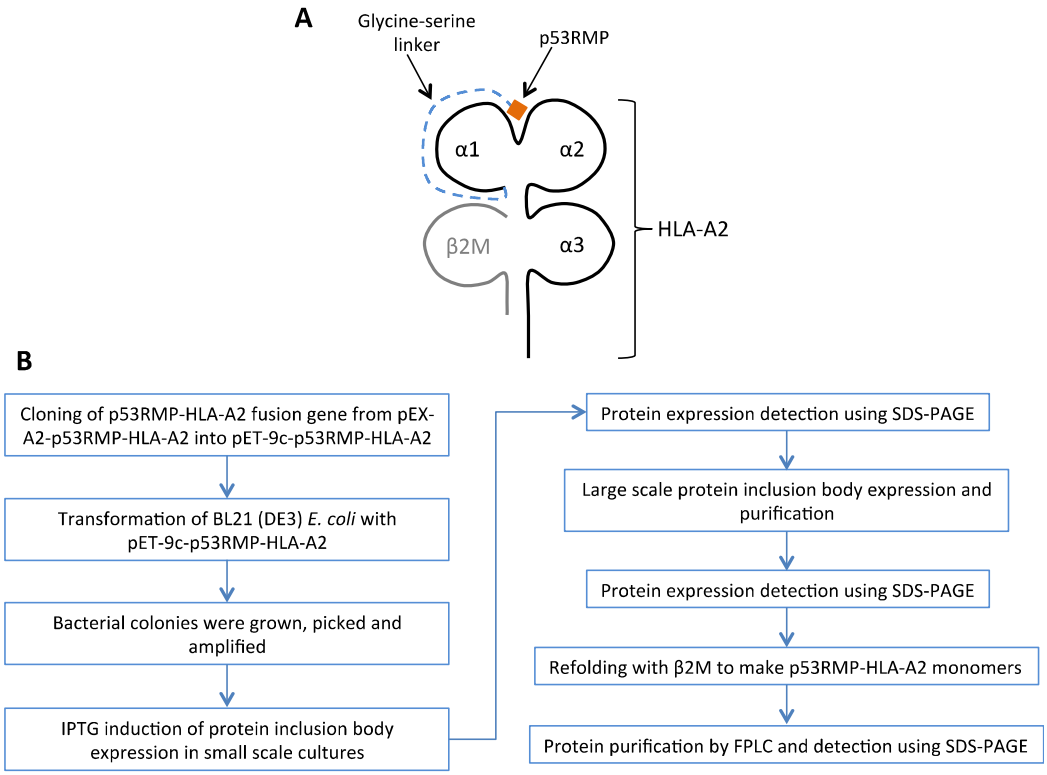

Figure 5.1 - Summary of the protocol for generating the p53RMP-HLA-A2 fusion protein. **A.** The structure of the p53RMP peptide covalently linked to HLA-A2. **B.** The steps in the method used for generating the p53RMP-HLA-A2 fusion protein.

To test this hypothesis, we generated a construct where the p53RMP peptide was linked covalently to the heavy chain of HLA-A2 via a glycine-serine linker in order to stabilise its binding to the HLA-A2 peptide cleft (Figure 5.1). This approach has been used by Kang *et al.* (1997) to covalently link two different melanoma epitopes to HLA-A*0201 in order to generate two fusion proteins, which were successfully recognised by HLA-A2-restricted CTLs specific for each epitope (Kang *et al.*, 1997). It has also been used to link peptides to the heavy chain of the mouse K^d molecule (Mottez *et al.*, 1995). The p53RMP-HLA-A2 recombinant protein was expressed in *E. coli* and purified as insoluble inclusion bodies (Figure 5.2).

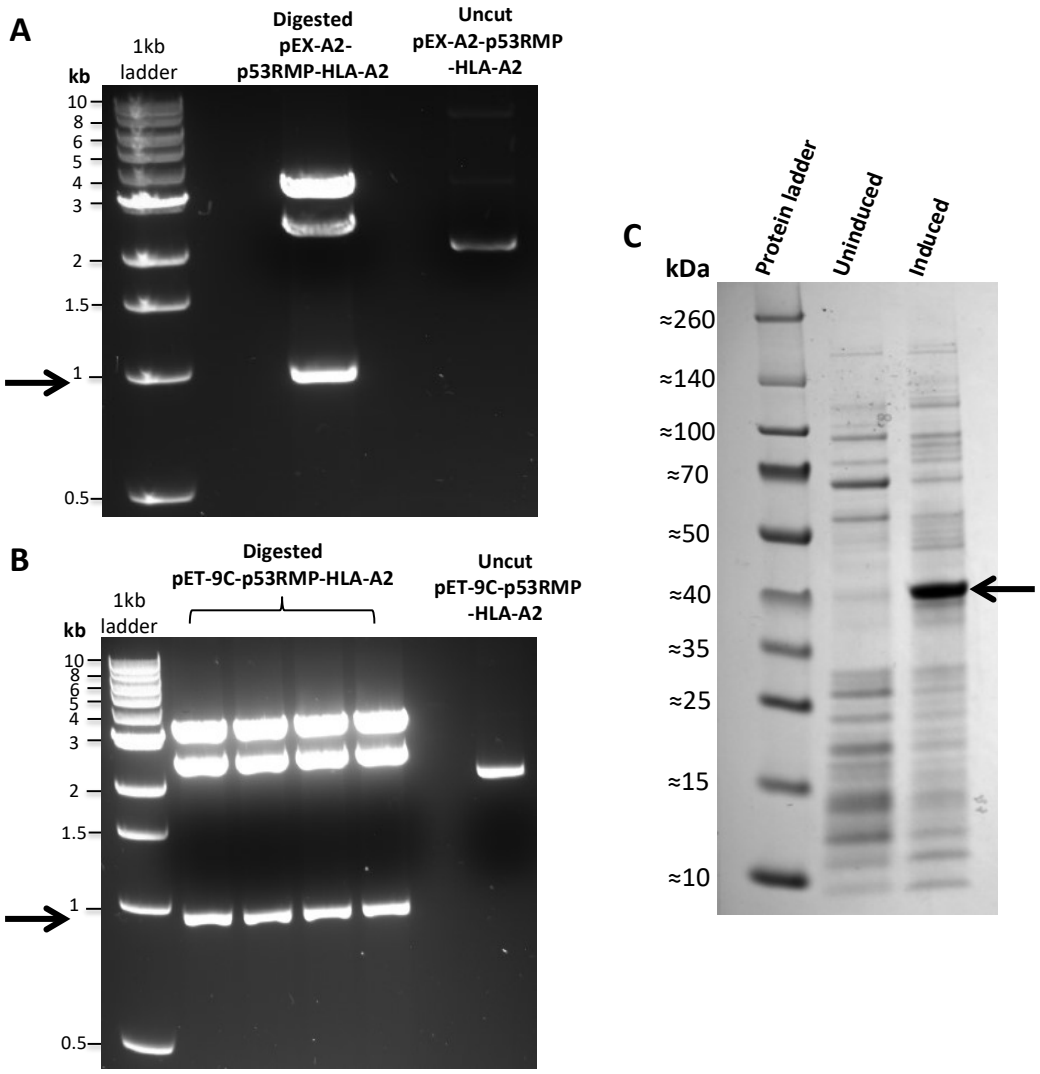

Figure 5.2 – Cloning of p53RMP-HLA-A2 fusion gene from pEx-A2 vector into pET-9c vector and SDS-PAGE detecting inclusion body protein.

A. Agarose gel showing the cloning of the construct. p53RMP-HLA-A2 cDNA was commercially synthesised and supplied in the pEX-A2 vector, which was digested with NdeI and BamHI restriction enzymes to release the 950bp band (indicated by the arrow) that contains the desired cDNA. **B.** The band was subsequently extracted and cloned into the expression vector pET9c, which was subsequently transformed into *E. coli*. The agarose gel shows the band extracted from four different bacterial colonies, which was digested with NdeI and BamHI to verify the presence of the insert (indicated by the arrow). The resulting expression construct was transformed into BL21 *E. coli* for protein expression by IPTG induction. **C.** SDS-PAGE was used to verify the size of the expressed protein. First lane: broad range protein ladder; second lane: uninduced sample (no IPTG) used as a negative control; third lane: the arrow indicates the prominent band at ≈40kDa, which is the p53RMP-HLA-A2 bacterial inclusion body protein, where IPTG was used to induce its expression.

Once purified, the recombinant HLA-A2 protein was refolded with β2M inclusion bodies to make a monomer, which was purified using fast protein liquid chromatography (FPLC) and validated by SDS-PAGE, shown in Figure 5.3A and 5.3B respectively. The MHC-I monomer was then used to coat an ELISA plate. Anti-HLA-A2 antibody (BB7.2) and anti-β2M antibody (BBM.1) were added to the ELISA, as positive controls, to validate the presence of the MHC-I molecule. Unlike BB7.2 and BBM.1, T1-116C did not stain the covalently linked p53RMP-HLA-A2 monomer (Figure 5.3C). However, in the same assay T1-116C did stain a p53RMP-HLA-A2 monomer where the p53RMP peptide was not covalently linked to the heavy chain of HLA-A2 (i.e. a monomer that is a non-covalently linked trimer of the p53RMP peptide, the HLA-A2 heavy chain, and β2M, like the one used to measure the K_D described in section 5.2 above).

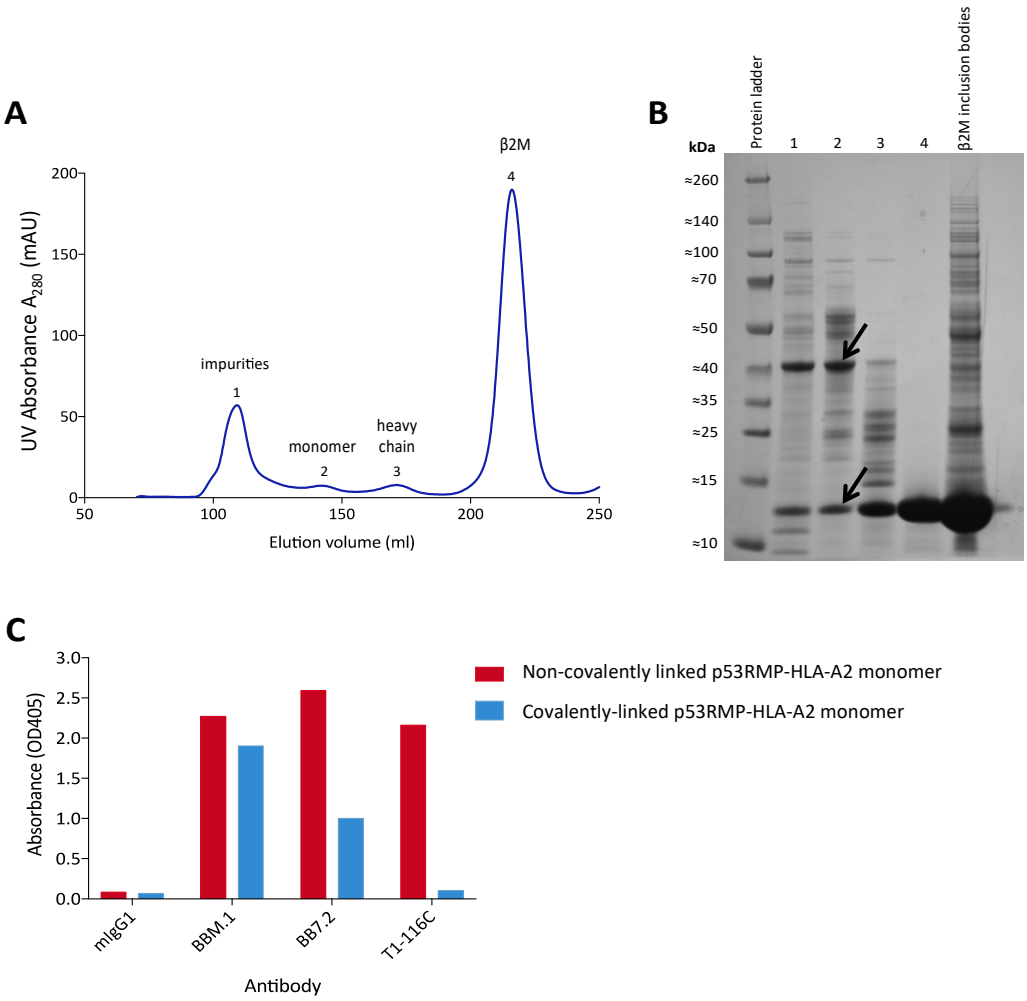

Figure 5.3 - Refolding and functional testing of covalently linked p53RMP–HLA-A2 monomers.

A. Covalently linked p53RMP-HLA-A2 was purified from BL21 *E. coli* inclusion bodies and refolded with β2M to make a monomer. FPLC was used to purify the refolded monomer. The FPLC chromatogram has four peaks: 1 – impurities (waste); 2 – refolded monomer; 3 – heavy chain of HLA-A2 covalently linked to p53RMP, which has not refolded with β2M; 4 - β2M, which has not refolded with the heavy chain of HLA-A2 that is covalently linked to p53RMP. Peak 2 is very small, indicating that a small amount of monomer has been formed. **B.** SDS-PAGE to validate the size of the protein present in each of the four FPLC peaks (same labelling of peaks 1 to 4 as in **A**). In the lane labelled "2", where refolded monomer was loaded, the top arrow indicates the heavy chain of HLA-A2 with the covalently linked p53RMP peptide (size of ≈40kDa). Also in this lane, the bottom arrow indicates the β2M molecule (size of ≈12kDa), which associates with p53RMP-HLA-A2 during the refolding process in order to form a monomer. A broad range protein ladder is in the first lane as a standard for protein size. The positive control is β2M inclusion bodies. C. ELISA coated with the FPLC-purified monomer shows that the covalently linked monomer does not bind T1-116C but does bind BB7.2 and BBM.1 (anti-β2M antibody). A p53RMP-HLA-A2 monomer in the conventional non-covalently linked format, which is known to bind to BBM.1, BB7.2, and T1-116C, was used as a control. The isotype control antibody is a mouse IgG1 antibody; n=2.

One possible explanation for the T1-116C staining of the un-linked monomer, but not the covalently linked monomer, could be that the glycine-serine linker is obstructing T1-116C binding to its target. It could also be possible that poor refolding of the monomer affected T1-116C staining, because the monomer yield in both refolding experiments was low. Furthermore, the higher BBM.1 binding in the ELISA, compared to the lower BB7.2 (while these are at similar levels for the non-covalently linked monomer), suggests that there was excess β2M and therefore perhaps misfolding. The refolding experiments were performed twice; the results were similar in both experiments, with T1-116C binding to the covalently linked peptide remaining negative. Due to the time-consuming nature of the procedure, we decided against a third repetition. At this point in time, our decision was also aided by the concurrent findings of our collaborators in the University of Oxford's Oncology Department. They performed cell surface avidity studies using surface plasmon resonance (Biacore) and found that the avidity of T1-116C was 92nM (Dr Bart Cornelissen, personal communication), which encouraged us to investigate T1-116C in the CAR format.

5.3 CAR production and validation based on the T1-116C TCRm antibody

All of the p53-targeting TCRm antibody CARs were based on the second generation CD19-targeting FMC63-28-CD3ζ CAR developed by Kochenderfer *et al.* (Kochenderfer *et al.*, 2009). As per this model, the T1-116C CAR has a spacer and transmembrane region derived from CD28 (Figure 5.4). The endodomain of the T1-116C CAR has two components: (i) a co-stimulatory region, which is derived from the intracellular portion of CD28, and (ii) the activating domain for signal transduction, which is

derived from the CD3ζ chain of the TCR. The scFv of T1-116C was used to provide the antigen-targeting moiety of the CAR. Two separate CARs were designed to reflect the two possible heavy and light chain orientations of the scFv: V_HV_L or V_LV_H. We tested the two possible scFv orientations in order to determine whether both have similar transfection efficiencies and similar specificity for the p53RMP-HLA-A2 target. A commercial supplier was used to synthesise the entire CAR genes (GeneART® Gene Synthesis, Invitrogen). The gene design and the subsequent cloning were performed in our laboratory, and all constructs were sequenced commercially to confirm they had the correct sequences.

5.3.1 Production and transient transfection of T1-116C CARs

The commercially synthesised T1-116C CAR minigenes were amplified by PCR then subcloned from the entry vector into the lentiviral expression vector pLenti 7.3, which has a bicistronically encoded GFP gene, under the control of a separate SV40 promoter, to facilitate downstream detection (Figure 5.4). The pLenti 7.3 vector was chosen as it is routinely used in our laboratory and it is very practical when used as part of the ThermoFisher Gateway™ Vector Kit.

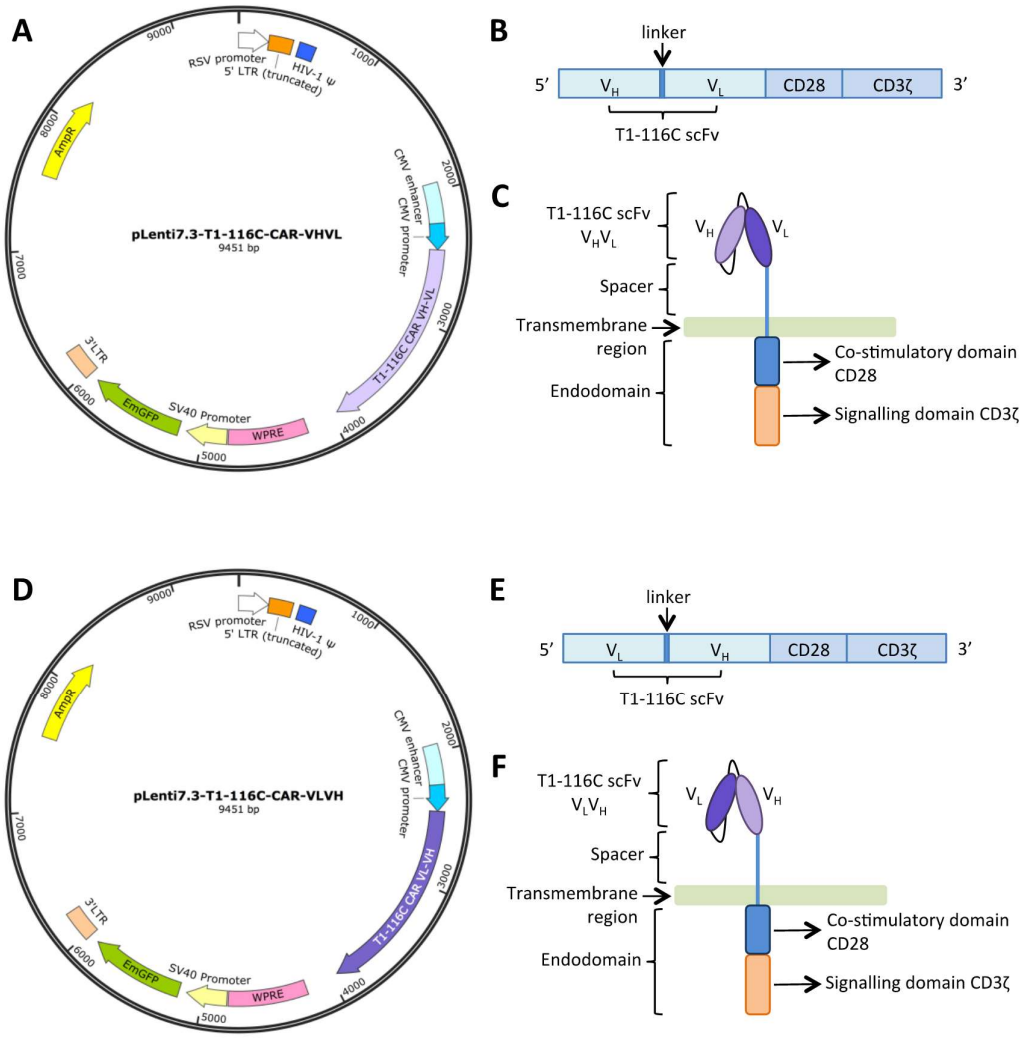

Figure 5.4 - T1-116C CAR constructs.
A. The plasmid map of the V_HV_L T1-116C CAR construct in the expression vector pLenti7.3. **B.** The V_HV_L T1-116C CAR construct. **C.** The structure of the V_HV_L T1-116C CAR on the cell surface. **D.** The plasmid map of the V_LV_H T1-116C CAR construct in the expression vector pLenti7.3. **E.** The V_LV_H T1-116C CAR construct. **F.** The V_LV_H T1-116C CAR structure on the cell surface. RSV – Rous sarcoma virus; LTR – long terminal repeat; HIV-1 Ψ – human immunodeficiency virus-1 psi packaging element; WPRE – Woodchuck post-transcriptional regulatory element from the woodchuck hepatitis virus allows increased transgene expression; EmGFP – emerald green fluorescent protein; AmpR – ampicillin resistance gene to enable selection of the plasmid in *E. coli*.

The first step was to transiently transfect HEK293T cells with the T1-116C CAR plasmids. HEK293T cells were selected because they grow fast, they are easily transfectable, and they contain the SV40 large T antigen, which enhances plasmid DNA replication of vectors containing the SV40 origin of replication, leading to

increased protein production (Lin *et al.*, 2014). Transient transfection with both CAR-containing plasmids had similar transfection efficiencies and GFP expression, as demonstrated by the similar MFI values for the two different scFv orientations (MFI 179 for V_HV_L and 190 for V_LV_H) (Figure 5.5). GFP expression was lower than that from cells transfected with the empty vector, which probably reflects better transfection efficiency of the smaller plasmid and the cell machinery only having to express one recombinant protein.

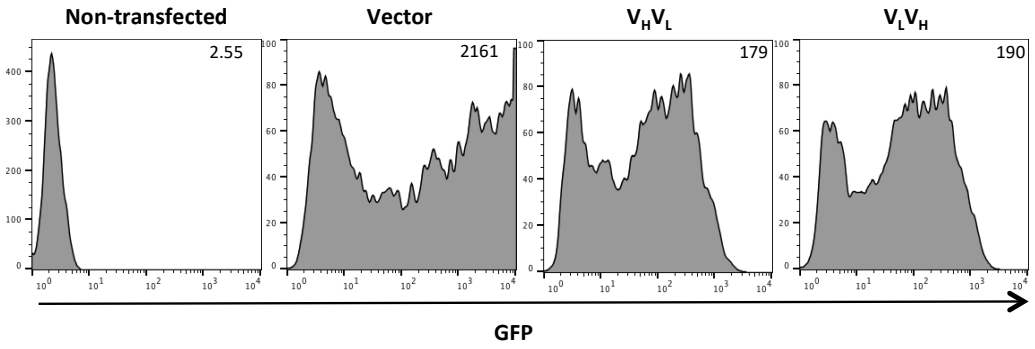

Figure 5.5 - HEK293T cell transfection with the T1-116C CAR in the V_HV_L or V_LV_H scFv orientation.
The vector (pLenti 7.3) containing the CAR construct is GFP-positive, and was used as a positive control. Non-transfected HEK293T cells were used as a negative control. The values in the upper right corner represent the MFI of the GFP expression, indicating the transfection efficiency. Transfection with either scFv orientation of the T1-116C CAR was successful. The experiment was performed three times and plots from one representative experiment are shown. Results from one of three replicative experiments are shown.

5.3.2 Tetramer staining of T1-116C CAR-transfected HEK239T cells

After establishing that both T1-116C CAR vectors could be used to transiently transfect HEK293T cells, the next step was to assess whether both CARs were equally effectively expressed on the cell surface and whether the T1-116C binding activity, and its specificity, were retained in the CAR format. APC-conjugated peptide-MHC-I

tetramers were used for this purpose. Two non-specific tetramers containing flu peptide or an irrelevant p53 peptide (p53GLA) were used as negative controls. Streptavidin-APC was included as a control, as it was used to cluster the monomers into tetramers. The results showed that both CAR formats were expressed on the surface, as they each bound their specific target p53RMP-HLA-A2 tetramers (Figure 5.6A). Both CAR formats also showed some non-specific recognition of the two irrelevant tetramers, however the MFIs of these were lower than the MFIs observed with the p53RMP tetramer. The T1-116C V_LV_H CAR was selected for further experiments as it showed higher p53RMP tetramer binding than the V_HV_L CAR (Figure 5.6B). The T1-116C V_LV_H CAR will be referred to as the T1-116C CAR from this point forward.

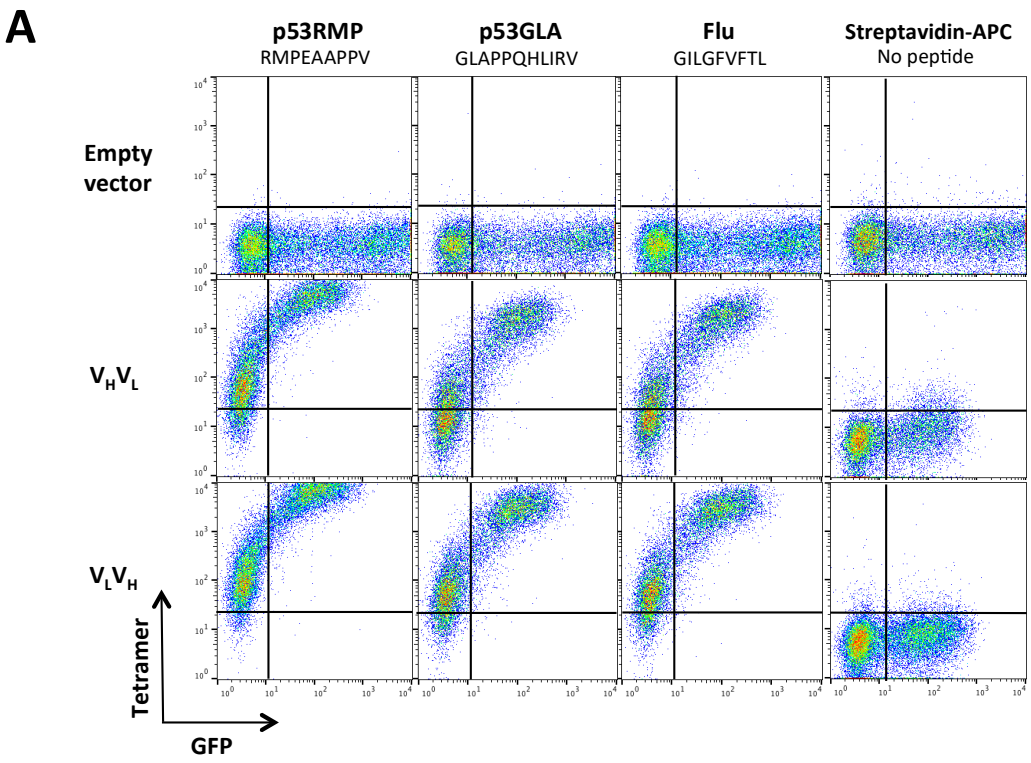

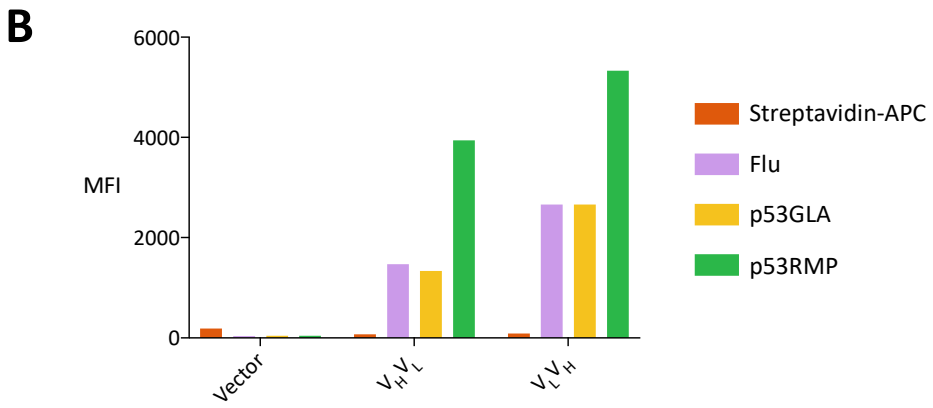

Figure 5.6. Functional validation of T1-116C CAR constructs.

A. HEK293T cells were transiently transfected with the two orientations of the T1-116C CAR (V_HV_L or V_LV_H). p53RMP tetramers were used to assess surface expression of the CARs. Flu-HLA-A2 and p53GLA-HLA-A2 tetramers, and streptavidin-APC were used as negative controls. Empty vector-transfected HEK293T cells were used as a negative control for transfection. The sequence of the peptide in each tetramer is: RMPEAAPPV (p53RMP), GLAPPQHLIRV (p53GLA), and GILGFVFTL (flu). The experiment was repeated two times and representative dot plots from one experiment are shown. **B.** The MFI of the tetramer binding from (**A**) is represented in a bar graph, showing that the p53RMP-HLA-A2 tetramer has the highest binding to T1-116C CAR-transfected cells compared to the controls. Of the two CARs, the V_LV_H CAR has the higher tetramer binding of the two scFv orientations.

Despite the non-specific binding of the T1-116C CARs towards the irrelevant tetramers in the HEK293T system, we went on to test such binding in T cells. The rationale is that CAR expression on the transiently transfected HEK293T cells will differ from that on the CAR-transduced T cells and, furthermore, using T cells will enable the testing of effector functions against target-expressing cell lines.

5.3.3 Lentiviral transduction of the Jurkat cell line with the T1-116C CAR

Having selected the V_LV_H CAR for further experiments, we generated a cell line with stable expression of the T1-116C CAR in order to perform more comprehensive studies of CAR specificity and activity against target cell lines. Jurkat cells were selected because they are immortalised human T lymphocytes that are easy to grow in culture and can produce T-cell cytokines such as IL-2 upon activation by target cells, which enables the assessment of CAR-directed activity. A drawback of Jurkat cells is that they are not cytotoxic and therefore cannot be used to determine whether CAR-directed target recognition will induce target cell killing, as is possible with primary human T cells. However the advantages outweigh the disadvantages at this stage in the T1-116C CAR evaluation, and Jurkat cells were selected for initial testing of CAR specificity and activity.

A stable Jurkat cell line expressing the T1-116C CAR (Jurkat-T1-116C-CAR) was generated by lentiviral transduction of the T1-116C V_LV_H CAR construct. Following initial lentiviral transduction, there were very few GFP-positive cells (Figure 5.7A), suggesting that the transduction efficiency of the experiment was low. Subsequent FACS sorting successfully enriched the GFP-positive population (Figure 5.7B).

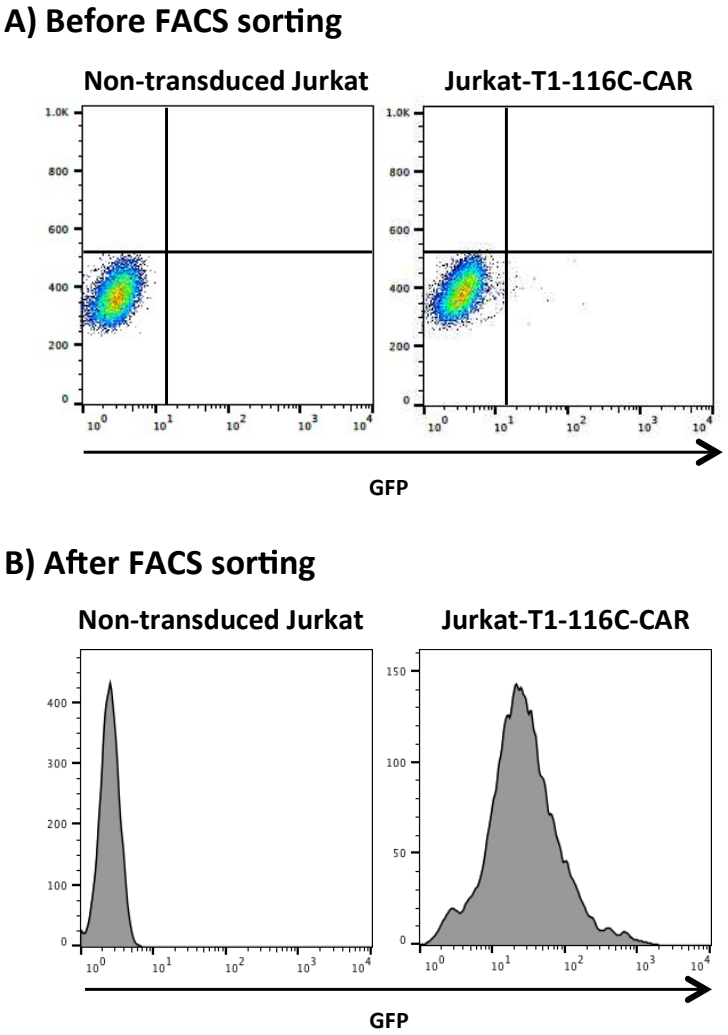

Figure 5.7 – Transduction of Jurkat cells with T1-116C CAR.
Jurkat cells were transduced with the T1-116C CAR (V_LV_H orientation) to generate a cell line (Jurkat-T1-116C-CAR) with stable expression of the T1-116C CAR. **A.** Jurkat-T1-116C-CAR cells before FACS sorting. Non-transduced Jurkat cells are presented in the left dot plot as a negative control. T1-116C CAR-transduced Jurkat cells are shown in the right dot plot, where very few GFP-positive cells are detected following lentiviral transduction. **B.** Jurkat-T1-116C-CAR cells after FACS sorting. Non-transduced Jurkat cells are shown as a negative control in the left panel. FACS sorted GFP-positive Jurkat-T1-116C-CAR cells were shown in the right panel.

5.3.4 The T1-116C CAR expressed by Jurkat cells specifically recognised p53RMP-HLA-A2 tetramers

While GFP expression may be indicative of CAR expression because they are expressed from the same vector, it does not directly correlate with CAR expression on the cell surface because the two genes are controlled by different promoters (CAR by CMV, GFP by SV40) and GFP is expressed intracellularly.

In order to confirm CAR expression on the surface of the Jurkat-T1-116C-CAR cell line and assess its binding activity, we stained the cell line with the target p53RMP-HLA-A2 tetramers. The cells were also stained with two irrelevant tetramers (flu or p53GLA). The Jurkat-T1-116C-CAR cell line showed specific binding to the p53RMP-HLA-A2 tetramer, but did not bind the irrelevant tetramers (Figure 5.8). Thus expression of the T1-116C-CAR on Jurkat cells seemed to overcome the non-specific binding observed with the transiently transfected HEK293T cells above (Figure 5.6). This experiment validated that the T1-116C CAR was expressed on the Jurkat-T1-116C-CAR cell surface and that it had retained its specificity, as assessed by tetramer binding.

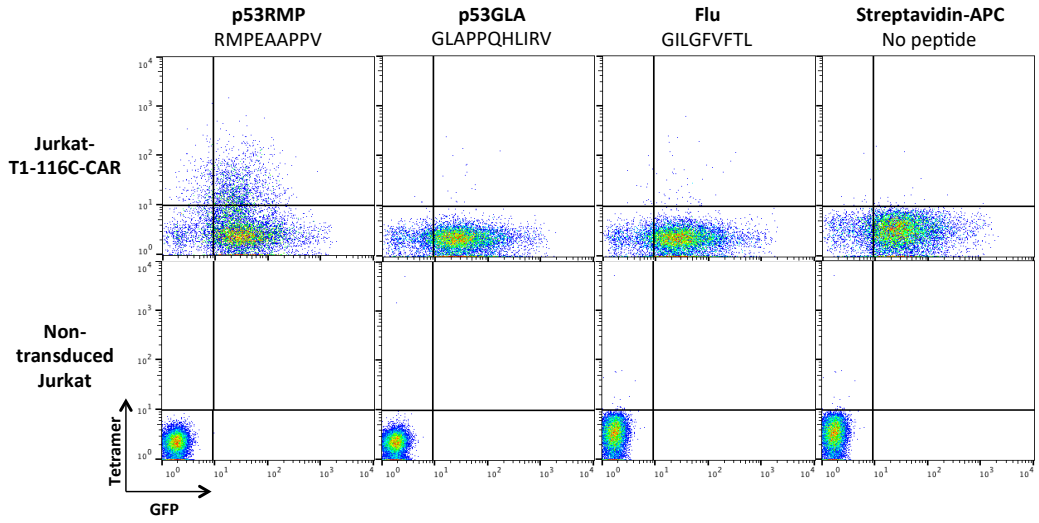

Figure 5.8 – Tetramer staining of Jurkat-T1-116C-CAR cells.
Tetramers were used to stain Jurkat-T1-116C-CAR cells to validate cell surface CAR expression and specificity for target tetramers. Streptavidin and irrelevant tetramers (flu-HLA-A2 or p53GLA-HLA-A2) were used as negative controls. Non-transduced Jurkat cells were used as a negative control. The sequence of the peptide in each tetramer is: RMPEAAPPV (p53RMP), GLAPPQHLIRV (p53GLA), and GILGFVFTL (flu). The Jurkat-T1-116C-CAR cells bind p53RMP tetramers but not the control tetramers. Results from one of three replicative experiments are shown.

The Jurkat-T1-116C-CAR cells stained with the target p53RMP-HLA-A2 tetramer show two distinct populations: a population that is only GFP-positive, and a population that is APC and GFP double positive. This suggests that the former population represents the Jurkat cells that are GFP-positive but that either: (i) do not express the CAR on the cell surface, and therefore cannot bind APC-conjugated tetramers, or (ii) do not express enough copies of the CAR on the cell surface to reach the sensitivity threshold for detection by flow cytometry (however the few CARs that are expressed could still be able to bind the APC-conjugated tetramers). The latter (APC and GFP double positive) population represents the Jurkat cells that are GFP-positive and that express the CAR on the cell surface at sufficient numbers for detection by flow cytometry, as demonstrated by binding the APC-conjugated tetramers. Hence

this indicated that not all transduced cells are capable of expressing the CAR at high levels, and that CAR expression levels vary between cells.

5.3.5 The T1-116C CAR did not retain its antigen specificity against target cell lines

To further characterise the T1-116C CAR, we investigated whether the Jurkat-T1-116C-CAR cells retained their T1-116C-mediated specificity, and became activated to produce IL-2 upon encountering target-expressing cell lines. Jurkat-T1-116C-CAR cells or non-transduced Jurkat cells were co-cultured for approximately 18 hours with: peptide-presenting T2 cells, Jurkat cells expressing recombinant HLA-A2, or cancer cell lines with previously established HLA-A2 and T1-116C binding profiles (Li *et al.*, 2017a). IL-2 secretion was assessed using an ELISA assay (Figure 5.9). All HLA-A2-positive cell lines stimulated IL-2 secretion, to various extents, while the HLA-A2-negative cell line, CEM, was the only cell line that did not. Although there were noticeable differences in the levels of IL-2 secretion between different peptide-loaded T2 cells and between different cancer cell lines, these were not statistically significant.

Although the HL-60 cell line is HLA-A2-negative and does not express p53, it has been shown to be T1-116C-positive by flow cytometry, and the epitope that is bound by T1-116C is unknown (Li *et al.*, 2017a). But in this particular assay, it is worth noting that HL-60 cells stimulated IL-2 secretion by both the non-transduced and T1-116C-transduced Jurkat cells to similar levels. In conclusion, the T1-116C CAR does

not retain the critical dual antigen specificity that would be required for it to progress as a therapeutic in the format of a CAR.

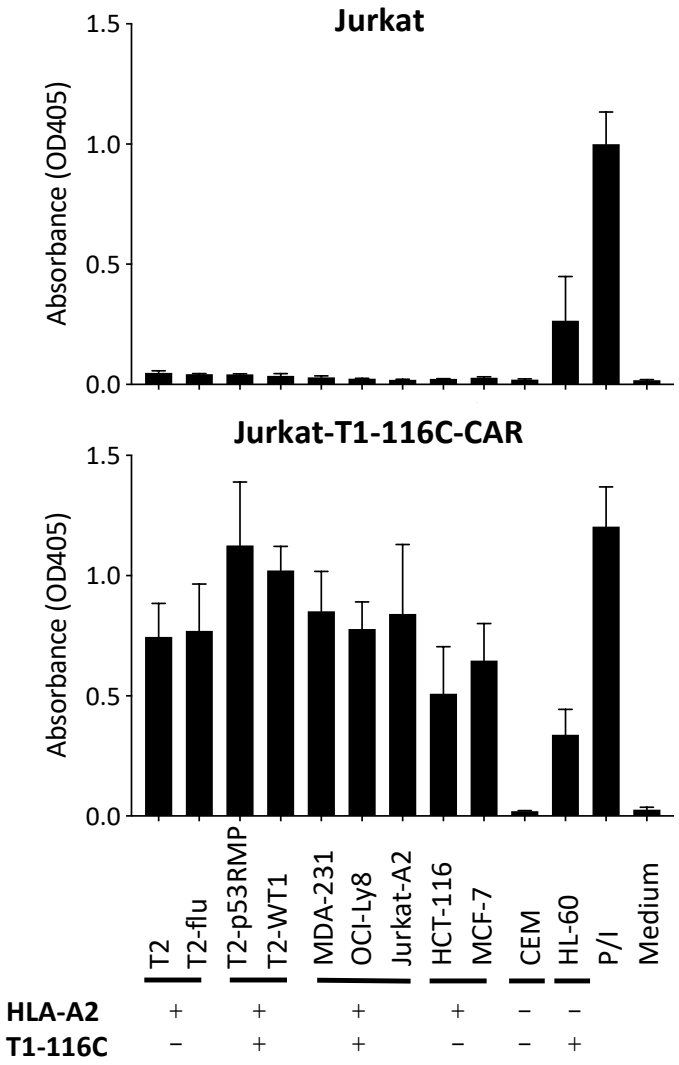

Figure 5.9 – IL-2 ELISA of Jurkat-T1-116C-CAR cells.

Non-transduced Jurkat cells (top graph) or Jurkat-T1-116C-CAR cells (bottom graph) were co-cultured overnight with different cell lines: T2 cells pulsed with different peptides, cancer cell lines (MDA-MB 231, OCI-Ly8, HCT-116, MCF-7, CEM and HL-60) or Jurkat cells with stable expression of HLA-A2 (Jurkat-A2). An ELISA was used to assess secreted IL-2 levels. The positive control was PMA/Ionomycin (P/I), while the negative control was the culture medium. The bottom panel summarises the HLA-A2 expression and T1-116C binding profiles of the cell lines as determined by flow cytometry. The error bars represent the standard deviation. One-way ANOVA was performed for the statistical analysis and there were no statistically significant differences between the peptide pulsed T2 cells or the HLA-A2-positive cell lines. n=3

5.4 CARs using alternative p53-targeting TCRm antibodies

Prior to the start of this DPhil project, members in the laboratory had generated a panel of p53-targeting TCRm antibodies and evaluated their binding to a variety of cancer cell lines by flow cytometry (Figure 5.10, patent WO2017037440A1). The T1-116C antibody was the only TCRm antibody that showed clearly positive binding to a variety of cancer cell lines. After discovering that the naked T1-116C antibody recognised multiple target antigens and that the T1-116C CAR did not retain its dual antigen specificity, we hypothesised that the cancer cell line FACS staining displayed by T1-116C might derive from its ability to recognise multiple tumour antigens and not just p53. Thus the development of CARs using the T2-2A, T2-116A, and T1-29D p53-targeting TCRm antibodies was investigated further as their lack of FACS positivity on cancer cell lines might indicate greater p53 specificity, rather than a lack of binding activity. It was possible that the copy numbers of p53 target epitopes on the target cell lines were below the threshold for detection by flow cytometry, hence the negative flow cytometry staining. CARs provide an attractive approach with which to test this as T cells require only tens of target peptides to enable their activation, while quantiBRITE bead-based calibration suggested 100-150 molecules per cell was the threshold for detection of binding using FACS (Li *et al.*, 2017a). Target epitope density is key for mAb function, as the engagement of antibody-dependent effector mechanisms requires relatively larger numbers of antibody molecules bound per cell. Therefore CAR T cells would be more effective at targeting low-density antigens than naked TCRm antibodies.

The T2-2A, T2-116A and T1-29D TCRm antibodies did not show obvious binding to any of the cancer cell lines (Figure 5.10); there were only slight shifts on some of the cell lines with strongest T1-116C binding, hinting that there might be very weak detection of their target (e.g. T2-116A on SW480 and NCI-H1395). Furthermore, peptide titrations in T2 assays showed that T2-2A, T2-116A and T1-29D bound their target p53 peptide-pulsed T2 cells more effectively than T1-116C did at lower peptide concentrations (patent WO2017037440A1). Thus it was possible that they had higher specificity for their target p53 peptide and it was unlikely that they would display weaker binding than T1-116C to p53 peptides on cancer cell lines (unless the conformation of the epitope on T2 cells and cancer cells had a critical difference that impaired their binding on cancer cell lines).

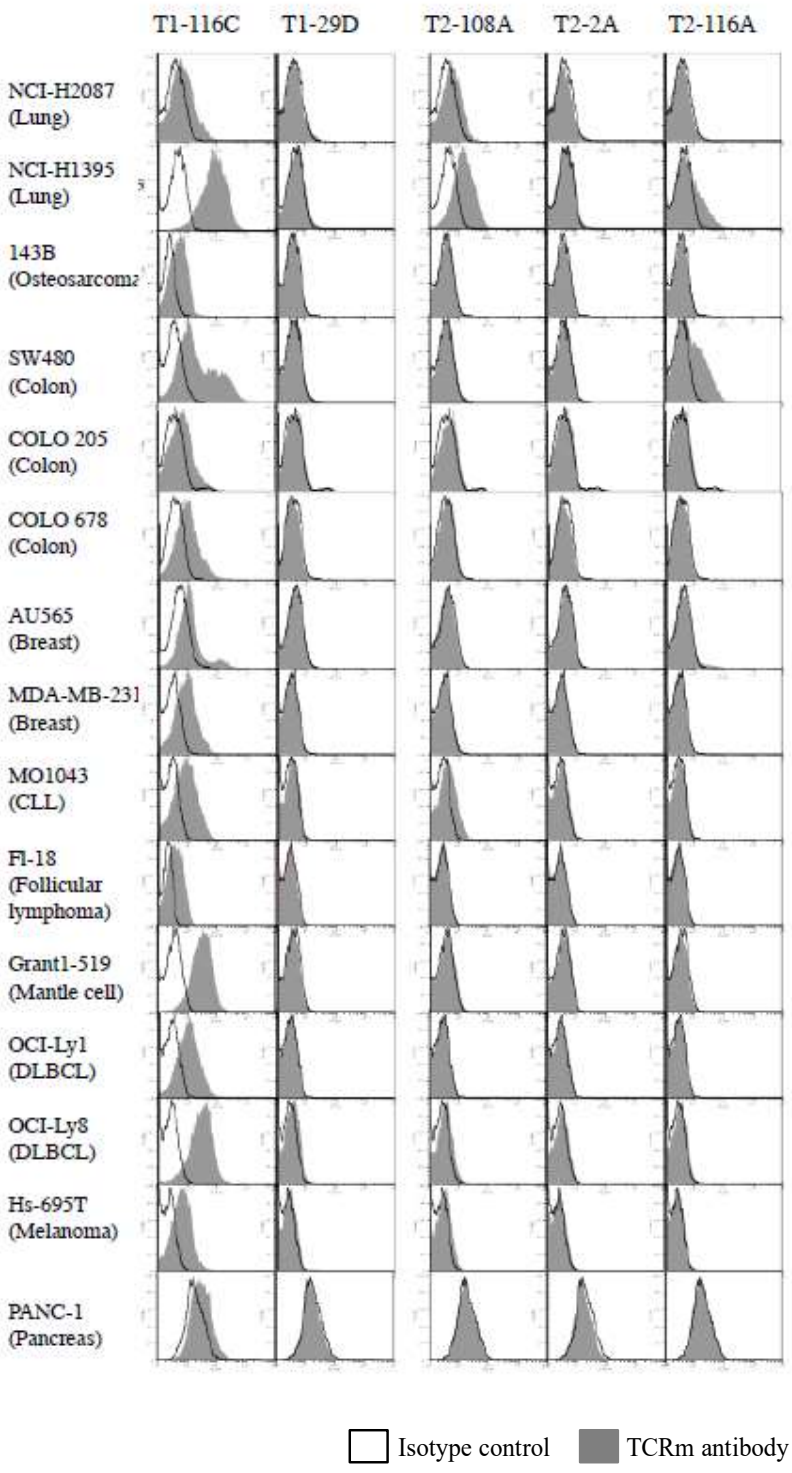

Figure 5.10 - Staining of cancer cell lines with a panel of p53-targeting TCRm antibodies.
Flow cytometry data showing the cancer cell line binding profiles of T1-116C, T2-2A, T1-29D, T2-116A and T2-108A. This Figure originates from the published patent for T1-116C and these experiments were performed by members of the laboratory prior to the start of this DPhil project (patent WO2017037440A1).

Table 5.1 lists the TCRm antibodies that were investigated for use in the CAR format or that were used as part of the experiments in this chapter (e.g. T2-108A was not a suitable candidate for CAR development because it previously displayed cross-reactivity with the negative control flu peptide, as reported in patent WO2017037440A1, however it was still useful as a control in later experiments).

Table 5.1 - TCRm antibodies used in this chapter and their specificity.

TCRm antibody	p53 peptide	Peptide sequence	Isotype	T2 specificity
T1-116C	p53RMP	RMPEAAPPV	IgG1	Specific
T1-29D	p53RMP	RMPEAAPPV	IgG1	Specific
T2-2A	p53GLA	GLAPPQHLIRV	IgG2a	Specific
T2-116A	p53GLA	GLAPPQHLIRV	IgG1	Specific
T2-108A	p53GLA	GLAPPQHLIRV	IgG1	Insufficient

The TCRm antibodies that are used in this chapter, either for the development of CARs (T1-116C, T1-29D, T2-2A, T2-116A) or as an experimental control (T2-108A) are summarised. Their target peptide is either p53RMP ($p53_{65-73}$) or p53GLA ($p53_{187-197}$). Their target peptide specificity when staining peptide-pulsed T2 cells is also indicated.

5.4.1 Isolation of T2-2A and T2-116A variable region cDNA sequences

Before the start of this DPhil project, the variable region heavy and light chain cDNA sequences of T1-29D had previously been isolated. The *Ig* genes of the T2-2A and T2-116A TCRm antibodies had not been sequenced previously and frozen hybridoma cells were available from which to isolate the variable region cDNA sequences and determine the sequence for the scFv of the CAR constructs. The variable heavy and light chain genes of T2-2A were isolated successfully using PCR and then sequenced. However we were unable to obtain a complete variable heavy chain gene sequence

for the T2-116A antibody, despite multiple attempts, and therefore did not pursue it further (Figure 5.11).

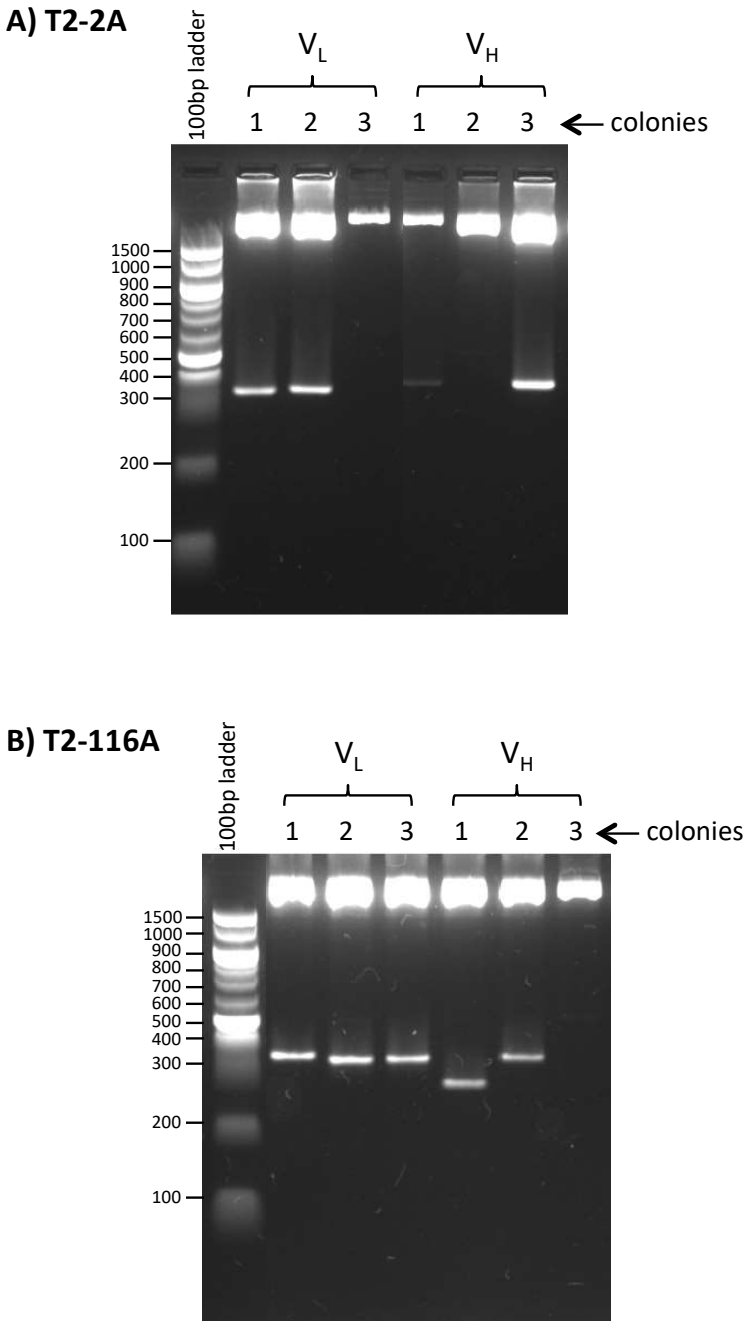

Figure 5.11 - Isolation of the variable heavy and light chain genes for T2-2A and T2-116A.
The variable heavy and light chain genes for T2-2A (A) and T2-116A (B) were isolated using PCR. PCR products were cloned into the ZeroBlunt® TOPO® vector, which was used to transform *E. coli*. Miniprep DNA was digested with EcoRI and run on an agarose gel (DNA from three different colonies is shown in A and B). The DNA band of interest is approximately 350bp long. Complete open reading frame (ORF) sequences were obtained for T2-2A, however a complete ORF sequence for the T2-116A variable heavy chain gene was not obtained because the sequences contained stop codons.

5.4.2 Production of T2-2A and T1-29D CARs

Except for the sequences of the scFv, the T2-2A and T1-29D CARs had the same structure as that of the T1-116C CAR. The T2-2A and T1-29D CARs were designed in the V_LV_H orientation. A commercial supplier (GeneART® Gene Synthesis, Invitrogen) synthesised the genes encoding the CARs for each TCRm mAb, while the gene design and the subcloning were performed in our laboratory. The CAR minigenes were first amplified by PCR, and then subcloned from the entry vector into the lentiviral expression vector pLenti 7.3. Constructs were sequenced commercially to confirm the correct sequences. The T2-2A and T1-29D CAR constructs and their schematic structures are depicted in Figure 5.12.

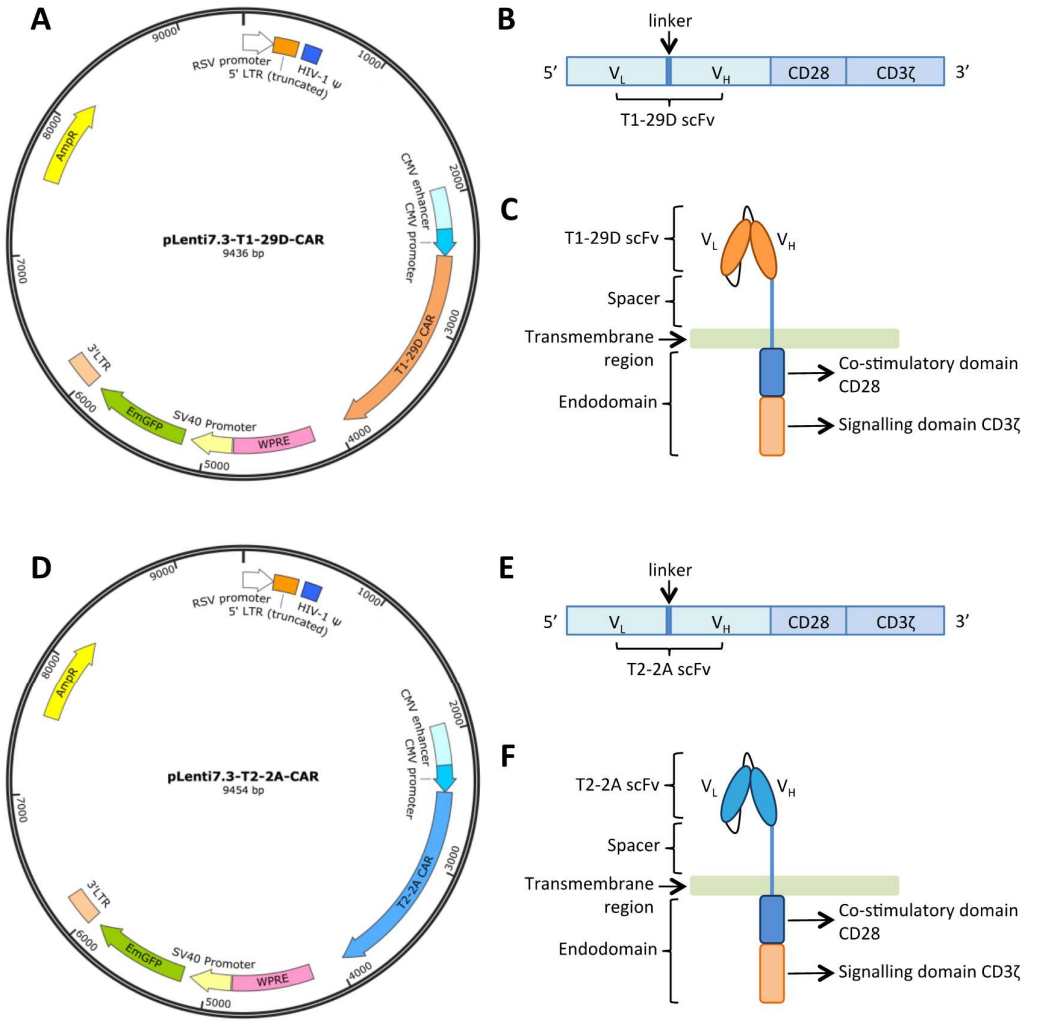

Figure 5.12 – T2-2A and T1-29D CAR constructs.

A. The plasmid map of the T1-29D CAR construct in the expression vector pLenti7.3. **B.** The T1-29D CAR construct. **C.** The structure of the T1-29D CAR on the cell surface. **D.** The plasmid map of the T2-2A CAR construct in the expression vector pLenti7.3. **E.** The T2-2A CAR construct. **F.** The T2-2A CAR structure on the cell surface. RSV – Rous sarcoma virus; LTR – long terminal repeat; HIV-1 Ψ – human immunodeficiency virus-1 psi packaging element; WPRE – Woodchuck post-transcriptional regulatory element from the woodchuck hepatitis virus; EmGFP – emerald green fluorescent protein; AmpR – ampicillin resistance gene.

5.4.3 The T2-2A CAR specifically recognised p53GLA-HLA-A2 tetramers

In order to initially assess whether the two CARs can be expressed on the cell surface and whether they specifically bind their target tetramers, we transfected HEK293T cells with either the T2-2A or the T1-29D CAR. GFP expression suggests, but does not directly correlate with, surface expression of the CAR. As with the T1-116C CAR, the tetramers were conjugated to APC. The target tetramer of each CAR (p53GLA-HLA-A2 for T2-2A, or p53RMP-HLA-A2 for T1-29D) was tested, as well as five irrelevant tetramers: flu peptide, two different peptides from PASD1 and two different peptides from Survivin (peptide sequences are specified in Figure 5.13). The results showed that the T2-2A CAR was expressed on the cell surface and it recognised its target p53GLA tetramer. It also showed some non-specific binding to the flu peptide-HLA-A2 tetramer but at much lower levels than observed with T1-116C (Figure 5.13). Importantly it did not recognise tetramers presenting other irrelevant tumour epitopes.

The T1-29D CAR did not bind any of the tetramers. It was possible that there was no CAR expression on the cell surface, despite the GFP expression confirming successful transfection, because these two genes are under the control of different promoters. It was also possible that the cloned variable genes did not encode the T1-29D mAb, which frequently happens either due to non-specific PCR amplification or the existence of multiple clones within the hybridoma.

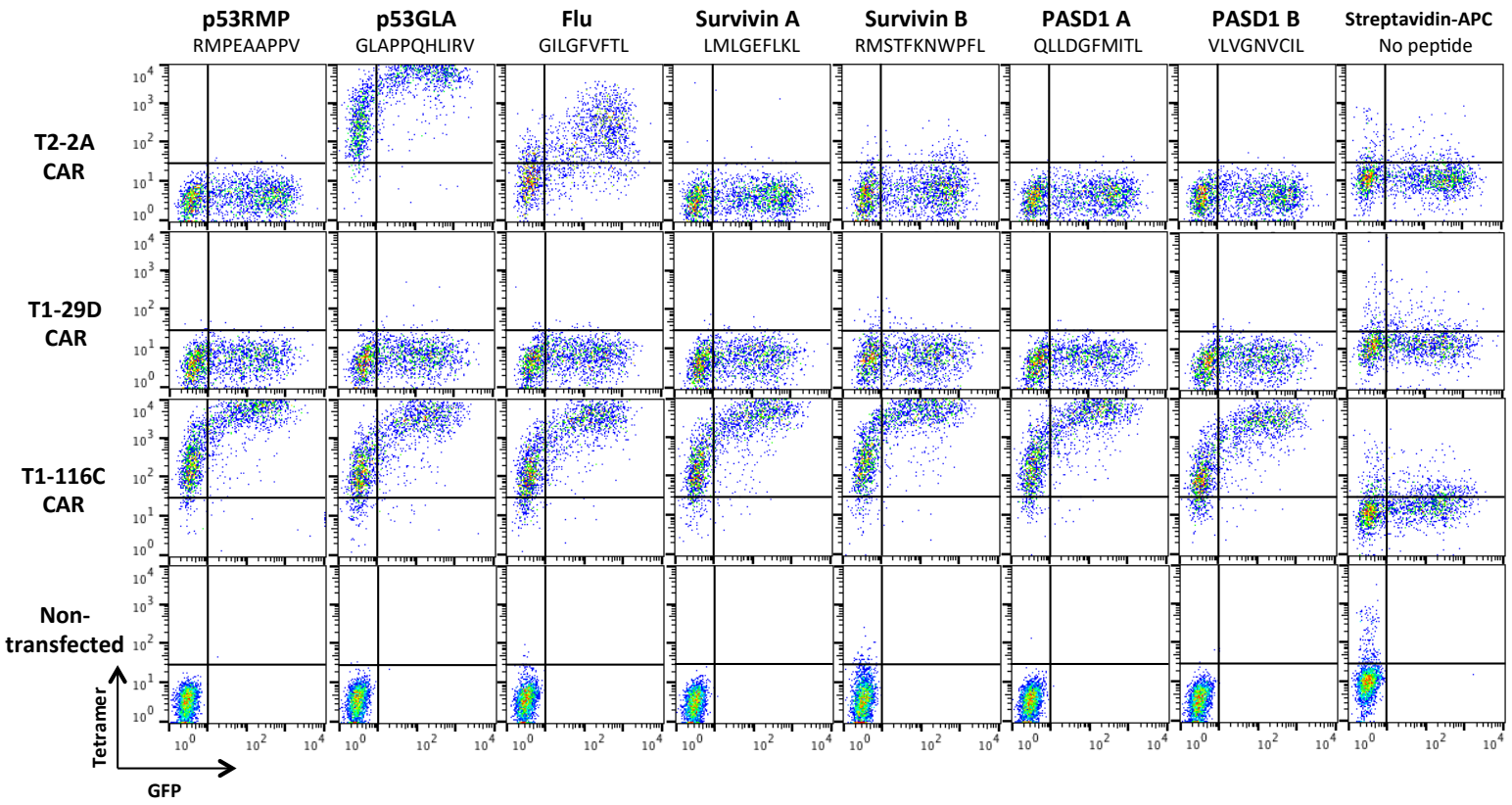

Figure 5.13 – Tetramer staining of HEK293T cells transfected with the T2-2A or the T1-29D CAR.
p53GLA tetramers (GLAPPQHLIRV peptide) were used to detect cell surface expression of the T2-2A CAR, and p53RMP tetramers (RMPEAAPPV peptide) were used to assess surface expression of the T1-29D CAR. Control tetramers included peptides from flu (GILGFVFTL), two different survivin peptides (Survivin A: LMLGEFLKL, and Survivin B: RMSTFKNWPFL) and two different PASD1 peptides (PASD1 A: QLLDGFMITL, and PASD1 B: VLVGNVCIL). A streptavidin control was also included. T1-116C CAR-transfected HEK293T cells were used as a control. The experiment was repeated three times and representative dot plots from one experiment are shown.

This panel of tetramers was an expansion on the panel used for the T1-116C CAR experiment described previously in Figures 5.6 and 5.8. This was the first time that T1-116C CAR binding to the PASD1 and Survivin peptides was tested, and it showed non-specific binding to all of these irrelevant tetramers. The results demonstrated that the T2-2A CAR was considerably more specific than the T1-116C CAR at this early stage of testing. This finding encouraged further characterisation of the T2-2A CAR, while the T1-29D CAR was no longer pursued.

5.4.4 Lentiviral transduction of the Jurkat cell line with the T2-2A CAR

To assess the activity of the T2-2A CAR further, we generated a Jurkat cell line with stable expression of the T2-2A CAR. Similarly to the T1-116C CAR, we used lentiviral transduction to produce the Jurkat cell line expressing the T2-2A CAR (Jurkat-T2-2A-CAR), which showed very low transduction efficiency (Figure 5.14A). We therefore used FACS sorting to successfully enrich for the GFP-positive population of Jurkat-T2-2A-CAR cells (Figure 5.14B).

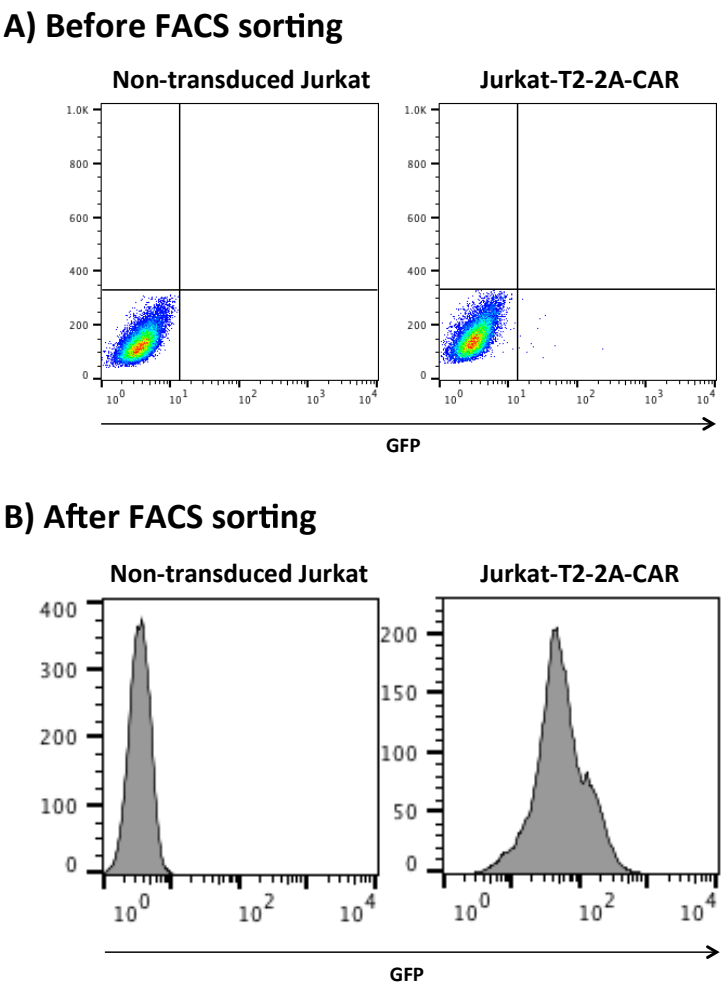

Figure 5.14 – Transduction of Jurkat cells with the T2-2A CAR.
A. Jurkat-T2-2A-CAR cells before FACS sorting: non-transduced Jurkat cells are shown in the left dot plot. Jurkat cells transduced with the T2-2A CAR are shown in the right dot plot. Few GFP-positive cells are detected following transduction. **B.** Jurkat-T2-2A-CAR cells after FACS sorting: the left histogram shows non-transduced Jurkat cells. In the right histogram, the GFP-positive Jurkat-T2-2A-CAR population were enriched by using FACS sorting.

5.4.5 Jurkat-T2-2A-CAR cells specifically recognised p53GLA-HLA-A2 tetramers

We used tetramer staining to validate that the T2-2A CAR is expressed on the cell surface and that it retains its T2-2A-mediated binding specificity. The Jurkat-T2-2A-CAR cells successfully recognised their target p53GLA-HLA-A2 tetramer, and unlike the T1-116C CAR (which recognised PASD1 and Survivin tetramers), showed no non-specific binding of irrelevant tetramers (Figure 5.15). As seen with T1-116C (Figure 5.8 and Figure 5.15), there were also two distinct populations of Jurkat-T2-2A-CAR cells: a GFP single positive population, and an APC and GFP double positive population. This indicates that the T2-2A CAR expression levels differ between the transduced Jurkat cells, and therefore not all transduced cells express the T2-2A CAR at high levels. Using the Jurkat-T1-116C-CAR cells as a control in this experiment demonstrated their non-specific binding of PASD1 and Survivin tetramers for the first time. In retrospect, had we tested the T1-116C CAR against this larger panel of tetramers initially, we would have had an indication of its lack of specificity at an earlier stage. This experiment not only confirmed that the T2-2A CAR is expressed on the surface of the Jurkat-T2-2A-CAR cells, but importantly, its specificity for the target p53GLA-HLA-A2 tetramer is retained, and it showed greater specificity than the T1-116C CAR at this stage.

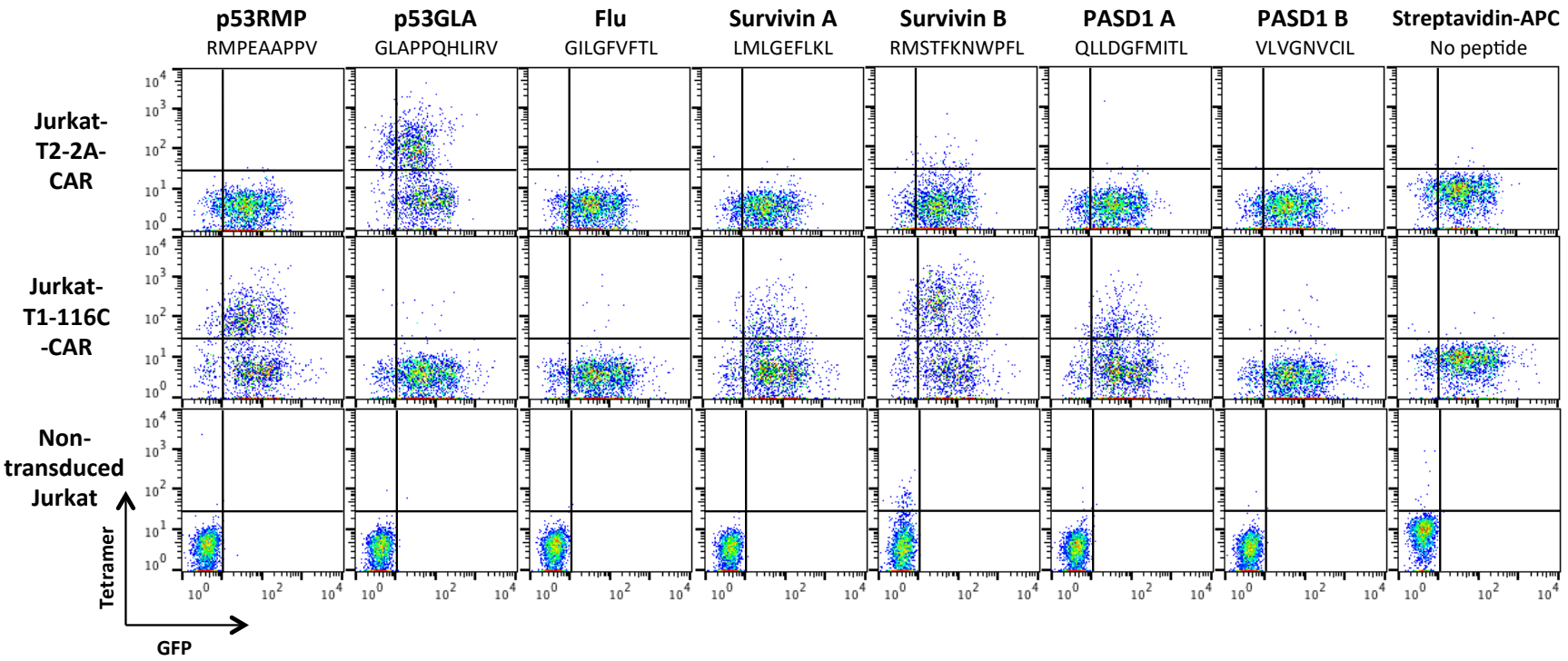

Figure 5.15 - Tetramer staining of Jurkat-T2-2A-CAR cells.

The Jurkat-T2-2A-CAR cells were stained with tetramers to confirm the expression of the T2-2A CAR on the cell surface and assess its specificity. Streptavidin and the previously used panel of irrelevant tetramers including peptides from flu (GILGFVFTL), p53RMP (RMPEAAPPV), two different survivin peptides (Survivin A: LMLGEFLKL, and Survivin B: RMSTFKNWPFL) and two different PASD1 peptides (PASD1 A: QLLDGFMITL, and PASD1 B: VLVGNVCIL) were used as controls. Jurkat-T1-116C-CAR cells were used as a control. Non-transduced Jurkat cells were used as a control. The experiment was repeated three times and representative dot plots from one experiment are shown.

5.4.6 Jurkat-T2-2A-CAR cells were activated to produce IL-2 by cancer cell lines

To assess whether T2-2A CAR engagement with cell lines expressing its target activated CAR-expressing Jurkat cells, we performed overnight co-cultures with a diverse panel of peptide-pulsed T2 cells, cancer cell lines or Jurkat cells expressing recombinant HLA-A2. All of the target cell lines, except the Jurkat cell line, were HLA-A2-positive. We then used an ELISA assay to evaluate IL-2 production by the CAR-expressing cells (Figure 5.16). The T2-2A flow cytometry results provided no clear indication of potential target cell lines (Figure 5.10). We therefore selected a panel of cell lines that covered a diverse range of cancers. We included those that were most strongly recognised by T1-116C, some of which were also very weakly recognised by the other p53GLA-targeting TCRm antibodies, as this could be an indication of target epitope expression at the sensitivity threshold for flow cytometry.

The positive control of T2 cells pulsed with the p53GLA peptide showed the highest levels of IL-2 secretion, as we would have expected because of the large number of target epitopes presented on peptide pulsed T2 cells (Figure 5.16). Indeed, levels of IL-2 secretion were nearly as high as achieved by non-specific T-cell activation with PMA/ionomycin. Importantly, no activation was achieved with T2 cells pulsed with a non-target p53 peptide or with a flu peptide. MO1043 (CLL) and Granta-519 (mantle cell NHL) were the only cancer cell lines that stimulated IL-2 production by the Jurkat-T2-2A-CAR cells. Importantly, Jurkat cells expressing recombinant HLA-A2 did not stimulate the Jurkat-T2-2A-CAR cells, suggesting that the requirement for the dual antigen epitope with a specific target p53 peptide was retained, which is an improvement on the T1-116C CAR. However, it was not possible to confirm that the

T2-2A CAR is binding the p53GLA-HLA-A2 target epitope in the MO1043 and Granta-519 cell lines. Overexpression of wt p53 in HEK293 (HEK293-p53) cells did give a modest, albeit non-significant, increase in IL-2 secretion, suggesting that the target peptide could be processed and presented from the full-length antigen.

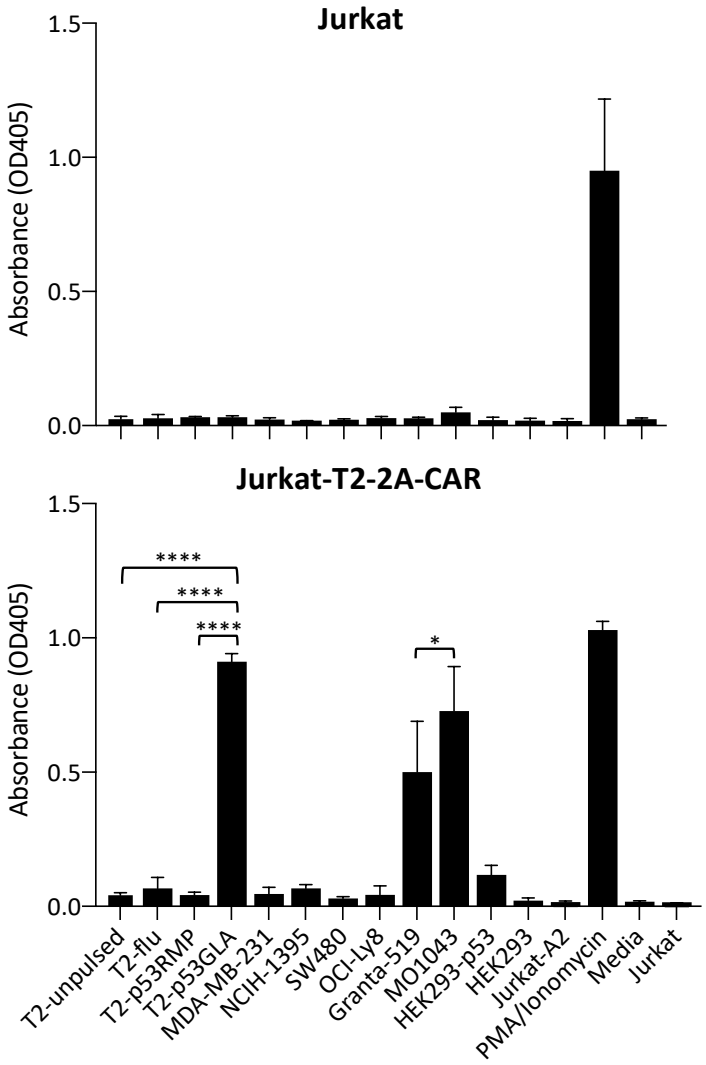

Figure 5.16 – IL-2 ELISA of Jurkat-T2-2A-CAR cells.
IL-2 ELISA of non-transduced Jurkat cells (top graph) or Jurkat-T2-2A-CAR cells (bottom graph). Jurkat cells were co-cultured overnight with different cell lines: T2 cells pulsed with different peptides, cancer cell lines (MDA-MB 231, NCIH-1395, SW480, OCI-Ly8, Granta-519, MO1043), Jurkat cells with stable expression of HLA-A2 (Jurkat-A2), or HEK293 cells over-expressing wt p53 (HEK293-p53). An ELISA was used to assess secreted IL-2 in response to T2-2A CAR-directed recognition of target cells. The positive control was PMA/Ionomycin (P/I), while the negative control was culture media. One-way ANOVA was used for statistical analysis; * indicates p-value ≤ 0.05; **** indicates p-value = ≤ 0.0001. The error bars represent the standard deviation. n=3

5.4.7 IL-2 response of the Jurkat-T2-2A-CAR cells was modestly reduced by competitive blocking with p53GLA-HLA-A2-targeting TCRm antibodies

As the T2-2A antibody did not stain the MO1043 and Granta-519 cell lines by flow cytometry, we had no evidence (other than the Jurkat-T2-2A-CAR IL-2 ELISA) to suggest that the T2-2A scFv can target these cell lines. We attempted to elucidate whether the Jurkat-T2-2A-CAR cells recognised the T2-2A target epitope (p53GLA-HLA-A2) on the MO1043 and Granta-519 cell lines. In order to do this, we investigated whether cellular binding of TCRm antibodies targeting the same p53GLA-HLA-A2 epitope could block the CAR's recognition of its target.

We plated the target cell lines, as in the previous co-culture experiment in Figure 5.16, however before adding the Jurkat-T2-2A-CAR cells to the co-culture, we pre-incubated the cells with one of two different p53GLA-targeting TCRm antibodies or an isotype control antibody, for one hour. The TCRm antibodies were either the T2-2A antibody, from which the CAR scFv is derived, or the T2-108A antibody, which had the same p53GLA-HLA-A2 target as the T2-2A antibody, but did not share an identical epitope with T2-2A (Figure 5.17). Both the T2-2A and isotype control antibodies were of the mIgG2a isotype, whereas T2-108A was of the mIgG1 isotype. Ideally, we should have also included a mIgG1 isotype control antibody, but on the basis of the added cost and time delay of including an additional ELISA plate in every experiment we excluded this extra control.

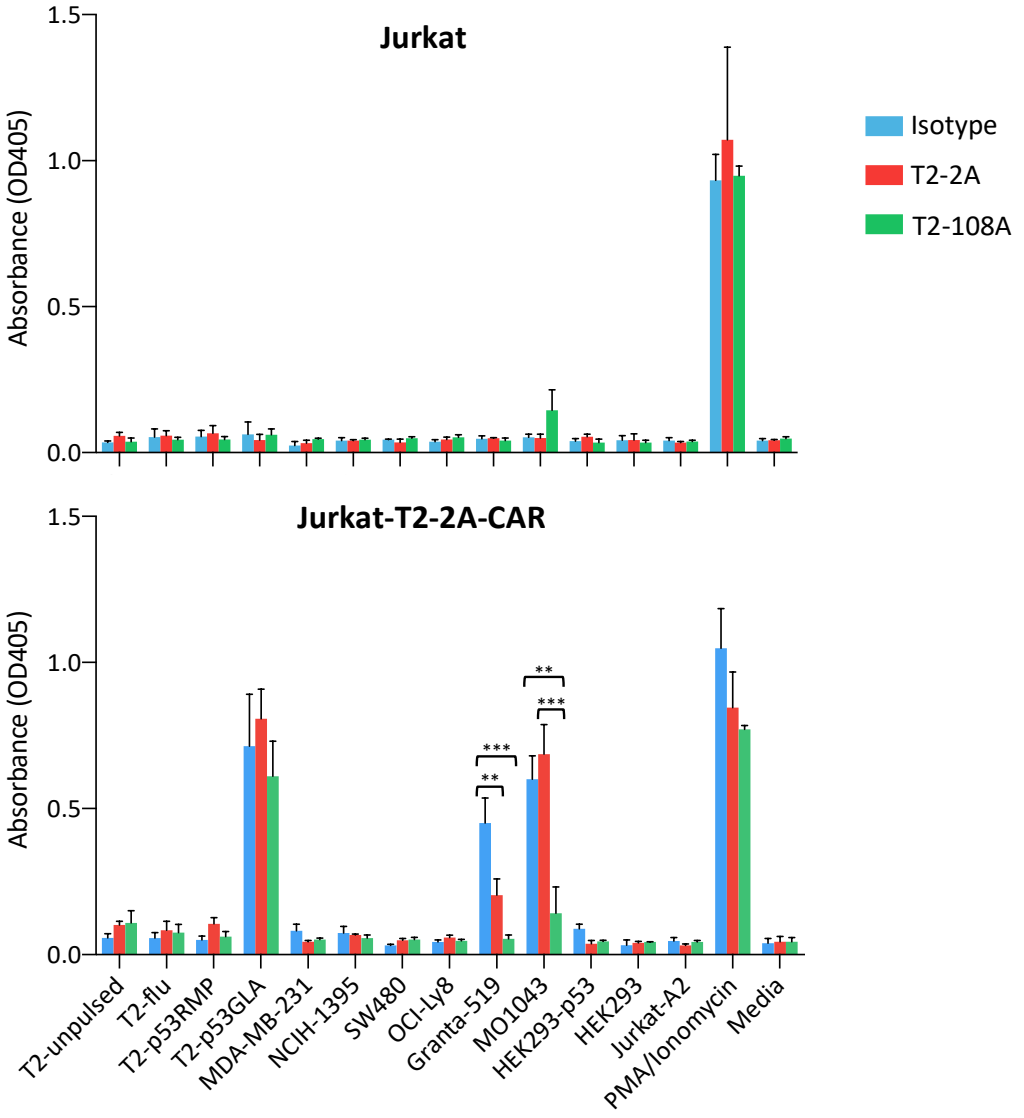

Figure 5.17 - IL-2 ELISA with TCRm antibody blocking.
IL-2 ELISA of non-transduced Jurkat cells (top graph) or Jurkat-T2-2A-CAR cells (bottom graph) cultured with a panel of target cell lines. Prior to adding the Jurkat-T2-2A-CAR or non-transduced Jurkat cells to the target cells, the target cells were incubated with either isotype, T2-2A or T2-108A TCRm antibodies in order test whether their binding to the epitope reduced the IL-2 response observed. One-way ANOVA was performed for the statistical analysis; ** indicates p-value ≤ 0.01; *** indicates p-value ≤ 0.001. Comparisons that were not statistically significant are not indicated on the graph. The error bars represent the standard deviation. n=3.

Contrary to our expectations, the greatest trend in reduction in IL-2 response was caused by pre-incubation with the T2-108A antibody, rather than T2-2A itself (Figure 5.17); this was observed with both the Granta-591 and MO1043 cells. Surprisingly, no significant reduction in IL-2 levels was observed when targeting the p53GLA-pulsed T2 cells used as an epitope specific positive control. Potentially this may reflect the latter's expression of the highest target density, with sufficient unbound p53 epitopes remaining to maintain effective CAR binding and T-cell activation.

The IL-2 response of the Jurkat-T2-2A-CAR cells against p53 overexpressing HEK293 cells was not significantly induced and assessing the levels of intracellular p53 over time by flow cytometry, showed that the levels of p53 had decreased in the HEK293-p53 cells to levels comparable to the parental HEK293 cells (Figure 5.18). Thus it is likely that using the cells at later passages compromised this cell line as a positive control.

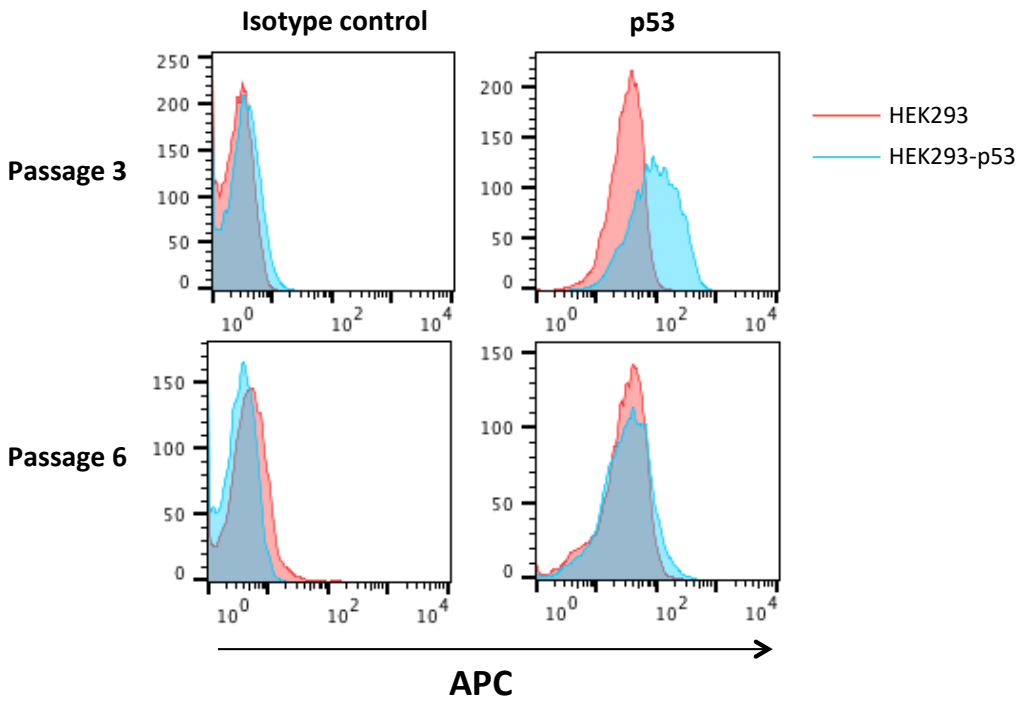

Figure 5.18 - Intracellular staining of HEK293 cell line over-expressing wild type p53.
At passage 3, the HEK293-wt p53 cell line displays higher levels of p53 than the HEK293 cell line. This difference is no longer observed at passage 6, as culture time progresses. An anti-p53-APC antibody was used to stain HEK293 (parental cells not over-expressing wt p53, shown in red) and HEK293-p53 (blue) cells.

The greater reduction of IL-2 levels by the T2-108A antibody was unexpected, because the T2-2A antibody shares an identical epitope with the T2-2A CAR. However, as previously mentioned, the T2-108A antibody was shown to be insufficiently specific for the p53GLA peptide in T2 assays (patent WO2017037440A1) so it is possible that its binding is not p53 peptide-restricted. It would be interesting to test whether a mAb binding HLA-A2 (such as BB7.2) would have a similar effect to T2-108A by preventing T2-2A CAR binding through steric hindrance.

We hypothesised that perhaps T2-108A might have a higher affinity for the target epitope than T2-2A. We have not previously determined the affinities of these antibodies, and only T2-2A, but not T2-108A, had been tested in peptide titration experiments previously. An antibody titration experiment was performed to provide a rough idea of the relative affinities of T2-2A and T2-108A. Decreasing concentrations of either T2-2A or T2-108A antibody were added to p53GLA-pulsed T2 cells. Interestingly, T2-2A achieved maximal binding at a lower antibody concentration than T2-108A (Figure 5.19). This suggested that it was possible that T2-108A did not have a higher affinity than T2-2A that could have explained its stronger effect on IL-2 reduction. A drawback of this experiment was that the secondary mAb (anti-mouse IgG-PE) binds more effectively to the mIgG2a isotype than it does to the mIgG1 isotype. Therefore the difference observed between T2-2A (mIgG2a) and T2-108A (mIgG1) in Figure 5.19 might not reflect the true difference in their binding affinities. The temperature of the incubator (37°C) during the co-culture could have had an effect on TCRm binding, and it was also possible that the off/on rates of the two TCRm mAbs were different; if T2-2A had a faster off-rate it would show weaker binding. It was also possible that T2-108A had higher binding avidity or caused more prolonged target internalisation than T2-2A.

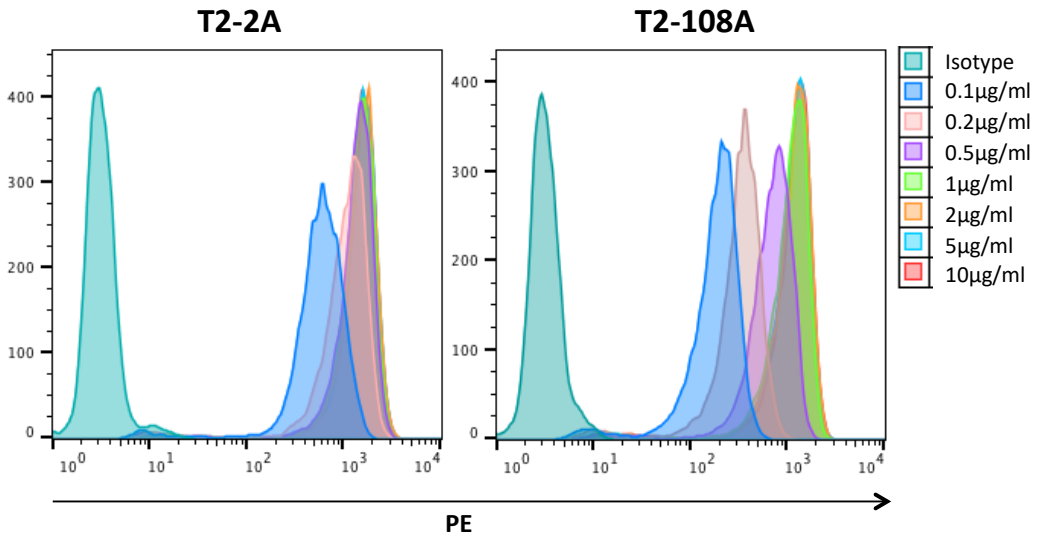

Figure 5.19 - Comparison of T2-2A and T2-108A binding to p53GLA-pulsed T2 cells.
The concentrations of T2-2A (mIgG2a) and T2-108A (mIgG1) were decreased in order to investigate which antibody had a higher affinity for the target-expressing cells. T2-2A showed stronger binding as the antibody concentrations decreased. A secondary anti-mouse IgG-PE antibody was used. The decreasing antibody concentrations that were tested are shown in the legend.

5.5 Discussion

In order to determine whether T1-116C would be suitable for the CAR platform, we first investigated its affinity. Affinity and avidity are one of the key differences between native TCRs and antibodies. TCRs tend to have relatively low affinity, which lies in the µM range, while their avidity is high because of the presence of multiple TCRs on the cell surface (Oren *et al.*, 2014). Antibodies have high affinity in the nM range, however their avidity is lower as it is restricted to the monovalent format in the case of an scFv and a Fab fragment, or the bivalent format for IgG molecules (Oren *et al.*, 2014). The T1-116C affinity had previously been shown to be approximately 1µM, which was surprising because T1-116C showed good binding to cell lines and *in vivo* activity. Ideally high affinity therapeutic antibodies typically have an affinity for their target in the low nM range. The refolding experiments to

test whether T1-116C affinity would be improved by stabilisation of the p53RMP interaction with MHC-I were inconclusive. However, the concurrent findings of our collaborators in the Oncology Department found that the avidity of T1-116C is 92nM. The T1-116C affinity and its 92 nM avidity were more characteristic of a TCR rather than a mAb. This indicated that T1-116C could be therapeutically more effective at redirecting T cells, rather than being used as a naked antibody, thereby encouraging the evaluation of T1-116C as the targeting moiety of a CAR.

The design of the CAR that we used was based on the FMC63-28-CD3ζ CAR, which was used to target CD19 in the treatment of B-cell malignancies (Kochenderfer *et al.*, 2009). CD28 and CD3 were chosen because they correlated with high level CAR expression and antigen-specific cytokine production (Kochenderfer *et al.*, 2009). The CD19-targeting CAR has since been used in clinical trials, where it has produced successful clinical responses in cancer patients whose prognosis was once thought to be terminal if treated with the existing standard of care (Kochenderfer *et al.*, 2013, 2012; Lee *et al.*, 2015; Locke *et al.*, 2017). Axicabtagene ciloleucel, as the CAR is known generically (also known as Yescarta commercially), eventually obtained FDA approval for the treatment of NHL. We selected the V_LV_H orientation of the T1-116C CAR in Figure 5.6 because the MFI of the p53RMP tetramer staining of the V_LV_H CAR was higher than that of the V_HV_L CAR. In retrospect, it would be interesting to know whether the V_HV_L CAR would show greater ability to discriminate between the target tetramer and the irrelevant tetramers, due to differences in scFv orientation or binding affinity.

Both retroviral and lentiviral vectors have been used to integrate CAR genes into host T cells, but retrovirus requires mitotic cells, while lentivirus can transduce quiescent cells, as well as dividing cells (Sadelain, 2017). Integration into the host genome allows long-term expression of the gene of interest. This can be beneficial for CAR T-cell therapy because if the modified T cells have long-term persistence in the patient, then continued CAR expression can ensure a prolonged therapeutic effect. However the benefit of this will need to be evaluated, as long-term persistence beyond the length of a therapeutic regimen may not be desirable; although methods to control this, such as inducible suicide genes, are being investigated (Bonini *et al.*, 1997; Straathof *et al.*, 2005; Di Stasi *et al.*, 2011).

Additionally, the internal promoters used in lentiviral vectors can affect the efficacy of CAR T-cell therapy because they drive transcription of the encoded CAR gene (Jones *et al.*, 2009). Early studies used the CMV immediate early gene promoter, which resulted in efficient expression in actively dividing cell lines (Jones *et al.*, 2009). However the efficacy of promoters varies between cell lines and primary cells, such as T cells, where constitutively active cellular promoters may be more effective (Jones *et al.*, 2009). A study investigating the optimal internal promoter for CAR expression compared the efficacy of a CMV promoter and the elongation factor-1α (EF-1α) promoter (Milone *et al.*, 2009). The CMV promoter drove high expression of a GFP transgene soon after transduction, however it was unable to maintain this level of expression, which decreased over the culture period. The EF-1α promoter was more efficient because it induced the highest level of GFP expression, as well as

maintaining this expression level in CD4 and CD8 cells, over the same culture period (Milone *et al.*, 2009).

The CAR gene in our studies is under a CMV promoter within the lentiviral vector, while GFP is under an SV40 promoter. The GFP reporter gene provided an initial indication of transduction efficiency, however as the GFP and CAR genes were under different promoters, GFP expression did not directly correlate with CAR expression. According to the studies described above, CMV is not the best promoter for driving long-term CAR expression, and this should be considered for future T2-2A CAR experiments in primary T cells. This could explain why even within the FACS sorted CAR-transduced Jurkat cells, not all were able to bind their target tetramer (Figures 5.8 and 5.15). It is possible that inefficient transcription of the CAR gene by the CMV promoter resulted in varying levels of surface CAR expression between cells. It is possible to evaluate CAR surface expression by adding a tag to the extracellular portion of the CAR that can then be detected by flow cytometry following antibody staining. Myc and FLAG-tags are commonly used and detected by their respective antibodies, and naturally occurring epitopes in the extracellular spacer region can also be used. We did not include a tag in the design of the CAR in order to keep the sequence as close as possible to what would be clinically applicable. Instead we used tetramer staining to assess surface CAR expression and CAR specificity. Tetramers are widely used to analyse the expression and peptide specificity of the TCR on T cells, and this approach is equally applicable to TCRm mAbs (Altman *et al.*, 1996; Wooldridge *et al.*, 2009).

IL-2 is a cytokine that is secreted by activated T cells, and assessing IL-2 production by CAR T cells has been used in the literature to evaluate CAR T-cell activity (Finney *et al.*, 1998; Maher *et al.*, 2002; Pulè *et al.*, 2005). IL-2 plays an important immunostimulatory role by promoting the proliferation of blood cells, including T cells (thus IL-2 functions through both paracrine and autocrine signalling). When the TCRs of T cells engage their pMHC target, a cascade of cellular signalling pathways is initiated that lead to cellular proliferation, differentiation and cytokine production, including that of IL-2 (Courtney *et al.*, 2018). The TCR forms a complex with CD3 molecules, which have immunoreceptor tyrosine-based activation motifs (ITAMs). Tyrosine phosphorylation of the ITAMs of CD3, mediated by Src family protein tyrosine kinases (PTKs), triggers the activation of the Src PTKs, Lck and Fyn. Subsequently, Zap70 binds to phosphorylated ITAMs and becomes phosphorylated and activated (Courtney *et al.*, 2018). These phosphorylation events trigger further downstream pathways, including the nuclear factor-κB (NF-κB), nuclear factor of activated T Cells (NFAT), extracellular signal-regulated kinase (ERK) and c-Jun N-terminal kinase (JNK) pathways, which result in the transcription of genes that regulate cellular responses such as cytokine production and proliferation (Courtney *et al.*, 2018).

Studies investigating how many pMHC complexes are required for T-cell activation have concluded that the number can be as low as ≈50 copies of antigen complexes per cell, with some reporting that ≈10 or even fewer epitopes are sufficient (Christinck *et al.*, 1991; Brower *et al.*, 1994; Sykulev *et al.*, 1996; Irvine *et al.*, 2002). The number will vary as it depends on the cell that is presenting the antigen, and

similarly, TCR affinity for its target will also determine how many complexes are required for T-cell activation (Hunt *et al.*, 2007). We do not know how many p53RMP-HLA-A2 or p53GLA-HLA-A2 complexes were presented on the surface of the cell lines that we used in the IL-2 ELISAs described in this chapter. However, the numbers of T1-116C molecules bound to p53RMP-pulsed T2 cells, and MDA-MB-231 and OCI-Ly8 cancer cell lines has been estimated previously (Li *et al.*, 2017a). QuantiBRITE PE-coupled calibration beads were used to generate a standard curve in order to estimate the number of PE-conjugated T1-116C antibodies bound to the cell surface. T2 cells were pulsed with a range of p53RMP concentrations, and it was found that the threshold for detection above background levels was approximately 100-150 T1-116C-PE molecules bound per cell (at the lowest p53RMP concentration of 0.5µM) (Li *et al.*, 2017a). At a p53RMP concentration of 50µM, which was used in the experiments in this chapter, there were approximately 22,000 T1-116C-PE molecules bound per cell. In comparison, the number of T1-116C-PE molecules bound per cell was ≈5,800 for OCI-Ly8, and ≈2,000 for MDA-MB-231 (Li *et al.*, 2017a). Although the estimated number of T1-116C-PE molecules bound per cell does not directly correlate with the number of available epitopes on the target cell, it provides an approximation of epitope numbers. The difference in estimated epitope numbers between the p53RMP-pulsed T2 cells and both the OCI-Ly8 and MDA-MB-231 cell lines is large; thus it is likely that the strongest IL-2 response induced by both the T1-116C and the T2-2A CARs was seen with the p53RMP- or p53GLA-pulsed T2 cells respectively, due to the higher epitope density on the pulsed T2 cells, as compared to the lower physiological levels on the cancer cell lines.

Bossi *et al.* used high affinity monoclonal TCRs and single-molecule fluorescence microscopy to quantify the number of different TAA-derived epitopes (gp100, WT1 and TERT) presented on T2 cells, at different concentrations of exogenous peptide (Bossi *et al.*, 2013). The advantages of using single-molecule fluorescence microscopy over flow cytometry are that the number of epitopes presented by individual cells can be detected and this approach has higher detection sensitivity than flow cytometry (Bossi *et al.*, 2013). They found that T2 cells pulsed with peptide concentrations between 10^{-8} and 10^{-10} M, presented on average 4 to 80 epitope copies per cell. This is similar to the reports of another study, where 10 to 50 copies of NY-ESO-1-derived epitopes were detected on T2 cells, using peptide concentrations between 10^{-9} and 10^{-11} M (Purbhoo *et al.*, 2006). Bossi *et al.* also found that pulsing T2 cells with nanomolar concentrations of gp100-derived peptides produced cell surface epitope numbers that correlated with the number of gp100-derived epitopes presented naturally on Mel526 and Mel624 melanoma cell lines. They found that partial T-cell activation occurred when using T cells transduced with wild-type TCRs against T2 cells pulsed with peptide concentrations of 10^{-8} to 10^{-10} M, which correspond to a physiological amount of epitopes (Bossi *et al.*, 2013). Thus, testing the T-cell response at concentrations of peptide that correspond to physiological levels is important as it will provide a more accurate representation of the likely response under physiological conditions. As a future experiment, it will be important to titrate the p53GLA peptide to generate lower levels of presentation on T2 cells and to test its effect on Jurkat-T2-2A-CAR cell activation. It would also be useful to perform single molecule fluorescence microscopy studies with the p53-targeting TCRm antibodies and TCRm-based CARs to study their cancer cell line and

normal tissue binding, as flow cytometry is not always sensitive enough at low antigen densities.

As the majority of peptides derived from intracellular proteins are presented at low densities on the cell surface, the agents used to target pMHC complexes will have to be very sensitive to low epitope numbers. IgG class antibodies are bivalent, as they have two antigen-binding sites, and their bivalency allows the binding of two targets by one IgG molecule simultaneously. This contributes to the avidity of the antibody, facilitating the activation of immune effector mechanisms, such as ADCC. The binding of multiple IgG molecules to multiple target antigens in close proximity to each other facilitates the cross-linking of Fc receptors on NK cells, activating the NK cells to kill the target cell (Scott *et al.*, 2012a). As the distance between the two Fab arms of the IgG molecule is restricted to 150Å, the bivalent function of IgG molecules can only be engaged when the target antigen is expressed at sufficiently high densities that are compatible with the IgG's physical flexibility (Hadzhieva *et al.*, 2017). The low physiological densities of peptide-HLA (pHLA) targets, such as those derived from TAAs, means that target epitopes will be thinly dispersed across the cell membrane and many mAbs will therefore be physically unable to bind multiple targets, which in turn will impair the activation of effector mechanisms. It is more likely that binding to an antigen will be monovalent, wherein the affinity of the mAb will dictate the stability of the interaction. It seems likely that T1-116C's ability to recognise multiple peptide targets is responsible for its high copy number binding to cancer cell lines and ability to engage immune effector functions. Therefore the density of the target antigen will determine the most suitable therapeutic strategy

and its mechanism of action. For example, using an ADC (Lowe *et al.*, 2017) or CAR-based T-cell approach to target low-density pHLA epitopes would be more effective than using a naked TCRm that functions through ADCC or CDC.

FDA-approved traditional mAbs typically target antigens that are expressed on the cell surface at densities that are much higher than those reported for pHLA targets. For example, in normal cells, CD20 has been reported to be expressed at ≈40,000 to 160,000 epitopes per cell, and CD19 densities have been reported to be ≈20,000 to 30,000 epitopes per cell. It has been shown that the expression levels of both of these antigens can be downregulated in B-cell malignancies, with epitope numbers reported at ≈10,500 to 30,500 per cell for CD20, and ≈5,400 to 13,300 per cell for CD19 (Bikoue *et al.*, 1996; Gratama *et al.*, 1998; Olejniczak *et al.*, 2006; Rossmann *et al.*, 2007). While this is a decrease from the levels on normal B cells, the range of epitope densities is still higher than those of low-density pHLA complexes. The average number of EGFR epitopes per cell have been found to be downregulated from ≈30,700 on normal cervical epithelial cells, to ≈14,700 on cervical squamous cell (Kimmig *et al.*, 1997). HER2 is another TAA that is targeted by mAbs and it is upregulated in cancer; in various tumour types it can undergo an upregulation from ≈50,000 epitopes per cell in normal cells, to ≈2,000,000 epitopes per cell in malignant cells (Brand *et al.*, 2006). As a result of targeting relatively higher antigen densities, traditional mAbs (that do not rely on inactivating the function of their target antigen) can engage immune effector functions such as ADCC and CDC, which are more effective at higher antigen densities (Golay *et al.*, 2001; Golay *et al.*, 2002; Kubo *et al.*, 2003; Van Meerten *et al.*, 2006).

As the low epitope density of pMHC complexes on the cell surface limits TCRm antibody-based therapies that rely on antibody dependent effector functions, it can be addressed by selecting target epitopes that have relatively higher cell surface expression in order to maximise therapeutic success. Alternatively, increasing the expression of MHC-I in tumours (for example by using IFN-γ), designing TCRm antibodies with higher sensitivity to low density epitopes, or selecting effector mechanisms or T-cell based strategies that do not require high epitope density for cytotoxicity could be possible methods to overcome the difficulties of targeting low-density epitopes. Strategies to enhance the ADCC function of mAbs are also available. For example, in fucosylation modification the fucose residues are removed from Fc *N-glycans* in order to increase binding to FcγRIIIa and consequently achieve higher ADCC (Scott *et al.*, 2012a). The ESK1 TCRm antibody targeting the WT1-derived RMFPNAPYL peptide presented by HLA-A2 functions primarily through ADCC *in vitro* and *in vivo* (Dao *et al.*, 2013). The Fc glycosylation of ESK1 was altered in the TCRm antibody ESKM, and this resulted in increased potency and efficacy against its low-density target *in vitro* and *in vivo* (Veomett *et al.*, 2014). Through this glycoengineering strategy, ESKM binding to Fcγ receptors was altered in two ways: (i) ESKM had a higher affinity for binding human FcγRIIIa, which enhanced ADCC, and (ii) and it had reduced affinity for the inhibitory human FcγRIIb, which limited inhibitory receptor activation (Veomett *et al.*, 2014).

It will be important to test the cytotoxic capacity of T2-2A CAR-transduced primary T cells in future experiments. The chromium release assay is a gold standard assay that uses target cells labelled with radioactive chromium (^{51}Cr) to assess CAR T-cell-

mediated cytotoxicity (Brunner *et al.*, 1968; Zaritskaya *et al.*, 2010). CAR T cells are incubated with the radioactive target cells, and if they cause cytolysis of the target cells, the radioactive ^{51}Cr label will be released. After centrifugation to pellet the cells and debris, the radioactivity in the supernatant can be measured in order to quantify the cytotoxic activity. However not all institutions have facilities with the appropriate safety and security measures for working with radioactive materials and therefore require alternative methods to test cytotoxicity. There are flow cytometry-based assays that can be used to assess cytotoxicity, such as the CD107a degranulation assay. Degranulation is a precondition for induction of the perforin/granzyme killing pathway in cytotoxic T cells. Perforin and granzyme are released from pre-formed lysosomes that reside within the cytoplasm. The membrane of the lysosomes is composed of a lipid bilayer, which includes various lysosomal associated membrane glycoproteins (LAMPs), including CD107a (LAMP-1). When degranulation occurs, the lysosomal membrane fuses with the plasma membrane of the CD8+ T cells, releasing the perforin and granzyme into the immunological synapse and externalising CD107a, which can then be detected by antibodies (Peters *et al.*, 1991).

Jurkat cells are not cytotoxic or CD8+, however we performed a CD107a degranulation assay with the Jurkat-T2-2A-CAR cells in order to assess whether they degranulate in response to recognition of target cells and whether this could provide an indication of the cytotoxic capacity of the T2-2A CAR. However we found that Jurkat cells are constantly degranulating and are therefore inappropriate for this assay (Appendix C). It will be interesting to repeat the CD107a degranulation assay

with T2-2A CAR-transduced primary human T cells. If the results of the *in vitro* cytotoxicity tests using human primary T cells were promising, the next step would be to test the *in vivo* cytotoxicity of the T2-2A CAR to further characterise its functional activity.

By developing CARs with our TCRm antibodies, we discovered that one of our existing TCRm antibodies has therapeutic potential even though it did not stain cancer cell lines as a naked TCRm in flow cytometry experiments. Thus some of our other existing TCRm antibodies may also have therapeutic potential; it is possible that their lack of staining of cancer cell lines as naked antibodies is not an indication of a lack of functional activity, but instead of greater specificity for their target peptide. The differences between the T1-116C and T2-2A staining of cancer cell lines, in conjunction with their differential specificity and activity in the CAR format, suggest that T2-2A could be more suitable for therapeutic applications in the CAR format than T1-116C. Other laboratory members have investigated the specificity of the T2-2A antibody further since T1-116C was shown to lack the required specificity (unpublished data). Initial findings showed that amino acid substitutions within the p53GLA peptide that caused the greatest reduction in T2-2A binding were located at both the p53GLA N-terminus and at its central residues. This suggests that, unlike T1-116C, T2-2A binding to its target is not solely focused at the N-terminus, and perhaps its specific need for multiple residues within p53GLA will allow less scope for variation and thereby limit cross-reactivity.

The results of the T2-2A CAR have opened the doors for future work on both the T2-2A TCRm and CAR, which could potentially lead to a new patent. It will be important to characterise the specificity of the T2-2A antibody and the T2-2A CAR, as well as to further evaluate the functional activity of the T2-2A CAR in primary T cells, ideally both *in vitro* and *in vivo*. Using techniques that are more sensitive than flow cytometry will be important for this purpose in order to accurately detect the low densities of pMHC targets.

6 Discussion

6.1 Developing anti-p53/HLA-A*0201 TCRm antibodies against cancer

During this DPhil project we have assessed the specificity and safety of T1-116C, both of which are crucial aspects for its clinical application. We found that T1-116C lacks the required dual antigen specificity for p53 and HLA-A2 and can recognise peptides derived from multiple antigens. Its lack of specificity made it unsuitable for further development as a CAR targeting moiety. However, if the naked antibody does not bind strongly to any normal tissues it may yet retain potential as a cancer therapeutic where binding multiple tumour epitopes may help counter the loss of individual target epitopes under therapeutic selection pressure. Furthermore, we have discovered that the T2-2A CAR shows higher specificity for its dual antigen epitope than the T1-116C CAR. As the low antigen density may be insufficient for the naked T2-2A antibody to effectively engage antibody dependent immune effector functions, it is possible that the T2-2A antibody is most suited for use as a CAR.

6.2 Challenges and opportunities in the development of TCRm antibodies for clinical applications

Both recombinant TCRs and TCRm antibodies are used to target peptides presented by MHC-I, and both can be generated to be soluble and high affinity therapeutics. The TCR and TCRm approaches have become interchangeable, where TCRm antibodies can be used to replace a TCR as the targeting moiety of a CAR for cellular therapy, while TCRs can be fused to an Ig Fc region to activate TCR-directed ADCC

(Mosquera *et al.*, 2005; Oren *et al.*, 2014; Zhang *et al.*, 2014). ImmTACs are soluble affinity-enhanced TCRs that are linked to an anti-CD3 scFv, and through their bispecificity they redirect T cells to eradicate cancer cells expressing the target pMHC complex (Oates *et al.*, 2015). As TCR- and TCRm antibody-based therapies are connected by the fact that they both target pMHC epitopes, they share similar challenges in their development for clinical application.

6.2.1 Preclinical specificity and efficacy evaluation

Due to the dual antigen epitope of TCRm antibodies and TCR-based therapies, conventional *in vivo* models present multiple limitations to efficacy and specificity/safety testing of these therapies and they are often not suitable for this purpose. The MHC-I molecule and the presented peptide, as well as the immune system required to mediate the therapeutic effect, are both human-specific, therefore an intact human peptidome and immune system would be required to fully evaluate the efficacy and specificity of these therapeutics *in vivo*. Animal models can be unsuitable for testing TCRm antibody/TCR immunotherapies because (i) the human and murine proteomes are different and so present different peptides, and (ii) the human and murine immune systems are different, and therefore an immune response observed in a mouse model, or a lack thereof, is not necessarily predictive of a human immune response. Humanised mouse models, such as the HHD mouse model, have been engineered to overcome some of these limitations by expressing human MHC-I. Despite this advantage, HHD mice still present peptides derived from murine proteins that have been generated by the murine processing machinery. Harper *et al.* estimate that approximately 40% of the human MHC-I

peptidome is shared with mice, which suggests that the majority of human pMHC molecules (60%) cannot be assessed in mouse models (Harper *et al.*, 2018).

In order to overcome the limitations of animal models in Immunocore's development of ImmTACs, Harper *et al.* proposed a completely *in vitro*-based approach to preclinical efficacy, specificity and safety testing of ImmTACs, which could also be applied to other TCR-based therapies (Harper *et al.*, 2018). Their methodology tests the therapeutic efficacy of ImmTACs by culturing a panel of target cell lines with effector cells (which are T cells derived from both healthy donors and cancer patients), and assessing T-cell activation by measuring IFN-γ release at different concentrations of ImmTAC, using an enzyme-linked immunospot (ELISpot) assay. For the target cells, indication-relevant tumour cells that express the pHLA target, as well as antigen-negative HLA-relevant tumour cells are tested in order to assess whether antigen specificity is retained. In future experiments, the T2-2A CAR will be transduced into human PBMCs and CAR T-cell activation will be assessed against a panel of antigen-positive and –negative HLA-A2-positive cell lines.

To assess the level of target epitope presentation on target cell lines and how this correlates with cytotoxicity, Harper *et al.* assessed gp100 mRNA transcript levels, HLA-A2 protein levels and apoptosis of target cells at different ImmTAC concentrations (Harper *et al.*, 2018). They proposed that the high levels of apoptosis of the Mel526 and Mel624 cell lines correlated with high gp100 transcript levels and high HLA-A2 surface expression (as assessed by flow cytometry). These two cell lines were previously shown to present similar levels of gp100 epitopes at the cell surface

by single-molecule fluorescence microscopy (Bossi *et al.* 2013). MeWo cells, which have high gp100 mRNA levels but low surface HLA-A2 protein, and WM266-4 cells, which have a contrasting profile of low gp100 mRNA levels but high surface HLA-A2 protein levels, both demonstrated lower levels of cell death than Mel526 and Mel624. They concluded that peptide expression is governed by cellular mRNA levels and HLA-A2 protein expression, both of which will dictate ImmTAC efficacy (Harper *et al.*, 2018). This is interesting, as mRNA expression levels and peptide presentation are not necessarily directly linked. *TP53* transcript levels in a panel of cancer cell lines were determined before this DPhil project, and the results showed that higher transcript levels did not necessarily correlate with stronger TCRm mAb binding by flow cytometry (patent WO2017037440A1). In the IL-2 ELISA of the T2-2A CAR, a response was observed against MO1043 and Granta-519 cell lines, but not against the MDA-MB-231 cell line, which had higher *TP53* transcript levels (patent WO2017037440A1). While it is important to evaluate mRNA levels, these observations indicate that mRNA levels may not always be predictive of the target cell lines that will display the highest response.

Multiple experiments were performed to test the cross-reactivity of the ImmTACs. First, as gp100 is also present in healthy melanocytes, in order to assess the on-target off-tumour activity for ImmTAC-gp100, Harper *et al.* assessed ImmTAC-gp100-directed activation of T cells by measuring IFN-γ release against melanocytes from gp100-positive HLA-A2-positive donors (using the Mel526 melanoma cell line as a positive control). Different doses of ImmTAC-gp100 were tested, and IFN-γ release was measured for the most sensitive donor at ImmTAC-gp100 concentrations

between 1-10 pM. Therefore skin-related off-tumour toxicity could be expected at this concentration in sensitive patients. Second, to assess off-target off-tumour activity, due to recognition of a similar peptide presented by HLA-A2 (or a compatible HLA-A2 subtype), cytokine release in whole blood was measured in order to evaluate the ability of ImmTACs to trigger broad immune responses. ImmTAC-nybr1 was incubated with whole blood from healthy HLA-A2-positive donors and release of IL-2, IFN-γ, IL-6 and TNF-α was measured using the Meso Scale Discovery (MSD) assay. Finally, to test the alloreactivity of ImmTAC-mageA3, 25 target cells or cell lines were used, each of which presents a different HLA type, and IFN-γ release was measured. Similar experiments could be performed for the T2-2A CAR, assessing its on-target off-tumour activity against p53-positive HLA-A2-positive normal cells, as well as assessing cytokine release in whole blood. It would also be important to test the alloreactivity of the T2-2A CAR against a panel of cells and/or cell lines. Harper *et al.* also used comprehensive amino acid substitution, the X-scan described previously, to assess the specificity of their ImmTACs. They draw on their experience from the preclinical testing of many ImmTACs, one of which is currently in clinical trials (ImmTAC-gp100, known in the clinic as IMC-gp100), in order to assemble an *in vitro* methodology for predicting clinical toxicity and determining a safe clinical starting dose, elements of which can be applied to the preclinical evaluation of TCRm antibodies and TCRm-based CARs.

Additionally, pMHC array technology could potentially be useful in assessing the specificity of T2-2A CAR-transduced T cells for different pMHC tetramers. Generally, pMHC arrays provide a high throughput strategy for the detection of CD8+ T-cell

populations found in patient blood samples (Brooks *et al.*, 2015; Bentzen & Hadrup, 2017). Fluorescently labelled pMHCs are printed onto distinct spots on a hydrogel slide and purified CD8+ T cells lipophyllically dyed with DiD are incubated with the pMHC array and CD8+ T-cell populations specific for pMHCs printed on the hydrogel can be detected using a microarray scanner (Brooks *et al.*, 2015). A single microarray advantageously has the capacity to hold up to 1000 tetramer spots that can represent different peptides and HLA restrictions for testing alloreactivity. Furthermore, a small number of T cells (0.8-1.25x10^6/array) is required, which is particularly advantageous when testing primary blood samples that may have limited cell numbers (Brooks *et al.*, 2015). The pMHC array approach could be used to test the specificity of T2-2A CAR-transduced T cells using pMHC tetramers that include different HLA restrictions and potentially cross-reactive peptides identified from *in silico* analyses. Where T2-2A CAR-transduced T cells are found to bind any cross-reactive pMHC tetramers, the results can be confirmed using flow cytometry and further *in vitro* analyses to assess the safety risk. It will be important to validate T2-2A CAR-transduced T-cell binding of cells or cell lines presenting the cross-reactive pMHC where possible, in order to assess CAR binding to cell surface pMHC.

6.2.2 Microscopy platforms to detect and quantify low-density pMHC epitopes

A large proportion of MHC-I molecules are occupied by peptides derived from the most abundant cellular proteins that have the highest synthesis rates, such as ribosomal and heat shock proteins, or viral proteins in the case of viral infection (Yewdell *et al.*, 2003). As a result, less abundant cellular proteins, such as TAAs, are likely to be presented at much lower levels. While it has been shown that low pMHC

numbers are sufficient for T-cell activation, it is still important to quantify epitope numbers because they will determine: (i) whether the antigen is targetable by immunotherapy, and (ii) the type of immunotherapy that is most suitable (higher epitope density is suitable for naked mAbs, while low epitope density is more suitable for ADCs and for TCRm/TCR T-cell based therapies). Thus screening methods are needed that are sensitive enough to identify the binding of these reagents to cells expressing low copy numbers of target pMHC.

Single-molecule fluorescence microscopy has been shown to be effective in quantifying pMHC density at the cell surface. Importantly, it can be used to assess the specificity of TCR-based therapies for target cells and to assess their efficacy even against low-density epitopes during their preclinical evaluation (Purbhoo *et al.*, 2006; Bossi *et al.*, 2013). Purbhoo *et al.* reported using single-molecule fluorescence microscopy in combination with high-affinity soluble TCRs, to detect and quantify the number of NY-ESO-$1_{157\text{-}165}$/HLA-A2 epitopes presented on the surface of peptide-pulsed T2 cells, cancer cell lines and primary tumours (Purbhoo *et al.*, 2006). They used an affinity-enhanced soluble TCR specific for NY-ESO-$1_{157\text{-}165}$/HLA-A2, which is biotinylated and can therefore be stained with streptavidin-PE. They imaged the entire 3D cell surface in order to detect single PE molecules. Biotinylated-TCR/pHLA complexes were labelled with streptavidin-PE in a 1:1 ratio, therefore the number of PE molecules detected represented the number of pHLA epitopes presented on the entire cell surface. This highly sensitive approach was able to detect as low as ≈10 epitopes on the surface of T2 cells pulsed with as little as a 10^{-10} M peptide concentration. Thus they found that single-molecule fluorescence microscopy is

more sensitive than FACS, which had a maximal sensitivity for PE that lies between 200 to 500 PE molecules per cell (Purbhoo *et al.*, 2006).

Purbhoo *et al.* also determined the number of epitopes on HLA-A2-positive melanoma cell lines, and found that cell surface NY-ESO-$1_{157-165}$/HLA-A2 antigen could not be detected with the soluble TCR by FACS (Purbhoo *et al.*, 2006). They proposed that the antigen levels were below the threshold for flow cytometric detection, and indeed showed that single-molecule fluorescence microscopy could quantify the number of antigens on individual melanoma cells (Purbhoo *et al.*, 2006). They reported that SK-Mel-37 presented an average of 25 epitopes per cell, while Mel-624 presented an average of 45 epitopes per cell, with antigen levels varying between individual cells and likely representing the heterogeneity of antigen expression found in tumours (Purbhoo *et al.*, 2006). They verified that these antigen levels were sufficient to induce IFN-y secretion by target-specific CTLs, and showed that primary melanoma cells expressed similar antigen numbers, which are representative of physiological surface densities (Purbhoo *et al.*, 2006).

Thus the use of single molecule microscopy is more sensitive than flow cytometry and it could help evaluate the specificity of TCRm mAbs and TCRm-based CAR T cells for a target antigen with very low cell surface expression. It can also be used in the preclinical assessment of TCRm antibodies to quantify the number of antigens on different target cell lines and thereby determine the number of antigens required for a cytotoxic response (thus assessing the sensitivity of the TCRm antibody and its suitability as a therapeutic agent).

6.2.3 MHC-I restriction of TCRm antibody therapies

The MHC-I-restricted nature of TCRm antibodies advantageously provides their unique specificity for human pMHC complexes and allows the targeting of intracellular proteins. However it can also be a disadvantage, as it confines their applicability to a limited population of patients that present the targeted HLA haplotype. In order to maximise the applicability of TCRm therapies and cover the largest possible proportion of the world population, researchers have focused on designing TCRm antibodies that target the most widely expressed HLA haplotypes. For example, the HLA-A2 haplotype is the most prevalent haplotype in Caucasians, covering approximately 40% of this population, and it is also present in populations of other ethnicities, but to a lower extent (Dao *et al.*, 2013). It is also possible that TCRm antibodies targeting the HLA-A*0201 subtype could be used to target other HLA-A2 subtypes because of minimal differences between their sequences that still enable TCRm binding, thus further widening the patient population that could benefit from therapy. HLA-A24 is a dominant haplotype in Asian populations; therefore targeting HLA-A24-restricted peptides could have wider applicability in Asian populations (DeLeo *et al.*, 2008).

For patients who do not present the targeted HLA haplotype, analogous TCRm mAbs would have to be designed, and this would depend on whether the same target peptide can be presented by other haplotypes. As explained previously, another disadvantage of the requirement for MHC-I in TCRm antibody therapy is that MHC-I downregulation is a tumour escape mechanism. To overcome this, using a combination of TCRm-based therapies that target different epitopes on the same

antigen or that target multiple tumour antigens could promote better tumour eradication and reduce immune evasion through MHC-I and antigen downregulation.

6.2.4 Prospects for the clinical application of TCRm antibodies

TCRm antibodies represent an immunotherapeutic approach that expands the target antigen repertoire of mAbs to include intracellular proteins. Generating large quantities of high-affinity and peptide-specific TCRm antibodies using traditional hybridoma technology or phage display has been difficult. However, with the development of enhanced display technologies, which enable the isolation of fully human antibodies within short timeframes, there are prospects for improving future TCRm antibody development (Frenzel *et al.*, 2017). The generation of more TCRm antibodies, in combination with a better understanding of their required characteristics and target expression profiles, will increase the chances of discovering new therapeutic agents. Importantly, TCRm antibodies have multiple applications: in the laboratory they can be used as research tools to study antigen presentation, while in the clinic they can be used as theranostics.

TCRm antibodies have yet to progress to clinical studies, however the partnership between Novartis, Eureka Therapeutics and Memorial Sloan Kettering Cancer Centre could see one of their TCRm antibodies, such as ESK1, advance to be the first TCRm antibody to be tested in humans (Martz, 2017). Manufacture and regulatory approval for TCRm antibodies is likely to share aspects that are common to both traditional mAbs and TCR-based therapies due to the dual antigen target. The preclinical assessment of TCRm-based therapies will have to be customised based on

the characteristics of the dual antigen epitope and the availability of appropriate *in vitro*, *in vivo*, and *in silico* techniques. As more TCRm antibodies are generated and tested, the experience and knowledge gained from these studies will aid in establishing systematic approaches to preclinical specificity and efficacy evaluation.

6.3 Future directions and final conclusions

While the ability of T1-116C to target multiple tumour antigens could be useful in minimising escape variants, it makes it difficult to define exactly which tumour antigens it is likely to target, in both the antibody and CAR format. Moreover, T1-116C was shown to be capable of binding peptides derived from normal tissue antigens, and so its reactivity is not limited to tumour antigens. This lack of defined specificity may make it difficult to acquire regulatory approval for the use of T1-116C as a therapeutic agent, without further data, perhaps from imaging studies. Nevertheless, T1-116C could still be a valuable research tool in the laboratory. Solving the crystal structure of T1-116C could be useful in order to define the residues in the p53RMP peptide and the HLA-A2 molecule that form part of its epitope, as well as to define its binding orientation. Knowing which residues are recognised by T1-116C could also aid in predicting cross-reactive peptides more conclusively.

Through this DPhil project, T2-2A has emerged as a promising TCRm antibody to pursue in future studies. The T2-2A CAR was more specific than the T1-116C CAR in the IL-2 ELISAs. The initial findings of the comprehensive scanning of the p53GLA peptide performed by other members in the laboratory suggest that T2-2A binding is

not centred around the residue in position 1; the T2-2A epitope seems to involve multiple residues at the N-terminus and in the central portion of the peptide, which could potentially limit variation and cross-reactivity. The T2-2A peptide specificity will have to be analysed further in order to map its epitope and identify any cross-reactive peptides. Solving the crystal structure of the T2-2A TCRm antibody binding to its p53GLA-HLA-A*02:01 target would make an important contribution to epitope mapping.

The ability of the T2-2A antibody and the T2-2A CAR to label primary tumours will have to be analysed, as well as analysing their cytotoxicity against target cell lines and primary cells. It will be important to use target cell lines that have different combinations of p53 and HLA-A2 expression profiles (including different HLA-A2 subtypes), as well as testing target cell lines that have different HLA haplotypes, in order to comprehensively assess the specificity for the dual antigen epitope. Analysing T2-2A antibody staining of cancer cell lines by flow cytometry was unsuccessful, therefore a more sensitive technique, such as single molecule microscopy could be useful to assess whether the naked T2-2A antibody does in fact stain cancer cell lines. The peptides from any T2-2A-positive cancer cell lines could then be eluted and identified using mass spectrometry (for example, this could be done for Granta-519 and MO1043, which were recognised by the T2-2A CAR), in order to investigate the endogenous presentation of the target p53GLA peptide.

For further evaluation of the T2-2A CAR, primary T cells will be transduced with the T2-2A CAR and their cytotoxicity evaluated. The lack of appropriate *in vivo* models

for the evaluation of TCR-based therapies makes the *in vivo* evaluation of such therapeutics difficult. In order to perform an extensive preclinical assessment that is in line with research in the field, the biodistribution of the T2-2A TCRm antibody could be analysed in HHD mice, despite the limitations of this model. The efficacy of the T2-2A antibody and the T2-2A CAR could also be tested against tumour xenografts, as well as assessing their biodistribution in these studies. Assessing the biodistribution of the T2-2A antibody using *in vivo* imaging studies of a subtherapeutic dose of the T2-2A antibody could be an opportunity for early clinical safety studies.

In conclusion, we have shown that T2-2A could be a suitable TCRm antibody for the development of p53-targeting cancer immunotherapies. This is an impactful discovery because there is a lack of TCRm antibodies targeting wt p53-derived peptides, and there is a need to develop immunotherapies targeting wt p53, which is recognised as an important cancer antigen. As this antibody was not claimed in the original patent application, and as its sequence was not disclosed, further work is ongoing to obtain sufficient therapeutic efficacy data to file a subsequent application to protect the T2-2A antibody. We have furthered our understanding of the T1-116C specificity and safety using the comprehensive amino acid scanning in combination with *in silico*, *in vitro* and *in vivo* methods. Moreover, assessing the use of the TCRm antibodies as CARs has shown that this immunotherapeutic platform could be more suitable for the targeting of low-density wt p53/HLA-A*02:01 targets. The knowledge and experience acquired through this DPhil project have contributed to advancing

the development of TCRm antibody-based therapies in our laboratory and have laid the foundations for future characterisation of the T2-2A antibody and T2-2A CAR.

References

Ahmed, M., Lopez-Albaitero, A., Pankov, D., Santich, B. H., Liu, H., Yan, S., Xiang, J., Wang, P., Hasan, A. N., Selvakumar, A., O'Reilly, R. J., Liu, C., & Cheung, N. V. (2018). TCR-mimic bispecific antibodies targeting LMP2A show potent activity against EBV malignancies. *Journal of Clinical Investigation Insight*, *3*(4), e97805.

Altman, J. D., Moss, P. A., Goulder, P. J., Barouch, D. H., McHeyzer-Williams, M. G., Bell, J. I., McMichael, A. J., & Davis, M. M. (1996). Phenotypic analysis of antigen-specific T lymphocytes. *Science*, *274*(5284), 94–96.

Angell, T. E., Lechner, M. G., Jang, J. K., LoPresti, J. S., & Epstein, A. L. (2014). MHC class I loss is a frequent mechanism of immune escape in papillary thyroid cancer that is reversed by interferon and selumetinib treatment in vitro. *Clinical Cancer Research*, *20*(23), 6034–6044.

Ataie, N., Xiang, J., Cheng, N., Brea, E. J., Lu, W., Scheinberg, D. A., Liu, C., & Ng, H. L. (2016). Structure of a TCR-Mimic Antibody with Target Predicts Pharmacogenetics. *Journal of Molecular Biology*, *428*(1), 194–205.

Backert, L., & Kohlbacher, O. (2015). Immunoinformatics and epitope prediction in the age of genomic medicine. *Genome Medicine*, *7*(119).

Barfoed, A. M., Petersen, T. R., Kirkin, A. F., Thor Straten, P., Claesson, M. H., & Zeuthen, J. (2000). Cytotoxic T-lymphocyte clones, established by stimulation with the HLA-A2 binding $p53_{65-73}$ wild type peptide loaded on dendritic cells in vitro, specifically recognise and lyse HLA-A2 tumour cells overexpressing the p53 protein. *Scandinavian Journal of Immunology, 51*(2), 128-133.

Barouch, D. H., Friede, T., Stevanovic, S., Tussey, L., Smith, K., Rowland-Jones, S., Braud, V., McMichael, A. J., & Rammensee, H. G. (1995). HLA-A2 subtypes are functionally distinct in peptide binding and presentation. *The Journal of Experimental Medicine*, *182*(6), 1847–1856.

Bassani-Sternberg, M., Pletscher-Frankild, S., Jensen, L. J., & Mann, M. (2015). Mass spectrometry of human leukocyte antigen class I peptidomes reveals strong effects of protein abundance and turnover on antigen presentation. *Molecular and Cellular Proteomics, 14*(3), 658-673.

Beatty, G. L., & Gladney, W. L. (2015). Immune escape mechanisms as a guide for cancer immunotherapy. *Clinical Cancer Research*, *21*(4), 687–692.

Bentzen, A. K., & Hadrup, S. R. (2017). Evolution of MHC-based technologies used for detection of antigen-responsive T cells. *Cancer Immunology, Immunotherapy*, *66*(5), 657–666.

Bernardeau, K., Gouard, S., David, G., Ruellan, A. L., Devys, A., Barbet, J., Bonneville, M., Chérel, M., & Davodeau, F. (2005). Assessment of CD8 involvement in T cell clone avidity by direct measurement of HLA-A2/Mage3 complex density using a high-affinity TCR like monoclonal antibody. *European Journal of Immunology*, *35*(10), 2864–2875.

Betts, M. R., Brenchley, J. M., Price, D. A., De Rosa, S. C., Douek, D. C., Roederer, M., & Koup, R. A. (2003). Sensitive and viable identification of antigen-specific CD8+ T cells by a flow cytometric assay for degranulation. *Journal of Immunological Methods*, *281*(1-2), 65–78.

Bhattacharya, R., Xu, Y., Rahman, M. A., Couraud, P. O., Romero, I. A., Weksler, B. B., Weidanz, J. A., & Bickel, U. (2010). A novel vascular targeting strategy for brain-derived endothelial cells using a TCR mimic antibody. *Journal of Cellular Physiology*, *225*(3), 664–672.

Bikoue, A., George, F., Poncelet, P., Mutin, M., Janossy, G., & Sampol, J. (1996). Quantitative analysis of leukocyte membrane antigen expression: Normal adult values. *Communications in Clinical Cytometry*, *26*(2), 137–147.

Blottière, H. M., Steplewski, Z., Herlyn, D., & Douillard, J. Y. (1991). Human anti-murine immunoglobulin responses and immune functions in cancer patients receiving murine monoclonal antibody therapy. *Human Antibodies*, *2*(1), 16–25.

Bonini, C., Ferrari, G., Verzeletti, S., Servida, P., Zappone, E., Ruggieri, L., Ponzoni, M., Rossini, S., Mavilio, F., Traversari, C., & Bordignon, C. (1997). HSV-TK gene transfer into donor lymphocytes for control of allogeneic graft-versus-leukemia. *Science*, *276*(5319), 1719–1724.

Bossi, G., Gerry, A. B., Paston, S. J., Sutton, D. H., Hassan, N. J., & Jakobsen, B. K. (2013). Examining the presentation of tumor-associated antigens on peptide-pulsed T2 cells. *OncoImmunology*, *2*(11), e26840.

Brand, F. X., Ravanel, N., Gauchez, A. S., Pasquier, D., Payan, R., Fagret, D., & Mousseau, M. (2006). Prospect for anti-HER2 receptor therapy in breast cancer. *Anticancer Research*, *26*(1B), 463–470.

Brentjens, R. J., Latouche, J. B., Santos, E., Marti, F., Gong, M. C., Lyddane, C., King, P. D., Larson, S., Weiss, M., Rivière, I., & Sadelain, M. (2003). Eradication of systemic B-cell tumors by genetically targeted human T lymphocytes co-stimulated by CD80 and interleukin-15. *Nature Medicine*, *9*(3), 279–286.

Brentjens, R. J., Davila, M. L., Riviere, I., Park, J., Wang, X., Cowell, L. G., Bartido, S., Stefanski, J., Taylor, C., Olszewska, M., Borquez-Ojeda, O., Qu, J., Wasielewska, T., He, Q., Bernal, Y., Rijo, I. V., Hedvat, C., Kobos, R., Curran, K., Steinherz. P., Jurcic, J., Rosenblat, T., Maslak, P., Frattini, M., & Sadelain, M. (2013). CD19-targeted T cells rapidly induce molecular remissions in adults with

chemotherapy-refractory acute lymphoblastic leukemia. *Science Translational Medicine*, *5*(177), 177ra38.

Brocker, T., Peter, A., Traunecker, A., & Karjalainen, K. (1993). New simplified molecular design for functional T cell receptor. *European Journal of Immunology*, *23*(7), 1435–1439.

Brocker, T., & Karjalainen, K. (1995). Signals through T cell receptor-zeta chain alone are insufficient to prime resting T lymphocytes. *The Journal of Experimental Medicine*, *181*(5), 1653–1659.

Brocks, B., Garin-Chesa, P., Behrle, E., Park, J. E., Rettig, W. J., & Pfizenmaier, K. und Moosmayer, D. (2001). Species-crossreactive scFv against the tumor stroma marker "fibroblast activation protein" selected by phage display from an immunized FAP-/- knock-out mouse. *Molecular Medicine*, *7*(7), 461–469.

Brooks, S. E., Bonney, S. A., Lee, C., Publicover, A., Khan, G., Smits, E. L., Sigurdardottir, D., Arno, M., Li, D., Mills, K. I., Pulford, K., Banham, A. H., Van Tendeloo, V., Mufti, G. J., Rammensee, H. G., Elliott, T. J., Orchard, K. H., & Guinn, B. A. (2015). Application of the pMHC array to characterise tumour antigen specific T cell populations in leukaemia patients at disease diagnosis. *PLoS ONE*, *10*(10), e0140483.

Brower, R. C., England, R., Takeshita, T., Kozlowski, S., Margulies, D. H., Berzofsky, J. A., & Delisi, C. (1994). Minimal requirements for peptide mediated activation of CD8+ CTL. *Molecular Immunology*, *31*(16), 1285–1293.

Brunner, K. T., Mauel, J., Cerottini, J. C., & Chapuis, B. (1968). Quantitative assay of the lytic action of immune lymphoid cells on 51-Cr-labelled allogeneic target cells in vitro; inhibition by isoantibody and by drugs. *Immunology*, *14*(2), 181–196.

Cameron, B. J., Gerry, A. B., Dukes, J., Harper, J. V., Kannan, V., Bianchi, F. C., Grand, F., Brewer, J. E., Gupta, M., Plesa, G., Bossi, G., Vuidepot, A., Powlesland, A. S., Legg, A., Adams, K. J., Bennett, A. D., Pumphrey, N. J., Williams, D. D., Binder-Scholl, G., Kulikovskaya, I., Levine, B. L., Riley, J.L., Varela-Rohena, A., Stadtmauer, E. A., Rapoport, A. P., Linette, G. P., June, C. H., Hassan, N. J., Kalos, M., & Jakobsen, B. K. (2013). Identification of a Titin-Derived HLA-A1-Presented Peptide as a Cross-Reactive Target for Engineered MAGE A3-Directed T Cells. *Science Translational Medicine*, *5*(197), 197ra103.

Campoli, M., & Ferrone, S. (2008). HLA antigen changes in malignant cells: Epigenetic mechanisms and biologic significance. *Oncogene*, *27*(45), 5869–5885.

Casadevall, A. (1996). Antibody-Based Therapies for Emerging Infectious Diseases. *Emerging Infectious Diseases*, *2*(3), 200–208.

Chaise, C., Buchan, S. L., Rice, J., Marquet, J., Rouard, H., Kuentz, M., Vittes, G. E., Molinier-Frenkel, V., Farcet, J. P., Stauss, H. J., Delfau-Larue, M. H., & Stevenson, F. K. (2008). DNA vaccination induces WT1-specific T-cell responses with potential clinical relevance. *Blood*, *112*(7), 2956–2964.

Chames, P., Hufton, S. E., Coulie, P. G., Uchanska-Ziegler, B., & Hoogenboom, H. R. (2000). Direct selection of a human antibody fragment directed against the tumor T-cell epitope HLA-A1-MAGE-A1 from a nonimmunized phage-Fab library. *Proceedings of the National Academy of Sciences*, *97*(14), 7969–7974.

Chames, P., Willemsen, R. A., Rojas, G., Dieckmann, D., Rem, L., Schuler, G., Bolhuis, R. L., & Hoogenboom, H. R. (2002). TCR-Like Human Antibodies Expressed on Human CTLs Mediate Antibody Affinity-Dependent Cytolytic Activity. *Journal of Immunology*, *169*(2), 1110–1118.

Chames, P., Van Regenmortel, M., Weiss, E., & Baty, D. (2009). Therapeutic antibodies: Successes, limitations and hopes for the future. *British Journal of Pharmacology*, *157*(2), 220–233.

Chang, A. Y., Dao, T., Gejman, R. S., Jarvis, C. A., Scott, A., Dubrovsky, L., Mathias, M. D., Korontsvit, T., Zakhaleva, V., Curcio, M., Hendrickson, R. C., Liu, C., & Scheinberg, D. A. (2017). A therapeutic T cell receptor mimic antibody targets tumor-associated PRAME peptide/HLA-I antigens. *Journal of Clinical Investigation*, *127*(7), 2705–2718.

Cheever, M. A., Allison, J. P., Ferris, A. S., Finn, O. J., Hastings, B. M., Hecht, T. T., Mellman, I., Prindiville, S. A., Viner, J. L., Weiner, L. M., & Matrisian, L. M. (2009). The prioritization of cancer antigens: A National Cancer Institute pilot project for the acceleration of translational research. *Clinical Cancer Research*, *15*(17), 5323–5337.

Christinck, E. R., Luscher, M. A., Barber, B. H., & Williams, D. B. (1991). Peptide binding to class I MHC on living cells and quantitation of complexes required for CTL lysis. *Nature*, *352*(6330), 67–70.

Cohen, C. J., Hoffmann, N., Farago, M., Hoogenboom, H. R., Eisenbach, L., & Reiter, Y. (2002). Direct detection and quantitation of a distinct T-cell epitope derived from tumor-specific epithelial cell-associated mucin using human recombinant antibodies endowed with the antigen-specific, major histocompatibility complex-restricted specificity of T cells. *Cancer Research*, *62*(20), 5835–5844.

Cohen, M., & Reiter, Y. (2013). T-Cell Receptor-Like Antibodies: Targeting the Intracellular Proteome Therapeutic Potential and Clinical Applications. *Antibodies*, *2*(3), 517–534.

Conforti, A., Peruzzi, D., Giannetti, P., Biondo, A., Ciliberto, G., Monica, N. La, & Aurisicchio, L. (2009). A novel mouse model for evaluation and prediction of

HLA-A2-restricted CEA cancer vaccine responses. *Journal of Immunotherapy*, *32*(7), 744–754.

Courtney, A. H., Lo, W. L., & Weiss, A. (2018). TCR Signaling: Mechanisms of Initiation and Propagation. *Trends in Biochemical Sciences*, *43*(2), 108–123.

CRUK. Cancer Research UK, Cancer Statistics for the UK, 2019. https://www.cancerresearchuk.org/health-professional/cancer-statistics-for-the-uk#heading-One

Cunningham, B. C., & Wells, J. A. (1989). High-Resolution Epitope Mapping of hGH-Receptor Interactions by Alanine-Scanning Mutagenesis. *Science*, *244*(4908), 1081–1085.

Dahan, R., & Reiter, Y. (2012). T-cell-receptor-like antibodies - generation, function and applications. *Expert Reviews in Molecular Medicine*, *14*, e6.

Dao, T., Yan, S., Veomett, N., Pankov, D., Zhou, L., Scott, A., Whitten, J., Maslak, P., Casey, E., Tan, T., Liu, H., Zakhaleva, V., Curcio, M., Doubrovina, E., Richard, J., Reilly, O., Liu, C., & Scheinberg, D. A. (2013). Targeting the Intracellular WT1 Oncogene Product with a Therapeutic Human Antibody. *Science Translational Medicine*, *5*(176), 1–22.

Dao, T., Pankov, D., Scott, A., Korontsvit, T., Zakhaleva, V., Xu, Y., Xiang, J., Yan, S., De Morais Guerreiro, M. D., Veomett, N., Dubrovsky, L., Curcio, M., Doubrovina, E., Ponomarev, V., Liu, C., O'Reilly, R. J., & Scheinberg, D. A. (2015). Therapeutic bispecific T-cell engager antibody targeting the intracellular oncoprotein WT1. *Nature Biotechnology*, *33*(10), 1079–1086.

Dattamajumdar, A. K., Jacobson, D. P., Hood, L. E., & Osman, G. E. (1996). Rapid cloning of any rearranged mouse immunoglobulin variable genes. *Immunogenetics*, *43*(3), 141–151.

Davila, M. L., Riviere, I., Wang, X., Bartido, S., Park, J., Curran, K., Chung, S. S., Stefanski, J., Borquez-Ojeda, O., Olszewska, M., Qu, J., Wasielewska, T., He, Q., Fink, M., Shinglot, H., Youssif, M., Satter, M., Wang, Y., Hosey, J., Quintanilla, H., Halton, E., Bernal. Y., Bouhassira, D.C., Arcila, M. E., Gonen, M., Roboz, G. J., Maslak, P., Douer, D., Frattini, M. G., Giralt, S., Sadelain, M., & Brentjens, R. (2014). Efficacy and toxicity management of 19-28z CAR T cell therapy in B cell acute lymphoblastic leukemia. *Science Translational Medicine*, *6*(224), 224ra25.

DeLeo, A. B., & Whiteside, T. L. (2008). Development of multi-epitope vaccines targeting wild-type-sequence p53 peptides. *Expert Review of Vaccines*, *7*(7), 1031–1040.

Denkberg, G., Cohen, C. J., Lev, A., Chames, P., Hoogenboom, H. R., & Reiter, Y. (2002). Direct visualization of distinct T cell epitopes derived from a melanoma

tumor-associated antigen by using human recombinant antibodies with MHC-restricted T cell receptor-like specificity. *Proceedings of the National Academy of Sciences*, *99*(14), 9421–9426.

Denkberg, G., Lev, A., Eisenbach, L., Benhar, I., & Reiter, Y. (2003). Selective Targeting of Melanoma and APCs Using a Recombinant Antibody with TCR-Like Specificity Directed Toward a Melanoma Differentiation Antigen. *Journal of Immunology*, *171*(5), 2197–2207.

DeVita, V. T., & Chu, E. (2008). A history of cancer chemotherapy. *Cancer Research*, *68*(21), 8643–8653.

Di Stasi, A., Tey, S. K., Dotti, G., Fujita, Y., Kennedy-Nasser, A., Martinez, C., Straathof, K., Liu, E., Durett, A. G., Grilley, B., Liu, H., Cruz, C. R., Savoldo, B., Gee, A. P., Schindler, J., Krance, R. A., Heslop, H. E., Spencer, D. M., Rooney, C. M., & Brenner, M. K. (2011). Inducible Apoptosis as a Safety Switch for Adoptive Cell Therapy. *New England Journal of Medicine*, *365*(18), 1673–1683.

Donehower, L. A., Harvey, M., Slagle, B. L., McArthur, M. J., Montgomery, C. A., Butel, J. S., & Bradley, A. (1992). Mice deficient for p53 are developmentally normal but susceptible to spontaneous tumours. *Nature*, *356*(6366), 215–221.

Dübel, S., Breitling, F., Fuchs, P., Zewe, M., Gotter, S., Welschof, M., Moldenhauer, G., & Little, M. (1994). Isolation of IgG antibody Fv-DNA from various mouse and rat hybridoma cell lines using the polymerase chain reaction with a simple set of primers. *Journal of Immunological Methods*, *175*(1), 89–95.

Dundas, C. M., Demonte, D., & Park, S. (2013). Streptavidin-biotin technology: Improvements and innovations in chemical and biological applications. *Applied Microbiology and Biotechnology*, *97*(21), 9343–9353.

Epel, M., Carmi, I., Soueid-Baumgarten, S., Oh, S., Bera, T., Pastan, I., Berzofsky, J. A., & Reiter, Y. (2008). Targeting TARP, a novel breast and prostate tumor-associated antigen, with T-cell receptor-like human recombinant antibodies. *European Journal of Immunology*, *38*(6), 1706–1720.

Eshhar, Z., Waks, T., Gross, G., & Schindler, D. G. (1993). Specific activation and targeting of cytotoxic lymphocytes through chimeric single chains consisting of antibody-binding domains and the gamma or zeta subunits of the immunoglobulin and T-cell receptors. *Proceedings of the National Academy of Sciences*, *90*(2), 720–724.

Ferrara, N., Hillan, K. J., Gerber, H. P., & Novotny, W. (2004). Discovery and development of bevacizumab, an anti-VEGF antibody for treating cancer. *Nature Reviews Drug Discovery*, *3*(5), 391–400.

Finney, H. M., Lawson, A. D., Bebbington, C. R., & Weir, A. N. (1998). Chimeric receptors providing both primary and costimulatory signaling in T cells from a single gene product. *Journal of Immunology*, *161*(6), 2791–2797.

Freed-Pastor, W. A., & Prives, C. (2012). Mutant p53: One name, many proteins. *Genes and Development*, *26*(12), 1268–1286.

Frenzel, A., Kügler, J., Helmsing, S., Meier, D., Schirrmann, T., Hust, M., & Dübel, S. (2017). Designing Human Antibodies by Phage Display. *Transfusion Medicine and Hemotherapy*, *44*(5), 312–318.

Garboczi, D. N., Hung, D. T., & Wiley, D. C. (1992). HLA-A2-peptide complexes: refolding and crystallization of molecules expressed in *Escherichia coli* and complexed with single antigenic peptides. *Proceedings of the National Academy of Sciences*, *89*(8), 3429-3433.

Golay, J., Lazzari, M., Facchinetti, V., Bernasconi, S., Borleri, G., Barbui, T., Rambaldi, A., & Introna, M. (2001). CD20 levels determine the in vitro susceptibility to rituximab and complement of B-cell chronic lymphocytic leukemia: Further regulation by CD55 and CD59. *Blood*, *98*(12), 3383–3389.

Golay, J., Gramigna, R., Facchinetti, V., Capello, D., Gaidano, G., & Introna, M. (2002). Acquired immunodeficiency syndrome-associated lymphomas are efficiently lysed through complement-dependent cytotoxicity and antibody-dependent cellular cytotoxicity by rituximab. *British Journal of Haematology*, *119*(4), 923–929.

Gong, M. C., Latouche, J. B., Krause, A., Heston, W. D., Bander, N. H., & Sadelain, M. (1999). Cancer patient T cells genetically targeted to prostate-specific membrane antigen specifically lyse prostate cancer cells and release cytokines in response to prostate-specific membrane antigen. *Neoplasia*, *1*(2), 123–127.

Gratama, J. W., D'hautcourt, J. L., Mandy, F., Rothe, G., Barnett, D., Janossy, G., Papa, S., Schmitz, G., & Lenkei, R. (1998). Flow cytometric quantitation of immunofluorescence intensity: problems and perspectives. European Working Group on Clinical Cell Analysis. *Cytometry*, *33*(2), 166–178.

Gray, B. P., & Brown, K. C. (2014). Combinatorial peptide libraries: Mining for cell-binding peptides. *Chemical Reviews*, *114*(2), 1020–1081.

Gross, G., & Eshhar, Z. (2016). Therapeutic Potential of T Cell Chimeric Antigen Receptors (CARs) in Cancer Treatment: Counteracting Off-Tumor Toxicities for Safe CAR T Cell Therapy. *Annual Review of Pharmacology and Toxicology*, *56*(1), 59–83.

Grupp, S. A., Kalos, M., Barrett, D., Aplenc, R., Porter, D. L., Rheingold, S. R., Teachey, D. T., Chew, A., Hauck, B., Wright, J. F., Milone, M. C., Levine, B. L., & June, C. H.

(2013). Chimeric antigen receptor-modified T cells for acute lymphoid leukemia. *New England Journal of Medicine*, *368*(16), 1509–1518.

Gudkov, A. V., & Komarova, E. A. (2010). Pathologies associated with the p53 response. *Cold Spring Harbor Perspectives in Biology, 2*(7), a001180.

Hadzhieva, M., Pashov, A. D., Kaveri, S., Lacroix-Desmazes, S., Mouquet, H., & Dimitrov, J. D. (2017). Impact of Antigen Density on the Binding Mechanism of IgG Antibodies. *Scientific Reports*, *7*(1), 3767.

Hansel, T. T., Kropshofer, H., Singer, T., Mitchell, J. A., & George, A. J. T. (2010). The safety and side effects of monoclonal antibodies. *Nature Reviews Drug Discovery*, *9*(4), 325–338.

Harper, J., Adams, K. J., Bossi, G., Wright, D. E., Stacey, A. R., Bedke, N., Martinez-Hague, R., Blat, D., Humbert, L., Buchanan, H., Le Provost, G. S., Donnellan, Z., Carreira, R. J., Paston, S. J., Weigand, L. U., Canestraro, M., Sanderson, J. P., Botta Gordon-Smith, S., Lowe, K. L., Rygiel, K. A., Powlesland, A. S., Vuidepot, A., Hassan, N. J., Cameron, B. J., Jacobsen, B. K., & Dukes, J. (2018). An approved in vitro approach to preclinical safety and efficacy evaluation of engineered T cell receptor anti-CD3 bispecific (ImmTAC) molecules. *PLoS ONE*, *13*(10), e0205491.

Hawkins, O., Verma, B., Lightfoot, S., Jain, R., Rawat, A., McNair, S., Caseltine, S., Mojsilovic, A., Gupta, P., Neethling, F., Almanza, O., Dooley, W., Hildebrand, W., & Weidanz, J. (2011). An HLA-Presented Fragment of Macrophage Migration Inhibitory Factor Is a Therapeutic Target for Invasive Breast Cancer. *Journal of Immunology*, *186*(11), 6607–6616.

Held, G., Matsuo, M., Epel, M., Gnjatic, S., Ritter, G., Lee, S. Y., Tai, T. Y., Cohen, C. J., Old, L. J., Pfreundschuh, M., Reiter, Y., Hoogenboom, H. R., & Renner, C. (2004). Dissecting cytotoxic T cell responses towards the NY-ESO-1 protein by peptide/MHC-specific antibody fragments. *European Journal of Immunology*, *34*(10), 2919–2929.

Held, G., Wadle, A., Dauth, N., Stewart-Jones, G., Sturm, C., Thiel, M., Zwick, C., Dieckmann, D., Schuler, G., Hoogenboom, H. R., Levy, F., Cerundolo, V., Pfreundschuh, M., & Renner, C. (2007). MHC-peptide-specific antibodies reveal inefficient presentation of an HLA-A*0201-restricted, Melan-A-derived peptide after active intracellular processing. *European Journal of Immunology*, *37*(7), 2008–2017.

Hilton, H. G., & Parham, P. (2013). Direct binding to antigen-coated beads refines the specificity and cross-reactivity of four monoclonal antibodies that recognize polymorphic epitopes of HLA class I molecules. *Tissue Antigens*, *81*(4), 212–220.

Hoffmann, T. K., Donnenberg, A. D., Finkelstein, S. D., Donnenberg, V. S., Friebe-Hoffmann, U., Myers, E. N., Appella, E., DeLeo, A. B., & Whiteside, T. L. (2002).

Frequencies of tetramer+ T cells specific for the wild-type sequence p53(264-272) peptide in the circulation of patients with head and neck cancer. *Cancer Research*, *62*(12), 3521–3529.

Hogan, K. T., & Brown, S. L. (1992). Localization and characterization of serologic epitopes on HLA-A2. *Human Immunology*, *33*(3), 185–192.

Houbiers, J. G., Nijman, H. W., Van der Burg, S. H., Drijfhout, J. W., Kenemans, P., van de Velde, C. J., Brand, A., Momburg, F., Kast, M. W., & Melief, C. J. (1993). In vitro induction of human cytotoxic T lymphocyte responses against peptides of mutant and wild-type p53. *European Journal of Immunology, 23*(9), 2072-2077.

Hülsmeyer, M., Chames, P., Hillig, R. C., Stanfield, R. L., Held, G., Coulie, P. G., Alings, C., Wille, G., Saenger, W., Uchanska-Ziegler, B., Hoogenboom, H. R., & Ziegler, A. (2005). A major histocompatibility complex-peptide-restricted antibody and T cell receptor molecules recognize their target by distinct binding modes: Crystal structure of human leukocyte antigen (HLA)-A1-MAGE-A1 in complex with Fab-Hyb3. *Journal of Biological Chemistry*, *280*(4), 2972–2980.

Humar, M., Maurer, M., Azemar, M., & Groner, B. (2009). DNA vaccination with a mutated p53 allele induces specific cytolytic T cells and protects against tumor cell growth and the formation of metastasis. *Journal of Cancer Research and Clinical Oncology*, *135*(4), 567–580.

Hünig, T. (2012). The storm has cleared: Lessons from the CD28 superagonist TGN1412 trial. *Nature Reviews Immunology*, *12*(5), 317–318.

Hunt, D., Henderson, R., Shabanowitz, J., Sakaguchi, K., Michel, H., Sevilir, N., Cox, A., Appella, E., & Engelhard, V. (2007). Characterization of peptides bound to the class I MHC molecule HLA-A2.1 by mass spectrometry. *Journal of Immunology*, *179*(5), 2669–2671.

Inaguma, Y., Akahori, Y., Murayama, Y., Shiraishi, K., Tsuzuki-Iba, S., Endoh, A., Tsujikawa, J., Demachi-Okamura, A., Hiramatsu, K., Saji, H., Yamamoto, Y., Yamamoto, N., Nishimura, Y., Takahashi, T., Kuzushima, K., Emi, N., & Akatsuka, Y. (2014). Construction and molecular characterization of a T-cell receptor-like antibody and CAR-T cells specific for minor histocompatibility antigen HA-1H. *Gene Therapy*, *21*(6), 575–584.

Irvine, D. J., Purbhoo, M. A., Krogsgaard, M., & Davis, M. M. (2002). Direct observation of ligand recognition by T cells. *Nature*, *419*(6909), 845–849.

Joerger, A. C., & Fersht, A. R. (2010). The tumour suppressor p53: from structures to drug discovery. *Cold Spring Harbor Perspectives in Biology, 2*(6), a000919.

Jones, P. T., Dear, P. H., Foote, J., Neuberger, M. S., & Winter, G. (1986). Replacing the complementarity-determining regions in a human antibody with those from

a mouse. *Nature, 321(6069),* 522-525.

Jones, S., Peng, P. D., Yang, S., Hsu, C., Cohen, C. J., Zhao, Y., Abad, J., Zheng, Z., Rosenberg, S. A., & Morgan, R. A. (2009). Lentiviral Vector Design for Optimal T Cell Receptor Gene Expression in the Transduction of Peripheral Blood Lymphocytes and Tumor-Infiltrating Lymphocytes. *Human Gene Therapy*, *20*(6), 630–640.

Joseph-Pietras, D., Gao, Y., Zojer, N., Ait-Tahar, K., Banham, A. H., Pulford, K., Rice, J., Savelyeva, N., & Sahota, S. S. (2010). DNA vaccines to target the cancer testis antigen PASD1 in human multiple myeloma. *Leukemia*, *24*(11), 1951–1959.

Kang, X., Robbins, P. F., Fitzgerald, E. B., Wang, R. F., Rosenberg, S. A., & Kawakami, Y. (1997). Induction of melanoma reactive T cells by stimulator cells expressing melanoma epitope-major histocompatibility complex class I fusion proteins. *Cancer Research*, *57*(2), 202–205.

Khanna, R. (1998). Tumour surveillance: Missing peptides and MHC molecules. *Immunology and Cell Biology*, *76*(1), 20–26.

Khoo, K. H., Verma, C. S., & Lane, D. P. (2014). Drugging the p53 pathway: understanding the route to clinical efficacy. *Nature Reviews Drug Discovery*, *13*(3), 217–236.

Kimmig, R., Pfeiffer, D., Landsmann, H., & Hepp, H. (1997). Quantitative determination of the epidermal growth factor receptor in cervical cancer and normal cervical epithelium by 2-color flow cytometry: Evidence for down-regulation in cervical cancer. *International Journal of Cancer*, *74*(4), 365–373.

Klechevsky, E., Gallegos, M., Denkberg, G., Palucka, K., Banchereau, J., Cohen, C., & Reiter, Y. (2008). Antitumor activity of immunotoxins with T-cell receptor-like specificity against human melanoma xenografts. *Cancer Research*, *68*(15), 6360–6367.

Kochenderfer, J. N., Feldman, S. A., Zhao, Y., Xu, H., Black, M. A., Morgan, R. A., Wilson, W. H., & Rosenberg, S. A. (2009). Construction and preclinical evaluation of an anti-CD19 chimeric antigen receptor. *Journal of Immunotherapy*, *32*(7), 689–702.

Kochenderfer, J. N., Wilson, W. H., Janik, J. E., Dudley, M. E., Stetler-Stevenson, M., Feldman, S. A., Maric, I., Raffeld, M., Nathan, D. A. N., Lanier, B. J., Morgan, R. A., & Rosenberg, S. A. (2010). Eradication of B-lineage cells and regression of lymphoma in a patient treated with autologous T cells genetically engineered to recognize CD19. *Blood*, *116*(20), 4099–4102.

Kochenderfer, J. N., Dudley, M. E., Feldman, S. A., Wilson, W. H., Spaner, D. E., Maric, I., Stetler-Stevenson, M., Phan, G. Q., Hughes, M. S., Sherry, R. M., Yang, J. C.,

Kammula, U. S., Devillier, L., Carpenter, R., Nathan, D. A., Morgan, R. A., Laurencot, C., & Rosenberg, S. A. (2012). B-cell depletion and remissions of malignancy along with cytokine-associated toxicity in a clinical trial of anti-CD19 chimeric-antigen-receptor-transduced T cells. *Blood*, *119*(12), 2709–2720.

Kochenderfer, J. N., Dudley, M. E., Carpenter, R. O., Kassim, S. H., Rose, J. J., Telford, W. G., Hakim, F. T., Halverson, D. C., Fowler, D. H., Hardy, N. M., Mato, A. R., Hickstein, D. D., Gea-Banacloche, J. C., Pavletic, S. Z., Sportes, C., Maric, I., Feldman, S. A., Hansen, B. G., Wilder, J. S., Blacklock-Schuver, B., Jena, B., Bishop, M.R., Gress, R.E., & Rosenberg, S. A. (2013). Donor-derived CD19-targeted T cells cause regression of malignancy persisting after allogeneic hematopoietic stem cell transplantation. *Blood*, *122*(25), 4129–4139.

Koehne, G. (2017). Targeting WT1 in hematologic malignancies? *Blood*, *130*(18), 1959–1960.

Koehne, G., Devlin, S., Chung, D. J., Landau, H. J., Korde, N., Mailankody, S., Hassoun, H., Lesokhin, A. M., Lendvai, N., Giralt, S., & Landgren, C. O. (2017). WT1 heteroclitic epitope immunization following autologous stem cell transplantation in patients with high-risk multiple myeloma (MM). *Journal of Clinical Oncology*, *35*, 8016.

Köhler, G., & Milstein, C. (1975). Continuous cultures of fused cells secreting antibody of predefined specificity. *Nature*, *256*(5517), 495–497.

Kolb, H., Mittermuller, J., Clemm, C., Holler, E., Ledderose, G., Brehm, G., Heim, M., & Wilmanns, W. (1990). Donor leukocyte transfusions for treatment of recurrent chronic myelogenous leukemia in marrow transplant patients. *Blood*, *76*(12), 2462–2465.

Krause, A., Guo, H. F., Latouche, J. B., Tan, C., Cheung, N. K., & Sadelain, M. (1998). Antigen-dependent CD28 signaling selectively enhances survival and proliferation in genetically modified activated human primary T lymphocytes. *Journal of Experimental Medicine*, *188*(4), 619–626.

Kuball, J., Schuler, M., Antunes Ferreira, E., Herr, W., Neumann, M., Obenauer-Kutner, L., Westreich, L., Huber, C., Wölfel, T., & Theobald, M. (2002). Generating p53-specific cytotoxic T lymphocytes by recombinant adenoviral vector-based vaccination in mice, but not man. *Gene Therapy*, *9*(13), 833–843.

Kubo, M., Morisaki, T., Kuroki, H., Tasaki, A., Yamanaka, N., Matsumoto, K., Nakamura, K., Onishi, H., Baba, E., & Katano, M. (2003). Combination of Adoptive Immunotherapy with Herceptin for Patients with HER2-expressing Breast Cancer. *Anticancer Research*, *23*(6a), 4443–4449.

Kuckelkorn, U., Ferreira, E. A., Drung, I., Liewer, U., Kloetzel, P. M., & Theobald, M. (2002). The effect of the interferon-γ-inducible processing machinery on the

generator of a naturally tumor-associated human cytotoxic T lymphocyte epitope within a wild-type and mutant p53 sequence context. *European Journal of Immunology*, *32*(5), 1368–1375.

Kuwana, Y., Asakura, Y., Utsunomiya, N., Nakanishi, M., Arata, Y., Itoh, S., Nagase, F., & Kurosawa, Y. (1987). Expression of chimeric receptor composed of immunoglobulin-derived V regions and T-cell receptor-derived C regions. *Biochemical and Biophysical Research Communications*, *149*(3), 960–968.

Labrecque, S., Naor, N., Thomson, D., & Matlashewski, G. (1993). Analysis of the anti-p53 antibody response in cancer patients. *Cancer Research*, *53*(15), 3468–3471.

Lamers, C. H. J., Sleijfer, S., Vulto, A. G., Kruit, W. H. J., Kliffen, M., Debets, R., Gratama, J. W., Stoter, G., & Oosterwijk, E. (2006). Treatment of metastatic renal cell carcinoma with autologous T-lymphocytes genetically retargeted against carbonic anhydrase IX: first clinical experience. *Journal of Clinical Oncology*, *24*(13), e20–e22.

Lamers, C. H., Sleijfer, S., van Steenbergen, S., van Elzakker, P., van Krimpen, B., Groot, C., Vulto, A., den Bakker, M., Oosterwijk, E., Debets, R., & Gratama, J. W. (2013). Treatment of metastatic renal cell carcinoma with CAIX CAR-engineered T cells: clinical evaluation and management of on-target toxicity. *Molecular Therapy*, *21*(4), 904–912.

Lebien, T. W., & Tedder, T. F. (2008). B lymphocytes: How they develop and function. *Blood*, *112*(5), 1570–1580.

Lee, D. W., Gardner, R., Porter, D. L., Louis, C. U., Ahmed, N., Jensen, M., Grupp, S. A., & Mackall, C. L. (2014). Current concepts in the diagnosis and management of cytokine release syndrome. *Blood*, *124*(2), 188–195.

Lee, D. W., Kochenderfer, J. N., Stetler-Stevenson, M., Cui, Y. K., Delbrook, C., Feldman, S. A, Fry, T. J., Orentas, R., Wayne, A. S., & Mackall, C. L. (2015). T cells expressing CD19 chimeric antigen receptors for acute lymphoblastic leukaemia in children and young adults : a phase 1 dose-escalation trial. *Lancet*, *385*(9967), 517–528.

Lefèvre, F., Rémy, M. H., & Masson, J. M. (1997). Alanine-stretch scanning mutagenesis: A simple and efficient method to probe protein structure and function. *Nucleic Acids Research*, *25*(2), 447–448.

Lev, A., Denkberg, G., Cohen, C. J., Reiter, Y., Tzukerman, M., Skorecki, K. L., Chames, P., Hoogenboom, H. R., & Reiter, Y. (2002). Isolation and characterization of human recombinant antibodies endowed with the antigen-specific, major histocompatibility complex-restricted specificity of T cells directed toward the widely expressed tumor T-cell epitopes of the telomerase catalytic subunit. *Cancer Research*, *62*(11), 3184–3194.

Li, D., Bentley, C., Anderson, A., Wiblin, S., Cleary, K. L. S., Koustoulidou, S., Hassanali, T., Yates, J., Greig, J., Nordkamp, M. O., Trenevska, I., Ternette, N., Kessler, B. M., Cornelissen, B., Cragg, M. S., & Banham, A. H. (2017a). Development of a T-Cell Receptor Mimic Antibody against Wild-Type p53 for Cancer Immunotherapy. *Cancer Research*, *77*(10), 2699–2711.

Li, D., Bentley, C., Yates, J., Salimi, M., Greig, J., Wiblin, S., Hassanali, T., & Banham, A. H. (2017b). Engineering chimeric human and mouse major histocompatibility complex (MHC) class I tetramers for the production of T-cell receptor (TCR) mimic antibodies. *PLoS ONE*, *12*(4), e0176642.

Li, F. P., & Fraumeni, J. F. (1969a). Rhabdomyosarcoma in children: Epidemiologic study and identification of a familial caneer syndrome. *Journal of the National Cancer Institute*, *43*(6), 1365–1373.

Li, F. P., & Fraumeni, J. F. (1969b). Soft-tissue sarcomas, breast cancer, and other neoplasms. A familial syndrome? *Annals of Internal Medicine*, *71*(4), 747–752.

Lin, Y. C., Boone, M., Meuris, L., Lemmens, I., Van Roy, N., Soete, A., Reumers, J., Moisse, M., Plaisance, S., Drmanac, R., Chen, J., Speleman, F., Lambrechts, D., Van De Peer, Y., Tavernier, J., & Callewaert, N. (2014). Genome dynamics of the human embryonic kidney 293 lineage in response to cell biology manipulations. *Nature Communications*, *5*, 4767.

Linette, G. P., Stadtmauer, E. A., Maus, M. V, Rapoport, A. P., Levine, B. L., Emery, L., Litzky, L., Bagg, A., Carreno, B. M., Cimino, P. J., Binder-Scholl, G. K., Smethurst, D. P., Gerry, A. B., Pumphrey, N. J., Bennett, A. D., Brewer, J. E., Dukes, J., Harper, J., Tayton-Martin, H.K., Jakobsen, B.K., Hassan, N. J., Kalos, M., & June, C. H. (2013). Cardiovascular toxicity and titin cross-reactivity of affinity-enhanced T cells in myeloma and melanoma. *Blood*, *122*(6), 863–871.

Locke, F. L., Neelapu, S. S., Bartlett, N. L., Siddiqi, T., Chavez, J. C., Hosing, C. M., Ghobadi, A., Budde, L. E., Bot, A., Rossi, J. M., Jiang, Y., Xue, A. X., Elias, M., Aycock, J., Wiezorek, J., & Go, W. Y. (2017). Phase 1 Results of ZUMA-1: A Multicenter Study of KTE-C19 Anti-CD19 CAR T Cell Therapy in Refractory Aggressive Lymphoma. *Molecular Therapy*, *25*(1), 285–295.

Lowe, D. B., Bivens, C. K., Mobley, A. S., Herrera, C. E., McCormick, A. L., Wichner, T., Sabnani, M. K., Wood, L. M., & Weidanz, J. A. (2017). TCR-like antibody drug conjugates mediate killing of tumor cells with low peptide/HLA targets. *mAbs*, *9*(4), 603–614.

Ma, Q., Garber, H. R., Lu, S., He, H., Tallis, E., Ding, X., Sergeeva, A., Wood, M. S., Dotti, G., Salvado, B., Ruisaard, K., Clise-Dwyer, K., John, L. S., Rezvani, K., Alatrash, G., Shpall, E. J., & Molldrem, J. J. (2016). A novel TCR-like CAR with specificity for PR1/HLA-A2 effectively targets myeloid leukemia in vitro when expressed in human adult peripheral blood and cord blood T cells. *Cytotherapy*,

18(8), 985–994.

Maher, J., Brentjens, R. J., Gunset, G., Rivière, I., & Sadelain, M. (2002). Human T-lymphocyte cytotoxicity and proliferation directed by a single chimeric TCRzeta /CD28 receptor. *Nature Biotechnology*, *20*(1), 70–75.

Mak, T. W., & Saunders, M. E. (2006). Exploiting Antigen–Antibody Interaction. In *The Immune Response* (pp. 147–177).

Mareeva, T., Martinez-Hackert, E., & Sykulev, Y. (2008). How a T cell receptor-like antibody recognizes major histocompatibility complex-bound peptide. *Journal of Biological Chemistry*, *283*(43), 29053–29059.

Martz, L. (2017). Eureka moment for TCR mimics. *Biocentury Innovations: From Idea to IND*.

Maude, S. L., Frey, N., Shaw, P. A., Aplenc, R., Barrett, D. M., Bunin, N. J., Chew, A., Gonzalez, V. E., Zheng, Z., Lacey, S. F., Mahnke, Y. D., Melenhorst, J. J., Rheingold, S. R., Shen, A., Teachey, D. T., Levine, B. L., June, C. H., Porter, D. L., & Grupp, S. A. (2014). Chimeric Antigen Receptor T Cells for Sustained Remissions in Leukemia. *New England Journal of Medicine*, *371*(16), 1507–1517.

Maude, S. L., Laetsch, T. W., Buechner, J., Rives, S., Boyer, M., Bittencourt, H., Bader, P., Verneris, M. R., Stefanski, H. E., Myers, G. D., Qayed, M., De Moerloose, B., Hiramatsu, H., Schlis, K., Davis, K. L., Martin, P. L., Nemecek, E. R., Yanik, G. A., Peters, C., Baruchel, A., Boissel, N., Mechinaud, F., Balduzzi, A., Krueger, J., June, C. H., Levine, B. L., Wood, P., Taran, T., Leung, M., Mueller, K. T., Zhang, Y., Sen, K., Lebwohl, D., Pulsipher, M. A., & Grupp, S. A. (2018). Tisagenlecleucel in Children and Young Adults with B-Cell Lymphoblastic Leukemia. *New England Journal of Medicine*, *378*(5), 439–448.

Michaeli, Y., Denkberg, G., Sinik, K., Lantzy, L., Chih-Sheng, C., Beauverd, C., Ziv, T., Romero, P., & Reiter, Y. (2009). Expression hierarchy of T cell epitopes from melanoma differentiation antigens: unexpected high level presentation of tyrosinase-HLA-A2 Complexes revealed by peptide-specific, MHC-restricted, TCR-like antibodies. *Journal of Immunology*, *182*(10), 6328–6341.

Milone, M. C., Fish, J. D., Carpenito, C., Carroll, R. G., Binder, G. K., Teachey, D., Samanta, M., Lakhal, M., Gloss, B., Danet-Desnoyers, G., Campana, D., Riley, J. L., Grupp, S. A., & June, C. H. (2009). Chimeric receptors containing CD137 signal transduction domains mediate enhanced survival of T cells and increased antileukemic efficacy in vivo. *Molecular Therapy*, *17*(8), 1453–1464.

Morgan, R. A., Yang, J. C., Kitano, M., Dudley, M. E., Laurencot, C. M., & Rosenberg, S. A. (2010). Case report of a serious adverse event following the administration of T cells transduced with a chimeric antigen receptor recognizing ERBB2. *Molecular Therapy*, *18*(4), 843–851.

Mosquera, L. A., Card, K. F., Price-Schiavi, S. A., Belmont, H. J., Liu, B., Builes, J., Zhu, X., Chavaillaz, P. A., Lee, H. I., Jiao, J. A., Francis, J. L., Amirkhosravi, A., Wong, R. L., & Wong, H. C. (2005). In Vitro and In Vivo Characterization of a Novel Antibody-Like Single-Chain TCR Human IgG1 Fusion Protein. *Journal of Immunology*, *174*(7), 4381–4388.

Mottez, E., Langlade-Demoyen, P., Gournier, H., Martinon, F., Maryanski, J., Kourilsky, P., & Abastado, J. P. (1995). Cells expressing a major histocompatibility complex class I molecule with a single covalently bound peptide are highly immunogenic. *Journal of Experimental Medicine*, *181*(2), 493–502.

Neefjes, J., Jongsma, M. L. M., Paul, P., & Bakke, O. (2011). Towards a systems understanding of MHC class I and MHC class II antigen presentation. *Nature Reviews Immunology*, *11*(12), 823–836.

Neethling, F. A., Ramakrishna, V., Keler, T., Buchli, R., Woodburn, T., & Weidanz, J. A. (2008). Assessing vaccine potency using TCRmimic antibodies. *Vaccine*, *26*(25), 3092–3102.

Neller, M. A., López, J. A., & Schmidt, C. W. (2008). Antigens for cancer immunotherapy. *Seminars in Immunology*, *20*(5), 286–295.

Nijman, H. W., Van der Burg, S. H., Vierboom, M. P., Houbiers, J. G., Kast, W. M., & Melief, C. J. (1994). p53, a potential target for tumor-directed T cells. *Immunology Letters, 40*(2), 171-178.

Nijman, H. W., Lambeck, A., van der Burg, S. H., van der Zee, A. G. J., & Daemen, T. (2005). Immunologic aspect of ovarian cancer and p53 as tumor antigen. *Journal of Translational Medicine*, *3*, 34.

Nijman, H. W., Vermeij, R., Leffers, N., Van Der Burg, S. H., Melief, C. J., & Daemen, T. (2011). Immunological and clinical effects of vaccines targeting p53-overexpressing malignancies. *Journal of Biomedicine and Biotechnology*, *2011*.

Oates, J., Hassan, N. J., & Jakobsen, B. K. (2015). ImmTACs for targeted cancer therapy: Why, what, how, and which. *Molecular Immunology*, *67*(2), 67–74.

Offringa, R., Vierboom, M. P., van der Burg, S. H., Erdile, L., & Melief, C. J. (2000). p53: a potential target antigen for immunotherapy of cancer. *Annals of the New York Academy of Sciences*, *910*, 223–233.

Oldham, R. K., & Dillman, R. O. (2008). Monoclonal antibodies in cancer therapy: 25 Years of progress. *Journal of Clinical Oncology*, *26*(11), 1774–1777.

Olejniczak, S. H., Stewart, C. C., Donohue, K., & Czuczman, M. S. (2006). A quantitative exploration of surface antigen expression in common B-cell

malignancies using flow cytometry. *Immunological Investigations*, *35*(1), 93–114.

Oren, R., Hod-Marco, M., Haus-Cohen, M., Thomas, S., Blat, D., Duvshani, N., Denkberg, G., Elbaz, Y., Benchetrit, F., Eshhar, Z., Stauss, H., & Reiter, Y. (2014). Functional Comparison of Engineered T Cells Carrying a Native TCR versus TCR-like Antibody–Based Chimeric Antigen Receptors Indicates Affinity/Avidity Thresholds. *Journal of Immunology*, *193*(11), 5733–5743.

Park, J. H., Rivière, I., Gonen, M., Wang, X., Sénéchal, B., Curran, K. J., Sauter, C., Wang, Y., Santomasso, B., Mead, E., Roshal, M., Maslak, P., Davila, M., Brentjens, R. J., & Sadelain, M. (2018). Long-Term Follow-up of CD19 CAR Therapy in Acute Lymphoblastic Leukemia. *New England Journal of Medicine*, *378*(5), 449–459.

Parker, K. C., Bednarek, M. A., & Coligan, J. E. (1994). Scheme for ranking potential HLA-A2 binding peptides based on independent binding of individual peptide side-chains. *Journal of Immunology*, *152*(1), 163–175.

Pascolo, S., Bervas, N., Ure, J. M., Smith, A. G., Lemonnier, F. A., & Pérarnau, B. (1997). HLA-A2.1–restricted education and cytolytic activity of CD8(+) T lymphocytes from beta2 microglobulin (beta2m) HLA-A2.1 monochain transgenic H-2Db beta2m double knockout mice. *Journal of Experimental Medicine*, *185*(12), 2043–2051.

Peters, P. J., Borst, J., Oorschot, V., Fukuda, M., Krahenbuhl, O., Tschopp, J., Slot, J. W., & Geuze, H. J. (1991). Cytotoxic T lymphocyte granules are secretory lysosomes, containing both perforin and granzymes. *Journal of Experimental Medicine*, *173*(5), 1099–1109.

Pinilla, C., Appel, J., Blondelle, S., Dooley, C., Dörner, B., Eichler, J., Ostresh, J., & Houghten, R. A. (1995). A review of the utility of soluble peptide combinatorial libraries. *Biopolymers*, *37*(3), 221–240.

Pinilla, C., Rubio-Godoy, V., Dutoit, V., Guillaume, P., Simon, R., Zhao, Y., Houghten, R. A., Cerottini, J. C., Romero, P., & Valmori, D. (2001). Combinatorial peptide libraries as an alternative approach to the identification of ligands for tumor-reactive cytolytic T lymphocytes. *Cancer Research*, *61*(13), 5153–5160.

Polanski, M., & Anderson, N. L. (2007). A list of candidate cancer biomarkers for targeted proteomics. *Biomark Insights*, *1*, 1–48.

Porter, D. L., Levine, B. L., Kalos, M., Bagg, A., & June, C. H. (2011). Chimeric antigen receptor-modified T cells in chronic lymphoid leukemia. *New England Journal of Medicine*, *365*(8), 725–733.

Postow, M. A., Callahan, M. K., & Wolchok, J. D. (2015). Immune Checkpoint Blockade in Cancer Therapy. *Journal of Clinical Oncology*, *33*(17), 1974–1982.

Pulè, M. A., Straathof, K. C., Dotti, G., Heslop, H. E., Rooney, C. M., & Brenner, M. K. (2005). A chimeric T cell antigen receptor that augments cytokine release and supports clonal expansion of primary human T cells. *Molecular Therapy*, *12*(5), 933–941.

Purbhoo, M. A., Sutton, D. H., Brewer, J. E., Mullings, R. E., Hill, M. E., Mahon, T. M., Karbach, J., Jager, E., Cameron, B. J., Lissin, N., Vyas, P., Chen, J.-L., Cerundolo, V., & Jakobsen, B. K. (2006). Quantifying and Imaging NY-ESO-1/LAGE-1-Derived Epitopes on Tumor Cells Using High Affinity T Cell Receptors. *Journal of Immunology*, *176*(12), 7308–7316.

Qasim, W., Zhan, H., Samarasinghe, S., Adams, S., Amrolia, P., Stafford, S., Butler, K., Rivat, C., Wright, G., Somana, K., Ghorashian, S., Pinner, D., Ahsan, G., Gilmour, K., Lucchini, G., Inglott, S., Mifsud, W., Chiesa, R., Peggs, K. S., Chan, L., Farzeneh, F., Thrasher, A. J., Vora, A., Pule, M., & Veys, P. (2017). Molecular remission of infant B-ALL after infusion of universal TALEN gene-edited CAR T cells. *Science Translational Medicine*, *9*(374).

Rammensee, H. G., Bachmann, J., Emmerich, N. P. N., Bachor, O. A., & Stevanović, S. (1999). SYFPEITHI: Database for MHC ligands and peptide motifs. *Immunogenetics*, *50*(3-4), 213–219.

Rezvani, K., Brenchley, J. M., Price, D. A., Kilical, Y., Gostick, E., Sewell, A. K., Li, J., Mielke, S., Douek, D. C., & Barrett, A. J. (2005). T-cell responses directed against multiple HLA-A*0201-restricted epitopes derived from Wilms' tumor 1 protein in patients with leukemia and healthy donors: Identification, quantification, and characterization. *Clinical Cancer Research*, *11*(24), 8799–8807.

Rock, K. L., & Goldberg, A. L. (1999). Degradation of cell proteins and the generation of MHC class I-presented peptides: Presentation of Peptides on Major Histocompatibility Complex Class I Molecules. *Annual Review of Immunology*, *17*, 739–779.

Rock, K. L., York, I. A., Saric, T., & Goldberg, A. L. (2002). Protein degradation and the generation of MHC class I-presented peptides. *Advances in Immunology*, *80*, 1–70.

Rock, K. L., York, I. A., & Goldberg, A. L. (2004). Post-proteasomal antigen processing for major histocompatibility complex class I presentation. *Nature Immunology*, *5*(7), 670–677.

Rosano, G. L., & Ceccarelli, E. A. (2014). Recombinant protein expression in Escherichia coli: Advances and challenges. *Frontiers in Microbiology*, *5*, 172.

Rosenberg, S. A., Packard, B. S., Aebersold, P. M., Solomon, D., Topalian, S. L., Toy, S. T., Simon, P., Lotze, M. T., Yang, J. C., & Seipp, C. A. (1988). Use of tumor-infiltrating lymphocytes and interleukin-2 in the immunotherapy of patients with metastatic melanoma. A preliminary report. *New England Journal of Medicine*, *319*(25), 1676–1680.

Rosenberg, S. A. (2014). Finding suitable targets is the major obstacle to cancer gene therapy. *Cancer Gene Therapy*, *21*(2), 45–47.

Rossmann, E. D., Lenkei, R., Lundin, J., Mellstedt, H., & Österborg, A. (2007). Performance of calibration standards for antigen quantitation with flow cytometry in chronic lymphocytic leukemia. *Cytometry Part B - Clinical Cytometry*, *72*(6), 450–457.

Rubio, V., Stuge, T. B., Singh, N., Betts, M. R., Weber, J. S., Roederer, M., & Lee, P. P. (2003). Ex vivo identification, isolation and analysis of tumor-cytolytic T cells. *Nature Medicine*, *9*(11), 1377–1382.

Sadelain, M., Brentjens, R., & Rivière, I. (2009). The promise and potential pitfalls of chimeric antigen receptors. *Current Opinion in Immunology*, *21*(2), 215–223.

Sadelain, M., Rivière, I., & Riddell, S. (2017). Therapeutic T cell engineering. *Nature*, *545*(7655), 423–431.

Sadelain, M. (2017). CD19 CAR T Cells. *Cell*, *171*(7), 1471.

Saeed, M., Van Brakel, M., Zalba, S., Schooten, E., Rens, J. A. P., Koning, G. A., Debets, R., & ten Hagen, T. L. M. (2016). Targeting melanoma with immunoliposomes coupled to anti-MAGE A1 TCR-like single-chain antibody. *International Journal of Nanomedicine*, *11*, 955–975.

Sastry, S. R., Too, C. T., Kaur, K., Gehring, A. J., Low, L., Javiad, A., Pollicino, T., Li, L., Kennedy, P. T. F., Lopatin, U., Macary, P. A., & Bertoletti, A. (2011). Targeting Hepatitis B Virus-Infected Cells with a T-Cell Receptor-Like Antibody. *Journal of Virology*, *85*(5), 1935–1942.

Scheibenbogen, C., Letsch, A., Thiel, E., Schmittel, A., Mailaender, V., Baerwolf, S., Nagorsen, D., & Keilholz, U. (2002). CD8 T-cell responses to Wilms tumor gene product WT1 and proteinase 3 in patients with acute myeloid leukemia. *Blood*, *100*(6), 2132–2137.

Scott, A. M., Wolchok, J. D., & Old, L. J. (2012a). Antibody therapy of cancer. *Nature Reviews Cancer*, *12*(4), 278–287.

Scott, A. M., Allison, J. P., & Wolchok, J. D. (2012b). Monoclonal antibodies in cancer therapy. *Cancer Immunity*, *12*, 14.

Sergeeva, A., Alatrash, G., He, H., Ruisaard, K., Lu, S., Wygant, J., McIntyre, B. W., Ma, Q., Li, D., St John, L., Clise-Dwyer, K., & Molldrem, J. J. (2011). An anti–PR1 / HLA-A2 T-cell receptor–like antibody mediates complement-dependent cytotoxicity against acute myeloid leukemia progenitor cells. *Blood*, *117*(16), 4262–4272.

Snyder, A., & Chan, T. A. (2015). Immunogenic peptide discovery in cancer genomes. *Current Opinion in Genetics and Development*, *30*, 7–16.

Stebbings, R., Findlay, L., Edwards, C., Eastwood, D., Bird, C., North, D., Mistry, Y., Dilger, P., Liefooghe, E., Cludts, I., Fox, B., Tarrant, G., Robinson, J., Meager, T., Dolman, C., Thorpe, S. J., Bristow, A., Wadhwa, M., Thorpe, R., & Poole, S. (2007). "Cytokine Storm" in the Phase I Trial of Monoclonal Antibody TGN1412: Better Understanding the Causes to Improve Preclinical Testing of Immunotherapeutics. *Journal of Immunology*, *179*(5), 3325–3331.

Stern, L. J. (2007). Characterizing MHC-Associated Peptides by Mass Spectrometry. *Journal of Immunology*, *179*(5), 2667–2668.

Stewart-Jones, G., Wadle, A., Hombach, A., Shenderov, E., & Held, G. (2009). Rational development of high-affinity T-cell receptor-like antibodies. *Proceedings of the National Academy of Sciences*, *106*(14), 5784–5788.

Straathof, K. C., Pulè, M. A., Yotnda, P., Dotti, G., Vanin, E. F., Brenner, M. K., Heslop, H. E., Spencer, D. M., & Rooney, C. M. (2005). An inducible caspase 9 safety switch for T-cell therapy. *Blood*, *105*(11), 4247–4254.

Strano, S., Dell'Orso, S., Di Agostino, S., Fontemaggi, G., Sacchi, A., & Blandino, G. (2007). Mutant p53: An oncogenic transcription factor. *Oncogene*, *26*(15), 2212–2219.

Sudo, T., Kamikawaji, N., Kimura, A., Date, Y., Savoie, C., Nakashima, H., Furuichi, E., Kuhara, S., & Sasazuki, T. (1995). Differences in MHC class I self peptide repertoires among HLA-A2 subtypes. *Journal of Immunology*, *155*(10), 4749–4756.

Sykulev, Y., Joo, M., Vturina, I., Tsomides, T. J., & Eisen, H. N. (1996). Evidence that a single peptide-MHC complex on a target cell can elicit a cytolytic T cell response. *Immunity*, *4*(6), 565–571.

Teachey, D. T., Lacey, S. F., Shaw, P. A., Melenhorst, J. J., Maude, S. L., Frey, N., Pequignot, E., Gonzalez, V. E., Chen, F., Finklestein, J., Barrett, D. M., Weiss, S. L., Fitzgerald, J. C., Berg, R. A., Aplenc, R., Callahan, C., Rheingold, S. R., Zheng, Z., Rose-John, S., White, J. C., Nazimuddin, F., Wertheim, G., Levine, B. L., June, C. H., Porter, D. L., & Grupp, S. A. (2016). Identification of predictive biomarkers for cytokine release syndrome after chimeric antigen receptor T-cell therapy for acute lymphoblastic leukemia. *Cancer Discovery*, *6*(6), 664–679.

Themeli, M., Rivière, I., & Sadelain, M. (2015). New cell sources for T cell engineering and adoptive immunotherapy. *Cell Stem Cell*, *16*(4), 357–366.

Theobald, M. (1995). Targeting p53 as a General Tumor Antigen. *Proceedings of the National Academy of Sciences*, *92*(26), 11993–11997.

Theobald, M., Ruppert, T., Kuckelkorn, U., Hernandez, J., Häussler, A., Ferreira, E. A., Liewer, U., Biggs, J., Levine, A. J., Huber, C., Koszinowski, U. H., Kloetzel, P. M., & Sherman, L. A. (1998). The sequence alteration associated with a mutational hotspot in p53 protects cells from lysis by cytotoxic T lymphocytes specific for a flanking peptide epitope. *Journal of Experimental Medicine*, *188*(6), 1017–1028.

Theobald, M., & Offringa, R. (2003). Anti-p53-directed immunotherapy of malignant disease. *Expert Reviews in Molecular Medicine*, *5*(11), 1–13.

Theoret, M. R., Cohen, C. J., Nahvi, A. V., Ngo, L. T., Suri, K. B., Powell, D. J., Dudley, M. E., Morgan, R. A., & Rosenberg, S. A. (2008). Relationship of p53 Overexpression on Cancers and Recognition by Anti-p53 T Cell Receptor-Transduced T Cells. *Human Gene Therapy*, *19*(11), 1219–1231.

Trenevska, I., Li, D., & Banham, A. H. (2017). Therapeutic antibodies against intracellular tumor antigens. *Frontiers in Immunology*, *8*, 1001.

Tyler, E. M., Jungbluth, A. A., O'Reilly, R. J., & Koehne, G. (2013). WT1-specific T-cell responses in high-risk multiple myeloma patients undergoing allogeneic T cell-depleted hematopoietic stem cell transplantation and donor lymphocyte infusions. *Blood*, *121*(2), 308–317.

Van Meerten, T., Van Rijn, R. S., Hol, S., Hagenbeek, A., & Ebeling, S. B. (2006). Complement-induced cell death by rituximab depends on CD20 expression level and acts complementary to antibody-dependent cellular cytotoxicity. *Clinical Cancer Research*, *12*(13), 4027–4035.

Veomett, N., Dao, T., Liu, H., & Scheinberg, D. A. (2014). Therapeutic Efficacy of an Fc-Enhanced TCR-Like Antibody to the Intracellular WT1 Oncoprotein. *Clinical Cancer Research*, *20*(15), 4036–4404.

Verma, B., Neethling, F. A., Caseltine, S., Fabrizio, G., Largo, S., Duty, J. A., Tabaczewski, P., & Weidanz, J. A. (2010a). TCR Mimic Monoclonal Antibody Targets a Specific Peptide/HLA Class I Complex and Significantly Impedes Tumor Growth In Vivo Using Breast Cancer Models. *Journal of Immunology*, *184*(4), 2156–2165.

Verma, B., Hawkins, O. E., Neethling, F. A., Caseltine, S. L., Largo, S. R., Hildebrand, W. H., & Weidanz, J. A. (2010b). Direct discovery and validation of a peptide/MHC epitope expressed in primary human breast cancer cells using a TCRm monoclonal antibody with profound antitumor properties. *Cancer*

Immunology Immunotherapy, *59*(4), 563–573.

Verma, B., Jain, R., Caseltine, S., Rennels, A., Bhattacharya, R., Markiewski, M. M., Rawat, A., Neethling, F., Bickel, U., & Weidanz, J. A. (2011). TCR mimic monoclonal antibodies induce apoptosis of tumor cells via immune effector-independent mechanisms. *Journal of Immunology*, *186*(5), 3265–3276.

Vierboom, M., Nijman, H., Offringa, R., van der Voort, E., van Hall, T., van den Broek, L., Fleuren, G., Kenemans, P., Kast, W., & Melief, C. (1997). Tumor eradication by wild-type p53-specific cytotoxic T lymphocytes. *Journal of Experimental Medicine*, *186*(5), 695–704.

Vierboom, M. P. M., Zwaveling, S., Bos, G. M. J., Ooms, M., Krietemeijer, G. M., Melief, C. J. M., & Offringa, R. (2000). High steady-state levels of p53 are not a prerequisite for tumor eradication by wild-type p53-specific cytotoxic T lymphocytes. *Cancer Research*, *60*(19), 5508–5513.

Vigneron, N. (2015). Human Tumor Antigens and Cancer Immunotherapy. *BioMed Research International*, *2015*, 948501.

Vita, R., Overton, J. A., Greenbaum, J. A., Ponomarenko, J., Clark, J. D., Cantrell, J. R., Wheeler, D. K., Gabbard, J. L., Hix, D., Sette, A., & Peters, B. (2015). The immune epitope database (IEDB) 3.0. *Nucleic Acids Research*, *43*(D1), D405–D412.

Vita, R., Mahajan, S., Overton, J. A., Dhanda, S. K., Martini, S., Cantrell, J. R., Wheeler, D. K., Sette, A., & Peters, B. (2018). The Immune Epitope Database (IEDB): 2018 update. *Nucleic Acids Research*, *47(D1)*, D339–D343.

Vogelstein, B., Lane, D., & Levine, A. J. (2000). Surfing the p53 network. *Nature*, *408*(6810), 307–310.

Vormittag, P., Gunn, R., Ghorashian, S., & Veraitch, F. S. (2018). A guide to manufacturing CAR T cell therapies. *Current Opinion in Biotechnology*, *53*, 164–181.

Wang, X., Mathieu, M., & Brezski, R. J. (2018). IgG Fc engineering to modulate antibody effector functions. *Protein and Cell*, *9*(1), 63–73.

Warren, R. L., & Holt, R. A. (2010). A census of predicted mutational epitopes suitable for immunologic cancer control. *Human Immunology*, *71*(3), 245–254.

Weidanz, J. A., Nguyen, T., Woodburn, T., Neethling, F. A., Chiriva-Internati, M., Hildebrand, W. H., & Lustgarten, J. (2006). Levels of specific peptide-HLA class I complex predicts tumor cell susceptibility to CTL killing. *Journal of Immunology*, *177*(8), 5088–5097.

Weidanz, J. A., Hawkins, O., Verma, B., & Hildebrand, W. H. (2011). TCR-like Biomolecules Target Peptide/MHC Class I Complexes on the Surface of Infected and Cancerous Cells. *International Reviews of Immunology*, *30*(5-6), 328–340.

Weiner, G. J. (2015). Building better monoclonal antibody-based therapeutics. *Nature Reviews Cancer*, *15*(6), 361–370.

Weiss, G. A., Watanabe, C. K., Zhong, A., Goddard, A., & Sidhu, S. S. (2000). Rapid mapping of protein functional epitopes by combinatorial alanine scanning. *Proceedings of the National Academy of Sciences*, *97*(16), 8950–8954.

Wittman, V. P., Woodburn, D., Nguyen, T., Neethling, F. A., Wright, S., & Weidanz, J. A. (2006). Antibody Targeting to a Class I MHC-Peptide Epitope Promotes Tumor Cell Death. *Journal of Immunology*, *177*(6), 4187–4195.

Wooldridge, L., Lissina, A., Cole, D. K., Van Den Berg, H. A., Price, D. A., & Sewell, A. K. (2009). Tricks with tetramers: how to get the most from multimeric peptide-MHC. *Immunology*, *126*(2), 147–164.

Wooldridge, L., Ekeruche-Makinde, J., Van Den Berg, H. A., Skowera, A., Miles, J. J., Tan, M. P., Dolton, G., Clement, M., Llewellyn-Lacey, S., Price, D. A., Peakman, M., & Sewell, A. K. (2012). A single autoimmune T cell receptor recognizes more than a million different peptides. *Journal of Biological Chemistry*, *287*(2), 1168–1177.

Wucherpfennig, K. W. (2010). The First Structures of T Cell Receptors Bound to Peptide-MHC. *The Journal of Immunology*, *185*(11), 6391–6393.

Würtzen, P. A., Pedersen, L. O., Poulsen, H. S., & Claesson, M. H. (2001). Specific killing of p53 mutated tumor cell lines by a cross-reactive human HLA-A2-restricted p53-specific CTL line. *International Journal of Cancer, 93*(6), 855-861.

Yanuck, M., Carbone, D. P., Pendleton, C. D., Tsukui, T., Winter, S. F., Minna, J. D., & Berzofsky, J. a. (1993). A mutant p53 tumor suppressor protein is a target for peptide-induced CD8+ cytotoxic T-cells. *Cancer Research*, *53*(14), 3257–3261.

Yewdell, J. W., Reits, E., & Neefjes, J. (2003). Making sense of mass destruction: Quantitating MHC class I antigen presentation. *Nature Reviews Immunology*, *3*(12), 952–961.

Zaritskaya, L., Shurin, M. R., Sayers, T. J., & Malyguine, A. M. (2010). New flow cytometric assays for monitoring cell-mediated cytotoxicity. *Expert Review of Vaccines*, *9*(6), 601–616.

Zhang, G., Wang, L., Cui, H., Wang, X., Zhang, G., Ma, J., Han, H., He, W., Wang, W., Zhao, Y., Liu, C., Sun, M., & Gao, B. (2014). Anti-melanoma activity of T cells redirected with a TCR-like chimeric antigen receptor. *Scientific Reports*, *4*, 3571.

Zhang, M., Heldin, A., Palomar-Siles, M., Öhlin, S., Bykov, V. J. N., & Wiman, K. G. (2018). Synergistic Rescue of Nonsense Mutant Tumor Suppressor p53 by Combination Treatment with Aminoglycosides and Mdm2 Inhibitors. *Frontiers in Oncology*, *7*, 323.

Zhao, Q., Ahmed, M., Tassev, D., Hasan, A., Kuo, T. Y., Guo, H. F., O'Reilly, R., & Cheung, N. K. (2015). Affinity maturation of T-cell receptor-like antibodies for Wilms tumor 1 peptide greatly enhances therapeutic potential. *Leukemia*, *29*(11), 2238–2247.

Zwaveling, S., Vierboom, M. P., Ferreira Mota, S. C., Hendriks, J. A., Ooms, M. E., Sutmuller, R. P., Franken, K. L., Nijman, H. W., Ossendorp, F., Van Der Burg, S. H., Offringa, R., & Melief, C. J. (2002). Antitumor Efficacy of Wild-Type p53-specific CD4+ T-Helper Cells. *Cancer Research*, *62*(21), 6187–6193.

Appendix A

List of the 271 peptides identified by mining the IEDB.

Gene	Protein name	Peptide
ACTB	Actin, cytoplasmic 1	RLDLAGRDL
ACTB	Actin, cytoplasmic 1	RMQKEITAL
ACTB	Actin, cytoplasmic 1	RMQKEITAL
ACTG1	Actin, cytoplasmic 2	RPRHQGVMV
ADGRE1	Adhesion G protein-coupled receptor E1	RLSSVNAEV
ADPGK	ADP-dependent glucokinase	RLLEVVTSI
AKAP8L	A-kinase anchor protein 8-like	RMWEDPMGA
ANKRD35	Ankyrin repeat domain 35	RLQEENQQL
ARHGAP30	Rho GTPase activating protein 30	RLYDKFAEA
ARHGAP31	Rho GTPase-activating protein 31 (Kiaa1204)	RPAKSMDSL
ARL6IP5	ADP-ribosylation-like factor 6 interacting protein 5	RLTDYISKV
ATG16L1	Autophagy-related protein 16-1	RLQKELAEA
ATIC	Bifunctional purine biosynthesis protein PURH	RLDFNLIRV
ATP6V1H	V-type proton ATPase subunit H	RLNEKNYEL
ATXN2	Ataxin-2	RMVHILTSV
ATXN2L	Ataxin-2-like protein	RMLHFLTAV
B4GALT7	Beta-1,4-galactosyltransferase 7	RLYHITDQV
BICD2	Protein bicaudal D homolog 2	RLASVAQEL
BRD4	Bromodomain-containing protein 4	RLAELQEQL
C11ORF49	UPF0705 protein C11orf49	RLLAQVPGL
C12ORF65	Probable peptide chain release factor C12orf65, mitochondrial	RLWEKLTLL
C1ORF112	Uncharacterized protein C1orf112 homolog	RLFQKTLKL
C3	Complement C3	RLIQESPTL
C5AR2	C5a anaphylatoxin chemotactic receptor 2	RALPSIILL
CALCOCO1	Calcium-binding and coiled-coil domain-containing protein 1	RLAELGLHL
CARD14	Caspase recruitment domain-containing protein 14	RLKEENEKL
CBX6	Chromobox protein homolog 6	RISDVHFSV
CCND1	G1/S-specific cyclin-D1	RLTRFLSRV
CCNDBP1	Cyclin-D1-binding protein 1	RLNEAAVTV
CENPE	Centromere-associated protein E	RLAEVEEKL
CHPF2	Chondroitin sulfate glucuronyltransferase	RLSSLLALL
CHRM1	Muscarinic acetylcholine receptor M1	RYFSVTRPL
CKAP4	Cytoskeleton-associated protein 4	RISEVLQKL
CLASP1	CLIP-associating protein 1	RLLDGAFKL
CLTC	Clathrin heavy chain 1	RLAELEEFI
CNPY3	Protein canopy homolog 3	RLIEVTETI
COASY	Bifunctional coenzyme A synthase	RQVEKAWAL

Gene	Protein name	Peptide
COMMD9	COMM domain-containing protein 9	RLVDLDWRV
COPB1	Coatomer subunit beta	RLLHEMILV
COPS8	COP9 signalosome complex subunit 8	RLTDYVAFL
CSDE1	Cold shock domain-containing protein E1	RLLGYVATL
CYTH1	Cytohesin-1	RLKDEIAEV
DCTN2	p50 dynamitin/Dynactin subunit 2	RLTELETAV
DCTN2	Dynactin subunit 2/p50 dynamitin	RLLHEVQEL
DDB1	DNA damage-binding protein 1	RLYDGLFKV
DEK	Protein DEK	RLTMQVSSL
DEPDC1B	DEP domain-containing protein 1B	RLWNETVEL
DGKI	Diacylglycerol kinase iota	RLQEDLQSV
DMD	Dystrophin	RLLEDSKGV
DMTF1	Cyclin-D-binding Myb-like transcription factor 1	RLAEVVHEL
DNAAF5	Dynein assembly factor 5, axonemal	RLFDDVPQV
DNAJB12	DnaJ homolog subfamily B member 12	RLSEVQASL
DNM2	Dynamin-2	RTIGVITKL
DOCK2	Dedicator of cytokinesis protein 2	RLFESINNL
DUS2	tRNA-dihydrouridine(20) synthase [NAD(P)+]-like	RLFSSIVTV
DUSP2	Dual specificity protein phosphatase 2	RLDEAFDFV
EEF2	Elongation factor 2	RLMEPIYLV
EHD4	EH domain-containing protein 4	RLPEIYIQL
EI24	Etoposide-induced protein 2.4 homolog	RLFHKTVYL
EIF3G	Eukaryotic translation initiation factor 3 subunit G	RLTPKLMEV
EIF4E	Eukaryotic translation initiation factor 4E	RLISKFDTV
EIF4G1	Eukaryotic translation initiation factor 4 gamma 1	RLKEELEEA
ELOVL5	Elongation of very long chain fatty acids protein 5	RMGPPLHTV
EMC1	ER membrane protein complex subunit 1	RLSSQLILL
EMILIN1	EMILIN-1	RLGQLEGLL
ENTPD1	Ectonucleoside triphosphate diphosphohydrolase 1	RLYGKDYNV
EPHX2	Soluble epoxide hydrolase/Bifunctional epoxide hydrolase 2	RLMKGEITL
ESR2	Estrogen receptor beta	RLANLLMLL
EXOC2	Exocyst complex component 2	RLFENYIEL
FLNA	Filamin-A	RLIALLEVL
FOCAD	Focadhesin	RLALLKVLL
G6PC2	Glucose-6-phosphatase 2	RLLCALTSL
GALNT12	Polypeptide N-acetylgalactosaminyltransferase 12	RLHQINIYL
GAPDH	Glyceraldehyde-3-phosphate dehydrogenase	RVIISAPSA
GAPDH	Glyceraldehyde-3-phosphate dehydrogenase	RVPTANVSV
GBE1	1,4-alpha-glucan-branching enzyme	RLLEIDPYL
GEMIN4	Gem-associated protein 4	RLLETVIDV
GEMIN4	Gem-associated protein 4	RLLDSVRAI
GIT2	ARF GTPase-activating protein GIT2	RLVEIQYEL
GLE1	Nucleoporin GLE1	RMYELVHRM

Gene	Protein name	Peptide
GOLPH3L	Golgi phosphoprotein 3-like	RLLDRKVLL
GOSR1	Golgi SNAP receptor complex member 1	RLIEETISI
GRHPR	Glyoxylate reductase/hydroxypyruvate reductase	RLPEAIEEV
GRIPAP1	GRIP1-associated protein 1	RLLEQLQEI
GTF3C1	General transcription factor 3C polypeptide 1	RLIESLFTI
GTF3C4	General transcription factor 3C polypeptide 4	RLYETSYRL
GUSBP1	Putative inactive beta-glucuronidase-like protein SMA3	RLVNYQISV
HDAC3	Histone deacetylase 3	RMLPHAPGV
HECTD4	Probable E3 ubiquitin-protein ligase HECTD4, KIAA0614	RLSPYLEDV
HERC2	E3 ubiquitin-protein ligase HERC2	RLHEFDEQV
HIST1H2BK	Histone H2B type 1-K	RLLLPGELA
HIVEP2	Transcription factor HIVEP2	RPVSPGKDI
HNRNPC	Heterogeneous nuclear ribonucleoproteins C1/C2	RVPPPPPIA
HSPA4	Heat shock 70 kDa protein 4	RLMNETTAV
HSPB1	Heat shock protein 27/Heat shock protein beta-1	RLFDQAFGL
HSPH1	Heat shock protein 105 kDa	RLMNDMTAV
IFIT2	Interferon-induced protein with tetratricopeptide repeats 2	RLSDVQIYV
IFIT3	Interferon-induced protein with tetratricopeptide repeats 3	RLSDAQIYV
IKBIP	Inhibitor of nuclear factor kappa-B kinase-interacting protein	RLQEEINEV
INPP5B	Type II inositol 1,4,5-trisphosphate 5-phosphatase	RLVGIMLLL
INS	Insulin	RGIVEQCCT
INS	Insulin	RGFFYTPKT
INS-1	Proinsulin precursor	REAEDLQVG
INS-1	Proinsulin precursor	RLLPLLALL
IPO9	Importin-9	RLIPTLVSI
IRS2	Insulin receptor substrate 2	RVASPTSGV
ISOC2	Isochorismatase domain-containing protein 2	RLLEVPVML
ITGB7	Integrin beta-7	RLQEVTHSV
KANK2	KN motif and ankyrin repeat domain-containing protein 2	RLLDYVVNI
KAZN	Kazrin	RLQEEVHLL
KDM1A	Lysine-specific histone demethylase 1A	RLLEATSYL
KDM5B	Lysine-specific demethylase 5B	RLIDLGVGL
KDSR	3-ketodihydrosphingosine reductase	RLISETTSV
KIF15	Kinesin-like protein KIF15	RLAEETEKL
KRT18	Keratin, type I cytoskeletal 18	RLAADDFRV
KRT18	Keratin, type I cytoskeletal 18	RLASYLDRV
KRT9	Keratin 9	RLASYLDKV
LETM1	Mitochondrial proton/calcium exchanger protein	RLVPFLVFV
LMNA	Prelamin-A/C	RLADALQEL
LMNB1	Lamin B1	RLAVYIDKV
LRRC49	Leucine-rich repeat-containing protein 49	RLFGILAHV
LUC7L2	Putative RNA-binding protein Luc7-like 2	RLAETQEEI
MACF1	Microtubule-actin cross-linking factor 1	RLQDELVTL

Gene	Protein name	Peptide
MAP10	Microtubule-associated protein 10	RLLDFPTLL
MC1R	Melanocyte-stimulating hormone receptor	RLLGSLNST
MCM4	DNA replication licensing factor MCM4	RLAEAHAKV
MCM7	DNA replication licensing factor MCM7	RLAQHITYV
MCM9	DNA helicase MCM9	RLLESLIRL
MED13L	Mediator of RNA polymerase II transcription subunit 13-like	RMFPTPPSL
MEF2D	Myocyte-specific enhancer factor 2D	RPASAGAML
MFN2	Mitofusin-2	RLIALSFGL
MICAL1	[F-actin] monooxygenase MICAL1	RLNEIEAAL
MLLT6	Protein AF-17	RTDNGGWAH
MOB3A	MOB kinase activator 3A	RLFRVFVHV
MON2	Protein MON2 homolog	RLFESSQYL
MORC3	MORC family CW-type zinc finger protein 3/KIAA0136	RLIKAYEKV
MPDZ	Multiple PDZ domain protein	RQDENTPSV
MRPL19	39S ribosomal protein L19, mitochondrial	RLDDSLLYL
MRPL51	39S ribosomal protein L51, mitochondrial	RLWDWVPLA
MRPS2	28S ribosomal protein S2, mitochondrial	RLPDLIIFL
MSH2	DNA mismatch repair protein Msh2	RLYQGINQL
MSH6	DNA mismatch repair protein Msh6	RLLSKIHNV
MSMO1	Methylsterol monooxygenase 1	RIYKYIHKV
MTF2	Metal-response element-binding transcription factor 2	RVPPVPPNV
MTHFD1	C-1-tetrahydrofolate synthase, cytoplasmic	RMFGIPVVV
MTHFD1	C-1-tetrahydrofolate synthase, cytoplasmic	RLVPSVNGV
MYD88	Myeloid differentiation primary response protein MyD88	RLLELLTKL
MYH9	Myosin-9	RTFHIFYYL
MYH9	Myosin-9	RLTAKKQEL
MYH9	Myosin-9	RLQQELDDL
MYH9	Myosin-9	RLKQLKRQL
MYH9	Myosin-9	RLKKANLQI
MYH9	Myosin-9	RLFTKVKPL
MYH9	Myosin-9	RLEARIAQL
MYO19	Unconventional myosin-XIX	RLFDWLVSV
MYO19	Unconventional myosin-XIX	RLLEAIIRL
MYO1G	Unconventional myosin-Ig	RLIPIIVLL
MYO9B	Unconventional myosin-IXb	RLIFHLVKV
NCBP1	Nuclear cap-binding protein subunit 1	RLQEKVESA
NCKAP1L	Nck-associated protein 1-like	RMLDSVEKL
NDRG3	Protein NDRG3	RLNPINTTL
NFIB	Nuclear factor 1 B-type	RQADKVWRL
NIPBL	Nipped-B-like protein	RLMDNSTSV
NR4A1	Nuclear receptor subfamily 4 group A member 1	RLLGKLPEL
NUP133	Nuclear pore complex protein Nup133	RQHEIVLKV
NUP160	Nuclear pore complex protein Nup160	RLIEESVTV

Gene	Protein name	Peptide
ORAI3	Protein orai-3	RLQGELQAV
PAPLN	PAPLN protein/Papilin	RLLLLVPLL
PARP4	Poly [ADP-ribose] polymerase 4	RIIDTVAQV
PDXDC1	Pyridoxal-dependent decarboxylase domain-containing protein 1	RLLENMTEV
PIEZO1	Piezo-type mechanosensitive ion channel component 1	RLVPFLVEL
PIGQ	Phosphatidylinositol N-acetylglucosaminyltransferase subunit Q	RMFPGEVAL
PIPSL	Putative PIP5K1A and PSMD4-like protein	RILSKLHTV
PJA1	E3 ubiquitin-protein ligase Praja-1	RLAQAMETA
PLEC	Plectin	RLHERLVAI
PLP1	Myelin proteolipid protein	RMYGVLPWI
PNN	Pinin	RLLEQKVEL
PPP1R13L	RelA-associated inhibitor	RLNPLVLLL
PPP1R35	Protein phosphatase 1 regulatory subunit 35	RLFRDLVSL
PPP6R3	Serine/threonine-protein phosphatase 6 regulatory subunit 3	RVSDINFTL
PRAG1	Tyrosine-protein kinase PRAG1	RLAPEIVSA
PRKD2	Serine/threonine-protein kinase D2	RQASLSISV
PRKDC	DNA-dependent protein kinase catalytic subunit	RIMEFTTTL
PRPF8	Pre-mRNA-processing-splicing factor 8	RLMKHDVNL
PRTN3	Myeloblastin precursor	RLVNVVLGA
PSMA4	Proteasome subunit alpha type-4	RLIAQRYLL
PSMB1	Proteasome subunit beta type-1	RRFFPYYVY
PSMC3	26S protease regulatory subunit 6A	RLLDSEIKI
PSMD2	26S proteasome non-ATPase regulatory subunit 2	RLAAMLRQL
PTPRN2	Receptor-type tyrosine-protein phosphatase N2	RLYQEVHRL
PUM3	Pumilio homolog 3/KIAA0020 protein	RTLDKVLEV
PXDN	Peroxidasin homolog precursor	RLFSMAHTV
PXK	PX domain-containing protein kinase-like protein	RLLDLENSL
RAD21	Double-strand-break repair protein rad21 homolog	RLQESVMEA
RANGAP1	Ran GTPase-activating protein 1	RVIGTLEEV
RHOD	Rho-related GTP-binding protein RhoD	RLHDNVHAV
RIC8A	Synembryn-A (RIC8A protein)	RLAELLVSV
RNF213	E3 ubiquitin-protein ligase RNF213	RLLNFDTEL
RNF213	E3 ubiquitin-protein ligase RNF213	RLLQEQHQL
RPL7A	60S ribosomal protein L7a	RRHWGGNVL
RPLP2	60S acidic ribosomal protein P2	RLNKVISEL
RPS8	40S ribosomal protein S8	RIIDVVYNA
RPS9	40S ribosomal protein S9	RLFEGNALL
RRBP1	Ribosome-binding protein 1	RLQEELEKL
SAPCD2	Suppressor APC domain-containing protein 2	RLLPKVQEV
SAR1A	GTP-binding protein SAR1a	RLVESKVEL
SBF1	Myotubularin-related protein 5	RLLEELQRL

Gene	Protein name	Peptide
SCFD1	Sec1 family domain-containing protein 1	RLIDLHTNV
SCOC	Short coiled-coil protein	RLINQVLEL
SFT2D1	Vesicle transport protein SFT2A	RLLATIVML
SFXN4	Sideroflexin-4	RLLPVIFLV
SHC1	SHC transforming protein 1	RVPPPPQSV
SLC30A8	Zinc transporter 8	RLLYPDYQI
SLC30A8	Zinc transporter 8	REIAKALSK
SMARCA1	SMARCA1 protein, partial/Probable global transcription activator SNF2L1	RLLNILMQL
SMARCA2	Probable global transcription activator SNF2L2	RPSGPGPEL
SMARCA4	SMARCA4/Transcription activator BRG1	RLLNFQRQL
SMARCE1	SWI/SNF-related matrix-associated actin-dependent regulator of chromatin subfamily E member 1	RLCGLKVEV
SMC4	Structural maintenance of chromosomes protein 4	RLIEQEEYL
SMYD4	SET and MYND domain-containing protein 4/KIAA1936	RLQDLQQQV
SNTB2	Beta-2-syntrophin	RLGDAILSV
SNX1	Sorting nexin-1	RLPPPFPGL
SNX14	Sorting nexin 14	RLVSLITLL
SNX4	Sorting nexin-4	RVADRLYGV
SPAST	Spastin	RLSDFTESL
SPECC1L	Cytospin-A	RLQDAIAKV
SPTBN1	Spectrin beta chain, non-erythrocytic 1	RMLIKLLEV
SSR2	Translocon-associated protein subunit beta	RLLSFVVLA
SUN2	SUN domain-containing protein 2/UNC84B	RIRPTAVTL
SURF6	Surfeit locus protein 6	RLHEKIQEA
SYNM	Synemin	RTFSPTYGL
TBL1Y	F-box-like/WD repeat-containing protein TBL1Y	RLWDVEQGV
TCF4	Transcription factor 4	RLDDAIHVL
TIPRL	TIP41-like protein	RVMPSSFFL
TMEM69	Transmembrane protein 69	RLSEAIVTV
TRAF1	TNF receptor-associated factor 1	RVFENIVAV
TRAP1	Heat shock protein 75 kDa, mitochondrial	RLDTHPAMV
TRAPPC1	Trafficking protein particle complex subunit 1	RLDSYVRSL
TRIM14	Tripartite motif-containing protein 14	RLWEGAISI
TRIM39	E3 ubiquitin-protein ligase TRIM39	RPNRQLGSM
TRIM66	Tripartite motif-containing protein 66	RLANSISQV
TRIP11	Thyroid receptor-interacting protein 11	RLMGSILGV
TRIP12	E3 ubiquitin-protein ligase TRIP12	RLLDTNPEI
TRPC4AP	Short transient receptor potential channel 4-associated protein	RLLAYISQV
TRRAP	Transformation/transcription domain-associated protein	RVYERLLYV
TUBGCP4	Gamma-tubulin complex component 4	RLIEEENML
TUBGCP5	Gamma-tubulin complex component 5	RLQEFIDEV
TXNDC11	Thioredoxin domain-containing protein 11	RLSDQVLFV

Gene	Protein name	Peptide
UBE2C	Ubiquitin-conjugating enzyme E2 C	RLQQELMTL
UBE2L3	Ubiquitin-conjugating enzyme E2 L3	RLMKELEEI
UBXN2A	UBX domain-containing protein 2A	RLLDETLTL
USP11	Ubiquitin carboxyl-terminal hydrolase 11	RLYDTHITV
USP9Y	Probable ubiquitin carboxyl-terminal hydrolase FAF-Y	RLWGEPVNL
UTRN	Utrophin	RLHDVLMEL
VAMP1	Vesicle-associated membrane protein 1	RLQQTQAQV
VARS	Valine--tRNA ligase	RIPAYFVTV
VCL	Vinculin	RILGAVAKV
VIM	Vimentin	RLRSSVPGV
VPS33B	Vacuolar protein sorting-associated protein 33B	RLMEAMSEV
VRK2	Serine/threonine-protein kinase VRK2	RMLDVLEYI
VRK3	Inactive serine/threonine-protein kinase VRK3	RLLDALEFL
WTAP	Pre-mRNA-splicing regulator WTAP	RLSETDFKV
XPO4	Exportin-4	RVMELFFTV
XPOT	Exportin-T	RLAQVSPEL
ZBTB25	Zinc finger and BTB domain-containing protein 25	RLEEGIRFL
ZCCHC2	Zinc finger CCHC domain-containing protein 2	RLLPQVDSV
ZNF292	Zinc finger protein 292	RLQELELQL
-	Chain A, Model Of Actin-Fimbrin Abd2 Complex	RVAPEEHPV
-	Transient receptor potential-related channel 7, a novel putative Ca2+ channel protein	RVADVIAQV
-	Unknown protein eluted from human MHC allele	RQPDLVLRL
-	hCG1644522	RLLPDIRGV

Appendix B

Histograms showing the BB7.2, T1-116C and T1-116CV1 staining of T2 cells pulsed with the 25 IEDB peptides selected for *in vitro* testing in T2 stabilisation assays. The experiment was repeated three times, and one representative experiment is shown.

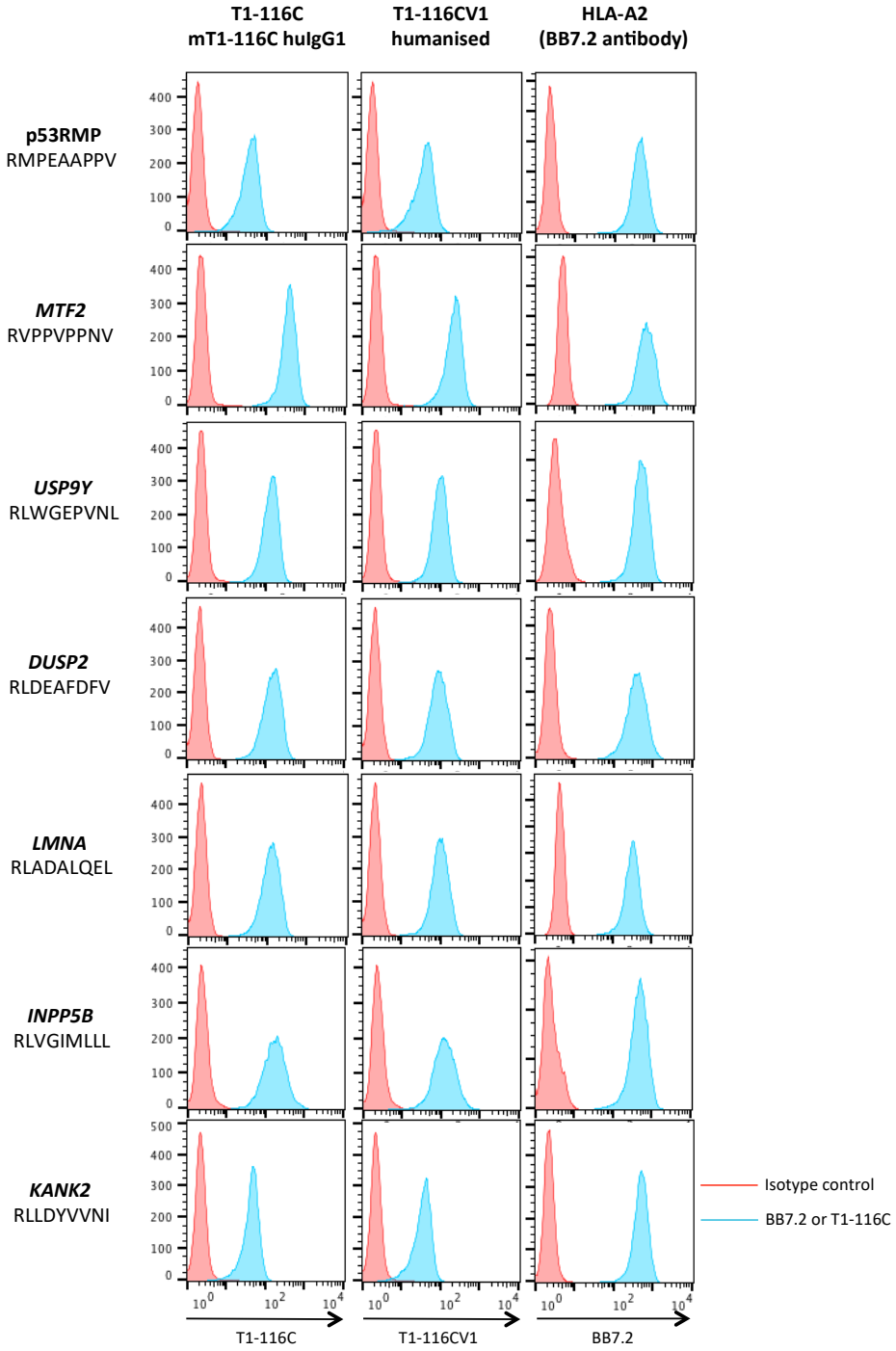

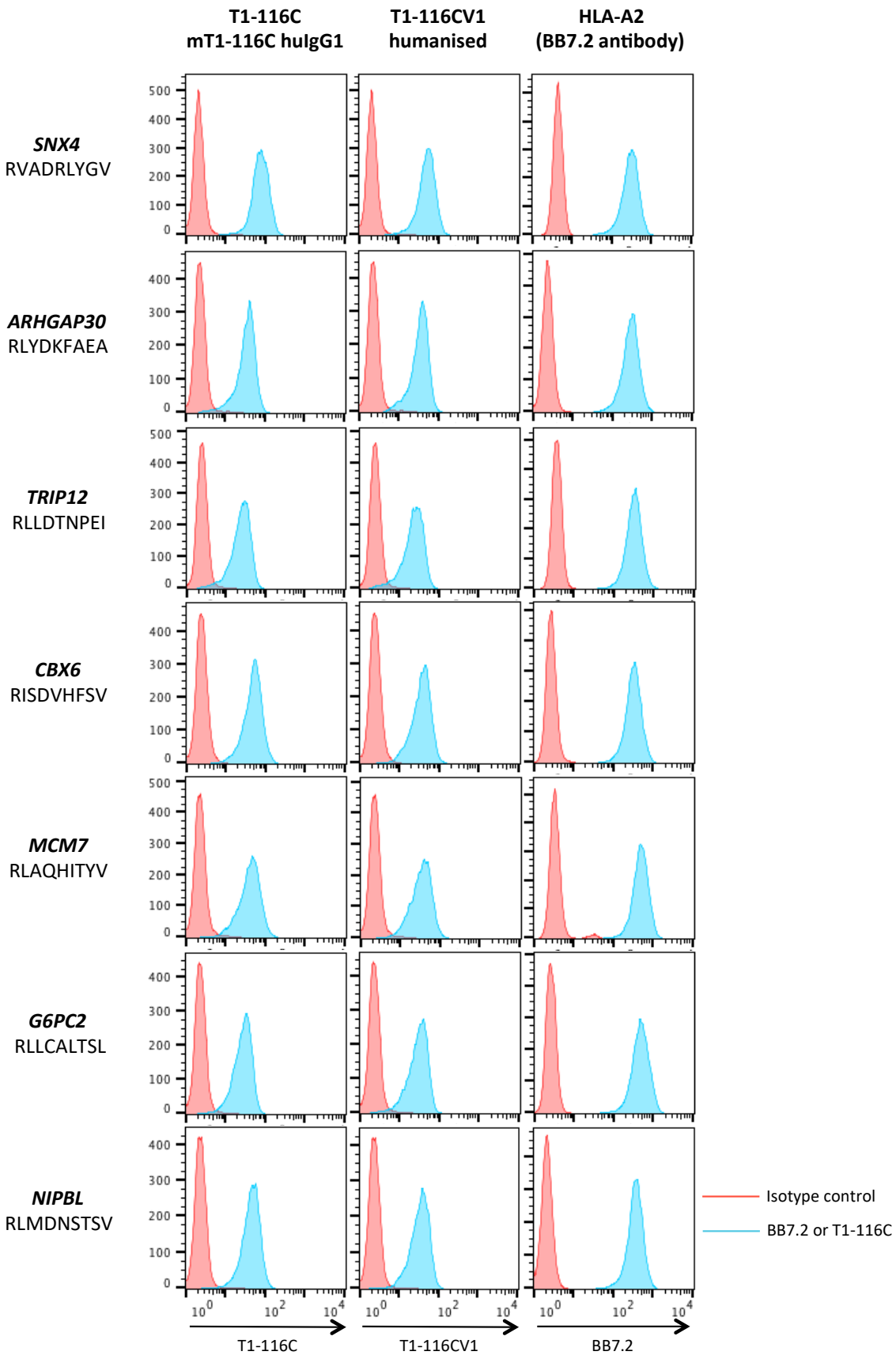
T1-116C
mT1-116C huIgG1
T1-116CV1
humanised
HLA-A2
(BB7.2 antibody)
SNX4
RVADRLYGV
ARHGAP30
RLYDKFAEA
TRIP12
RLLDTNPEI
CBX6
RISDVHFSV
MCM7
RLAQHITYV
G6PC2
RLLCALTSL
NIPBL
RLMDNSTSV
Isotype control
BB7.2 or T1-116C
T1-116C
T1-116CV1
BB7.2

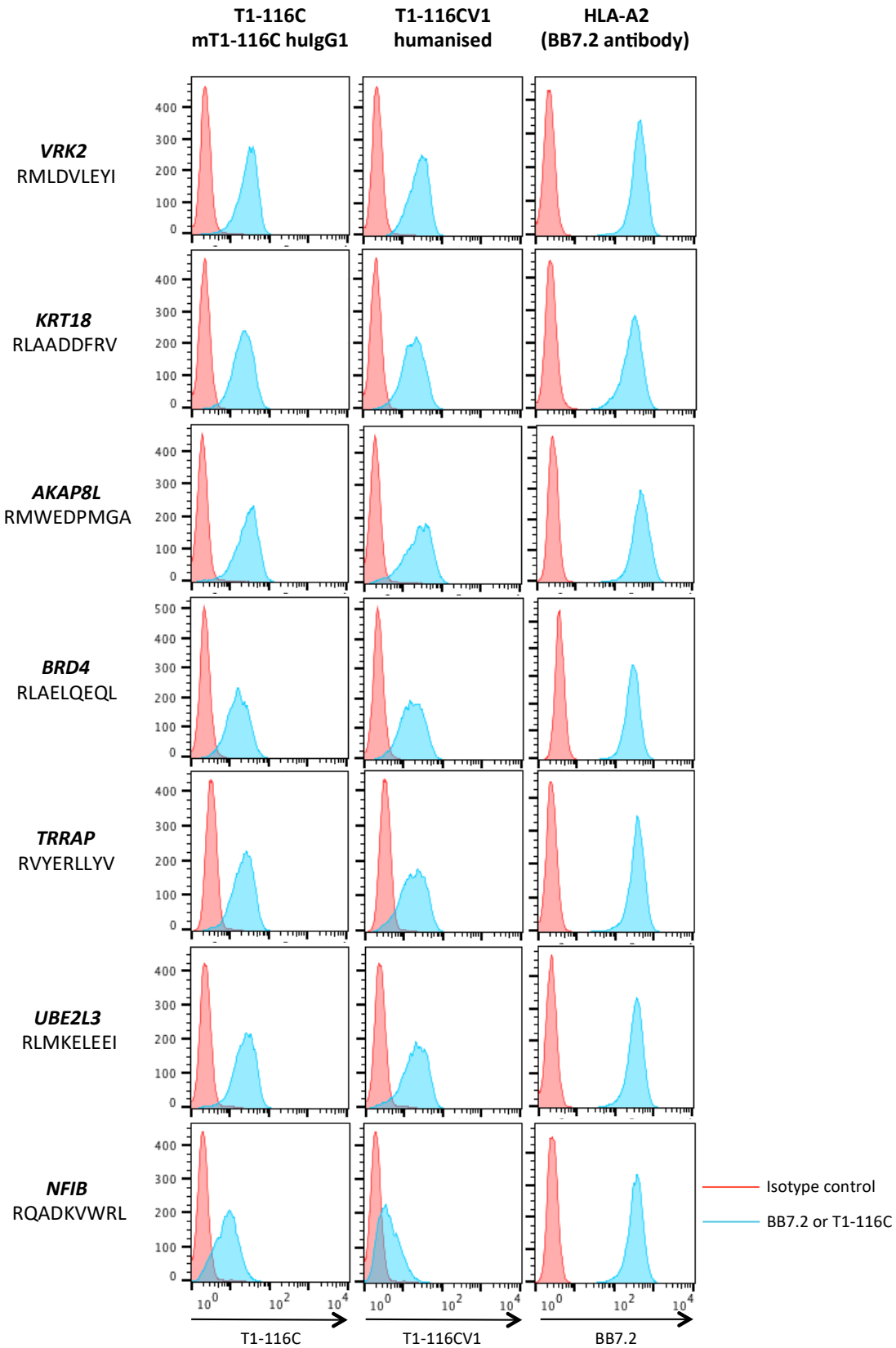
T1-116C
mT1-116C hulgG1
T1-116CV1
humanised
HLA-A2
(BB7.2 antibody)
VRK2
RMLDVLEYI
KRT18
RLAADDFRV
AKAP8L
RMWEDPMGA
BRD4
RLAELQEQL
TRRAP
RVYERLLYV
UBE2L3
RLMKELEEI
NFIB
RQADKVWRL
Isotype control
BB7.2 or T1-116C
T1-116C
T1-116CV1
BB7.2

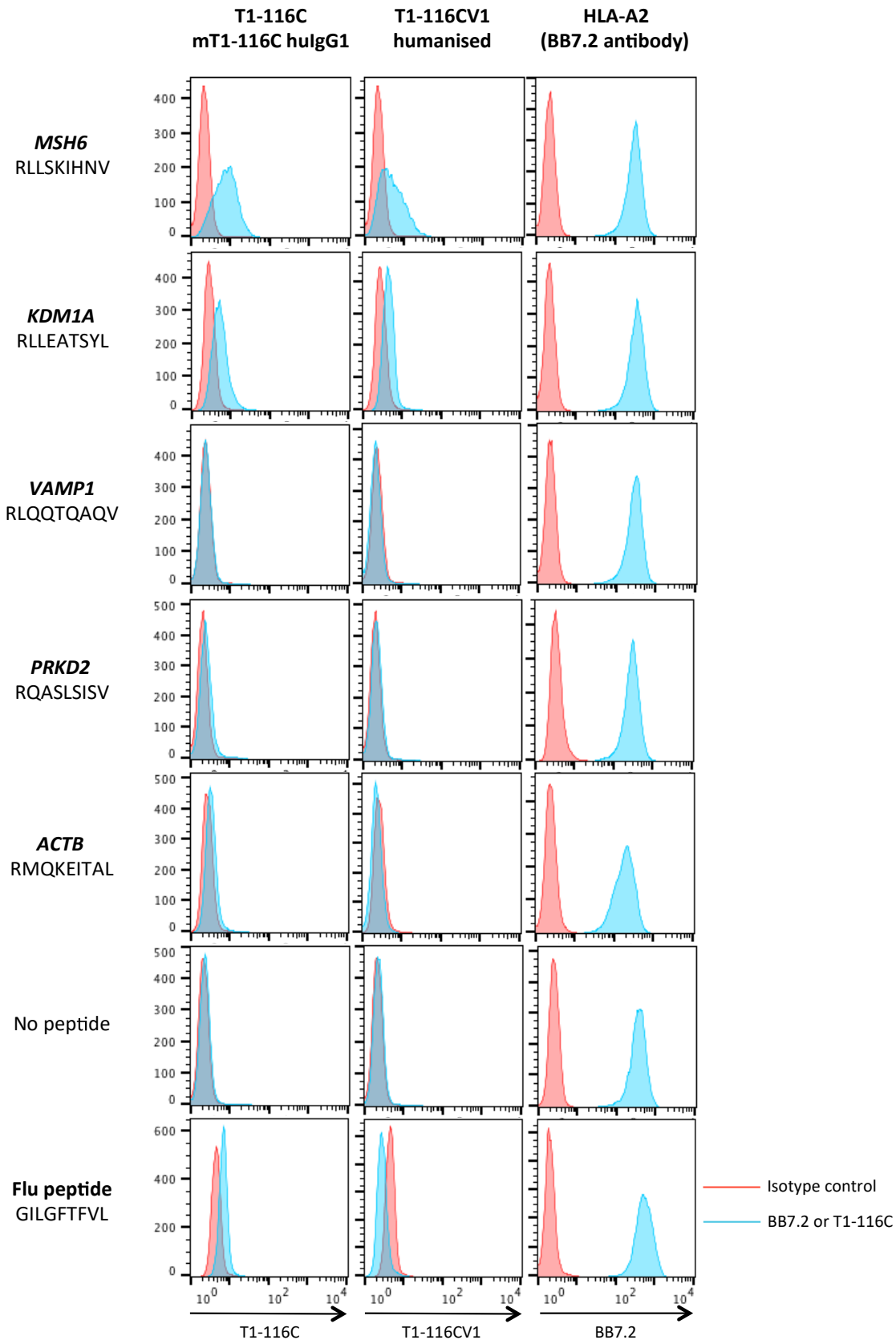
T1-116C
mT1-116C huIgG1
T1-116CV1
humanised
HLA-A2
(BB7.2 antibody)
MSH6
RLLSKIHNV
KDM1A
RLLEATSYL
VAMP1
RLQQTQAQV
PRKD2
RQASLSISV
ACTB
RMQKEITAL
No peptide
Flu peptide
GILGFTFVL
Isotype control
BB7.2 or T1-116C
T1-116C
T1-116CV1
BB7.2

Appendix C

In order to assess the cytotoxic ability of the T2-2A CAR, a cytotoxicity assay using CAR-transduced PBMCs should be performed. Due to the time constraints of the DPhil project, we did not have sufficient time to both establish the assay in the laboratory and complete the experiment. Instead, we elected to perform a degranulation assay with the Jurkat-T2-2A-CAR cells. Degranulation assays can be used as a surrogate for cytotoxicity assays using CAR-transduced PBMCs (Betts *et al.*, 2003; Rubio *et al.*, 2003). Although we did not find reports of degranulation assays performed with CAR-transduced Jurkat cells, we attempted to perform the experiment as it could give us an indication of whether activated T2-2A CAR-transduced T cells might indeed have cytotoxic potential.

The experiment involved the co-culture of the Jurkat-T2-2A-CAR cells with target cells, with the anti-CD107a antibody being added to the co-culture in order to detect the CD107a as it becomes externalised. After 5 hours of co-culture, the cells were harvested and stained with an anti-CD3 antibody, which enabled selection of the Jurkat cells. As target cells, we used the cell lines that were shown to stimulate IL-2 production in Figure 5.16, as well as flu peptide-pulsed T2 cells as a negative control. Unexpectedly, all of the cells, including the negative control cells and non-transduced Jurkat cells were found to be CD107a-positive (Figured C1). An isotype control antibody for the CD107a antibody did not give any labelling, indicating that this was not a consequence of non-specific antibody labelling (Figure C2).

The media only control in Figure C1 suggested that the Jurkat cells alone, without target cell stimulation, were positive for CD107a. We repeated this staining and confirmed that Jurkat cells and Jurkat-T2-2A-CAR cells alone were indeed positive for CD107a (Figure C3). These data indicated that the Jurkat cell line was unsuitable for this experimental approach.

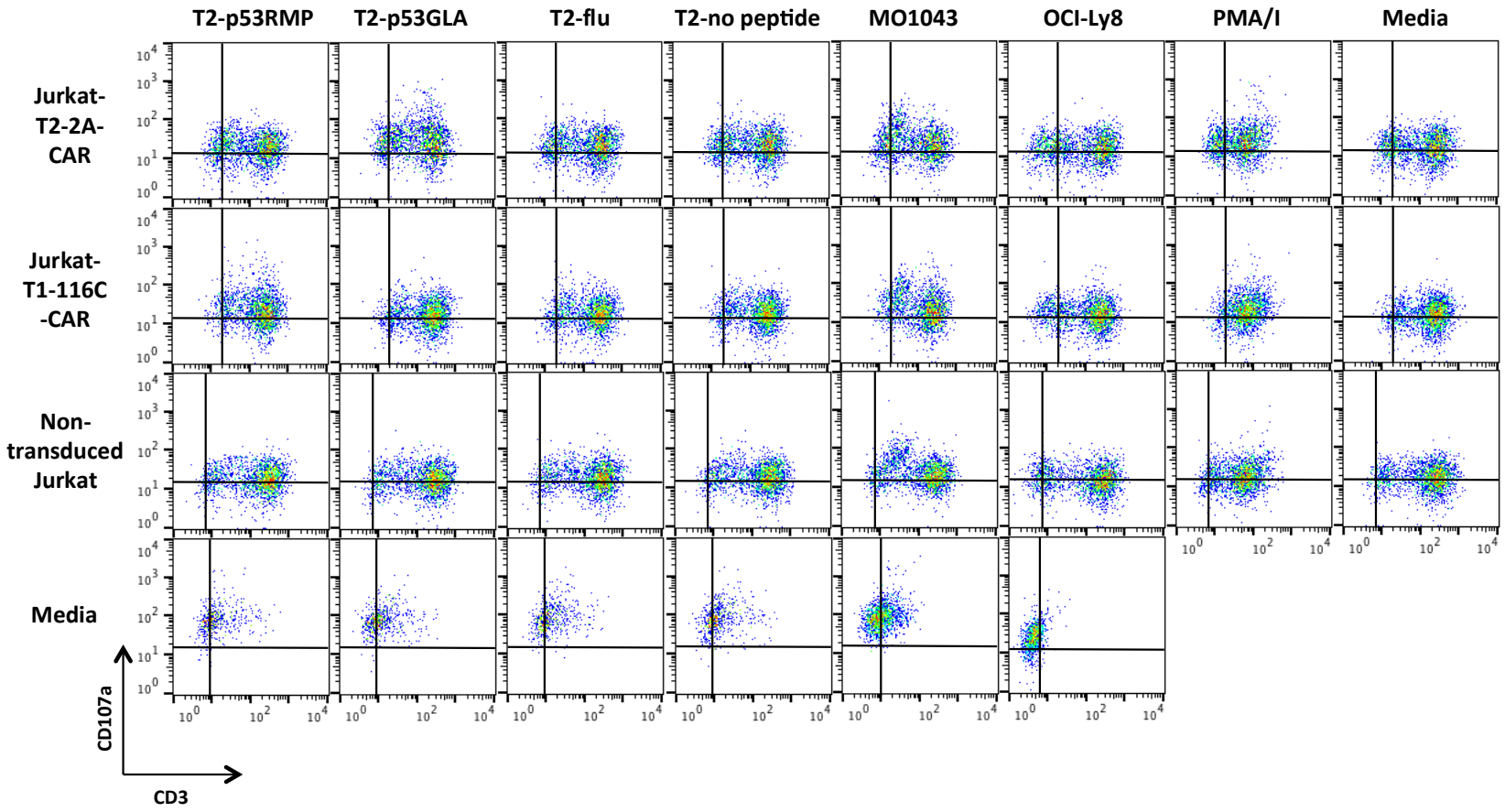

Figure C1 – Degranulation assay using Jurkat-T2-2A-CAR cells.

Jurkat-T2-2A-CAR cells or control cells (Jurkat-T1-116C-CAR or non-transduced Jurkat) were co-cultured with target cells and anti-CD107a antibody. Cells were harvested after a 5 hour incubation period and stained with anti-CD3 antibody to identify the T cells. Unexpectedly, all samples were CD107a-positive.

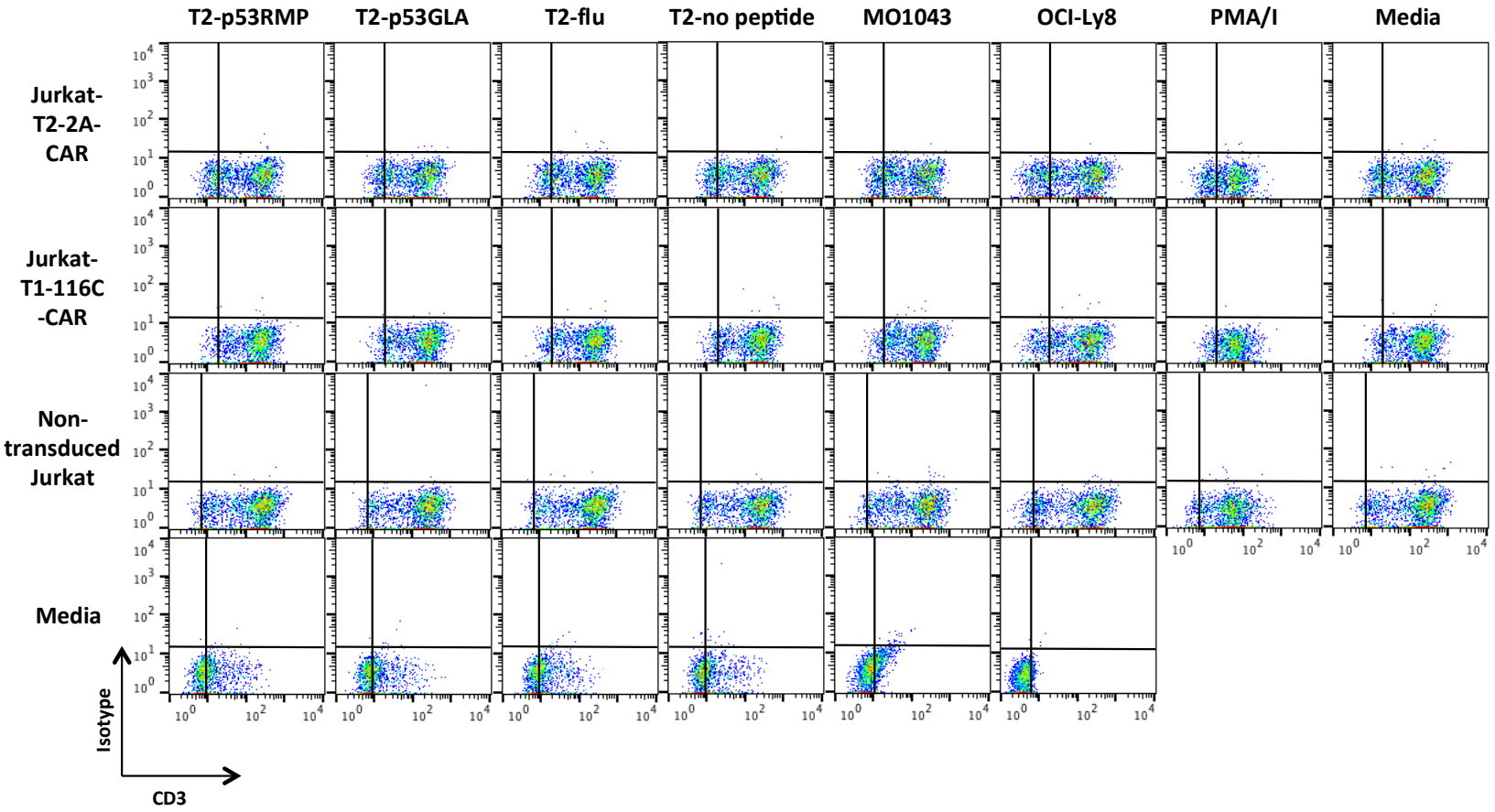

Figure C2 – Isotype control antibody staining for the Jurkat-T2-2A-CAR cell degranulation assay.
The same cell lines and co-cultures that were used in the degranulation assay, in Figure D1, were also stained with the isotype control antibody. As expected, all samples were CD107a-negative.

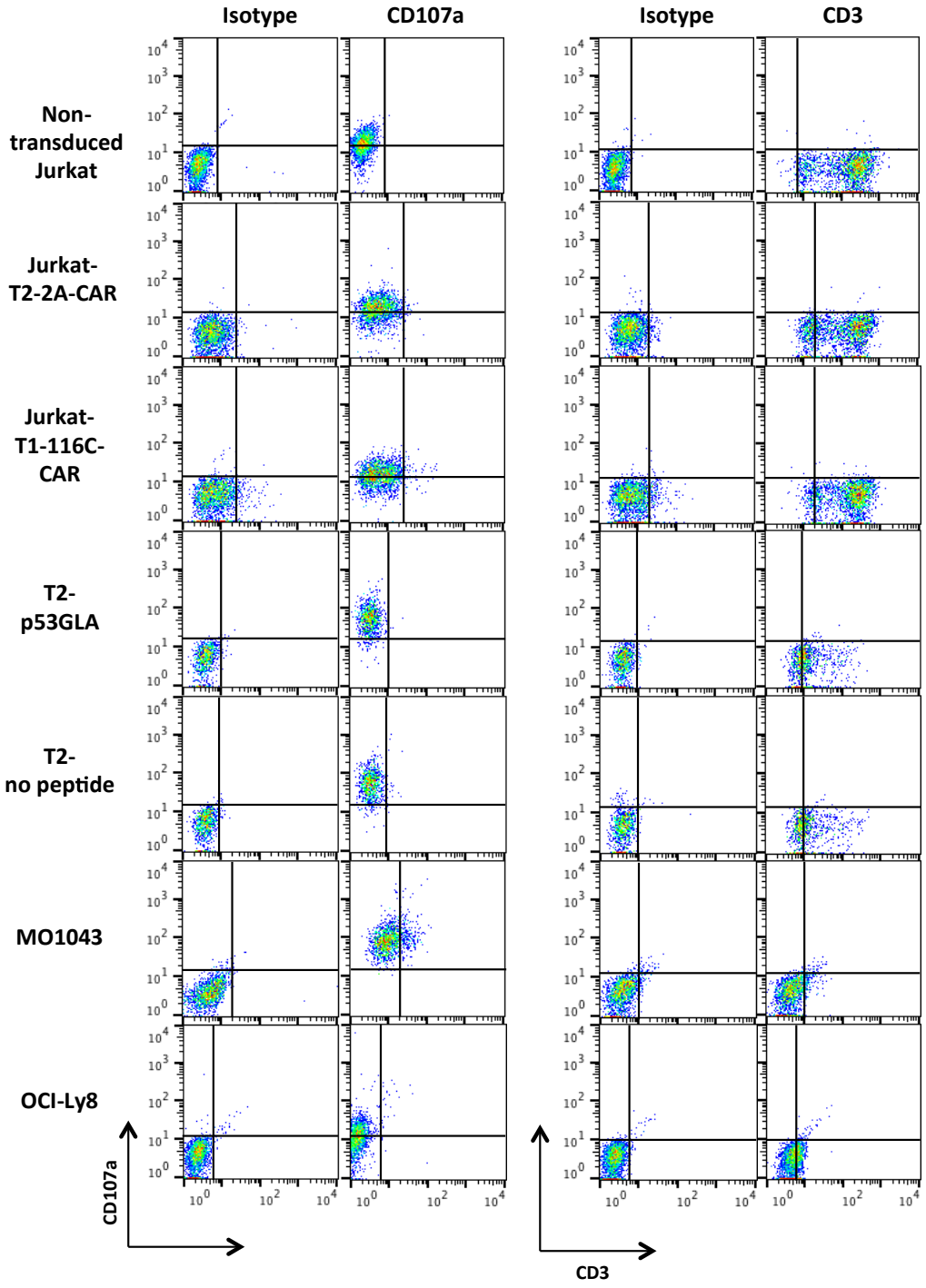

Figure C3 – CD107a and CD3 staining of cells used in the Jurkat-T2-2A-CAR cell degranulation assay.

Cell lines used in the degranulation assay in Figure D1 were stained individually with anti-CD107a and anti-CD3 antibody. All the cells lines show some CD107a positivity. Only the Jurkat cells should be CD3-positive, however the T2 cells show a slight shift toward CD3-positivity.